Systematics and biostratigraphy of Australian Early Cretaceous belemnites with contributions to the timescale and palaeoenvironmental assessment of the Australian Early Cretaceous System derived from stable isotope proxies

Thesis submitted by
Toni Williamson B. Sc. (Hons)

In August, 2006,
for the degree of Doctor of Philosophy
in the School of Earth Sciences,
James Cook University,
Australia

STATEMENT OF ACCESS

I, the undersigned, the author of this thesis, understand that James Cook University will make it available for use within the University Library and, via the Australian Digital Theses network, or other means, allow access to other users in other approved libraries.

All users consulting this thesis will have to sign the following statement:

" In consulting this thesis, I agree not to copy closely nor paraphrase it in whole or in part without written consent of the author; and to make proper public written acknowledgement for any assistance which I have obtained from it."

I understand that, as an unpublished work, a thesis has significant protection under the Copyright Act and I do not wish to place any restriction on access to this thesis.

Toni Williamson August 2006

STATEMENT OF SOURCES

DECLARATION

I, the undersigned, declare that this thesis is my own work and has not been submitted in any form from another degree, diploma or study at any university or other institution of tertiary education. Information derived from the published or unpublished work of others has been acknowledged in the text and a list of references is given.

Toni Williamson August 2006

STATEMENT OF CONTRIBUTION OF OTHERS

Stipend Support:	Australian Research Council (ARC) stipend James Cook University Earth Science Award
Supervision:	Prof. Bob Henderson
Editorial Assistance:	Prof. Bob Henderson
Laboratory Assistance:	Dr Yi Hu, Darren Richardson, Irena Kinaev
Analytical Assistance:	Advanced Analytical Centre James Cook University, Townsville Dr Yi Hu, Dr Kevin Blake
	Advanced Centre for Queensland University Isotope Research Excellence (ACQUIRE) Brisbane, Queensland Prof. Ken Collerson, Irena Kinaev
	The Australian National University Research School of Earth Sciences Canberra Dr Michael Gagan
Photographic Assistance:	Kirsten Perry
Use of Infrastructure External to JCU:	South Australian Museum, Palaeontology
	Geological Survey of South Australia, Palaeontology
	University of Adelaide, Earth Science Department, Palaeontology
	Museum of Victoria, Palaeontology
	Queensland Geological Survey, Core Library and Palaeontology

University of Queensland, Earth Science Department, Palaeontology

Queensland Museum, Palaeontology

Department of Palaeontology, Australian Museum

University of Sydney, Palaeontology

Commonwealth Palaeontological Collections Canberra

Western Australian Museum, Palaeontology

Geological Survey of Western Australia, Core Library and Palaeontology

University of Western Australia, School of Earth and Geographical Sciences, Palaeontology

Hunterian Museum, University of Glasgow, Department of Geology, Palaeontology

British Museum (Natural History), London, Palaeontology

ACKNOWLEDGEMENTS

Firstly, I would like to thank Prof. Bob Henderson for giving me this opportunity to work on this project. Bob's direction and enthusiasm throughout the duration of the project was inspirational and the thorough reviewing of my drafts is especially appreciated.

Thanks to the UWA (Prof. David Haig, Matt Dixon) and GSWA bunch (Arthur Mory), for inviting me to share and sample from the new cores, and also the invaluable help that you have been in providing me with your unpublished data from the west.

I also wish to thank Dr. Mike Gagan (RSES, ANU, Oxygen isotopes) and Prof. Ken Collerson (ACQUIRE, UQ, Strontium isotopes) for running my isotope samples in their respective labs. Thank you for sharing your geochemical knowledge that greatly aided the interpretation of the raw data and the construction of curves.

The assistance received in the lab from Dr. Yi Hu and guidance for using the CL machine by Dr. Kevin Blake, from the AAC, JCU, is greatly appreciated.

On a personal note, thank you to any one and everyone that leant a listening sympathetic ear to me during those dark times, consoled me during the trying times, and laughed with me in the good times. Your friendships are inexplicable and are appreciated beyond words!

Charlie, thanks for filling me with the inspiration to come back and submit. I am forever indebted to your persistent nagging that has finally allowed me to get this monkey off my back! Thanks, for just being you xxx.

Last but definitely not least, thanks to Mom and Dad for making regular visits to Townsville, and keeping me on the straight and narrow (or at least trying too!). Your guidance, enthusiasm and most importantly, support has been unbounding in magnitude, and never goes unappreciated. Thank you.

ABSTRACT

Belemnites are particularly common in Australian Early Cretaceous sequences but have attracted little contemporary examination. They offer potential for biostratigraphic zonation, as evaluated in the study presented here, based on an examination of very extensive collections that have accumulated in museum and university collections over more than a century. Most of these are from the Great Artesian Basin of eastern Australia and the Carnarvon Basin of Western Australia but small collections from the Maryborough Basin (coastal Queensland) and the Money Shoals Basin (Northern Territory) are also included in the study. Systematic revision has identified distinctive taxa of the Austral Family Dimitobelidae, and has determined their stratigraphic ranges. Contrary to the existing literature, the Aptian Stage is characterized by just two species: robust *Peratobelus oxys* Tenison-Woods characterized by an unusually large phragmocone, previously described under the name *P. selheimi* Tenison-Woods, and gracile *P. bauhinianus* Skwarko. Albian taxa include long-ranging *Dimitobelus diptychus* McCoy and *D. stimulus* Whitehouse but also the short-ranging *D. plautus* sp. nov. (early Albian), and *D. liversidgei* Etheridge (late Albian). *Dimitobelus hendersoni* sp. nov. is recognized from the Albian of Western Australia but its precise range is not known. A distinctive new, diminutive, Cenomanian belemnite genus *Microbelus* gen. nov. is established with two component species, *M. haigi* sp. nov. and *M. tumidus* sp. nov., based on collections from the West Australian Carnarvon Basin.

Many of the belemnite guards have retained pristine biogenic calcite, free from diagenetic overprint, as demonstrated by the luminescence properties of polished thin sections examined by electron microprobe imaging and by analysis for trace element contents by inductively coupled plasma technology. Belemnite guards arranged in stratigraphic sequence for the eastern Australian Great Artesian Basin and from drill core from the Carnarvon Basin have been analysed for Sr-isotope contents. Strontium isotopic curves for these two sequences have been used for timescale resolution of the Australian Early Cretaceous System, by comparison with the global curve established from a range of northern hemisphere studies. The evaluation indicates that some adjustment to biostratigraphic zonations applied in Australia for timescale purposes, particularly that related to dinoflagellates, requires adjustment. Substantial paraconformities are indicated for both documented successions, embracing the Aptian-Albian boundary interval.

Oxygen and carbon isotopic analysis has been applied to the same sample set examined for strontium contents, with the objective of illuminating the palaeoenvironmental context of Australian shallow marine environments of Early Cretaceous (Aptian-Cenomanian) age. The data indicate that oxygen and carbon isotopic systematics of epeiric association were perturbed by partial isolation from the global ocean. Isotope signatures for the sequence of the Great Artesian Basin reflect a combination of local scale influences, including dilution by riverine runoff, exchange with volcaniclastic sediment, unusual temperature regimes that applied in very

extensive, shallow epicontinental water bodies and the peculiarities of organic recycling in such an environment.

Oxygen-isotope values obtained from the Carnarvon Basin, representing an open-ocean continental margin sediment system, indicate southern hemisphere mid-latitude late Aptian sea surface temperatures, that differ little from those which presently apply. A warming trend is apparent for the Albian-Cenomanian interval, representing greenhouse climatic conditions. Carbon-isotope values through the same interval show a complementary negative trend in $\delta^{13}C$, attributed to CO_2 enhancement in the atmosphere that accompanied global warming. Short period temperature excursions of as much as 5°C are identified in the record, suggesting that climatic shifts of similar scale to those which characterised the Pleistocene Epoch also applied in the mid Cretaceous. Relative to values of $\delta^{13}C_{carb}$ available from other studies of Albian – Cenomanian biogenic carbonate, those obtained from the Carnarvon Basin are unusually low, suggesting that low productivity characterised the water body in which its sedimentary succession accumulated through this time interval. The carbon-isotope record is incomplete for the intervals that should register oceanic anoxic episodes 1a (early Aptian), 1b (Aptian-Albian boundary interval) and 1d (latest Albian). OAE 1b is expressed by a positive $\delta^{13}C_{carb}$ excursion across the euxinic interval of the Toolebuc Formation in the Great Artesian Basin succession and a correlative positive excursion is apparent for the succession of the Carnarvon Basin. It is dated as early late Albian, ~ 105Ma, but its global significance is open to question. A matching negative excursion in $\delta^{13}C_{org}$ across the Toolebuc interval of the Great Artesian Basin is attributed to the influence of organic matter of continental provenance.

TABLE OF CONTENTS

LIST OF FIGURES AND PLATES

SECTION A

SECTION B

SECTION C

SECTION D

SECTION E

LIST OF TABLES

SECTION C

SECTION D

SECTION A

Albian and Cenomanian belemnites of the Family *Dimitobelidae* from Australia

Section A. Albian and Cenomanian belemnites of the Family *Dimitobelidae* from Australia

A. 1 Abstract

Representatives of the Family *Dimitobelidae* (Mollusca:Cephalopoda) are abundantly represented in Australian Early Cretaceous shallow marine strata, especially those related to the epeiric sedimentary record of the Great Artesian Basin. The taxonomy, biostratigraphy and distribution of Albian and Cenomanian Australian representatives of the family are revised, utilising all known collections. The genus *Dimitobelus* Whitehouse (early Albian - mid Cenomanian) occurs in both the Great Artesian Basin of eastern Australia and the Carnarvon Basin of Western Australia. This genus embraces six named species: *D. diptychus* (McCoy) (earliest Albian - mid Cenomanian), *D. stimulus* Whitehouse (Albian), *D. dayi* Doyle (earliest Albian – early late Albian), *D. liversidgei* Etheridge (late Albian), *D. plautus* sp. nov (early Albian) and *D. hendersoni* sp. nov. (late Albian). A new genus, *Microbelus*, is represented by *M. haigi* sp. nov. and *M. tumidus* sp. nov. which are endemic to the Cenomanian upper Gearle Siltstone, Carnarvon Basin, Western Australia.

A. 2 Introduction

Dimitobelus is the characteristic genus of the Dimitobelidae, a distinctive group of Southern Hemisphere Cretaceous belemnites first recognised by Whitehouse (1924) and now known to be latitudinally restricted to the Austral Realm (Stevens, 1973; Doyle, 1988). The family is characterised by a cylindrical or clavate guard with anteriorly placed ventro-lateral grooves, and lacking ventral and apical grooves. Whitehouse originally separated four component genera, *Peratobelus*, *Dimitobelus*, *Tetrabelus* and *Cheriobelus*. *Dimitobelus* guards are characteristically depressed with dorsally curving ventro-lateral grooves.

The first representatives of *Dimitobelus* appeared in the earliest Albian within Australia and the genus enjoyed a wide distribution in Albian time (Australia, New Zealand, New Guinea, Antarctic Peninsula, Argentina and probably the Falkland Plateau). A similar distribution pattern occurred in the Cenomanian (Western Australia, New Zealand, ? New Guinea and the Antarctic Peninsula). However in the Late Cretaceous the genus became restricted to a southern polar distribution with records only from the Antarctic Peninsula (Campanian) and New Zealand (Santonian-Maastrichtian).

Six nominal species of *Dimitobelus* have been recorded from Australia. Most representatives of the genus have been documented from Albian formations of the Eromanga Basin, a very extensive epeiric sedimentary system developed in eastern Australia (Figure A. 2. 1)(Exon and Senior, 1976; Senior et al., 1978). *Dimitobelus* is also known from the Albian strata from the subjacent Carpentaria, Laura, Maryborough and Surat Basins. The genus is extensively represented in the Carnarvon Basin in Western Australia where it ranges through the Albian into the Cenomanian.

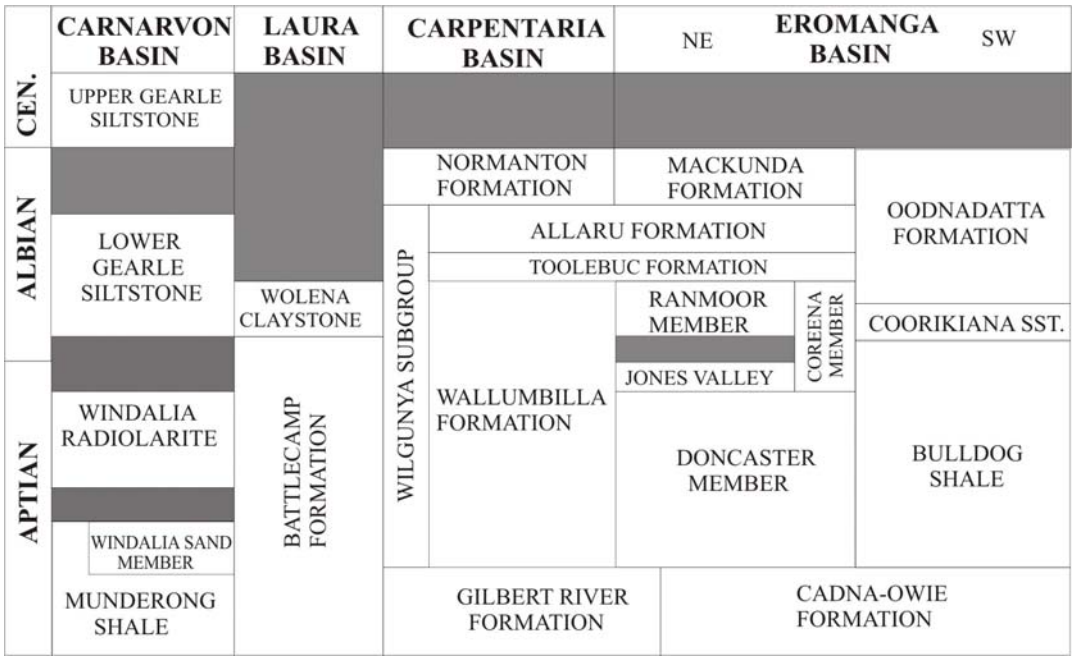

Figure A. 2. 1 Aptian – Albian marine lithostratigraphic units recognised in Cretaceous basins of Australia (modified from Haig and Lynch, 1993). Age assignments are based on strontium-isotope stratigraphy (Section C) and biostratigraphy.

This paper revises the Australian species of *Dimitobelus*, drawing on extensive collections now available. In the course of the study, a new genus, *Microbelus*, has been recognised from Cenomanian strata from the Western Australian Carnarvon Basin. This genus was probably more widely ranging in the Australian region. However, marine Cenomanian strata are lacking in eastern Australia due to widespread withdrawal of epicontinental seas at this time (Figure A. 2. 2).

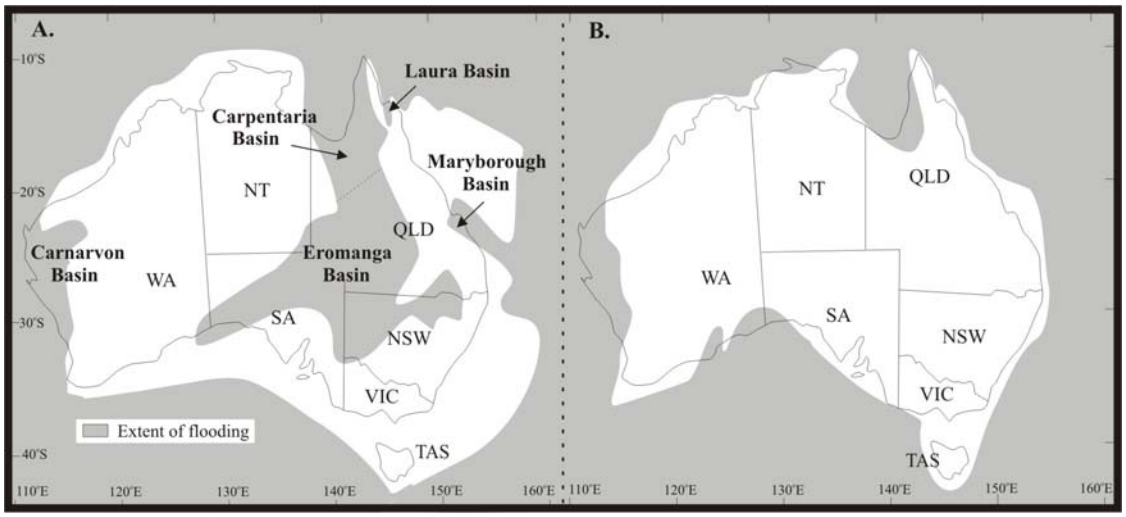

Figure A. 2. 2 Emergent areas (unshaded) and the extent of marine flooding (shaded) of Australia during the Albian (A) and Cenomanian (B) (after Frakes et al., 1987).

A. 3 Collections and localities

The specimen suite evaluated here is held by a number of repositories, as follows: SAM, South Australian Museum, Adelaide; GSSA, Geological Survey of South Australia; UA, University of Adelaide; NMV, Museum of Victoria; QGS, Queensland Geological Survey; UQ, University of Queensland; QM, Queensland Museum; JCU, James Cook University; AM, Department of Palaeontology, Australian Museum; US, University of Sydney; CPCC, Commonwealth Palaeontological Collections Canberra; WAM, Western Australian Museum; UWA, University of Western Australia; GSWA, Geological Survey of Western Australia; HM, Hunterian Museum, Department of Geology, University of Glasgow; BM, British Museum (Natural History), London. Locality numbers, prefixed 'L' refers to specific sites registered by these repositories. Modern collections are in general accurately located. However, locality records for older collections are commonly imprecise. Where possible these have been assigned approximate geographic coordinates.

In addition to the extensive collection of belemnites held by museums and other repositories, new field collections from the northern Eromanga Basin and

material from newly obtained drill core from the Carnarvon Basin have been included in the study. All collections have been placed within the lithostratigraphic framework of the basins to which they relate utilising published geological maps, generally at 1:250,000 scale. This in turn has provided the superpositional basis for biostratigraphic evaluation.

For the Carnarvon Basin, a suite of stratigraphic wells drilled in the last decade by the Geological Survey of Western Australia (GSWA) and collaborators has provided an especially useful suite of collections for which superpositional relationships are well established.

A. 3. 1 Morphological terminology and measurements

Guard terminology is based on the contributions of Swinnerton (1955), Glaessner (1945), Day (1968), Stevens (1965) and Challinor (1990). The apical region is that portion of the axis posterior to the position of maximum inflation; the stem region is that portion of the guard between the axis of maximum transverse inflation and the position of the protoconch; the alveolar region is that portion of the guard anterior to the protoconch.

The following order has been generally adopted in the systematic descriptions of belemnite guards:

1) General remarks: (i) size and shape of guard, (ii) ratio of length to maximum transverse diameter.
2) Outline of guard: (i) position of maximum transverse diameter (Dl_{max}), (ii) outline shape posterior to Dl_{max} including nature of apex and apical angle, (iii) outline shape anterior to Dl_{max}.
3) Profile of guard shape including the position of the maximum dorso-ventral diameter (Dv_{max}).
4) Cross-sectional shape of apical, stem and alveolar regions.
5) Grooves on surface of guard (if present).
6) Lateral lines on surface of guard (if present).

7) Internal structures: (i) apical line, (ii) alveolar angle, (iii) protoconch, (iv) phragmocone (if preserved).

The term `guard' is used in preference to the term `rostrum', which is favoured by European workers.

A. 3. 1. 1 Outline

The outline of the guard is its form as seen in dorsal or ventral view and is symmetrical in all known representatives of the Dimitobelidae. The outline may reflect hastate (spear-like), clavate (club-like), cylindrical or conical guard shapes and is considered an important taxonomic feature. In hastate guards, the position of maximum transverse inflation (Dl_{max}) is readily determined. It is clear on the guards of some taxa (e.g. *D. liversidgei*), whereas for others it is ill-defined and cannot be exactly located. In such cases Dl_{max} has been located at the most proximal apical site possible.

Posterior to Dl_{max} guard outlines may converge very gradually, defining an elongate, pointed apical region, or converge rapidly to produce a shortened, blunt apical region (see Swinnerton, 1955)(Figure A. 3. 1). Shape of the apical region commonly characterises individual species. In *Dimitobelus* the outline of the apical region is short and abrupt and either pointed or very obtuse to rounded, and in species with an apical canal an apical perforation is present (e.g. in *D. dayi*).

In hastate outlines, the sides of the guard converge anteriorly from Dl_{max} to the axis of minimum transverse diameter (Dl_{min}), which maybe located some distance anterior of the position of the protoconch. Anterior to this the sides diverge to accommodate the phragmocone. In *Dimitobelus*, the sides of the guard may at first converge quite rapidly anterior to Dl_{max}, producing a marked feature of the outline, but thereafter converge gradually.

In cylindrical guards, except for the apical region which is typically short, the sides are approximately parallel throughout the length of the guard, but usually diverge some distance anterior to the protoconch to accommodate the phragmocone. In conical guards the sides diverge throughout the length of the guard.

The degree of hastation may change during ontogeny. For instance, *D. diptychus* is usually more hastate in later growth stages.

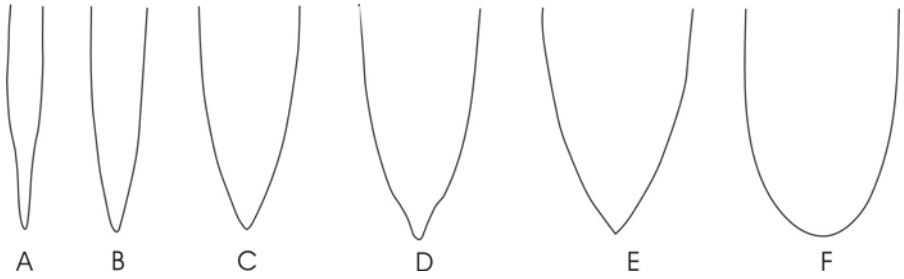

Figure A. 3. 1 Outline of apical region of belemnite guards (a) very acute and constricted (attenuated); (b) very acute; (c) acute; (d) moderately obtuse and constricted; (e) moderately obtuse; (f) very obtuse and rounded (after Swinnerton, 1955, Text Fig. 3, Stevens, 1965, fig. 14).

A. 3. 1. 2 Profile

The profile is shown in lateral views of the guard. In most species of *Dimitobelus* it is symmetrical or almost so and similar in shape to the outline, but is typically less hastate. In some species (e.g. *D. diptychus*), where the outline is clearly hastate, the profile is less so or not at all. The apex is eccentric in guards with an asymmetric profile and positioned dorsally with the line of the ventral surface is more distinctly curved than the line of the dorsal surface.

A. 3. 1. 3 Cross-section

The shape of the cross-sections provide a valuable specific characters, in addition to measurement of cross sectional dimensions. It varies from rounded to semi-elliptical and typically changes along the guard length.

A. 3. 1. 4 Surface grooves

Only ventro-lateral grooves and dorso-lateral grooves are present in *Dimitobelus*, and they are best developed in the anterior portion of the stem region becoming less clearly inscribed towards the apex. The detail of their morphology is useful in discriminating between species. In the alveolar region the ventro-lateral grooves are typically straight, narrow, and deeply incised, running approximately

parallel to venter. At about the position of the protoconch they curve sharply towards the mid-line of the flanks of the guard. The curved posterior portion of the ventro-lateral grooves in *Dimitobelus* connects with the anterior termination of the lateral lines. Though the actual junction of the groove with the lateral lines has been observed in few specimens it appears that the ventro-lateral line is essentially a continuation of the ventro-lateral groove. These two features either relate to the same structure, or to colinear and adjoining structures in the soft-part organization of *Dimitobelus*. A dorso-lateral groove may also be present in *Dimitobelus*, and may be colinear to a dorso-lateral line, mirroring relationships between the ventro-lateral groove and line. The two sets of grooves and lines are not symmetrical about the flank mid-line of the guard, but are dorsally offset. The dorso-lateral grooves follow a similar course to that of the ventro-lateral grooves, but their curvature is slight and they essentially continue the trend of the lateral lines, but may show a slight dorsal deflection towards the anterior. In most *Dimitobelus* species, the dorso-lateral grooves are obscure where only a faint dorso-lateral depression marks the groove position.

Whitehouse (1924) placed great emphasis on the relationships of lateral grooves to the lateral lines in the Dimitobelidae, and the issue of whether the grooves are independent of, or connected to, the lateral lines. Stevens (1965) considered that the lateral lines are dependent on the placement and depth of the lateral grooves, and their apparent independence merely reflected abrasional removal of the connecting portion of the lateral lines. The ventro-lateral grooves are usually well developed in *Dimitobelus*. Stevens (1965) considered that they mark the sites of prominent blood vessels.

A. 3. 1. 5 Lateral lines

Lateral lines are present on the flanks of many belemnite guards and may represent the course of longitudinal blood vessels in contact with the guard surface or the line of termination against the guard of the lateral structures such as fins. In his review of these features, Stevens (1965) suggested that if they represented the course of blood vessels, other vascular markings may be expected to occur as frequently as lateral lines, but they only occur in one family, the Belemnitellidae.

Lateral lines are present on the flanks of most species of *Dimitobelus*, though commonly they have been removed from individual specimens by corrosion. Stolley (1911) used the term `Laterallinien' for lateral grooves and `Doppellinien' for lateral lines. However in this study the term `lateral lines' is used for Stolley's `Doppellinien' and Swinnerton's `lateral grooves'. The term `lateral grooves' is restricted to true grooves as represented in the Dimitobelidae.

The paired lateral lines of *Dimitobelus* are a distinguishing feature for this southern hemisphere genus. Only single lateral lines are evident in northern hemisphere Early Cretaceous belemnites such as *Belemnitella* and *Actinocamax*, and such features are noticeably absent from others such as *Belemnellocamax* (Christensen, 1997a). The depth of incision of the lateral lines appears to vary between species being deeply incised in *D. diptychus* (McCoy), and less so in *D. liversidgei* (Etheridge). The paired lateral lines are commonly well preserved in the apical region, becoming indistinct in the stem and alveolar regions.

When well-preserved in *Dimitobelus* the lateral lines appear on the dorso-lateral surface of the posterior apex, and continue anteriorly along a slightly dorso-lateral or central course across the anterior apical and stem regions. In the anterior portion of the stem region, the lateral lines link with the ventro-lateral grooves and the dorso-lateral grooves (or depressions). The lateral lines are paired and remain together along all sections of the guard.

A. 3. 1. 6 Internal structures

The apical line is the central axis of the guard to which the calcite prisms of which it is constructed converge and marks successive positions of the apex during growth. In *Dimitobelus* the apical line is always markedly eccentric and ventrally placed. In some species such as *D. diptychus* and *D. dayi* an apical canal follows the course of the apical line and communicates to the exterior via an apical perforation.

The alveolar region of guards contains a conical hollow, the alveolus. The alveolar angle is the angle subtended by the alveolar walls as measured in the dorso-ventral plane. For *Dimitobelus* this angle is commonly within a range of 25°-27°.

The protoconch and phragmocone are rarely preserved in *Dimitobelus* but when present the protoconch is usually central or slightly ventral in position. The phragmocone is typically displaced a little towards the dorsum.

A pseudoalveolus (Stolley, 1911), a structure resulting from an enlargement of the alveolus by exfoliation of the alveolar walls, is commonly developed in *Dimitobelus* but is variably developed, or entirely lacking, in specimens representing individual species. It is developed where the anterior fringes of the growth lamellae abutting the alveolus are feebly crystalline. The development of a pseudoalveolus is usually accompanied by the development of an axial projection (`Nadelspitze' of Stolley, 1911, p. 186; Whitehouse, 1924, p. 413, 1925, pl. 2, figs. 8, 10, 11c), a needle-like spine that projects into the pseudoalveolus. Stolley (1911) regarded this structure as being the anterior extremity of the embryonic guard projecting into the pseudoalveolus, but Whitehouse (1924) considered that its development was unrelated to ontogeny of the guard. Stevens (1965) adapted Stolley's interpretation, envisaging the protoconch, and the apex of the alveolus, as being immediately anterior to the tip of the axial projection prior to the development of the pseudoalveolus.

Detailed studies of internal structures of the belemnite guard and the phragmocone of Boreal belemnites are due to Christensen (1925) and Hanai (1953). Though the shape of the guard is related to internal parameters such as the distance from the apex to the protoconch and the depth of the alveolus, the detail of internal structures of the guard have little taxonomic value. In northern hemisphere belemnites, such as *Belemnitella*, *Belemnella* and *Actinocamax*, the `Schatsky index', reflecting the distance between the protoconch and the beginning of the ventral fissure on the wall of the alveolar cavity, is important (Birkelund, 1957; Stevens, 1965). But for the belemnites in this study, the ventral groove, when present, is strictly a surface feature of the guard and not related to the development of a fissure connecting to the alveolus.

A. 3. 2 Dimensions

Measured dimensions (in millimetres) adopted for this study follow Avias (1953) and Stevens (1965)(Figure A. 3. 2) as follows:

L - total preserved length, i.e. from apex to the point where the sides of the guard intersect the sides of the phragmocone. Descriptive size terms related to length (L) are as follows: diminutive (< 10 mm), small (10-40 mm), medium (40-70 mm), and large (> 70 mm).

X - length from the apex to the Dl_{max}, position of maximum inflation shown in outline.

Dv_{max} - dorsoventral diameter at position of maximum inflation

Dl_{max} - lateral diameter at position of maximum inflation.

Terms and ratios used to describe the shape of the transverse section of the guard are:

Rounded - $Dl_{max}:Dv_{max} = 1$

Elliptical - $Dl_{max}:Dv_{max} = 1.1\text{-}1.2$

Semi elliptical - flattened on the ventral surface. $Dl_{max}:Dv_{max} = 1.3\text{-}1.4$

Depressed - flattened on both dorsal and ventral surfaces, subquadrate; $Dl_{max}:Dv_{max} \geq 1.4$

The value of the ratios varies from genus to genus, especially between hastate and non-hastate forms. Although the wide range of variability within belemnite species limits the usefulness of these ratios, they do provide a useful basis for comparison between species. With few exceptions, Australian Cretaceous belemnite guards are in general only partially preserved and complete specimens, from which the full range of measurements can be obtained, are uncommon. Suites of measurements that adequately define the range of variation are rarely obtained.

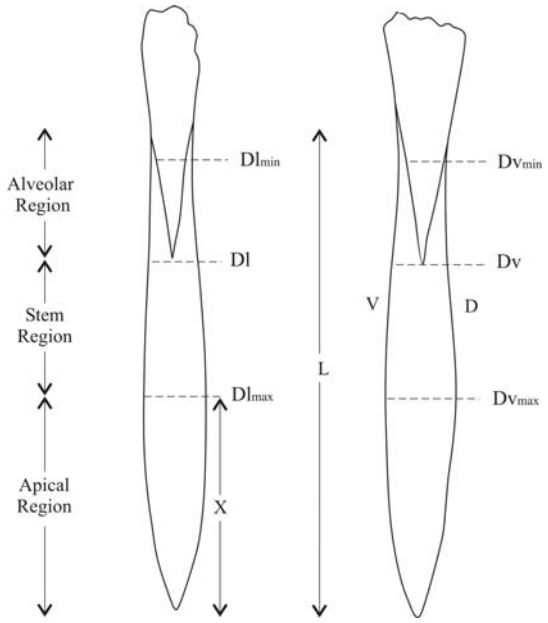

Figure A. 3. 2 Outline (left) and profile (right) of a belemnite guard to illustrate symbols used for measurements (modified from Stevens, 1965).

A. 3. 3 Illustrations

The diagrams of cross-sections were prepared by tracing the outline and internal structures showing in polished thin sections. This gives an accurate representation of width and the number of internal growth bands as well as presence (depth and location) of grooves and lines.

Specimens illustrated in the plates were coated with ammonium chloride sublimate prior to photography.

A. 4 Systematic Descriptions

Class CEPHALOPODA Cuvier, 1795

Subclass COLEOIDEA Bather, 1888

Order BELEMNITIDA Zittel, 1895

Suborder BELEMNOPSEINA Jeletzky, 1965

Family Dimitobelidae Whitehouse, 1924

Diagnosis: Cylindrical and clavate guards bearing a pair of ventro-lateral grooves at least on the anterior portion of the guard, in the alveolar region. Devoid of apical grooves; unpaired ventral or dorsal alveolar grooves are never present.

Discussion: The Family Dimitobelidae comprised of the genera *Peratobelus* Whitehouse, *Dimitobelus* Whitehouse, and *Tetrabelus* Whitehouse (=*Cheriobelus* Whitehouse) was established by Whitehouse (1924) for a group of Cretaceous belemnites from eastern Australia. It represents a distinctive Cretaceous belemnite clade characteristic of mid to high Southern Hemisphere latitudes where its members are diagnostic of the marine Austral Realm that developed in the Early Cretaceous Period and continued through to the end of the Cretaceous extinction event. The Dimitobelidae are likely to have evolved from a southern outlier of a more northern belemnite group in the late Early Cretaceous, perhaps the Tethyan *Hibolithes*, as this genus is characterised by well developed lateral lines and a commonly reduced single ventral alveolar groove (Doyle, 1987a).

This study has also recognised a new diminutive genus *Microbelus* referred to the Dimitobelidae and represented by two new species, *M. haighi* and *M. tumidus*.

Genus *Dimitobelus* Whitehouse, 1924

Dimitobelus Whitehouse, 1924, p. 412.

Cheriobelus Whitehouse, 1924, p. 414.

Type Species: by original designation. Objective synonym *Belemnites canhami* Tate 1880 (= *Belemnitella diptycha* McCoy 1867a; see Glaessner, 1957, p. 88); Albian, Great Artesian Basin.

Diagnosis: Guards hastate in outline, less so or cylindriconical in profile. Ventro-lateral grooves clearly inscribed are confined to the alveolar region and anterior portion of the stem region. Dorso-lateral grooves lacking or rudimentary, forming weak, obscure depressions or lines. Ventro-lateral grooves are straight in the alveolar region and lie sub-parallel to the venter, but posteriorly towards the stem region they curve towards the mid-line of the flanks and progressively weakening. Lateral lines paired, always present in apical and stem regions, centrally placed, becoming deflected dorsally near the apex.

Description: Diminutive to large, slender to robust guards, subhastate to hastate in outline and commonly markedly depressed in cross section. Profile subhastate to cylindriconical, asymmetrical or symmetrical. Ventral surface is commonly flattened. Transverse sections elliptical to subcircular in stem and apical regions, typically subquadrate in alveolar region. Paired, short ventro-lateral grooves are well developed; dorso-lateral grooves lacking or forming indistinct depressions or lines. Grooves are confined to the alveolar region and anterior portion of the stem region. Ventro-lateral grooves are initially straight and extend along one quarter to one third of the guard. They become weaker posteriorly where they deflect dorsally, curving towards the mid-line of the flanks to meet the lateral lines. Dorsal-lateral grooves, where developed, follow a similar course but curve more gently towards the mid-flank region. In stem and apical regions, lateral lines are generally well developed and centrally placed, becoming gently deflected dorso-laterally towards the apex. The phragmocone is slightly offset dorsally and has a ventrally incurved protoconch; it penetrates a quarter to a third of the guard. Apical line is excentric, offset slightly towards the ventral surface.

Range: Albian-Cenomanian of Australia, Antarctica, New Zealand and New Guinea.

Discussion: Originally described by Whitehouse (1924), *Dimitobelus* was established to encompass all "clavate (hastate) belemnites with dorso-lateral (ventro-lateral) grooves and lateral lines, both of which may be straight or somewhat curved. The alveolus is normal, but generally a pseudoalveolus with axial projection is developed. A ventro-lateral (dorso-lateral) groove may be formed by the furcation of the lateral lines, but it becomes isolated."

The nature and position of the ventro-lateral grooves is definitive for *Dimitobelus*. Whitehouse followed Tate (1880, p.104) and Etheridge (1902a, p. 45-47) in assigning the strongly developed grooves in *Dimitobelus* and *Cheriobelus* as dorso-lateral in position. This was questioned by Glaessner (1957; 1958) who regarded the dominant grooves in *Dimitobelus* as ventro-lateral in position, a view that has been followed by all subsequent authors and is adopted here.

Woods (1917) interpreted the dominant grooves in the New Zealand species *B. superstes* Hector and *B. lindsayi* Hector (designated by Whitehouse as the type species of *Cheriobelus*) as ventro-lateral. Although the phragmocone is rarely preserved in *Dimitobelus* (or *Cheriobelus*), due to development of a pseudoalveolus, it has been described *in situ* for both *Dimitobelus superstes* and *Dimitobelus lindsayi* by Stevens (1965) where the position of the siphuncle clearly indicates the orientation of the guard and confirms the ventro-lateral position for the dominant pair of grooves.

Whitehouse (1924) placed great taxonomic importance upon the relationships of the grooves to the lateral lines. For *Dimitobelus* he considered that the `dorso-lateral' grooves and the `ventro-lateral' grooves (if developed) connected with the lateral lines. According to Whitehouse, in *Cheriobelus*, lateral lines are lacking and the `dorso-lateral' grooves and rudimentary dorso-lateral grooves, if present, are independent whereas for *Tetrabelus* Whitehouse he considered the lateral lines as derived from the dorso-lateral grooves and the ventro-lateral groove as independent.

Cheriobelus was originally characterised as having a clavate guard, with dorso-lateral grooves that do not continue as lateral lines. However the genus has been placed as a synonym of *Dimitobelus* by several authors (Glaessner, 1957; Stevens, 1965; Doyle, 1987a) because specimens of the type species of both genera (*B. canhami* Tate

and *B. lindsayi* Hector) typically show a confluence of ventro-lateral grooves with the lateral lines.

There has been some confusion in the separation of *Tetrabelus* and *Dimitobelus*. *Tetrabelus* was originally erected by Whitehouse (1924), with the Indian *Belemnites seclusus* Blanford (1861) as the type species, to encompass "clavate (hastate) belemnites provided with dorso-lateral lines, but having, in addition, independent ventro-lateral grooves". The taxon was grouped with, but considered as subgenetically distinct from *Dimitobelus sensu stricto* by Glaessner (1958) and Stevens (1965). However, Doyle (1985) retained it as of full generic status, based on its compressed transverse section and ventrally curving grooves whereas *Dimitobelus* has a depressed section and dorsally curving grooves.

Although Whitehouse (1924) recorded *Tetrabelus* as occurring in Australia, this has proven to be incorrect. The specimen described by Gürich (1901, pl. 29, figs. 2, 3) from White Cliffs, N. S. W. as *Belemnites kleini* and referred to *Tetrabelus* by Whitehouse has a subcircular section and long ventro-lateral grooves and represents *Peratobelus*. The specimen figured by Etheridge (1902b, pl. 9, figs. 3, 4) also referred to as *Tetrabelus* by Whitehouse (1924) has a depressed guard typical of *Dimitobelus*. *Tetrabelus macgregori* Glaessner (1945) originally described from New Guinea and also recorded from New Zealand by Stevens (1965) is considered here as a synonym of *Dimitobelus diptychus*.

Peratobelus Whitehouse is allied to *Dimitobelus* Whitehouse, but distinguished by the presence of long, straight, ventro-lateral grooves. *Dimitobelus* guards are typically more hastate and show lateral lines and a pseudoalveolus, features not shown by *Peratobelus*.

Skwarko (1966) described *Dimitobelus (?) youngensis* from the Mullaman Beds of the Northern Territory but these are now assigned a pre-Albian age (Henderson, 1998a) and this species is probably a synomyn of Aptian *Peratobelus bauhinianus* (Skwarko, 1966, see Section B).

Within Australia, *Dimitobelus* has previously been described only from Albian strata, but the range extends into the Cenomanian. Other ranges of *Dimitobelus* are

noted as Albian – Campanian in Antarctica (Doyle, 1987a), Albian – Maastrichtian in New Zealand (Stevens, 1965), and Albian – Cenomanian? of the New Guinea Papuan Basin, contiguous with Carpenteria Basin (Glaessner, 1945; 1958). Four previously described species of *Dimitobelus* are recognised in this study: *Dimitobelus diptychus* (McCoy, 1867a), *Dimitobelus stimulus* (Whitehouse, 1925), *Dimitobelus liversidgei* (Etheridge, 1892) and *Dimitobelus dayi* (Doyle, 1987a), as well a two new species *Dimitobelus hendersoni* and *Dimitobelus plautus* and two unnamed taxa *Dimitobelus* sp. nov. ? 1 and sp. nov. ? 2.

***Dimitobelus diptychus* McCoy**

Pl. 1, figs. 1-13

Synonymy:

1867a	*Belemnitella diptycha* McCoy, p. 356.
1867b	*Belemnitella diptycha* McCoy, p. 42.
1867c	*Belemnitella diptycha* McCoy, p. 196.
1870	*Belemnites australis* Phillips *in* Moore, p. 258, pl. 16, figs. 3 and 4 only.
1880	*Belemnites canhami* Tate, p. 104, pl. 4, figs. 2a-c.
1889	*Belemnites canhami* Tate; Tate, p. 230.
1892	*Belemnites canhami* Tate; Etheridge *in* Jack and Etheridge, p. 490, pl. 35, figs. 3-5, 7-9, 12-14.
1902a	*Belemnites canhami* Tate; Etheridge, p. 49.
1902a	*Belemnites eremos* Tate; Etheridge, p. 51, pl. 7, figs. 18-21.
1902b	*Belemnites canhami* Tate; Etheridge, p. 45, pl. 8, figs. 8-9; pl. 9, fig. 2.
1902b	*Belemnites* sp.; Etheridge, p. 46, pl. 9, figs. 3-4.
1902	*Belemnites canhami* Tate; Etheridge and Dun, p. 80.
1902	*Belemnites eremos* Tate; Etheridge and Dun, p. 81.
1924	*Dimitobelus canhami* (Tate); Whitehouse, p. 412, figs. 2, 3, 7.
1925	*Dimitobelus canhami* (Tate); Whitehouse, p. 35, pl. 2, figs. 1-7, 9-11.
1957	*Dimitobelus diptychus* (McCoy); Glaessner, p. 88.
1958	*Dimitobelus macgregori* Glaessner, p.219, fig. 5.
1959	*Dimitobelus diptychus* (McCoy); Dorman and Gill, p. 91, pl. 8, figs. 1-2.

1965 *Dimitobelus macgregori* (Glaessner); Stevens, p. 121, 135, pl. 21, figs. 10-12; pl. 24, figs. 1-3.

1965 *Dimitobelus diptychus* (McCoy); Day, p. 419.

1966 *Dimitobelus diptychus* (McCoy); Ludbrook, p. 191, pl. 27, figs. 1-11.

1968 *Dimitobelus diptychus* (McCoy); Hill et al., p. k.7, pl. KII, figs. 14 a-c.

1969 *Dimitobelus diptychus* (McCoy); Day, p. 145, 148.

Types: Lectotype NMV P2177, Allaru Formation (Albian), collected by J. Sutherland and D. Carson from west bank of Flinders River at the base of Walker's Table Mountain, Queensland, 20°56'S, 144°13'E, and described by McCoy (McCoy, 1867a, p.356). This specimen was designated the holotype by Doyle (1987a) but is one of four specimens assigned to this species by McCoy.

Remainder of type series: NMV P2178-80, Base of Walker's Table Mountain, west bank of Flinders River, Allaru Formation, Qld 20°56'S, 144°13'E.

Additional Material: Approximately 260 specimens.

Eromanga Basin, Queensland: SAM P31592, 20 km north of Hughenden, Doncaster Member, 20°38'S, 144°13'E; NMV P 310419-24, 5 miles SE of Roma, Doncaster Member, c.26°36'S, 148°51'E; QGS L1512, Tambo, Doncaster Member, 24°502'S, 146°16'E; QGS L813, south bank of Flinders River at Sussex Rush, 6 miles WNW of Hughenden, Ranmoor Member, 20°48'S, 144°07'E; QGS F1369, Cambridge Downs Run, Flinders River, 7 ml from Richmond Downs Station, Ranmoor Member, 20°35'S, 143°18'E; QGS F1370, Aramac Well at 238 ft, Aramac Town, Coreena Member, 22°59'S, 145°15°'E; QGS F1372, Aramac Well, Coreena Member, 22°58'S, 145°14'E; QM F1307, western Queensland (unlocalised); QM F2105, Tarbrax Station, near Maxwellton, Mackunda Formation, 21°06'S, 142°26'E; QM F1383, F1407, Hughenden, Ranmoor Member, 20°50'S, 144°11'E; QM F2727, F27742, Richmond, Allaru Formation, 20°44'S, 143°08'E; QGS 270, Barcaldine Downs, Mackunda Formation, 23°42'S, 145°33'E; QM F27918, F6152-6157, Winchester Downs, 50 miles SW of Richmond, Mackunda Formation, 21°11'S, 142°37'E; QM F36160, Flinders River at Marathon Homestead, Allaru Formation, 20°49'S, 143°35'E; JCU 11616-11617, Quarry 15 km east of Julia Creek, Toolebuc Formation, 20°38'02''S, 141°54'01''E; JCU L910, Flinders River, east of

Glendower homestead, Ranmoor Member, 20°40'S, 144°32'E; JCU L912, Flinders River, east of Glendower homestead, not in situ, Ranmoor Member, 20°41'S, 144°34'E; JCU F11632 L913, and approximately 30 specimens, Flinders River, east of Glendower homestead, lower Ranmoor Member, 20°42'S, 144°36'E; JCU L914 (approximately 15 specimens), east of Wongalee Station, Ranmoor Member, 20°38'S, 144°29'E; JCU L916 (3 specimens), near Jones Valley Station, not in situ, Ranmoor Member, 20°32'S, 143°58'E; JCU L921 (approximately 15 specimens), Flinders River, east of Glendower, Ranmoor Member, 20°49'S, 144°20'E; AM F10475-6, south central Queensland, locality unknown; AM F10924-F10925, Marion Downs Station, Toolebuc Formation, 23°22'S, 139°39'E; AM F113967-113973, 113975-113987, Dunraven Station, west of Hughenden, Toolebuc Formation, 20°28'S, 143°57'E; AM F7125, near watershed of Baroo and Ward Rivers, Allaru Formation, c. 24°58'S, 146°09'E; AM F87634, Hughenden district, Ranmoor Member, 20°50'S, 144°11'E.

Eromanga Basin, South Australia: SAM T 1311, described by Etheridge (Etheridge, 1902a, pl. 7, fig. 18), as *Belemnites canhami* Tate, SAM T 1312, described by Etheridge (1902a, pl. 7, figs. 19-20), as *Belemnites eremos* Tate, SAM 7011, T1326, T1328, Stuart's Creek, southern end of Lake Eyre, Oodnadatta Formation, 29°42'S, 137°02'E; SAM P36629, Wooldridge Creek (Fossil Creek), Iodnonden Station, N.W. of Oodnadatta, Oodnadatta Formation, 27°15'S, 135°58'E; GSSA M2472, 6 miles northeast of Lagoon Hill, 5 miles southeast of Primrose Hill, Oodnadatta Formation, 28°13.75'S, 136°28'E; GSSA M2473-81, Kurillina run, north side of Neales River, Oodnadatta Formation, 28°02'S, 136°14'E; NMV P310414-18, Lake Eyre, Oodnadatta Formation, 28°14'S, 136°35'E; NMV P5975, near Warrina, South of Oodnadatta, Oodnadatta Formation, 28°11'S, 135°49'E; NMV P2223-9, Woodduck Creek, Peake Station, Central Australia, Oodnadatta Formation, 27°56'S, 136°13'E; NMV P2232, Kuryapundy Swamp, from a well 100ft. deep (locality uncertain); NMV P310426-29, 14 miles SE of Algebuckinna, Oodnadatta Formation, 28°075'S, 135°59'E; NMV P 310449-51, Cootanoorina district, Oodnadatta Formation, 28°00' S, 135°18' E; NMV P310467, Primrose Springs, Peake Station, Oodnadatta Formation, 28°05'S, 135°50'E; NMV P310468, Woodduck Creek, Peake Station, Oodnadatta Formation, 27°56'S, 136°13'E; HM S8430-8477, Woodduck

Creek, northwest of Lake Eyre, South Australia, Oodnadatta Formation, 27°56′S, 136°13′E; AM F87632, S.A./N.S.W. border, locality uncertain.

Laura Basin, Queensland: QGS F9681, L925, tributary of Piccaninny Creek about 1 mile upstream from NE side of road, Coen district (unlocalised); QM F33235, Hahn Tableland, west of Laura, Wolena Claystone, 15°50′S, 144°20′E; JCU 11620-11621, Laura, Tablelands, Far North Queensland 15°56′S, 144°10′E.

Carpentaria Basin, Queensland: SAM P18962, Near Kamileroi, 108 miles north of Cloncurry, Normanton Rd, Allaru Formation, 19°233′S, 139°717′E.

Carnarvon Basin, Western Australia: NMV P310425, 1 mile south of Cardibia Pool, Cardibia Station, Carnarvon, Gearle Siltstone, 23°15′S, 114°07′E; WAM 70.1146a-g, some 6.5 miles east of Murchison House homestead, basal Gearle Siltstone, 27°38′S, 114°20′E; WAM 83.582, Winning Station, hill 2 km south along Vermin fence, south from Bannawong bore, basal Gearle Siltstone, 23°22′S, 114°52′E; WAM 91.808-810, Cardabia Station, marly hill near Cardabia Creek, SE from Point Cloates, basal Gearle Siltstone, 23°34′S, 113°42′E; WAM 91.818-822, Wandagee Station, dam excavation on the plain near the shearing shed, ~ 15 ft. below the surface, basal Gearle Siltstone, 23°45′S, 114°33′E; WAM 91.827-837, Murchison House Station, basal Gearle Siltstone, 27°38′S, 114°14′E; WAM 91.838-845, 91.847, white cliff, ~ 4 miles NW of Murchison House, basal Gearle Siltstone, 27°36′S, 114°12′E; WAM 97.705, Alinga Point, Alinga Formation, 27°37′S, 114°10′E; WAM 97.721, 1.2 km south of Giralia No. 1, upper Gearle Siltstone, 23°00′S, 114°10′E; UWA CS-MM (approximately 20 specimens), Cardibia Station, Mia Mia, basal Gearle Siltstone ,114°20′E, 23°22′S; UWA TP-PP (approximately 10 specimens), Thiridine Point, Pillawarra Plateau, upper Gearle Siltstone, 27°36′S, 114°13′E; UWA 2/11/99-15 (approximately 15 specimens), Hill Springs Station, Whitby dam, basal Gearle Siltstone, 24°23′S, 115°01′E; UWA 2/11/99-16-1 to 3 and approximately 10 unnumbered specimens, upper Gearle Siltstone, Cenomanian, MacDonald Dam, 24°10′S, 114°29′E; UWA 23/3/93 (approximately 13 specimens), Alinga Point, Alinga Formation, 27°35′S, 114°11′E; GSWA Barrabiddy 1, see Appendix A. 1, Gearle Siltstone, 23°49′57″S, 114°20′E; GSWA Boologooro 1, see Appendix A. 2, Gearle Siltstone, 24°19′27.3″S, 113°53.3″E; GSWA Edaggee 1, see Appendix A. 3, Gearle Siltstone, 25°21′27.0″S, 114°14′04.9″E.

Diagnosis: Medium to large, elongated, robust guards. Outline symmetrical, hastate; profile asymmetrical, cylindroconical. Transverse sections depressed elliptical in stem region. Deeply incised, well-developed ventro-lateral grooves are inscribed on the anterior part of the guard; they extend along one third of rostrum, curving slightly dorsally in anterior portion of stem region. Lateral lines well developed and dorsally placed. Alveolar region narrow, apical region obtuse. The apical line is arched, tracing a gentle ventrally concave curve.

Dimensions (mm):

	L	**X**	**Dv_{max}**	**Dl_{max}**
UWA TP-PP-2	11.4	2.5	1.7	2.8
UWA 2/11/99-16-12	14.0	6.8	2.7	3.3
UWA 2/11/99-16-7	14.6	6.8	2.6	3.2
UWA 2/11/99-16-11	15.3	6.7	2.8	3.1
UWA 2/11/99-16-10	16.2	6.0	2.6	3.5
UWA 2/11/99-16-8	16.8	9.0	3.2	4.3
UWA 2/11/99-16-9	16.9	6.0	3.1	3.8
UWA TP-PP-3	17.8	7.4	3.1	4.3
UWA TP-PP-1	19.0	5.7	4.9	6.9
UWA TP-PP-4	28.4	11.6	5.5	7.9
NMV P310468 2	41.1	19.9	4.9	6.4
HM S5583	46.9	25.9	6.8	9.5
HM S5584	47.7	20.9	6.2	8.5
NMV P310467 2	50.2	19.9	6.4	8.8
JCU 11617	52.8	23.2	9.9	11.2
HM S5582	52.9	23.7	7.1	14.0
UWA 2/11/99-15-7	53.0	23.6	10.5	13.0
HM S5581	54.5	32.2	8.1	11.6
SAM T1324 B	54.8	24.2	6.8	9.4
UWA 2/11/99-15-8	55.1	21.0	12.1	14.4
UWA 23/3/93-1	55.2	23.0	12.6	15.0
UWA 23/3/93-2	54.9	18.8	12.4	15.8
NMV P310414	60.7	25.5	6.9	8.5
NMV P310467 1	64.1	24.9	8.0	11.8
SAM T1324 A	65.4	27.3	9.5	13
NMV P310416	65.8	28.9	~	~
NMV P310467 3	73.6	28.9	~	~
SAM T1311	74.3	35.0	9.3	13.2
JCU 11621	81.0	43.1	15.5	20.6
SAM T1312	81.6	39.3	~	~
QM F36160	83.2	40.3	11.1	17.1
JCU 11620	83.8	43.5	17.2	21.7
NMV P310468 1	90.7	42.9	13.2	19.9
NMV P2177	93.0	47.8	13.2	18.8
SAM T1324	100.2	48.8	16.1	24.9
NMV P310443	102.1	48.9	15.2	23.8

Description: Medium to large *Dimitobelus*; with a weakly hastate outline, and the guard length more than five times the diameter. Apical region obtuse, tapering to a distinct point; apex mucronate. Alveolar region narrow in comparison; the stem extends from the position of the protoconch to the point of maximum inflation (Figure A. 3. 2). Profile asymmetrical and cylindroconical, with the ventral surface commonly flattened and slightly arched, especially towards the apex. Dorsal surface is flat and broad. Lateral surfaces are gently convex. Transverse section is semi-elliptical in stem and apical regions but almost equi-dimensional in the alveolar region (Figures A. 4. 1 to A. 4. 4). Two deeply incised ventro-lateral grooves in alveolar region extend onto the anterior part of the stem. They are straight in alveolar region, then deflected dorsally in stem region. Dorso-lateral grooves faintly impressed, and gently curved to almost straight. On mid-stem region, in line with the termination of the phragmocone, the ventro-lateral and the dorso-lateral grooves converge. Paired lateral lines variably impressed, strongly marked on some guards, obscure on others. They are positioned just dorsal of mid-flank, almost straight, and extend across the stem region almost to the apex. The phragmocone is central to slightly dorsal in position, with a small bulbous protoconch, and penetrates a third to a quarter the length of the guard. A pseudo-alveolus and apical canal are commonly developed. The apical line is in general ventrally offset and gently arched towards the ventral surface, most noticeably in the apical region.

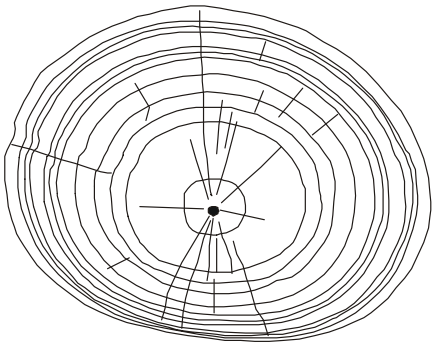

Figure A. 4. 1 *Dimitobelus diptychus* (McCoy). JCU F11632 L913, Flinders River east of Glendower homestead, Ranmoor Member, northern Eromanga Basin. Transverse section at axis of maximum inflation, with growth lines that show faint and variable records of the lateral lines. Section is elliptical with apical line ventrally placed. Growth lines crowded on the ventral surface which is flattened. Magnification: x 2.75.

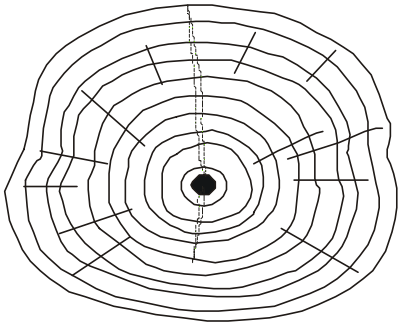

Figure A. 4. 2 *Dimitobelus diptychus* (McCoy). WAM 91.839, Murchison House Station, basal Gearle Siltstone, Carnarvon Basin. Transverse section at axis of maximum inflation, showing clearly inscribed lateral lines. Section is elliptical and slightly flattened on the ventral surface. Magnification: x 3.5.

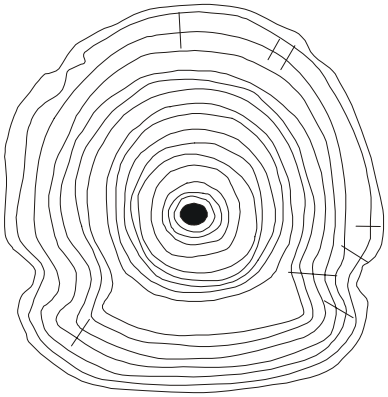

Figure A. 4. 3 *Dimitobelus diptychus* McCoy. UWA 23/3/93-L1, Alinga Point, lower Alinga Formation, Carnarvon Basin. Transverse section of most anterior stem region (or most posterior alveolar region) showing weakly inscribed dorso-lateral grooves as well as ventro-lateral grooves. Apical canal is centrally placed. Magnification: x

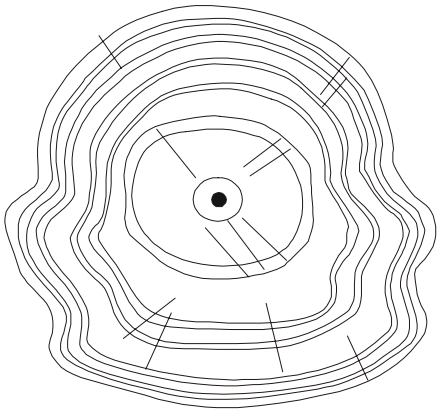

Figure A. 4. 4. *Dimitobelus diptychus* McCoy. UWA 23/3/93-L2, Lower Alinga Formation, Alinga Point, Carnarvon Basin. Transverse section of most anterior stem region (or most posterior alveolar region) showing pronounced dorso- and ventro-lateral grooves. Apical canal is centrally placed.

Remarks: *D. diptychus* McCoy (1867a) was originally placed in *Belemnitella* because its paired grooves were mistakenly considered as dorso-lateral in position, as characteristic of this northern hemisphere genus. Following description by Tate (1880) of *B. canhami*, this species was designated the type species of *Dimitobelus* by Whitehouse (1924) but is now is regarded as a synonym of *D. diptychus*. The lectotype of *D. canhami* (NMV P2177) was first figured by Dorman and Gill (1959, pl. 8, figs. 1, 2) and is refigured here (pl. 1, fig. 11). In guard shape and disposition of the ventro-lateral grooves and dorso-lateral lines, this specimen is indistinguishable from *D.*

diptychus. Similarly, the specimen figured by Phillips (Phillips, 1870, pl. 16, figs. 3, 4) as *B. australis* is indistinguishable from, and synonymous with, *D. diptychus*.

Some intraspecific variation is apparent within *Dimitobelus diptychus*. The stem ranges in cross-sectional shape from elliptical to sub-circular (Figure A. 4. 5). Tapering of the stem towards the alveolar region is also is variable within the species with some specimens noticeably more hastate than others. The axial line is always ventrally curved (cyrtolineate) but the degree of curvature is variable. There is marked variation in the depth to which ventro-lateral grooves are incised, but their length is consistent within the species. This may be an artefact of preservation caused by post mortem degradation of the guard surface through abrasion, or by solution during exposure, diagenesis or during passage through the alimentary tract of a predator. Taper of the apical region is acute, generally subtending an angle of about 30°, but the range is from 18° to 40°. Intraspecific variation is also apparent between specimen suites from eastern and western basins. The dorso-lateral grooves are much more deeply inscribed in the Western Australian specimens of *D. diptychus* than in their eastern counterparts. Samples from Western Australia tend to be broader in outline in the comparison with eastern specimens, which are somewhat wider in profile view relative to the outline (Figure A. 4. 5).

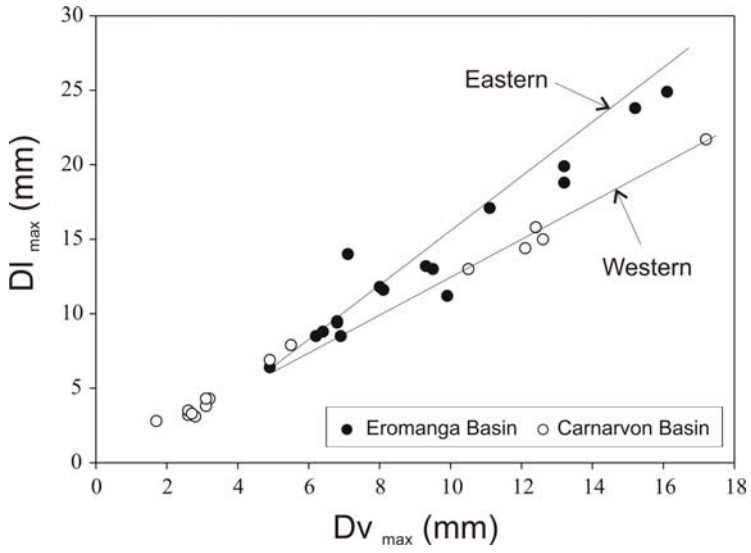

Figure A. 4. 5 Cross-sectional measurements for *Dimitobelus diptychus*. Variation in the degree of depression separates the eastern and western specimen suites at maturity.

JCU 11620 (pl. 2, fig. 12) from the Albian Wolena Claystone of the Laura Basin is a pathological specimen with the robust profile, outline and transverse section and deeply incised, well-developed ventro-lateral grooves diagnostic of *D. diptychus*. However, it has an unusually inflated posterior stem region, an unusually depressed anterior sector and a bent, acute apex. Dl_{max}:Dv_{max} is 1.3 for this specimen, within the range established for *D. diptychus* as is the apical angle (18°).

D. diptychus also exhibits distinct ontogenetic variation. Juveniles show a weaker cyrtolineate apical line in comparison to more mature specimens. The immature forms are commonly more cylindrical, with flattening of the dorsal and ventral surfaces less apparent. The ventro-lateral and lateral lines become more deeply incised mid-way through ontogeny, presumably due to an increase in bulk muscular tissue attaching to the guard. The cross-section in early growth is rounded but is progressively transformed by the addition of growth laminae that are variable in thickness into a cross-section that is more sub-quadrate (see Figures A. 4. 3 and A. 4. 4). Guards also become more tapered towards the alveolar region as growth proceeds. Slender, juvenile specimens of *D. diptychus* somewhat resemble *D. stimulus* but are distinguishable by a more robust, and more clearly hastate, morphology. A more substantial juvenile specimen suite is available from collections from the Carnarvon Basin, largely from the lower Gearle Siltstone, than from eastern Australia. Comparable juvenile growth stages are represented in collections from the Ranmoor Member of the northern Eromanga Basin.

Discussion: *D. diptychus* has been compared to *D. supertes* (Hector) from New Zealand by Whitehouse (1925) and to *D. macgregori* (Glaessner) from New Guinea by Doyle (1985). Stevens (1965) considered *D. superstes* as distinct, being discriminated by more prominent ventro-lateral grooves, a more cylindrical shape, with less clearly marked lateral lines. In New Zealand, *D. superstes* ranges from Motuan to Mangaotanean (middle Albian to Coniacian-Santonian).

Glaessner (1958) described *D. macgregori* from Albian strata of New Guinea, and based separation of this species from *D. diptychus* (McCoy) on the less clavate shape of the guard, with less severe flattening of the dorso-lateral surface. He measured Dl_{max}:Dv_{max} as 1.3 (range 1.2 - 1.4) indicating a slightly less depressed shape

than typical of *D. diptychus* where this ratio has an average of 1.4, (range 1.3 to 1.5). However, the cross-sectional shape of Glaessner's species fits into the range of variation shown by *D. diptychus.* The less clavate shape attributed to *D. macgregori* relates to the large size of the type specimen with *D. diptychus* becoming more hastate when mature. As a consequence of these observations, *D. macgregori* is also regarded here as a synonym of *D. diptychus.* The established range of the species in New Guinea (upper Albian to Cenomanian) overlaps with that known from Australian (Albian to Cenomanian).

Skwarko (1966) described *D. diptychus* from the Albian of Northern Territory but, as noted by Doyle (1987b), the material is poorly preserved rendering specific assignment questionable.

Dimitobelus stimulus (Whitehouse) closely resembles *D. diptychus* but is more slender, less hastate and is weakly depressed (Dl_{max}:Dv_{max} 1.1 for *D. stimulus* compared to *D. diptychus* Dl_{max}:Dv_{max} 1.4). *D. diptychus* differs from *D. liversidgei* primarily in adult size and in the nature of its apical region. Its apex is obtuse and eccentric whereas that of *D. liversidgei* is acute and almost central in position. Day (1968) noted that in Queensland these two species appear to be stratigraphically separated, with *D. diptychus* occurring in the pre-Toolebuc units (Ranmoor and Coreena Members of the Wallumbilla Formation) and *D. liversidgei* in the Toolebuc, Allaru and Mackunda Formations. However, both species are recorded here as having the same range confirming the observation of Whitehouse (1925) and Ludbrook (1966) who noted the two species as occurring together in South Australia strata.

Distribution and Age: The type series of *D. diptychus* described by McCoy (1867a) was collected from the lower Allaru Formation exposed at the base of Walker's Table Mountain near Hughenden Queensland. The species is widely distributed in the northern Eromanga Basin where it ranges through the upper, Ranmoor Member, of the Wallumbilla Formation, and the Toolebuc, Allaru and Mackunda Formations, spanning the Albian Stage (see Section C). Within the Hughenden district, the species is especially prolific within the Ranmoor Member.

The species is represented in the Allaru Formation of the Carpentaria Basin and the Wolena Claystone of the Laura Basin, both units of Albian age. Within the

southern Eromanga Basin, *D. diptychus* is prolific in the Albian Oodnadatta Formation, with collections from this unit known from Woodduck Creek, Primrose Springs, Wooldridge Creek, Algebuckinna and the Oodnadatta district. Ludbrook (1966) identified specimens from the Albian Oodnadatta Formation from the north bank of the River Neales as *D. diptychus*, which occurs in association with prolific *D. stimulus*. Other specimens are from Stuart's Creek, Lake Eyre district, as figured by Etheridge (1892a, pl. 7, figs. 18, 19, 21).

D. diptychus is well represented in the Carnarvon Basin where it ranges from early Albian to Cenomanian. It is represented in the early Albian lower Gearle Siltstone by collections from Murchison House, Wandagee, Cardabia, Winning, Giralia and Hills Springs Stations. Recently drilled stratigraphic core holes intersecting this unit contain a prolific record of *D. diptychus*. The best record is from Boologooro 1 where the species is represented through ~65 m of section representing the entire lower Gearle Siltstone but the species is also common in core of this unit from Barrabiddy 1 and Edaggee 1. There are also records for the Albian Alinga Formation, from Alinga Point and from south of Giralia Bore No. 1 (see McWhae et al., 1958).

D. diptychus is also characteristic of the upper Gearle Siltstone of Cenomanian age, with collections from Thiridine Point, Pillawarra Plateau and from core intersections from Edaggee 1 and Boologooro 1. Occurrences from Cenomanian strata of the Carnarvon Basin have been noted by Stevens (1965) and Pirrie et. al. (1995). *D. diptychus* has not been documented from Cenomanian strata of eastern Australia because marine sequence of this age is not represented.

Reports by Etheridge (1902a; 1902b) of *D. diptychus* occurring in the White Cliffs opal fields in New South Wales is anomalous. Whitehouse (Whitehouse, 1926, p. 277) and others (David, 1950, p. 486; Vallance and Packham, 1959, p. 162) tentatively assigned the White Cliffs strata as Aptian. Specimens held by the Australian Museum from this locality are undoubtedly *Peratobelus*, consistent with this age assignment.

***Dimitobelus stimulus* Whitehouse**

Pl. 2, figs. 3-7

Synonymy:

1925 *Dimitobelus stimulus* Whitehouse; Whitehouse, p. 35, pl. 2, figs. 8, 12-17.

1925 *Dimitobelus stimulus* var. *extremus* Whitehouse, p. 35, pl. 2, figs. 18-20.

1965 *Dimitobelus stimulus* Whitehouse; Stevens, p. 121.

1966 *Dimitobelus stimulus* Whitehouse; Ludbrook, p. 192, pl. 27, figs. 12-21.

1966 *Dimitobelus stimulus* var. *extremus* Whitehouse; Ludbrook, p. 192.

1987 *Dimitobelus stimulus* Whitehouse; Doyle p. 163-166, pl. 22, figs. 11-15.

1987 *Dimitobelus stimulus* var. *extremus* Whitehouse; Doyle p. 166, pl. 22, fig. 16, pl. 23, figs. 1 and 2.

2001 *Dimitobelus (Dimitobelus) stimulus* Whitehouse; Stilwell and Crampton, p. 391-394, figs. 2a-c.

Type: Holotype: HM S5594, Kurillina run 4, south bank of Kurillina Creek, Oodnadatta Formation (Albian), Woodduck Creek district, South Australia 27°57.5'S, 136°11.5'E as described and figured by Whitehouse (1925).

Remainder of type series: HM S5590-5593 and HM S5595-97, 6 miles northeast of Lagoon Hill, 5 miles southeast of Primrose Hill, Oodnadatta Formation (Upper Albian), South Australia 28°13.75'S, 136°28'E.

Additional Material: Approximately 65 specimens.

Eromanga Basin, Queensland: QGS 270A.1, Barcaldine Downs Station, Mackunda Formation, 23°42'S, 145°33'; QSQ F1372, figured by Etheridge 1892, pl. 35, fig. 18, Allaru Formation, Aramac district, c. 22°55', 145°13'; UQ F16922, Currane Station, 9 miles north of Dartmouth, Allaru Formation, 23°24'S, 144°45'E; QM F6152-6157, Winchester Downs Station, 50 miles SW of Richmond, Mackunda Formation, 21°11'S, 142°37'E; JCU F11633 L910, and approximately 20 unnumbered specimens, Flinders River east of Glendower homestead, Ranmoor Member, 20°40'S, 144°32'E; JCU F11634 L914 and approximately 10 unnumbered specimens, east of Wongalee Station, Ranmoor Member, 20°38'S, 144°29'E; AM F87634, Hughenden district, Ranmoor Member, 20°50'S, 144°11'E; AM F7125, watershed of the Barcoo and Ward rivers,

Allaru Formation, c. 24°58′S, 146°09′E; AM F113974, F113988 & 113989 Dunraven, Hughenden district, Toolebuc Formation, 20°28′S, 143°57′E; NMV P2231, Kuryapundy Swamp, Central Australia (from a well 100ft. deep), (unlocalised).

Eromanga Basin, South Australia: NMV P310411-13, Lake Eyre, Oodnadatta Formation, 28°14'S, 136°35'E; NMV P310446-8, Dalhousie Station, Oodnadatta district, Oodnadatta Formation, 26°27'S, 135°31'E; NMV P310430-442, cliff banks of Neales River, 14 miles SE of Algebuckinna, Oodnadatta Formation, 28°075'S, 135°59'E; NMV P310452-58, Woodduck Creek, Peake Station, Oodnadatta Formation, 27°58'S, 136°125'E; GSSA M2481-95, Kurillina run, north side of Neales River, Oodnadatta Formation, 28°02′S, 136°14′E; HM S8478-S8536, Woodduck Creek, Oodnadatta Formation, 27°56'S, 136°13'E.

Laura Basin, Queensland: QM F33230, F33237, F33240, Hann Tableland, south of Laura, Wolena Claystone, 16°54'S, 145°14'E; JCU 11622, tablelands north of Laura, Wolena Claystone, 15.6°S, 144°10'E; JCU 11619, tableland north of Laura, Wolena Claystone, 15°56′S, 144°10′E.

Carpentaria Basin, Queensland: UQ L679, Little Bynoe Crossing, Little Bynoe River, Normanton Formation, 17°54′S, 140°51′E.

Carnarvon Basin, Western Australia: WAM 01.92, Barrow Island, Mardie Greensands Member, 20°47'S, 115°24'E; WAM 91.823-6, Wandagee Station, ~ 15 ft. below the surface, Gearle Siltstone 23°45'S, 114°33'; UWA CS-MM (approximately 20 specimens), Cardibia Station, Mia Mia, basal Gearle Siltstone, 114°20′E, 23°22′S; UWA 2/11/99-15 (approximately 25 samples), Hill Springs Station, Whitby Dam, Kennedy Range, basal Gearle Siltstone, 24°09'S, 114°26'E; GSWA Barrabiddy 1, see Appendix A. 1, basal Gearle Siltstone, 23°49′57″S, 114°20′E; GSWA Boologooro 1, see Appendix A. 2, Gearle Siltstone, 24°19′27.3″S, 113°53.3″E; GSWA Edaggee 1, see Appendix A. 3, Gearle Siltstone, 25°21′27″S, 114°14′04.9″E; GSWA Yinni 1, see Appendix A. 4, basal Gearle Siltstone, 26°03′22.8″S, 114°48′58.5″E.

Other: SAM P3016, Northern Territory (unlocalised).

Diagnosis: Medium sized, slender, subhastate to subcylindrical *Dimitobelus*. Outline symmetrical and subhastate, as is profile. Apex acute. Transverse sections are

elliptical and slightly depressed. Lateral lines paired and well developed, straight and centrally placed, but posteriorly may converge to a single structure and become deflected dorsally in the apical region. Pseudoalveolus and axial projection are common in this species.

Dimensions (mm):

	L	**X**	**Dvmax**	**Dlmax**
UWA CS-MM-1	34.3	12.2	5.1	5.7
UWA CS-MM-2	37.4	19.6	6.9	7.1
UWA 2/11/99-4	43.0	21.0	7.0	8.0
NMV P310456	43.0	21.0	6.5	8.0
UWA 2/11/99-1	43.5	20.0	6.0	8.0
HM S5594	46.7	21.5	5.6	4.7
UWA 2/11/99-5	47.0	16.0	7.0	8.0
HM S5593	48.3	23.1	6.9	5.7
NMV P310455	49.0	16.0	6.8	8.0
HM S5592	49.2	21.4	5.8	6.8
UWA 2/11/99-2	50.0	27.0	8.3	10.0
HM S5591	50.4	17.7	6.5	7.8
NMV P310412	51.0	29.5	6.0	7.0
NMV P310411	52.0	29.0	6.3	7.5
NMV P310453	53.0	24.5	6.0	7.5
NMV P310454	53.0	28.0	5.8	6.0
GSSA M2488	55.2	28.8	6.9	8.0
JCU 11622	57.5	28.3	10.0	12.0
GSSA M2485	59.0	32.0	9.0	10.2
UWA 2/11/99-3	59.5	30.0	11.0	13.0
GSSA M2484	60.3	27.0	7.5	9.0
HM S5590	66.6	28.8	8.2	9.8
HM S5589	71.9	29.4	~	9.4

Description: Medium sized, subhastate to subcylindrical, slender guards with the length ranging to 80 mm and more than five times the diameter. Outline symmetrical and subhastate; maximum point of inflation at mid-length of the guard, or displaced slightly towards the apical region. Profile is subhastate and symmetrical with the dorsal and ventral surfaces slightly flattened. Transverse section weakly depressed (Dl_{max}:Dv_{max} 1.1; Figures A. 4. 6 and A. 4. 7), becoming more flattened towards the alveolar region. In alveolar region, the ventro-lateral grooves curve dorsally to join with straight, well-developed and centrally placed lateral lines. Lateral lines are paired, some 1mm apart and extend for the entire length of the guard. Dorso-lateral grooves commonly developed on the alveolar region and straight. The phragmocone is commonly not well preserved due to development of a pseudoalveolus. The apical

line is curved slightly ventrally with the development of an apical canal common in this species.

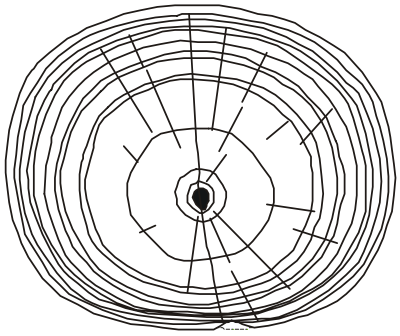

Figure A. 4. 6 *Dimitobelus stimulus* Whitehouse. JCU F11633 L910, Ranmoor Member, Eromanga Basin. Cross section through the point of maximum inflation, at the boundary between the stem and apical regions; weakly depressed. Magnification: x 3.6.

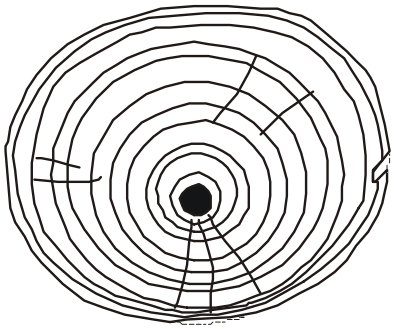

Figure A. 4. 7 *Dimitobelus stimulus* Whitehouse. JCU F11634 L914, Lower Ranmoor Member, Eromanga Basin. Juvenile specimen sectioned in the anterior stem region, showing a large apical canal. Magnification: x 4.5

Discussion: *Dimitobelus stimulus* was established by Whitehouse (1925), for slender guards, with a depressed cross-section. Whitehouse noted that the lateral lines appeared straight and centrally placed, giving rise anteriorly to either a single groove or pair of diverging grooves.

Specimens figured by Whitehouse (1925) were lodged in the Hunterian Museum (HM S5595-5597) along with four other guard fragments (HM S8433-8436). It may be presumed that this collection represents the type series for the species. However, re-examination of specimens HM S8433-8436 shows them to be *D. diptychus* due to their characteristically flattened rostra and the distinctively placed, off-centre lateral lines.

Dimitobelus stimulus is similar to *D. diptychus* such that both species generally develop diverging dorso-lateral and ventro-lateral grooves. Whitehouse (1925) considered *D. stimulus* as distinctive in its less clavate shape and in the lateral lines which are straight and central. The profile of *D. stimulus* is more subhastate than that

of *D. diptychus* and transverse sections are less depressed (Dl_{max}:Dv_{max} ~1.1 compared to ~1.4). *D. stimulus* resembles juveniles of *D. diptychus*, but can be easily distinguished by the subhastate profile, and near perfectly elliptical transverse section. Most other species of *Dimitobelus* are more flattened (semi-elliptical) and hastate than *D. stimulus*.

D. liversidgei Etheridge Jnr (1892) was previously included as a synonym of *D. stimulus* by Day (1968) as both have slender guards with acute, almost central apices. However, *D. liversidgei* is distinguished by its long, acutely pointed apical region, distinctly clavate outline, more depressed cross-section (Dl_{max}:Dv_{max} ~1.3) and weaker development of ventro-lateral grooves.

Variation in shape has been noted for *D. stimulus*. Whitehouse (1925) proposed the varietal name *D. extremis* for longer, more cylindrical and more gently tapering forms which retained the straight and strictly central lateral lines characteristic of *D. stimulus sensu stricto*. However, Ludbrook (1966) re-examined the type series (HM S5595-S5597) of this form but could not discriminate it from the *D. stimulus* s. s.. *D. stimulus* var. *extremis* represents extreme morphs of this taxon where guards are particularly long and slender but there is no break in the range of variation linking to *D. stimulus s.s.*. Slender guards described by Doyle (1987a) from the Albian Kotick Point Formation of the Antarctic Peninsula and assigned as *D. stimulus* var. *extremus* are closely comparable to Whitehouse's lectotype. The specimen from Alexander Island, West Antarctica, described by Willey (1972) as *D. macgregori* was reassigned by Doyle (1987a) to *D. stimulus*. However, it is poorly preserved and its identity is uncertain.

Distribution and Age: The type series described by Whitehouse (1925) was collected from the Oodnadatta Formation from Woodduck Creek in the southern sector of the Eromanga Basin, South Australian. Other collections from this formation are from the Lake Eyre district, Neales River Algebuckinna district and Dalhousie Station. An Albian age was assigned to this unit (Ludbrook, 1966).

D. stimulus is also represented in the northern Eromanga Basin, mostly by collections from the Ranmoor Member of the Wallumbilla Formation (early to mid Albian) exposed along the Flinders River east of Hughenden but also the late Albian

Mackunda Formation. In the Laura Basin *D. stimulus* is present in early Albian Wolena Claystone.

The species is prolific in the basal Gearle Siltstone (Albian) of the Carnarvon Basin exposed on Hills Springs, Wandagee and Cardibia Stations. A single specimen is recorded from the upper Aptian Mardie Greensand at Barrow Island Western Australia but was not collected in situ and its provenance is suspect. *D. stimulus* is present in all four cored stratigraphic wells from the Carnarvon Basin where it occurs throughout the lower Gearle Siltstone.

D. stimulus Whitehouse ranges through the Albian; it commonly occurs with *D. diptychus* (McCoy) and *D. dayi* (Doyle) in the Great Artesian and Carnarvon basins.

***Dimitobelus liversidgei* Etheridge**

Pl. 2, figs. 1-2

Synonymy:

1892	*Belemnites? Liversidgei* Etheridge , p. 491, pl. 35, figs. 17, 20.
1902a	*Belemnites? Liversidgei* Etheridge; Etheridge, p. 48.
1902b	*Belemnites? liversidgei* Etheridge; Etheridge, p. 81.
1968	*Dimitobelus? liversidgei*; Etheridge; Hill et. al., p. k.7, pl. KII, fig. 17.

Types: Lectotype (designated here): QGS F1371, figured by Etheridge 1892, pl. 35, fig. 17, Allaru Formation, Rockwood Station, Aramac district.

Remainder of the type series: QGS F5631, figured by Etheridge 1892, pl. 35, fig. 20, F5629, F5630 and eighteen unnumbered specimens, within the same rock slab as the lectotype.

Additional material: Approximately 30 guards.

NMV P310444-5, Kingston Station, near Longreach, Allaru Formation, 144°13'E, 23°24'S; JCU F11624-F11630 L924, Daunton South Station, Ilfacombe, upper Allaru Formation, Eromanga Basin, Queensland, 144°49'59"E, 23°17'18"S; JCU F11631, L925 and 15 unnumbered specimens, Glenferrie Station, upper Allaru Formation, Eromanga Basin, Queensland, 144°45'21.5"E, 23°30'21.5"S.

Diagnosis: Diminutive, slender, hastate, weakly depressed guards with an acute, sharply pointed apex and an elongate and a highly attenuated anterior segment which tapers almost to a point. Grooves and lines not evident.

Dimensions (mm):

	L	**X**	**Dvmax**	**Dlmax**
JCU F11630	11.2	3.0	-	1.1
JCU F11624	13.1	3.2	-	1.1
NMV P310445	13.2	4.0	2.2	-
JCU F11628	14.7	2.5	1.7	-
NMV P310444	15.6	6.2	2.5	-
JCU F11629	16.9	4.3	2.2	-
JCU F11625	18.3	4.0	1.9	-
JCUF11626	18.8	5.0	1.9	
QGS F5629	24.0	14.9	~	2.8
JCU F11627	26.3	8.0	2.9	-

Description: Guard small, less than 40 mm long, hastate in shape with an elongate, strongly attenuated anterior segment which tapers to a termination that is less than 1 mm across. The point of maximum diameter is positioned adapically at about one third of the guard length. Alveolus not developed. Dv_{max} is approximately 8 to 10 times length of the guard, depending on the preservation of the delicate anterior extension. Outline and profile are symmetrical with the point of maximum diameter in apical third of guard. Apex is acute (~20°) and tapers to a point. Transverse section oval and slightly depressed. Axial line generally central but excentric near the apex and offset presumably towards the ventral surface. Ventro-lateral grooves and lateral lines are unknown for this species.

Discussion: The type series described by Etheridge (1892) was figured by Hill et al. (1968, pl. KII, fig. 17) and is re-illustrated here (pl. 2, fig. 3) consists of over 20 current aligned specimens partially exposed on a small slab of fine sandstone. Two of these specimens were individually illustrated as hand drawings, out of context, by Etheridge (1892) but can be recognised within the slab. One of the original illustrations (pl. 35, fig. 20) is an incomplete specimen with only the apex retained and is now numbered QGS F5631. The original of his plate 35, figure 17 can be recognised because it is translucent and shows the axial line as he noted in his figure caption and is the only specimen of the group with this attribute and resembling the illustration. It is now numbered QGS F5630 and is designated here as the lectotype. This specimen is

a substantially complete guard but the distinctive anterior portion is missing. Such is generally the case for the type series but some of the unnumbered specimens show a part of the guard anterior confirming that it is tapered and narrow. The specimen referred to *D. liversidgei* by Etheridge in his plate 35, figure 19 is not in evidence and its status is uncertain.

All of the specimens available are embedded in rock matrix which supports their delicate form especially the attenuated anterior portion. All specimens are slender with an attenuated, sharply pointed apex where preserved but within the type series some specimens are more slender than others. Most have been abraded on their exposed surfaces but some are sufficiently intact to show that surface lines and grooves are not developed. Measurements of both cross-sectional diameters can rarely be obtained but partial sections revealed by several specimens show that the cross-section is oval and weakly depressed (Dl_{max}:Dv_{max} ~1.1 – 1.2). Some specimens have preserved the anterior termination, in general only a fraction of a millimetre across, which shows only the presence the axial line which can be seen through translucent shell. An alveolus is not developed.

Guards of this species somewhat resemble those of juvenile *D. diptychus* in shape, being pinched in the posterior alveolar region, and with the maximum point of inflation located towards the apex. *D. liversidgei* is set apart from other Albian *Dimitobelus* by its small size, slender form, its very distinctively tapered and attenuated anterior segment of the guard, and absence of lateral grooves and lines.

Distribution and Age: D*imitobelus liversidgei* is known only from the Allaru Formation of the Aramac and Longreach – Ilfracombe districts and is of late Albian age.

***Dimitobelus dayi* Doyle**

Pl. 2, figs. 9-11

Synonymy:

1987a *Dimitobelus dayi* Doyle, p. 169, pl. 23, figs. 8-10.

Types: Holotype: BMNH C35019, Hughenden district, north Queensland, unlocalised. Remainder of type series: BMNH C 35000, 35002, 35010, Hughenden district, unlocalised.

Additional Material: Approximately 55 specimens.

Eromanga Basin, Queensland: NMV P31592, 20 km north of Hughenden, Ranmoor Member, 20°38′S, 144°14′E; QM F6149–6151, Mountain View Station, Hughenden, Ranmoor Member, 20°47'S, 144°19′E; JCU F116635 L910/3 and approximately 10 unnumbered specimens, Flinders River, east of Glendower homestead, Ranmoor Member, 20°40'S, 144°32′E; L912, Flinders River, east of Glendower homestead, not in situ, Ranmoor Member, 20°41'S, 144°34′E; L914, east of Wongalee Station, Ranmoor Member, 20°38′S, 144°29′E; L921, Flinders River, east of Glendower homestead, Ranmoor Member, 20°49′S, 144°20′E; AM F17715-17717, Prairie district, unlocalised.

Laura Basin, Queensland: JCU 11623, tableland north of Laura, Wolena Claystone, 15°56′S, 144°10′E.

Carnarvon Basin, Western Australia: UWA 2/11/99-15 (6 specimens), Whitby Dam, Kennedy Range, near Hills Springs Station, basal Gearle Siltstone, 24°23'S, 115°01'E; WAM 91.846, white cliffs, NW of Murchison House, basal Gearle Siltstone, 27°36′S, 114°12′E; UWA CS-MM (10 specimens), Cardibia Station, Mia Mia, basal Gearle Siltstone, 114°20′E, 23°22′S.

Diagnosis: Medium sized, tumid *Dimitobelus*. Outline is symmetrical and hastate, as is profile. Transverse sections depressed elliptical to sub-circular. Axis of maximum diameter located close to apex which is abbreviated and rounded. Paired lateral lines prominent.

Dimensions (mm):

	L	**X**	**Dvmax**	**Dlmax**
UWA 2/11/99-15-5	43.2	14.7	9.5	12.1
UWA 2/11/99-15-6	46.0	22.8	10.6	12.2
UWA 2/11/99-15-3	47.2	20.9	10.4	11.3
QM F6149	52.4	20.0	15.0	16.9
UWA 2/11/99-15-4	56.0	27.0	11.8	13.9
UWA 2/11/99-15-2	56.2	22.7	11.3	14.9
UWA 2/11/99-15-1	57.1	18.7	15.1	17.8
QM F6151	58.0	25.2	16.1	19.8
QM F6150	60.5	23.6	14.7	16.2
JCU 11623	66.2	27.0	15.5	17.7

Description: Guard medium sized, robust, with a hastate outline. Profile is sub-symmetrical and hastate with the ventral and dorsal surfaces gently arched. Guard length approximately five times the maximum diameter. Point of maximum inflation occurs in posterior portion of guard. Apex is obtuse, rounded, rarely terminating in a sharp point. Transverse sections are semi-elliptical and depressed (Dl_{max}:Dv_{max} 1.2) and the ventral surface may show some flattening (Figures A. 4. 8 and A. 4. 9). Apical canal positioned ventrally and commonly well developed. Apical line curved, convex towards the ventral surface, typically excavated as a canal. Pseudoalveolus generally developed. Ventro-lateral grooves variably developed, commonly obscure; they are deflected dorsally converging on the lateral line on some specimens, including the holotype. The lateral lines are deeply incised, centrally placed, and continuous from the alveolar to the apical region.

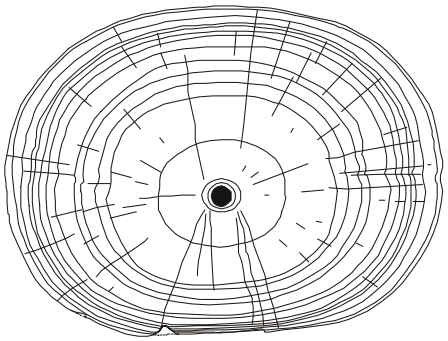

Figure A. 4. 8 *Dimitobelus dayi* Doyle. JCU F11635, Ranmoor Member, northern Eromanga Basin. Transverse section at posterior of stem region showing semi-elliptical, depressed outline, slightly ventrally placed apical canal and clearly incised, centrally placed lateral lines. Magnification x 2.5.

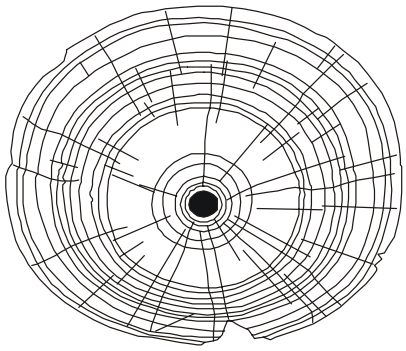

Figure A. 4. 9 *Dimitobelus dayi* Doyle. JCU F11623, Wolena Claystone, Laura Basin. Small specimen sectioned in the stem region showing a weakly elliptical outline and weak registration of lateral lines. Magnification x 2.8.

Discussion: Doyle (1987a) based the original description of his *D. dayi* on specimens from the Wilkins Collection held by the British Museum of Natural History, from the Hughenden area, Queensland. As reported by Doyle (1987a), the species had previously been identified as a variant of *D. diptychus* (McCoy) by Day (1969) in his

review of the Tambo fauna. However, its specific identity is clear. The tumid shape of the guard with a rounded apical termination, weak to absent ventro-lateral grooves but distinctive paired lateral lines set *D. dayi* apart from other members of the genus. *D. dayi* has a symmetrical profile, whereas that of *D. diptychus* is asymmetrical and its apex terminates in a distinct point. *D. dayi* is slightly less depressed in cross-section than most *D. diptychus* (Figure A. 4. 10).

Dimitobelus dayi exhibits some intraspecific variation. Although all specimens show an abrupt apex, the apical angle varies between 50°-75°. An apical canal and pseudoalveolus are typical but variably developed, features reflecting quality of preservation. Whereas the ventral surface is always convex in cross-section, the dorsal surface may show incipient flattening.

For some juveniles, the lateral lines are more dorsally placed than typical of the species and extend the entire length of the guard. In general, lateral grooves are more deeply incised on specimens that show dorsal flattening of the guard.

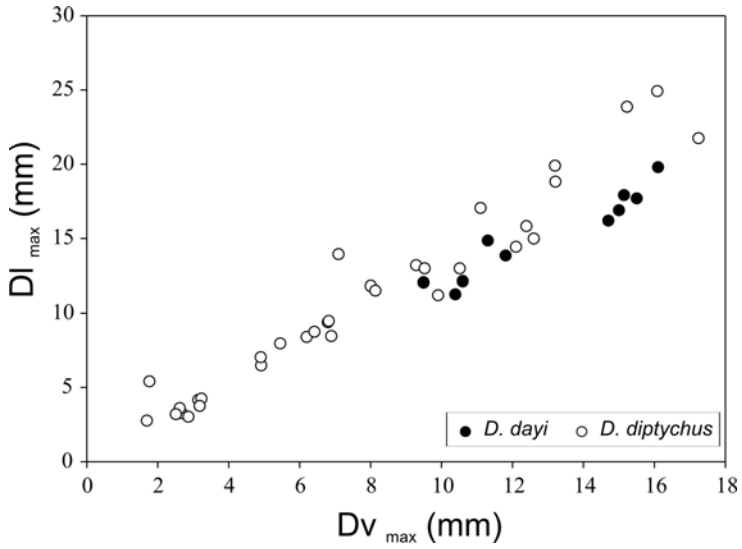

Figure A. 4. 10 Relationship of Dv_{max} with Dl_{max} for *D. diptychus* and *D. dayi*.

Distribution and Age: *D. dayi* has been principally found in the early Albian Ranmoor Member exposed along the Flinders River to the east of Hughenden. It is likely that the type series for which locality details are not known other than the district of Hughenden, are also from this unit.

D. dayi is present in the early Albian Wolena Claystone from the Laura Basin (JCU F11623). In the Western Australian Carnarvon Basin the species is represented in the basal Gearle Siltstone outcropping in the Murchison House district and near the Hills Springs Station (UWA 2/11/99-15). Other specimens are from the basal Gearle Siltstone at Mia Mia, Cardibia Station.

The species is early Albian in age and is characteristic of the older part of the Tambo fauna.

***Dimitobelus (?) hendersoni* sp. nov.**

Pl. 3, figs. 5-6

Type Material: Holotype: GSWA F51430; Paratypes F51431, UWA CS-MM (approximately 25 un-numbered specimens). All from Cardibia Station, Mia Mia, Carnarvon Basin, Western Australia, basal Gearle Siltstone, 114°20'E, 23°22'S.

Additional material: GSWA Barrabiddy 1, see Appendix A. 1, basal Gearle Siltstone, 23°49'57"S, 114°20'E; GSWA Boologooro 1, see Appendix A. 2, Gearle Siltstone, 24°19'27.3"S, 113°53.3"E.

Etymology: In recognition of Professor Bob Henderson, James Cook University, who has provided invaluable contributions towards the completion of this manuscript.

Diagnosis: Medium sized, slender, cylindroconical guards. Outline and profile are symmetrical. Transverse sections are almost circular. Apex is acute. Grooves lacking, lateral lines faint or absent. Alveolus prominent, deeply set, extending to the mid-length of the guard.

Dimensions (mm):

	L	**X**	**Dvmax**	**Dlmax**
UWA CS-MM-3	18.6	8.1	3.3	3.2
UWA CS-MM-4	33.6	15.9	5.8	5.6
UWA CS-MM-5	35.9	20.7	7.2	7.0
UWA CS-MM-6	41.3	24.2	6.9	6.7
UWA CS-MM-7	42.0	24.0	7.1	7.0

Description: Guard slender, outline symmetrical and cylindroconical as is the profile. Apical region attenuated and apex is slightly dorsally deflected, apical angle approximately 20°. Apical line is centrally placed. Guard circular to very weakly compressed in cross-section. Transverse sections are subcircular to weakly compressed (Dl_{max}:Dv_{max} 0.96-1.0; Figure A. 4. 11). Dv_{max} is approximately 6 times the length of guard at maturity. Guard surfaces smooth, completely lacking grooves. Shallow, faint paired lateral lines are present in some specimens, and extend from the alveolus to the apex. Some specimens show a broad weak ventral groove in the alveolar region. Alveolus is centrally placed and deeply set, extending to the mid length of the guard. It is commonly accentuated by development of a pseudoalveolus.
Discussion: These guards are characteristically slender and cylindrical in form and most show well preserved outer surfaces. The anterior part of the alveolar region is missing from all specimens. However, for some the guard walls surrounding the alveolus are thin indicating that the missing anterior part of the alveolar region is small. Extrapolation to completeness, based on the thickness of the circum-alveolar guard walls, indicates that the maximum guard length at maturity does not exceed 55 mm. Juvenile specimens less than 30 mm long when reconstructed are particularly slender, with length some eight times the maximum diameter, and adults become more robust. Many specimens show exfoliation of growth laminae, both on the outer surface and also on the walls of the alveolus.

Given that ventro-lateral grooves cannot be demonstrated, although they could be represented on the missing anterior part of the alveolar region, reference to *Dimitobelus* is questionable. However, the paired lateral lines shown by some specimens clearly indicate affinities with this genus. In shape, the lack of grooves and the absence of lateral lines on many specimens, guards of *D. hendersoni* bear some resemblance to those of *D. liversidgei* from the Eromanga Basin. However, a larger size at maturity, the deep alveolus, and the lack of taper in the anterior region are clear discriminating characteristics.
Distribution and Age: *D. hendersoni* is known only from the basal Gearle Siltstone, which is assigned an Albian age, from a single locality in the Carnarvon Basin in association with adult and juvenile *D. diptychus*, *D. stimulus* and *D. dayi.*

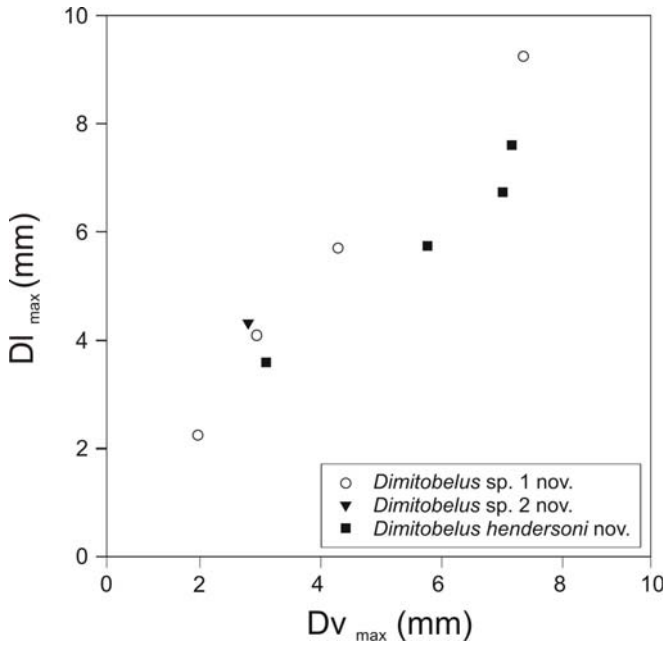

Figure A. 4. 11 Relationship of Dv_{max} and Dl_{max} for *Dimitobelus(?) hendersoni* nov, and *D*. sp. nov. ? 1, *D*. sp. nov.? 2.

***Dimitobelus plautus* sp. nov.**

Pl. 2, fig. 8

Type Material: Holotype: QM F33232; Paratypes QM F33231, F33236 and F33238. All from Hann Tableland, south of Laura, Laura Basin, far northern Queensland, Wolena Claystone, 16°54'S, 145°14'E.

Additional material: JCU F11655, F11656, Tablelands, north of Laura, Laura Basin, far northern Queensland, Wolena Claystone, 15°56'S, 144°10'E; QGS F9689, F9692, F9696 L925, tributary of Piccaninny Creek about 1 mile upstream from NE side of road, Coen, 13°09'S, 142°40'E,Carpentaria Basin.

Etymology: From the latin *plautus*, recognising the broad, flat cross-sectional profile of this species.

Diagnosis: Medium sized, hastate guards. Outline and profile are symmetrical. Transverse sections are elliptical with slightly flattened dorsal and ventral surfaces. Apical and alveolar regions are attenuated. Grooves faint, paired lateral lines evident.

Dimensions (mm):

	L	X	Dvmax	Dlmax
QM F 33232	44.6	20.3	6.2	7.8
QGS F9692	47.1	26.0	6.0	10.1
QM F33238	47.8	23.6	7.1	9.2
QGS F9689	47.8	28.0	6.0	9.9
QGS F9696	48.3	26.0	6.0	9.2
QM F33231	49.5	24.3	9.0	11.9
QM F 33236	55.0	25.5	11.1	13.0

Description: Medium sized *Dimitobelus* with flattened guards ranging to some 50 mm in length. Length of guard approximately six times the maximum diameter, which occurs around mid length. Outline hastate; profile mildly hastate, stem region long, gently tapering, apical region acute (apical angle ~ 20°). Apex positioned slightly dorsal of centre. Guards are depressed and elliptical in transverse section (Dl_{max}:Dv_{max} 1.3; Figure A. 4. 12).

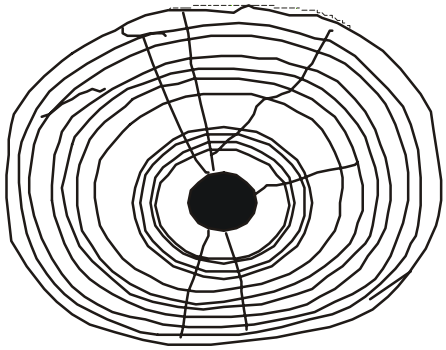

Figure A. 4. 12 *Dimitobelus plautus* sp. nov. QM F33238, Wolena Claystone, Laura Basin. Transverse section showing elliptical outline, with slightly flattened dorsal and ventral surfaces. Faint impressions of dorso-lateral grooves and lateral lines are evident. Point of maximum inflation at mid stem region. Magnification x 6.8.

Dorsal and ventral surfaces markedly flattened in profile. Ventro-lateral grooves faintly incised, straight in alveolar region and curving gently towards mid-region of anterior stem. Dorso-lateral grooves faintly impressed and broad; straight in alveolar region and gently curving on the anterior stem region towards the mid-line, then straightening to become parallel to ventro-lateral grooves. Paired lateral lines are centrally placed and extend from the stem region to the apex. Alveolus is relatively short and a pseudoalveolus with an axial projection is commonly developed. Phragmocone is not known. Axial line is gently curved towards the ventral surface.

Discussion: *Dimitobelus plautus* is most similar to *D. stimulus*. Both are slender guards with acute, almost central apices and prominent centrally placed paired lateral lines

and both have similar cross sections (Figure A. 4.13). However, they differ markedly in attenuatation of the apical and alveolar regions.

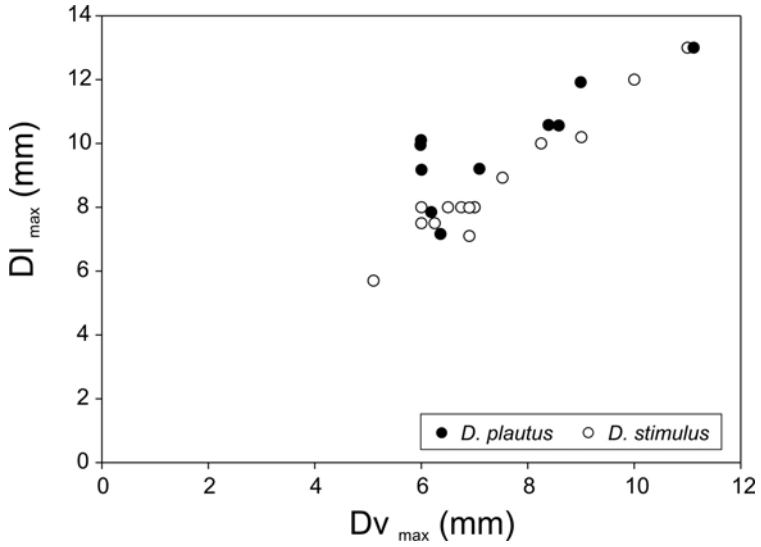

Figure A. 4. 13 Relationship of Dv_{max} and Dl_{max} for *Dimitobelus stimulus* and *D. plautus*.

The long, acutely pointed apical region of *D. plautus* separates the species from *D. diptychus* McCoy; and the size of the guard, depressed cross-section and surface grooves enables easy distinction from *D. liversidgei.*

Intraspecific variation within *D. plautus* is prominent. Flattening of ventral and dorsal surfaces in profile is variable with some specimens being more robust with greater inflation. The alveolar region is variously attenuated ranging from strongly tapered to less so (see pl. 2, fig. 10) and approaching *D. diptychus* in this regard.

Distribution and Age: *D. plautus* is best known from the Hann Tablelands near Laura within the Laura Basin where it occurs in the Wolena Claystone which is assigned as early Albian age (Haig and Lynch, 1993). Other specimens were located near Coen in the Carpentaria Basin(GQS F9689, 9692, 9696).

***Dimitobelus* sp. nov. ? 1**

Pl. 3, figs. 1-3

Material:

Carnarvon Basin, Western Australia: GSWA F51426, UWA TP-PP 5, Thiridine Point, Pillawarra Plateau, upper Gearle Siltstone, 27°36'S, 114°13'E; GSWA F51427 and

F51428, Boologooro 1, see Appendix A. 2, upper Gearle Siltstone, 24°19'27.3"S, 113°53.3"E; GSWA Edaggee 1, see Appendix A. 3, upper Gearle Siltstone, 25°21'27"S, 114°14'04.9"E.

Dimensions (mm):

	L	**X**	**Dvmax**	**Dlmax**
Boologooro 289m	14.7	7.0	2.1	2.3
Boologooro 294.4m	17.7	9.4	3.1	3.5
UWA TP-PP-5	27.2	15.8	4.4	5.8
Edaggee 245.9m	36.8	20.8	6.4	8.2

Description: Guard small in size with length ranging to 37 mm and nearly 5 times the diameter at the point of maximum inflation. The outline is symmetrical and semi-hastate; profile is asymmetrical and sub-cylindrical. The dorsal surface is more arched than its flattened ventral counterpart. The position of maximum inflation (Dl_{max}) occurs in the mid-flank of the guard, within the stem region. Transverse sections are semi- elliptical and depressed (Dl_{max}:Dv_{max} 1.2). The apex is not preserved but appears to be acute. Ventro-lateral grooves are visible in the alveolar region, and converge to meet faint lateral lines that extend from alveolar region to apex. Dorsal grooves faintly impressed and broad, straight in alveolar region and gently curving on the anterior stem region towards the mid-line at Dv_{max}, then recurving to become parallel to the ventro-lateral grooves. Paired lateral lines extend from alveolar to the apex. Apical line is ventrally placed, and an apical canal commonly forms.

Discussion: The juvenile form is more cylindrical, and transverse section not as depressed as in adult specimens. The outline of the juvenile guards is similar to that of the adults but the profile is less curved bounding surfaces. The apex is acute to very acute and Dv_{max} is at mid-flank, similarly to the adult form.

This species is similar in outline and profile to *D. diptychus* but the apical region, although incomplete in the material available, is decidedly more tapered. The point of maximum inflation is more anteriorly positioned than that of *D. diptychus*, with a gentle taper towards the alveolar region of the guard. The presence of ventro-lateral grooves, which converge to join lateral lines, places this form within *Dimitobelus*. *D. dayi* is similar in that it has weak to absent ventro-lateral grooves with

distinctive paired lateral lines, but differs in shape. *Dimitobelus* sp. nov.? 1 is most similar to *D. liversidgei* in transverse sections (Dl_{max}:Dv_{max} ~ 1.1-1.2 for *D. liversidgei*, 1.2 for *D*. sp. nov. ? 1) and the point of maximum inflation is also similarly positioned around the mid-flank of the guard. Difference in profile and alveolar regions separate *Dimitobelus* sp. 1 from *D. liversidgei*.

This small group of specimens, the largest of which may still be immature, appears to represent a discrete taxon but more material is needed before formal naming is warranted.

Distribution and Age: Specimens of *Dimitobelus* sp. nov.? 1 were collected from the upper Gearle Siltstone of the Carnarvon Basin at Thiridine Point, Pillawarra Plateau and from core obtained from GSWA Edaggee 1 and GSWA Boologooro 1. This unit is of Cenomanian age (see Section C).

***Dimitobelus* sp. nov. ? 2**

Pl. 3, fig. 4

Material: GSWA F51429, UWA 23/3/93 3, Alinga Formation, late Albian, Alinga Point, Carnarvon Basin 27°35'S, 114°11'E.

Dimensions (mm):

	L	**X**	**Dvmax**	**Dlmax**
UWA 23/3/93-3	14.5	5.0	2.9	3.6

Description: Guard diminutive, semi-clavate in shape. Outline is symmetrical and the profile almost so; point of maximum inflation decidedly posterior of the mid length. Transverse sections are semi-elliptical. Apex is moderately obtuse and the apical canal is centrally placed. Ventral and dorsal surfaces are flattened. Ventral surface has a central, broad, deep groove extending from the alveolar region almost to the apex. Faint ventro-lateral grooves are also present, positioned near the mid-flank and almost straight. The guard reduces in width anteriorly and shows a slight waist in profile near its anterior termination.

Discussion: This guard somewhat resembles juveniles of *D. diptychus* in shape, being pinched in the posterior alveolar region, and with the maximum point of inflation

located towards the apex. It is set apart from other Albian *Dimitobelus* by its diminutive size and prominent single ventro-lateral groove. Given that only a single, diminutive and possibly immature specimen with this distinctive form is available, it is left under open nomenclature. It could possibly represent a pathological example of *D. diptychus*.

Distribution and Age: The specimen is from the lower Alinga Formation of late Albian age.

Genus *Microbelus* nov.

Type Species: *Microbelus haigi* sp. nov.

Etymology: prefix *micro-*, reflecting to the diminutive size of the guard; suffix *-belus*, identifying membership of the Family Dimitobelidae.

Diagnosis: Guard diminutive, semi-clavate in shape, inflated with Dl_{max} located towards the apex. Transverse sections depressed with a flattened ventral surface. A single ventro-lateral groove extends almost the full length of the guard. Alveolus inconspicuous and phragmocone unknown.

Range: Cenomanian of Western Australia.

Discussion: The genus *Microbelus* is established here for distinctive diminutive belemnites that occur only from the Cenomanian upper Gearle Siltstone of the Carnarvon Basin, Western Australia. The two included species, *Microbelus haigi* and *M. tumidus* are unlike any previously described members of the family. They share a globular, clavate form with an inflated apical region. The presence of ventro-lateral grooves confirms reference to the Family Dimitobelidae.

The evolutionary derivation of *Microbelus* is uncertain. In some aspects of its morphology, the diminutive size and the tapered guard anterior and in the case of *Microbelus tumidus* the poor representation of ventro-lateral grooves, suggests a connection to the Albian *Dimitobelus liversidgei.*

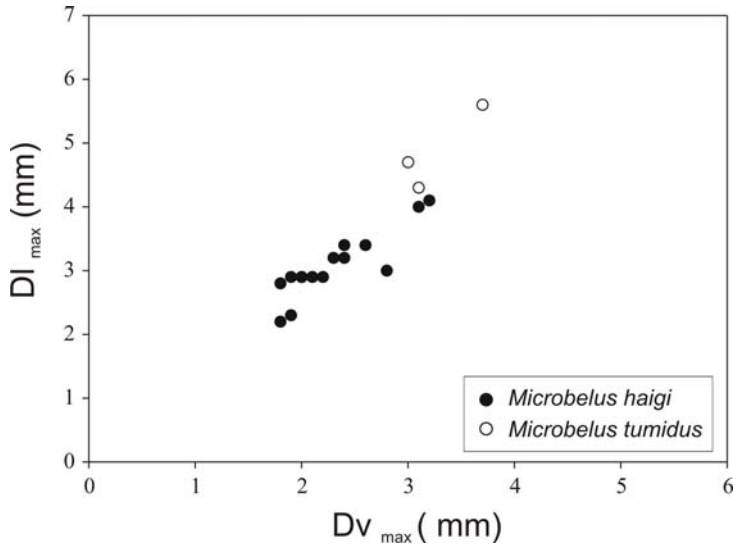

Figure A. 4. 14 Relationship of Dv_{max} and Dl_{max} in *Microbelus haigi* and *Microbelus tumidus*.

***Microbelus haigi* sp. nov.**

Pl. 3, figs. 9-13

Type specimens: GSWA F51432 (holotype), GSWA F51433- F51436 (paratypes), remainder of type series UWA 2/11/99-16 7– 2/11/99-16 20, upper Gearle Siltstone, Cenomanian, MacDonald Dam, Carnarvon Basin 24°10'S, 114°29'E.

Additional Material: approximately 74 guards (UWA 2/11/99-16), both fragmentary and complete, from the mid-Cenomanian (uppermost Gearle Siltstone), MacDonald Dam, Carnarvon Basin.

Etymology: In recognition of Professor David Haig, University of Western Australia, who collected most of the specimens.

Diagnosis: Guard diminutive and globular, less than 20 mm in length, semi-clavate in shape, point of maximum inflation well posterior of mid-length. Outline is symmetrical; profile asymmetrical. Transverse sections are semi-elliptical and depressed. Apex is eccentric and ventrally placed.

Dimensions (mm):

	L	**X**	**Dvmax**	**Dlmax**
UWA 2/11/99-16 19	8.2	3.8	1.8	2.2
UWA 2/11/99-16 13	8.8	2.7	1.9	2.3
UWA 2/11/99-16 12	11.0	3.0	1.9	2.9
UWA 2/11/99-16 11	11.1	3.3	1.8	2.8
UWA 2/11/99-16 20	11.2	3.9	2.0	2.9

UWA 2/11/99-16 14	11.9	4.0	2.2	2.9
UWA 2/11/99-16 15	11.9	4.3	2.4	3.4
UWA 2/11/99-16 21	13.2	5.3	2.0	2.9
UWA 2/11/99-16 7	13.8	4.1	2.3	3.2
UWA 2/11/99-16 10	14.3	4.5	2.6	3.4
UWA 2/11/99-16 18	14.8	6.1	2.1	2.9
UWA 2/11/99-16 8	15.1	3.9	3.2	4.1
UWA 2/11/99-16 16	17.2	5.1	2.8	3.0
UWA 2/11/99-16 17	17.6	7.0	2.4	3.2
UWA 2/11/99-16 9	18.0	5.6	3.1	4.0

Description: Extremely small in size, with guard length ranging to 18 mm. The guard length is approximately four times the diameter at the position of maximum inflation. The outline is symmetrical and clavate, narrowing anteriorly; profile is asymmetrical and sub-clavate. The maximum lateral (Dl_{max}) and ventral (Dv_{max}) diameters occurs in the posterior third of the guard. The apex ranges from acute to obtuse with apical angles ranging between 15° - 30°. Transverse sections are depressed and subquadrate (Dl_{max}:Dv_{max} 1.3; Figure A. 4. 14). Ventro-lateral grooves are well developed and deeply incised, extending from the alveolar region to the apex. They are positioned at the margin of the flattened ventral surface. Flanks and dorsal surface are weakly convex. A small pseudoalveolus is commonly developed, obscuring the nature of the alveolus proper. Phragmocone unknown. Apical line is centrally placed, and an apical canal is commonly present.

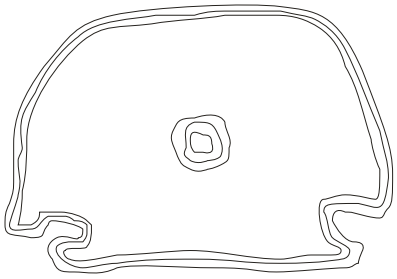

Figure A. 4. 15 *Microbelus haigi* sp. nov. UWA 2/11/99-16-1. Transverse section at point of maximum inflation, adapical of mid stem. Note the quadrate shape and flat venter, with two deeply incised ventro-lateral grooves running entire length of guard. Magnification x 30.

Discussion: *Microbelus haigi* sp. nov. is a miniature species with a guard which is subquadrate in transverse section, an attribute shared with juvenile *D. dayi* which is also clavate in form, being most inflated in the apical region and gradually tapering to the anterior margin. However, it is easily distinguished from this species other *Dimitobelus* by to its diminutive size and distinctive, strongly marked ventro-lateral

grooves that extend the entire length of the guard. A minute alveolus appears to be present but is commonly overprinted by a small pseudoalveolus, similar to that formed in *D. dayi*.

Microbelus haigi appears to have been a species with a short life span, extending over only a few years. Cross-sections (Figure A. 4. 15) show few growth laminae, apparently no more than five in some cases, although those first formed adjacent to the axial canal are poorly preserved and difficult to recognise. Most of the guard is comprised of just one or two thick annual increments followed by slow growth at maturity as registered by one or two thin laminae at the periphery.

Distribution and Age: *Microbelus haigi* sp. nov. is known only from the upper Gearle Siltstone, Carnarvon Basin which is Cenomanian in age (Hocking et al., 1987).

***Microbelus tumidus* sp. nov.**

Pl. 3, figs. 7-8

Type Material: GSWA F51437 (holotype); GSWA 51438, UWA TP-PP 1-2 (paratypes). All from Thiridine Point, Pillawarra Plateau, Carnarvon Basin, uppermost Gearle Siltstone, 27°36'S, 114°13'E.

Etymology: From the latin *tumidus*, recognising the rotund, bulbous outline of this species.

Diagnosis: Diminutive guards, less than 11 mm in length, clavate in shape. Apical and stem regions strongly inflated, alveolar region narrow. Transverse sections are semi-elliptical with a depressed ventral surface. Apex is centrally placed.

Dimensions (mm):

	L	**X**	**Dvmax**	**Dlmax**
GSWA F51438 1	7.2	2.9	3.7	5.6
GSWA F51437	8.8	3.1	3.1	4.3
GSWA F51438 2	10.8	3.8	3.0	4.7

Description: Extremely small in size with guard length ranging to approximately 11mm and approximately twice the diameter at the position of maximum inflation. The outline is symmetrical and strongly clavate; profile is almost symmetrical and clavate. Apex rounded, apical region is bulbous; the stem region is very short and

guards taper anteriorly to a narrow alveolar region. The maximum lateral diameter (Dl_{max}) is positioned just posterior of the guard mid-length. The dorsal surface and flanks are rounded, whereas the venter is flattened. Transverse sections are depressed and oval (Dl_{max}:Dv_{max} 1.5; Figure A. 4. 14). The apex is centrally placed and the apical angle is strongly obtuse. Faint ventro-lateral grooves extend from the apex to the alveolus, being a little more pronounced in the alveolar region. They are positioned close to the mid-flank. A pseudoalveolus is commonly developed, obscuring the form of the alveolus which is very small if indeed developed. Phragmocone unknown. Apical line is ventrally placed, and an apical canal is commonly formed.

Discussion: Although *Microbelus tumidus* sp. nov. is represented by only 3 specimens, it is very distinctive with a minute guard which is globular and abbreviated, narrowing abruptly to the alveolar region which is unusually slender. It is distinguishable from *M. haigi* sp. nov. by its more globular shape.

Age and Distribution: *Microbelus tumidus* is known only from the upper Gearle Siltstone exposed at Thiridine Point, Pillawarra Plateau, Carnarvon Basin, Western Australia where is associated with juvenile *D. diptychus* and *Dimitobelus* sp. nov ? 1. This unit is of Cenomanian age (Campbell and Haig, 1999).

A. 5 Biostratigraphic Summary

The geographic and age distributions of Albian and Cenomanian Dimitobelidae from Australia is summarised in Figure A. 5. 1. *Dimitobelus diptychus* is long ranging, distributed through the Albian and into the Cenomanian. *Dimitobelus dayi* and *D. stimulus* are confined to the Albian. *D. liversidgei*, *D. hendersoni* sp. nov. and *D. plautus* sp. nov have more limited ranges, both chronologically and geographically.. These species occur in separated basins and appear to be short-ranging. Two discrete species left under open nomenclature are restricted to the Carnarvon Basin and are of disjunct (Albian and Cenomanian) ages.

Microbelus is described from two different West Australian localities exposing the upper Gearle Siltstone (Cenomanian) of the Carnarvon Basin succession.

	CARNARVON BASIN	LAURA BASIN	CARPENTARIA BASIN	EROMANGA BASIN NE	EROMANGA BASIN SW
CENOMANIAN	*M. tumidus* nov. *M. haigi* nov. *D.* sp. nov. ? 1 *D. diptychus*				
ALBIAN	*D.* sp. nov. ? 2 *D. hendersoni* nov. *D. dayi* *D. stimulus* *D. diptychus*	*D. plautus* sp. nov. *D. diptychus* *D. stimulus*	*D. diptychus*	*D. liversidgei* *D. stimulus* *D. diptychus* *D. dayi*	*D. diptychus* *D. stimulus*

Figure A. 5. 1. Summary of the age and distribution of the *Dimitobelus* and *Microbelus* species that are represented within Australia. Diagram not to scale.

EXPLANATION OF PLATE 1

Figures 1-13. *Dimitobelus diptychus* (McCoy). 1-12, ventral outline, profile and dorsal outlines. 1, 5, 6, Albian, Carnarvon Basin, Western Australia. UWA 2/11/99-16-1 x2, UWA 2/11/99-16-2 x 2, UWA 2/11/99-16-3 x 2. 2-4, Cenomanian, Carnarvon Basin, Western Australia. UWA TP-PP1 x 1.5, UWA TP-PP2 x 1.5, UWA TP-PP3 x 2.5. 7, syntype, Albian, Eromanga Basin, South Australia. SAM T1311 x 1. 8, Albian, Eromanga Basin, South Australia. NMV P310414 x 1. 9, 10, Late Albian, Carnarvon Basin, West Australia. UWA 2/11/99-15-1 x 1, UWA 2/11/99-15-2 x 1. 11, cast of holotype, Albian, Eromanga Basin, Queensland. NMV P2177 x 1. 12, Albian, Eromanga Basin, Queensland. JCU F11617 x 1.5. 13, left profile and inner, Albian, Eromanga Basin, South Australia. SAM T1312 x 1.

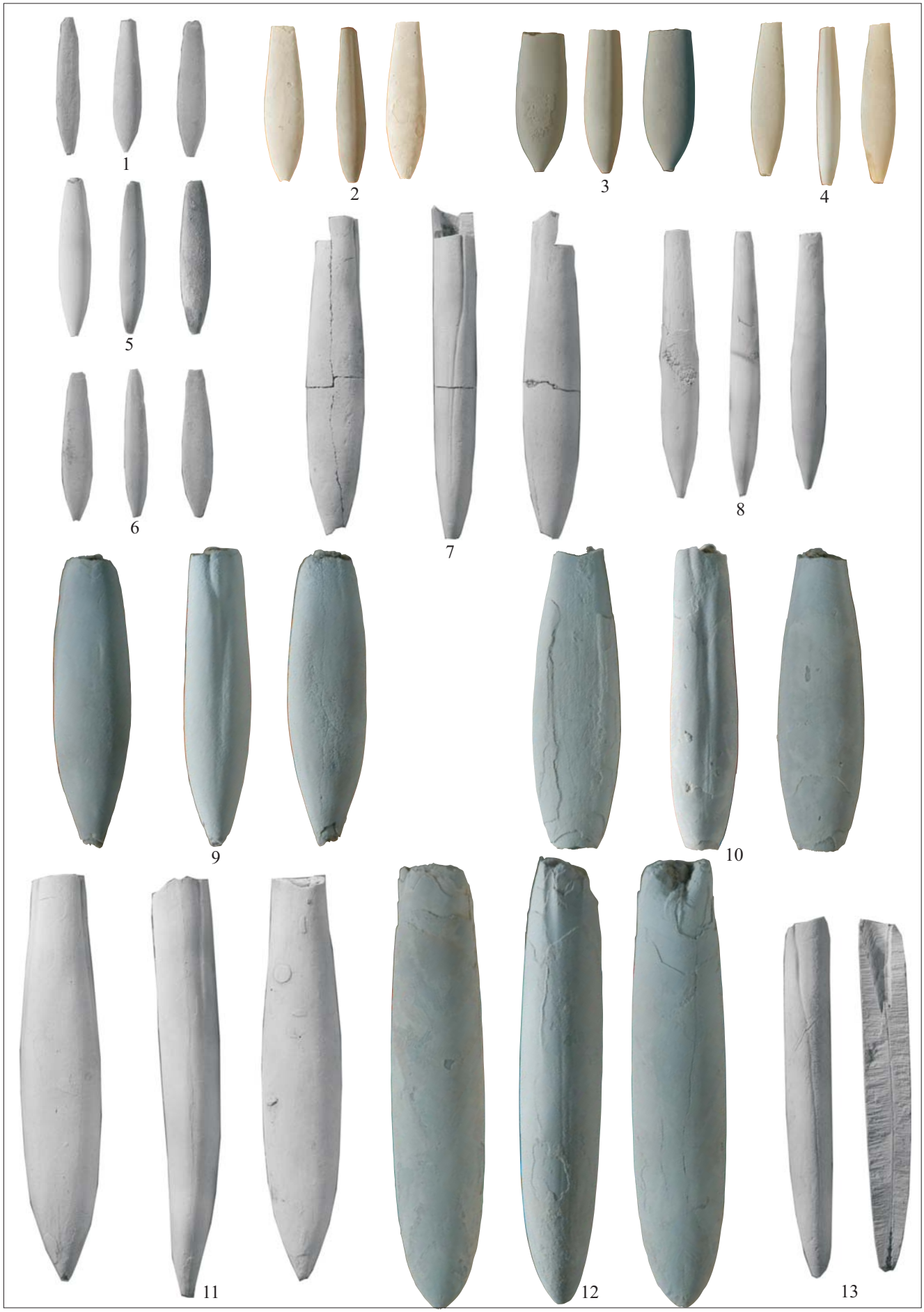
1
2
3
4
5
6
7
8
9
10
11
12
13

EXPLANATION OF PLATE 2

Figures 1-3. *Dimitobelus liversidgei* (Etheridge Jnr). 1, 2, 3 in situ specimens. 1, Albian, Eromanga Basin, Queensland. NMV P310444-5 x 1. 2, Albian, Eromanga Basin, Queensland. QGS F1372 x 1. 3, Albian, Eromanga Basin, Queensland. QGS F5629-5631 x 1.

Figures 4-6. *Dimitobelus stimulus* (Whitehouse). 4, 6, ventral outline, profile and dorsal outline. 4, designated lectotype, Albian, Eromanga Basin, South Australia. NMV P310453 x 1. 6, Albian, Carnarvon Basin, Western Australia. UWA 2/11/99-15-1 x 2. 5, left profile and inner, Albian, Carnarvon Basin, Western Australia. WAM 91.823 x 1.

Figures 7-9. *Dimitobelus dayi* (Doyle). 7, left profile and inner, Albian, Carnarvon Basin, Western Australia. UWA 2/11/99-15-3 x 1. 8, 9, ventral outline, profile and dorsal outline. 8, Early Albian, Carnarvon Basin, Western Australia. UWA 2/11/99-15-2 x 1. 9, Early Albian, Eromanga Basin, Queensland. QM F6149 x 1.

Figure 10. *Dimitobelus plautus* sp. nov. 10, ventral outline, profile and dorsal outline, Albian, Laura Basin, Far North Queensland. QMF 33232 x 1.

Figure 11. *Dimitobelus* sp. indet. 11, ventral outline, profile and dorsal outline. Albian, Laura Basin, Far North Queensland. JCU 11620 x1.

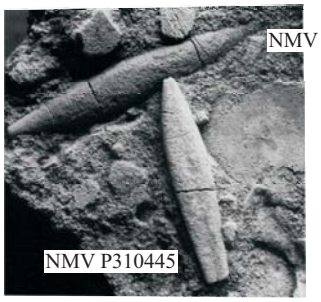

1

2

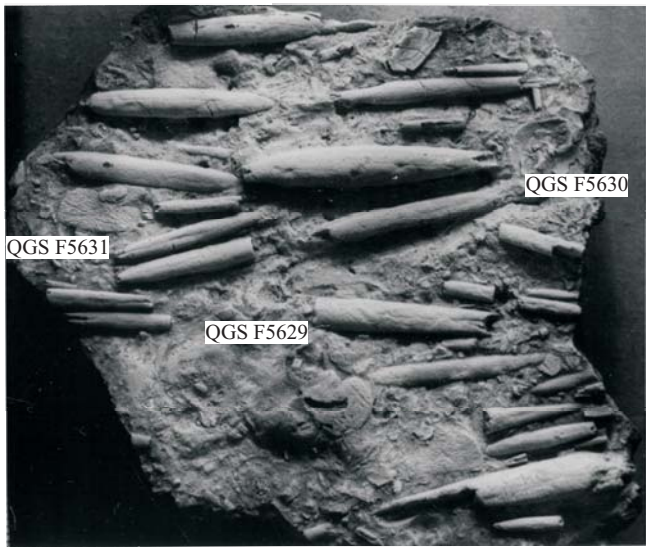

3

4 5 6 7

8

9

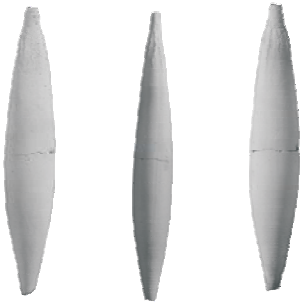

10

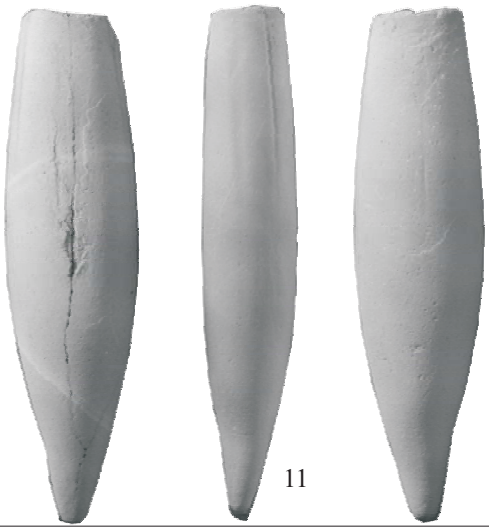

11

EXPLANATION OF PLATE 3

Figures 1 - 3. *Dimitobelus* sp. nov. ? 1. 1- 3 ventral outline, profile and dorsal outline. 1, upper Cenomanian, Carnarvon Basin, Western Australia. GSWA F51427 Boologooro 1 289.0 m, x 1.75. 2, Cenomanian, Carnarvon Basin, Western Australia x 1.5. GSWA F 51428 Boologooro 1 294.4 m, x 1.75. 3, Cenomanian, Carnarvon Basin, Western Australia. GSWA F51426, x 1.3.

Figure 4. *Dimitobelus* sp. nov. ? 2. 4, ventral outline, profile and dorsal outline. Late Albian, Carnarvon Basin, Western Australia. GSWA F51429 x 2.5.

Figure 5 and 6. *Dimitobelus (?)hendersoni* sp. nov. 5, 6 ventral outline, profile and dorsal outline. 5, Late Albian, Carnarvon Basin, Western Australia. GSWA F51430 x 1. 6, Late Albian, Carnarvon Basin, Western Australia. GSWA F51431 x 1.

Figure 7 and 8. *Microbelus tumidus* sp. nov. 7, 8 ventral outline, profile and dorsal outline. 7, holotype, Cenomanian, Carnarvon Basin, Western Australia. GSWA F 51437 x 3.5. 8, paratype, Cenomanian, Carnarvon Basin, Western Australia. GSWA F 51438 x 3.5.

Figs. 9-13. *Microbelus haigi* sp. nov. 9-13 ventral outline, profile and dorsal outline. 9, holotype, mid Cenomanian, Carnarvon Basin, Western Australia. GSWA F51432 x 3. 10, paratype, mid Cenomanian, Carnarvon Basin, Western Australia. GSWA F51433 x 3. 11-13, mid Cenomanian, Carnarvon Basin, Western Australia. GSWA F51434-F51436 x 3.

1

2

3

4

5

6

7

8

9

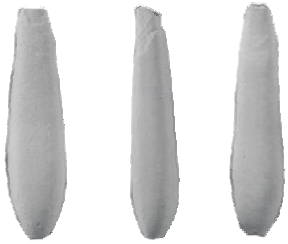

10

11

12

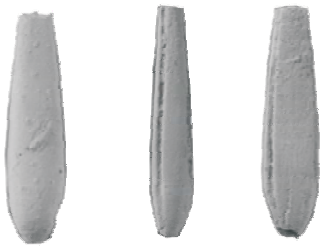

13

SECTION B

Aptian *Peratobelus* (*Dimitobelidae*) of Australia

Section B. Aptian *Peratobelus* (*Dimitobelidae*) of Australia

B. 1 Abstract

A review of Australian belemnites referred to the Aptian genus *Peratobelus* (Dimitobelidae) is presented, based on an evaluation of extensive collections from the Great Artesian Basin of eastern Australia, the Carnarvon Basin of Western Australia and the Money Shoals Basin of the Northern Territory. Only two species are recognised, gracile *Peratobelus bauhinianus* which had an Australia-wide distribution and robust *Peratobelus oxys* which is known only from the Great Artesian Basin in Australia but ranged to the Antarctic Peninsula. *Peratobelus oxys* Tenison-Woods was named from guards but is conspecific with *Peratobelus selheimi* Tenison-Woods which was based on a phragmocone. Guards and phragmocones of this species typically separated prior to fossilisation but co-occur in the same horizons and localities. This species possessed an unusually large phragmocone, up to 15 cm in length, among Cretaceous belemnites.

B. 2 Introduction

A distinctive belemnite assemblage characterised by *Hibolithes, Belemnopsis* and *Duvaliidae* spread south from Europe in the Late Jurassic, and characterised the Gondwana margins in the Neocomian (see Stevens, 1965; Challinor, 1991; 1992). It was largely replaced by members of the Family Dimitobelidae in the Aptian, entirely so in east Gondwana where taxa other than members of this group are unknown subsequent to the Neocomian. Dimitobelidae represent an important element of the Austral faunal realm which characterised the Cretaceous marine invertebrate fauna of Gondwana in general, and Australasia in particular, during the Cretaceous Period (see Henderson et al., 2000).

In guard shape and the nature of the phragmocone and the conical anterior cavity within the guard, the alveolus, in which it is housed the Dimitobelidae are unremarkable. However unique grooves are inscribed on their guards, considered to reflect a distinctive soft-part organisation (Stevens, 1965). No clear ancestral stock for the Dimitobelidae has been identified and their origin is uncertain. As noted by Stevens (1973) most authors have favoured an origin from Belemnopseidae or the Hastitidae. However in a more recent review of possible evolutionary connections, Doyle (1988) favoured ancestry from *Hibolithes.*

Early description of Australian belemnites, prior to the nineteenth century, invariably made use of European generic categories. Whitehouse (1924) was the first worker to recognise the distinctive character of Australian faunas and erected the Family Dimitobelidae for "cylindrical and clavate belemnites provided with lateral grooves on the anterior portion of the guard, but devoid of antero-ventral or apical grooves". *Peratobelus* was established by Whitehouse (1924) as the earliest (Aptian) representative of the group, characterised by a robust, cylindrical guard with long, straight ventro-lateral grooves. This genus was replaced throughout Australasia in the early Albian by *Dimitobelus* which persisted for the remainder of the Cretaceous and is readily distinguishable by a characteristically depressed guard with more dorsally positioned, curved ventro-lateral grooves which pass into paired lateral lines. A third genus of the family known only from India and the Antarctic Peninsula, *Tetrabelus*, has surface grooves restricted to the anterior part of the guard (Figure B .2 .1).

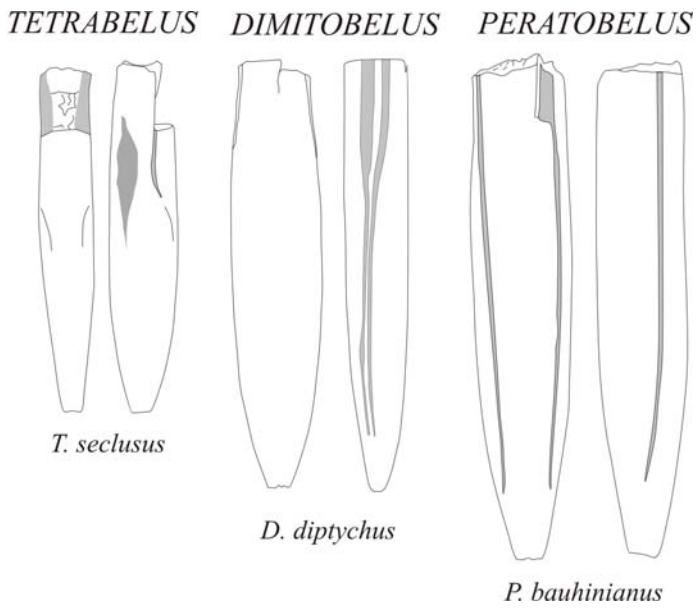

Figure B. 2. 1 Drawings illustrating the differences in surface markings between genera of the Dimitobelidae (modified from Doyle, 1988). The venter is illustrated on the furthest right of each outline view.

Morphological attributes of the groupings within *Peratobelus* are generally well constrained, with the shape, length and nature of the ventro-lateral grooves, and

guard size distinctively categorising individual species. Within *Peratobelus* stocks the majority of specimens are closely alike and hence the specific categories are morphologically distinctive and constrained. However, intraspecific variation does apply and imperfect preservation due to fragmentation and the loss of surface features through abrasion commonly impedes identification. Three species of *Peratobelus* have commonly been recorded from Australia: *P. oxys* (Tenison-Woods), *P. australis* (Phillips), and *P. selheimi* (Tenison-Woods).

Of these, *P. oxys* (= *P. selheimi*) is unusual, commonly being represented by a large and conspicuous phragmocone, rather than the guard as is the case for other species where the phragmocone is smaller and rarely preserved. The combination of guard and phragmocone is a universal attribute of belemnite morphology regarded as having had a buoyancy and trim function for the living animal. This is almost certainly the case for the phragmocone because its morphology is homologous with that of modern *Nautilus* for which a buoyancy function is well known (see Ward, 1987) and for a wide range of extinct ectocochleate cephalopods for which a similar function can be safely inferred. The guard probably acted as a counterbalance to the head and arms, with the buoyant phragmocone acting as a pivot (Stevens, 1965). The size of the phragmocone must be related not only to the weight of the guard but also the mass of soft parts vested in the living animal. It may be inferred that the larger the belemnite, the larger the phragmocone needed to counterbalance the total body and skeletal weight. The large, robust phragmocone of *P. oxys* is likely to reflect a large body size, considerably bigger than that of other *Peratobelus* species.

Most representatives of the genus have been documented from Aptian formations of the Eromanga and Carpentaria basins, deposited within a very extensive epeiric sedimentary system developed in eastern Australia at this time (Figure B. 2. 2; Exon and Senior, 1976; Senior et al., 1978). *Peratobelus* is also known from Aptian strata from the subjacent Maryborough Basin (Whitehouse, 1925, 1926) and there are additional records from Money Shoals Basin of northern Australia (Henderson, 1998a) and the Carnarvon Basin from Western Australia (Hocking et al., 1987).

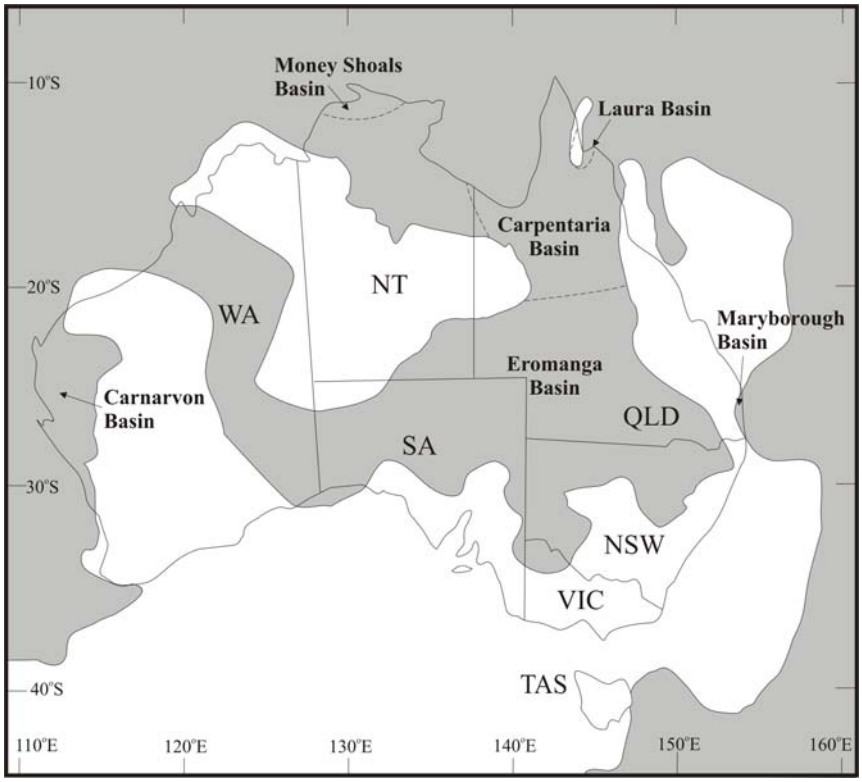

Figure B. 2. 2 Map showing the extent of Aptian flooding (shaded) for Australia (after Frakes et al., 1987) and the location of basins referred to in this paper.

This paper revises the Australian species of *Peratobelus*, drawing on the extensive collections now available. It recognises extensive synonymy amongst the species categories introduced in the older literature where taxa were commonly established on small collections where the specimens available were insufficient to establish the full morphology and/or the range of variation.

B. 3 Collections and localities

For this study, relevant collections held by museums, universities and geological surveys were extensively examined. In addition, it utilizes new collections from the northern Eromanga Basin, and collections newly acquired from stratigraphic drilling by the Geological Survey of Western Australia (GSWA) are of significance.

The specimen suite evaluated here is held by a number of repositories, as follows: AM, Australian Museum, Sydney; SAM, South Australian Museum, Adelaide; GSSA, Geological Survey of South Australia; UA, University of Adelaide; NMV, Museum of Victoria; QGS, Queensland Geological Survey; UQ, University of Queensland; QM, Queensland Museum; JCU, James Cook University; WAM, Western Australian Museum; UWA, University of Western Australia; GSWA, Geological Survey of Western Australia; CPC Commonwealth palaeontological collection, Geoscience Australia. Locality numbers prefixed `L' refer to specific sites registered in these repositories. Modern collections are in general accurately located. However, locality records for older collections are commonly imprecise. Where possible these have been assigned approximate geographic coordinates.

Ages assigned to the various localities are based on their position relative to the lithostratigraphic framework that applies in the regions where they occur. The lithostratigraphic succession of the Eromanga Basin is extensively expressed by surface outcrop as documented by regional mapping and detail of it is augmented by numerous stratigraphic core holes. A useful composite section, through the Aptian and Albian of the northern Eromanga Basin is provided by outcrop along the Flinders River, east of Hughenden.

For the Carpentaria Basin, the Walsh River and its tributaries expose the lower part of the Cretaceous succession and only a few isolated outcrops are known for Cretaceous marine strata of the Laura Basin.

For the Carnarvon Basin, a suite of stratigraphic wells drilled in the last decade by the Geological Survey of Western Australia (GSWA) and collaborators provide a concise record of belemnites from the latest Barremian through to the Cenomanian. These fully cored drill holes, together with collections from representative surface outcrops of the lithostratigraphic succession provide an extensive record of belemnites through the Early Cretaceous Epoch for the Western Australian continental margin.

B. 4 Systematic descriptions

Class CEPHALOPODA Cuvier, 1795

Subclass COLEOIDEA Bather, 1888

Order BELEMNITIDA Zittel, 1895

Suborder BELEMNOPSEINA Jeletzky, 1965

Family Dimitobelidae Whitehouse, 1924

Diagnosis: Cylindrical and clavate guards with two ventro-lateral grooves on the anterior portion of the guard. Antero-ventral grooves absent or rudimentary and apical grooves lacking.

Discussion: The Family Dimitobelidae was established by Whitehouse (1924) for a distinctive group of Cretaceous belemnites from eastern Australia. The position of the siphuncle in the phragmocone shows that grooves inscribed into the guard are ventro-lateral in position whereas the dorso-lateral surface is generally featureless. Successive workers have shown that the representatives of the family also occur in southern India (Whitehouse, 1924), New Zealand (Stevens, 1965), New Guinea (Glaessner, 1945; Glaessner, 1958; Challinor, 1990), Antarctica (Doyle, 1988), and Mozambique (Doyle, 1987b). The Dimitobelidae are now recognised as a distinctive Cretaceous belemnite clade characteristic of Southern Hemisphere mid to high latitudes.

Based largely on eastern Australian material, Whitehouse (1924) recognised four nominal genera within the Family Dimitobelidae: *Peratobelus, Dimitobelus, Tetrabelus* and *Cheriobelus*. Glaessner (1945; 1957) and others (Stevens, 1965; Doyle, 1987a) considered *Cheriobelus* to be a subjective synonym of *Dimitobelus*, thereby reducing the family to three genera. *Peratobelus* and *Dimitobelus* were wide-ranging but *Tetrabelus* is known only from India and the Antarctic Peninsula.

Genus *Peratobelus* Whitehouse, 1924

Peratobelus Whitehouse, 1924, p. 410.

Peratobelus Stevens, 1965, p. 61.

Peratobelus Doyle, 1987*a*, p. 153.

Type Species: *Belemnites oxys* Tenison-Woods 1883a, Aptian of the Great Artesian Basin.

Diagnosis: Slender to robust Dimitobelidae with guard outline subhastate to cylindroconical. Profile is asymmetrical to almost symmetrical, cylindroconical. Transverse sections subcircular, ventral surface generally flattened. Two well-developed, long ventro-lateral grooves are set close to the venter and run approximately parallel to it, extending at least to the stem region. For most or all of their course they are straight but dorsally directed curvature may occur towards their posterior termination. No other surface markings are present.

Range: Widespread in the Aptian of Australia, known also from the Aptian of the Antarctic Peninsula and Mozambique.

Discussion: *Peratobelus* is the oldest representative of the Dimitobelidae, being succeeded by *Dimitobelus* in the Albian. Whitehouse (1924, p. 410) erected the genus, distinguishing it as "cylindrical or clavate (hastate) guards with ventro-lateral grooves only. These grooves extend for about half the length of the guard; alveolus normal." Glaessner (1957) and Stevens (1965) restricted the genus to cylindroconical, non-hastate (non-clavate) species. However, Doyle (Doyle, 1987a, p. 154) observed that the type species *P. oxys* (Tenison-Woods) and related forms such as *P. australis* (Phillips) display some hastation.

The genus *Dimitobelus* Whitehouse (1924) has double lateral lines that are unknown in *Peratobelus* and its guards are generally set apart by being distinctly clavate rather than cylindroconical or weakly hastate. The most distinctive characteristic of *Peratobelus* is its elongate, relatively straight ventro-lateral grooves (Figure B. 2. 1).

Species described from Australian Cretaceous basins include *P. oxys* (Tenison-Woods), *P. australis* (Phillips), and *P. selheimi* (Tenison-Woods). Whitehouse (1924, p.

411) placed a single large guard from the upper Aptian of South Australia (BMNH C. 5309) as "an unnamed species of *Peratobelus*." The specimen was later referred to *Belemnites selheimi* Tenison-Woods by Woods (1961, p. 3), even though that species was originally described from phragmocones only (Tenison-Woods, 1883a, p. 250, pl. 7, fig. 1). *B. selheimi* has been generally regarded as a species of *Peratobelus* (Day, 1967a, 1967b; Hill et al., 1968) but Ludbrook (1966) referred the species to *Dimitobelus*. Doyle (1987a) remarked that *B. selheimi* should be restricted to the Tenison-Woods type, which cannot clearly be assigned to *Peratobelus*. He placed Whitehouse's unnamed species as a variant of *P. oxys*.

Only two Australian species of Aptian age are recognised here. The suite of material now available shows that *Peratobelus oxys* and *P. selheimi* are synonyms. Skwarko (1966) described belemnites that he assigned as *Dimitobelus* from strata he assigned as late Neocomian and Aptian. However, they represent *Peratobelus* as discussed below. The Neocomian age assignment made by Skwarko (1966) is in error as the lithostratigraphic unit from which they were collected also contains the ammonite *Australiceras* which is restricted to the Aptian.

Peratobelus oxys Tenison-Woods

Pl. 1, figs. 6-7; Pl. 2, figs. 1-9

?1862 *Belemnites ? barklyi* Clarke, p. 246, *nomen dubium*.

1870 *Belemnites paxillosus* Schlotheim; Phillips *in* Moore, p.240, pl. 16, figs. 6, 6a, 6b.

1870 *Belemnites australis* Phillips; Phillips *in* Moore p. 258-59, pl. 16, figs. 1, 2, 5 only.

1880 *Belemnites* sp.; Etheridge, p. 20, figs. 1-3.

1883a *Belemnites oxys* Tenison-Woods p. 237, pl. 13, figs. 1-3.

1883b *Belemnites selheimi* Tenison-Woods, p. 150, pl. 7, fig.1.

1889 *Belemnites eremos* Tate, p. 229-30.

1889 *Belemnites selheimi* Tenison-Woods; Tate, p. 230.

1892 *Belemnites australis* Phillips; Etheridge, p. 487, pl. 35, figs. 1-2

1892 *Belemnites oxys* Phillips; Etheridge, p. 487, pl. 35, figs. 1-2.

1892 *Belemnites eremos* Tate; Etheridge, p. 487, pl. 35, figs. 1-2.

1892 *Belemnites selheimi* Tension-Woods; Etheridge, p. 489, pl. 35, figs. 10-11

1902a *Belemnites oxys* Tenison-Woods; Etheridge, p. 48

1902a *Belemnites selheimi* Tenison-Woods; Etheridge, p. 50, pl. 7, figs. 16-17.

1902b *Belemnites oxys* Tenison-Woods; Etheridge, p. 48, pl. 6, figs. 4-6; pl. 7, figs. 5-7; pl. 8, figs. 4-7.

1902 *Belemnites oxys* Tenison-Woods; Etheridge and Dun, p. 81.

1902 *Belemnites selheimi* Tenison-Woods; Etheridge and Dun, p. 81.

1924 *Peratobelus oxys* (Tenison-Woods); Whitehouse, p. 410, figs. 1a-b.

1926 *Peratobelus oxys* (Tenison-Woods); Whitehouse, p. 277.

1961 *Peratobelus* sp. Woods, p. 6.

1961 *Peratobelus selheimi* Tenison-Woods; Woods, p. 3, 6.

1964 *Peratobelus oxys* (Tenison-Woods); Day, p. 18, table 3.

1964 *Peratobelus? selheimi* (Tenison-Woods); Day, p. 18, table 3.

1965 *Peratobelus oxys* (Tenison-Woods); Day, p. 418.

1965 *Peratobelus oxys* (Tension-Woods); Stevens, p. 61.

1966 *Peratobelus oxys* (Tenison-Woods); Ludbrook, p. 192, pl. 27, fig. 23.

1966 *Dimitobelus selheimi* (Tenison-Woods); Ludbrook, p. 192, pl. 27, fig. 22-25.

1968 *Peratobelus selheimi* (Tenison-Woods); Hill et al. p. 6, pl. figs. 12a, b.

1968 *Peratobelus selheimi?* (Tenison-Woods); Hill et al. p. 6, pl. figs. 16a-c.

1969 *Peratobelus oxys* (Tenison-Woods); Day, p. 144, 146.

1969 *Peratobelus*? *selheimi* (Tenison-Woods); Day, p. 144, 146.

1972 *Peratobelus oxys* (Tenison-Woods); Willey, p. 37, figs. 4d and e.

1972 *Dimitobelus* sp. aff. *D. macgregori* (Glassner); Willey, p. 32, figs. 3a, b only.

1987a *Peratobelus* cf. *oxys* (Tenison-Woods), Doyle, p. 154, pl. 21, figs. 1, 2.

Types: Lectotype by monotypy the specimen figured by Tenison-Woods (1883a, pl. 13, figs. 1-3), from a well near Mount Brown, NW NSW. The original was held by the

Macleay Museum, Sydney but presently cannot be located. A plaster cast of this specimen, numbered L1574, is held by the Australian Museum.

Additional Material: Approximately 72 guards and some 30 isolated phragmocones. Eight specimens showing part of both the guard and phragmocone.

Eromanga Basin, Queensland: UQ F12975, 12978, F12980, 12993 and L1160-64, Metowra Creek, near Metboura Woolshed, Tambo, Doncaster Member, 25°02'S, 146°27'E; UQ F35523, F 35781 and F35786, Bungeworgorai Creek, 1/4 mile west of Mount Abundance Homestead, Doncaster Member, 26°36'S, 148°41'E; UQ F35596 Bungeworgorai shell bed, south of Roma, Doncaster Member, 26°35'S, 148°41'E; UQ F35644-5, Bungeworgorai shell bed, 1/2 ml west of Mount Abundance Homestead, Doncaster Member, 26°36'S, 148°41'E; UQ F35816, Bungeworgorai shell bed, 1/4 mile west of Bungeworgorai Creek junction, Doncaster Member, 26°36'S, 148°42'E; UQ F35783-84, Clerk Creek 600 yards west of Bungeworgorai Creek junction, Doncaster Member, 26°37'S, 148°43'E; UQ F61084, 61086-7, 200 yards from the southern side of Warrego Highway, 100 yards west of Bungeworgorai Creek, Doncaster Member, 26°36'S, 148°42.5'E; UQ F64860 Wallumbilla Creek, Wallumbilla, Doncaster Member, 26°39’S, 149°13’E; QM F1308 Yeulba Creek, Doncaster Member, locality uncertain; QM F14320 Glendower Station, Flinders River, Doncaster Member, 20°44’S, 144°29’E; QM F1641, Winton District, Doncaster Member, 22°22'S, 143°02'E; QM F16432 no recorded locality, Queensland, lower Cretaceous; QM F2219 Tambo Station Upper Barcoo, Doncaster Member, 24°04'S, 144°50'E; QM F2568 Curra Station, Mt Abundance area, Doncaster Member, 26°40'S, 148°25'E; QM F27910, Rosevale, South of Muckidilla, Doncaster Member, c.20°42’S, 144°14’E; QM F27745, locality unknown; QM F43847, approximately 12 miles south of Tambo, Doncaster Member, 24°54 S, 146°20'E; QGS F13763 Barcaldine, Doncaster Member, 23°34’S, 145°18’E; QGS F1368 Flinders River near Hughenden, Doncaster Member, 20°51'S, 144°12'E; QGS F1373-4, 9 miles north of Tambo, on Blackall Road, Doncaster Member, 24°44'S, 146°15'E; QGS F1759, near Aramac, Doncaster Member, 22°59'S, 145°13'E; QGS F1763-4, Barcaldine, Doncaster Member, 23°34'S, 145°18'E; QGS F10485-86, Bungeworgorai Creek, near Mount Abundance Homestead, Doncaster Member, 26°36'S, 148°41'E; JCU F6814 Hughenden district, Jones Valley Member, 20°50’S, 144°11’E; JCU F11637, F11650 L912 and

approximately 40 unnumbered specimens, Flinders River, east of Glendower homestead, Jones Valley Member, 20°41’S, 144°34’E; JCU F11638 L916 and approximately 15 unnumbered specimens, near Jones Valley Station, Jones Valley Member, 20°32’S, 143°58’E; JCU F11639 L907 and 3 unnumbered specimens, Glendower Station, Flinders River, Doncaster Member, 20°40’S, 144°36’E; JCU F11636, F11645 L908 and 3 unnumbered specimens, Glendower Station, Flinders River, Doncaster Member, 20°40’S, 144°36’E; JCU F11640, F11651 L909 (approximately 5 unnumbered specimens), Glendower Station, Flinders River, Doncaster Member, 20°41’S, 144°33’E; JCU L911 (approximately 5 unnumbered specimens), Glendower Station, Flinders River, lower Doncaster Member, 20°41’S, 144°32’E; AM L1574 locality unknown; AM F10472-73 South central Queensland, locality unknown; AM F7118-F71120, Ward River Watershed, Doncaster Member, 24°58', 146°09'; AM F7123 watershed of the Barcoo and Ward rivers, Doncaster Member, c. 24°56’S, 146°13’E; AM F10318, F10319, 10474, F10619, F7283, South-central Queensland, locality unknown; AM F10609, Barcoo River, Doncaster Member, c. 24°46', 146°09'; SAM P29169 Wongalee Station, Hughenden, Doncaster Member, 20°36’S, 144°25’E.

Eromanga Basin, South Australia: SAM T1330 Lake Eyre, Bulldog Shale, 28°14'S, 136°35'E; SAM P18960, Marla Bore, NW South Australia, Bulldog Shale, 27°19'S, 133°33'E; SAM P19229, 40 miles north-west Oodnadatta, Bulldog Shale, 27°15'S, 135°58'E; SAM P10664, Stuarts Creek, central Australia, Bulldog Shale, 29°42'S, 137°02'E; SAM P21362, P19612, Cooper Pedy, Bulldog Shale, 28°55'S, 134°54'E; GSSA M2507, Toodina 7 5/570/7, 50kms from Algebuckina, Bulldog Shale, 28°56'S, 135°21'E; NMV P310459, P310460-2, P310464-5, P310463, P310466, P310467, Primrose Springs, Peake Station, Bulldog Shale, 28°05'S, 135°50'E; AM F9082 Mt Margaret, Bulldog Shale, 28°29’S, 136°04’E.

Carpentaria Basin, north Queensland: QM F1603 Hann Northern Expedition, Walsh River, Wallumbilla Formation, c. 16°53’S, 145°14’E; QM L682, Palmer River, Wallumbilla Formation, c. 16°04'S, 142°43'E; QM F33175-78, F33253, Boomers Hole, Wrotham Park Station, Wallumbilla Formation, 16°33’S, 143°47’E; QGS F8324, F8333, F8802 F10502, Elizabeth Creek, west of Wrotham Park Homestead, Wallumbilla Formation, 16°38’S, 143°56’E; QGS F8430, telegraph line crossing of Elizabeth Creek,

Wallumbilla Formation, 16°40′S, 143°59′E; QGS F8773, F8775, F8776, F8781, F10502, Elizabeth Creek, 0.2 mls west of Wrotham Park on Walsh Telegraph Station track crossing, Wallumbilla Formation, 16°39'S, 143°58'E; QGS F8802, near new Dunbar Road 0.4 miles west of telegraph line crossing, Wrotham Park Station, Wallumbilla Formation, 16°32′S, 143°54′E; QGS L 1318, 0.5 miles north of crossing of Emu Creek, Coen 13°47'S, 142°50'E; JCU F5170-2, 5175, Walsh River, Wallumbilla Formation, 16°39', 143°58'; JCU F8107, F8109 Boomers Hole, Walsh River, Wallumbilla Formation, 16°33′S, 143°47′E; JCU F8115, F8116, F8119, Elizabeth Creek, Wallumbilla Formation 16°40′S, 143°59′E; UQ F13146 Wrotham Park NW of Herberton, Wallumbilla Formation, 16°40′S, 143°59′E; AM F175, Walsh River, Wallumbilla Formation, c. 16°39', 143°58'.

Maryborough Basin, Queensland: QGS F7688, UQ 6304, UQ 5934 Woody Island, Maryborough district, Maryborough Formation, 16°23'S, 145°34'E; QM F12211 Jumpinpin, Crusoe Island, dredged sample, c. 27°45′S, 154°26′E; UQ unnumbered, L240, near Bromleys Farm, Nikembah, Maryborough District, Maryborough Formation, Maryborough Basin, 25°19'S, 152°48'E.

Money Shoals Basin, Northern Territory: JCU F1297-13001, 13003-13022,13024-13025,13027-13030, 13036, Imaluk Beach, Cox Peninsula, Darwin Formation, 12°26'S, 130°44'E.

Other: UQ L1304, Stanwell marine band, Stanwell Coal Measures, 23°32'S, 150°18'E; AM F66926-F66928, F37172, White Cliffs, N.S.W, Doncaster Member, 30°50'S, 143°05'E.

Diagnosis: Large, slender to robust *Peratobelus* terminating in a sharply pointed, dorsally offset, apex. Ventro-lateral grooves almost straight, terminating in the stem region. Alveolus extending some one third of the guard length, dorsally offset. Phragmocone large, robust, extending well beyond the anterior termination of the guard.

Dimensions: in millimetres (mm)

Guards only:

	L	**X**	**Dl_{max}**	**Dv_{max}**
SAM P21362	40.4	19.3	9.1	8.7
JCU F8109a	57.8	19.8	11.4	11.0
JCU F8109b	58.1	25.5	8.4	8.3

SAM P19612	61.8	28.8	10.4	8.7
UQ F35816	65.5	29.0	12.5	11.9
UQ F 35784	68.5	30.5	15.3	12.2
UQ F35781	69.2	21.5	15.0	13.2
QGS F1764	70.3	55.4	16.1	13.9
UQ F61086	73.1	32.7	9.9	9.8
AM F66928	73.2	32.4	12.9	10.8
QM F35523	78.2	37.2	15.9	14.5
QM F33252	78.2	47.8	20.1	16.7
GSSA M2470	79.9	39.9	14.1	13.4
UQ F35783	80.1	44.6	16.5	15.1
AM F66926	81.1	37.0	14.0	13.7
NMV P310467 a	82.8	48.0	23.6	21.0
UQ F35644	86.5	69.2	14.8	13.0
QGS F8430	87.6	66.3	23.2	19.1
QM F12211	89.2	61.2	31.9	29.8
GSSA M2507	90.1	43.1	15.8	14.0
QGS F8776 W14	96.9	44.3	20.5	18.8
UQ L1164b	98.2	55.0	12.0	10.9
UQ F61087	104.9	41.4	14.6	12.2
AM F66927	105.5	48.6	16.9	15.0
QGS F 8333	110.1	53.0	24.6	21.2
QM F 16432	112.9	56.6	29.6	26.1
UQ F12980	120.7	62.7	28.1	26.3

Phragmocones only (refer to Figure B. 4. 1 for schematic of measured parameters):

	L	**L_{total}**	**C**	**D_{max}**
QM F33178	32.0	32.0	32.0	10.9
QGS F8324	82.0	117.7	25.0	37.9
QGS F8802 W23	102.5	140.4	27.0	43.5
QM F33176	121.4	140.4	45.0	39.9
QM F5757	101.2	150.1	32.0	32.1
SAM P29169	87.2	150.7	26.0	39.2
QM F1703	121.0	160.2	25.0	44.7

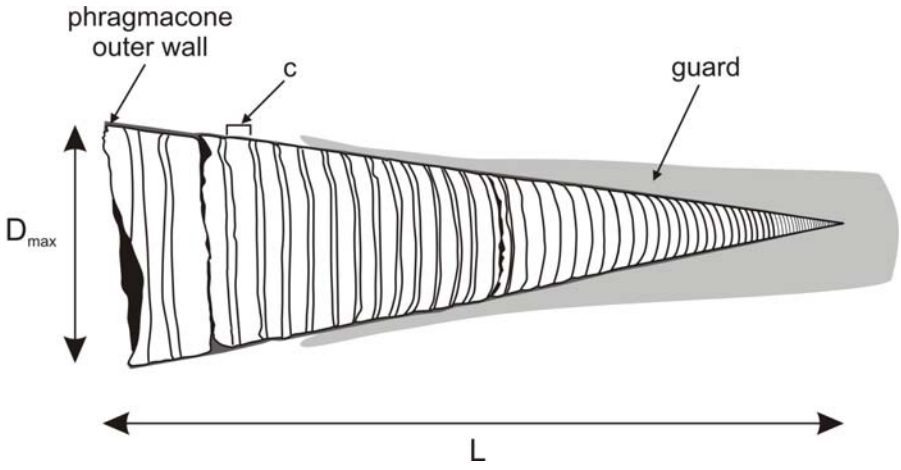

Figure B. 4. 1 Schematic line diagram of position of the phragmocone in relation to the guard, illustrating where measurements where taken. For the dimensions of phragmocones, the near perfect conical form allows a restored length (L_{total}) to be estimated for specimens where the earlier growth stages are missing due to breakage. C is the number of preserved chambers and D_{max} the maximum width of the last growth stage preserved.

Description: *Peratobelus* with large, slender to robust cylindroconical to weakly hastate guards almost symmetrical in profile, subcircular to weakly depressed in cross-section with the venter just slightly flattened at maturity (Figures B. 4. 2 to B. 4. 5). Guard length is 7 to 10 times the maximum width. Alveolar region, when fully preserved, flaring slightly at its anterior margin with alveolar walls tapering very gradually in thickness. Stem and alveolar regions approximately the same length and maintain an almost constant diameter. Apical region typically elongate with its margins in profile almost straight, tapering to a point, but may be blunt with its margins weakly arched in profile; the apex is slightly offset towards the dorsum. Apical angles vary from 15^{O} to 35^{O}. Deeply inscribed ventro-lateral grooves margin the venter. They are straight and extend to the posterior part of the stem region. Alveolus is deeply inset, extending a third of the guard length. Apical line offset towards the venter (Figures B. 4. 2 and B. 4. 5) and arched towards the ventral surface. Phragmocone regularly conical right to its origin, subcircular in cross-section, with the angle of taper varying from 12^{O} to 20^{O}. Up to 50 camerae separated by thin, concave septa are represented. Septa are thin, concave and very regularly spaced with the diameter spanning six to eight camerae in the immediately preceding portion of phragmocone. Siphuncle located at the ventral margin.

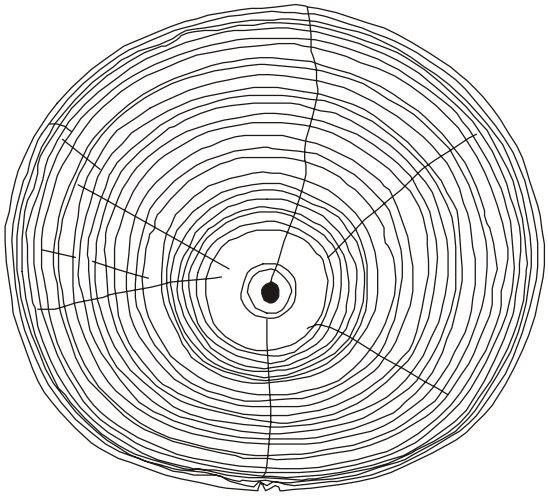

Figure B. 4. 2 *Peratobelus oxys* Tenison-Woods. QM F1641, upper Doncaster Member, northern Eromanga Basin. Transverse section in the stem region at point of maximum inflation, showing multiple growth lines indicating maturity. Impressions of grooves/lines are absent. Outline of guard is elliptical with apical line ventrally displaced, and growth lines more closely spaced in ventral sector. Dl_{max}: 22.8 mm; Dv_{max}: 20.7 mm. Magnification x 3.

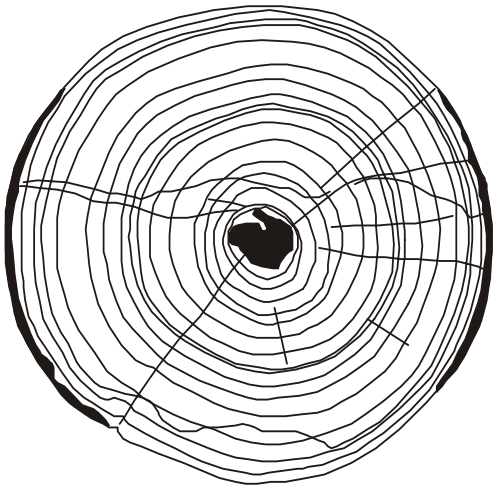

Figure B. 4. 3 *Peratobelus oxys* Tenison-Woods. SAM P19239, Bulldog Shale, southern Eromanga Basin. Transverse section at point of maximum inflation, of immature specimen with apical canal centrally placed. The guard outline is elliptical. No grooves are evident as section is in posterior stem sector were ventro-lateral grooves are lacking. Dl_{max}: 15.1 mm; Dv_{max}: 14.5 mm. Magnification x 4.

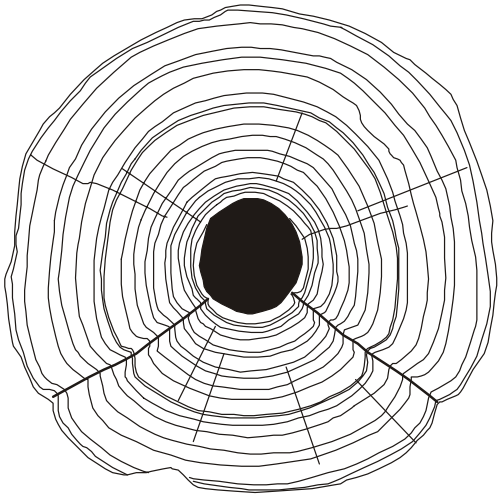

Figure B. 4. 4 *Peratobelus oxys* Tenison-Woods. QGS F8775, Wallumbilla Formation, Carpentaria Basin. Subcircular transverse section in posterior alveolar region, showing incised ventro-lateral grooves. Dl_{max}: 22.1 mm; Dv_{max}: 21.9mm. Magnification x 2.5.

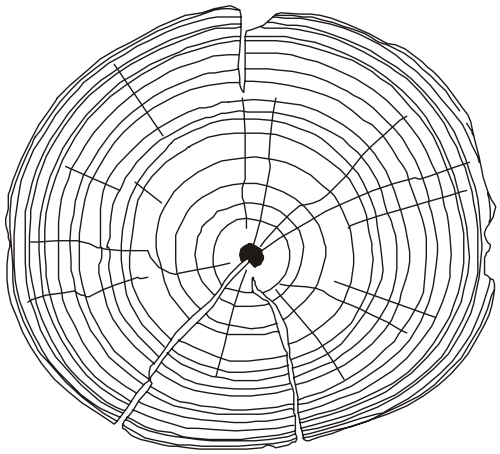

Figure B. 4. 5 *Peratobelus oxys* Tenison-Woods. JCU F11637 L912, Jones Valley Member, Eromanga Basin. Section in posterior of stem region showing slight ventral offset of apical canal. Outline is semi elliptical and slightly depressed. Dl_{max}: 19.3 mm; Dv max: 17.7 mm. Magnification x 2.7.

Discussion: It is now apparent that specimens used by Phillips (1870) in the establishment of *Belemnites australis* are conspecific with *P. oxys.* Phillips had a confused concept of *Belemnites australis*, including in it Albian *Dimitobelus diptychus* (McCoy, 1867a) as illustrated in his plate 16, figures 3, 4. The specimen in this illustration was largely the basis of his description of *B. australis* which notes in particular a hastate shape and the curved character of its ventro-lateral grooves. Also included in *B. australis* was the specimen illustrated in his plate 16, figures 1, 2, a large and robust, cylindroconical guard characterised by straight ventro-lateral grooves which extend only as far as the stem region. The latter has been taken by most subsequent authors as representing *P. australis* and the specimen on which the illustration was based was designated as the lectotype by Day (1967b, p. 6). A small, immature guard with part of a clearly chambered phragmocone attached (his plate 16, figures 6, 6a, 6b) was referred by Phillips to *Belemnites paxillosus* Schlotheim. Subsequently Tate (Tate, 1889, p. 229) considered it to represent a new species which he named *Belemnites eremos.* Both the designated lectotype of *B. australis,* and this specimen, represent *P. oxys,* fitting within the range of variation now established for this taxon. In particular the lectotype shows the shape and diagnostic straight ventro-lateral grooves of *P. oxys*. It shows a blunt apex, somewhat unusual for this species, but within the range of variation known for it. All of Phillips' material is missing, apparently lost in the `Garden Palace fire' which affected Sydney in 1882 as noted by Day (1969).

It might be argued that *P. australis* has priority over *P. oxys*. However, given that the description of *P. australis* was largely based on a specimen of *Dimitobelus diptychus* (McCoy, 1867a), that the type material is missing, and that the name *oxys* has been very widely used in the literature including being designated as the type species of *Peratobelus*, Phillips' name is not employed here. An appropriate action would be an application to the Commission of Zoological Nomenclature to have the name *australis* suppressed.

Previously phragmocones of this species have been referred to *Peratobelus selheimi* whereas guards have been assigned as *P. oxys*. Both commonly occur together, such as in the Doncaster Member of the Wallumbilla Formation exposed along the Walsh and Flinders Rivers in north Queensland, in the vicinity of Bungeworgorai Creek, southern Queensland and at Primrose Springs on Peake Station in South Australia. Very few specimens show both guard and phragmocone and where this is the case, the guard is almost always just a small fragment and/or is obscured by matrix. However, a key specimen, QM F14320, shows a substantially complete guard as characteristic of *P. oxys* and most of a phragmocone as characteristic of *P. selheimi*. It is clear that these two separately named elements belong to a single species.

Publications by Tenison-Woods establishing *Belemnites oxys* and *B. selheimi* both date from 1883. *B. oxys* is taken as the senior subjective synonym because a cast of the lectotype, a guard, is available for it. Given that belemnite species are universally diagnosed on guard characteristics, this specimen is more useful in species definition than the original of *P. selheimi* which is a phragmocone. The original specimens on which the two species were erected have both been lost and there is no replica available of that on which *B. selheimi* was based. An additional consideration in applying priority in this case is that *P. oxys* is the type species of *Peratobelus* and its retention as a species category is in the interests of nomenclatural stability.

The large phragmocone from Wallumbilla described by Philips (1870) undoubtedly must be *B. oxys* (= *selheimi*), "counting above forty septa; with the whole number must have been fifty, without reaching the last chamber… the phragmocone is nearly straight, with an angle of 18°". Clarke (1862) named a specimen from the

same locality as *B. barklyi*, for which McCoy (1866) wrote "a large species…..nearly related to the gigantic species of the Lower Oolite and Lias of Europe, but which cannot be fully characterised from the present specimen, as all the posterior portion of the guard is broken away". Etheridge (1892) suggested that this specimen is very likely to represent *B. selheimi*. However, Clarke's specimen was not figured and cannot be identified in contemporary collections. *B. barklyi* is therefore a *nomen dubium*.

The lectotype cast of *P. oxys*, AM L1574, represents a substantially complete, robust guard as figured by Tenison-Woods (Tenison-Woods, 1883a, pl. 13, figs 1-3), and refigured by Etheridge (Etheridge, 1902a, pl. 6, figs 4-6), apart from the apex which is missing, and shows the characteristic straight ventro-lateral grooves. A number of other guards are similarly robust and show an acute, attenuated apex as figured by that author. However, other specimens are more slender, ranging to AM F37172 and QMF33178 for which the maximum diameter is only one tenth of the full guard length, compared to some seven times the full length of robust morphs. The slender forms have an unusually long, gradually tapered apical region. There is continuous variation in these attributes, similar to that shown by *Dimitobelus stimulus*. This suggests that the animals of some belemnite species showed variation in length for the same body weight to which the buoyancy and trim imparted by the skeleton related. Variation in the shape of the apical region is also evident, with some morphs being less sharply pointed than others as shown by the range of apical angle. Some morphs show the alveolar region as a little more slender than the stem, imparting a weakly hastate outline to the guard, which could possibly be an ontogenetic feature.

The outer wall of the phragmocone is thin and is not fully preserved on specimens free from matrix. These invariably show the internal septa which were very regularly inserted, becoming progressively more widely spaced as growth proceeded. The largest phragmocone, AM F175, had a length of some 14 cm and there are a number of fragmentary specimens of equivalent size. QMF 33175 shows a complete phragmocone some 6 cm in length associated with the alveolar region of the guard which has a diameter of 9 mm. Using these measures to scale, on the basis that

the phragmocone is has a near-perfect conical form, the large phragmocones would have been associated with guards some 2 cm in diameter as is the case for the largest specimens in the collection, including the lectotype replica. Thus guard and phragmocone were of similar lengths and the total skeletal length of guard plus phragmocone combined would have been close to 20 cm when growth was complete.

Fossil occurrence for *P. oxys* shows that post-mortem separation of guard and phragmocone was clearly the norm. This suggests that buoyancy of the phragmocone persisted through destruction of the soft tissues and that it was not firmly attached to the guard. It is surmised that when the skeleton was exposed some time after death, the retained buoyancy of the phragmocone caused its separation from the guard with subsequent transport until the chambers became flooded, settlement occurred and fossilisation commenced.

Willey (1972, fig. 3d) assigned a specimen from south-east Alexander Island, Antarctica, as *P. oxys*. This probably also applies for the partially preserved specimen he referred to *Dimitobelus macgregori* (Glaessner). It is certainly the case for the specimen figured by Willey (1972, figs. 3a, b) as *Dimitobelus* sp. aff. *D. macgregori* (Glaessner) which has a guard shape and straight, undeflected ventro-lateral grooves terminating in the stem region as typical of *Peratobelus oxys*. The Alexander Island specimens assigned by Doyle (1987a) as *P*. cf. *oxys* are considered here as definite representatives of this species.

P. oxys is readily distinguished from *P. bauhinianus* Skwarko which is decidedly smaller at maturity (Figure B. 4. 6), with a generally less robust form, and has the ventro-lateral grooves extending onto the apical region and show a clear deflection towards the dorsum in their distal reach.

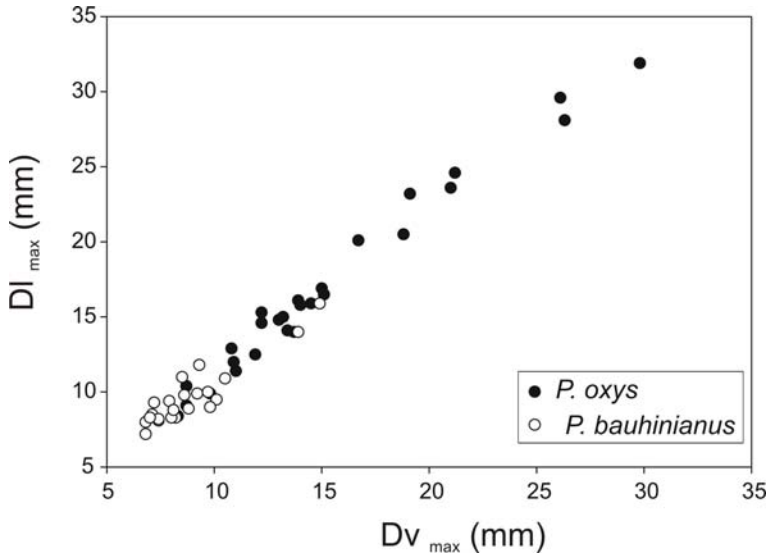

Figure B. 4. 6 Relationship of maximum diameters in *Peratobelus* species. *P. oxys* guards are typically more compressed and can grow to be much longer specimens than *P. bauhinianus*.

Distribution and Age: Within the northern Eromanga and Carpentaria Basins, *P. oxys* is well known from the late Aptian Doncaster and Jones Valley Members of the Wallumbilla Formation. It occurs in the Minmi Member of the Aptian Blythesdale Formation of the Surat Basin and in the Maryborough Formation of the Maryborough Basin of coastal southern Queensland. It is also extensively represented in the Aptian Bulldog Shale, of the south-western Eromanga Basin. Occurrences have also noted near Aramac in the northern Eromanga Basin from at the base of the Coreena Member, a lower division of the Albian Doncaster Formation. However these are considered as due to reworking from underlying Aptian strata as they are associated with Albian *Dimitobelus diptychus* in `belemnite conglomerates' formed on an omission surface (Day, 1969). The species is also known from Aptian strata of the Antarctic Peninsula.

Peratobelus bauhinianus Skwarko

Pl. 1, figs. 1-5

Synonymy:

?1964 *Peratobelus australis* (Phillips); Day, table 3.

1966 *Peratobelus* (?) *bauhinianus* Skwarko, p. 124, pl. 15, figs. 7-11.

?1966 *Dimitobelus* (?) *youngensis* Skwarko, p. 125, pl. 15, figs. 1-6, 12..

1967b *Peratobelus australis* (Phillips); Day, p. 6, pl. 1, figs. 22, 23; text-fig. 1a-d.

?1972 *Peratobelus* aff. *australis* (Phillips); Willey, p. 38, fig. 4f.

?1987 *Peratobelus* (?) sp.; Doyle, p. 155, p. 21, fig. 7.

1998 *Peratobelus forsteri* Doyle; Henderson, p. 119.

Type Specimens: Holotype CPC 4795, west of Borroloola, Northern Territory, Mulliman Beds, 16°06'S, 136°05'E. Paratypes CPC 4797, 4799, west of Borroloola, Northern Territory, Mulliman Beds, 16°06'S, 136°05'E; CPC 4796, 4798, WSW of Borroloola, Northern Territory, Mulliman Beds, 16°08'S, 136°02.5'E.

Material: Approximately 300 specimens.

Northern Eromanga Basin, Queensland: QM F27909-F27915, Rosevale, south of Muckadilla, 26°40'S, 148°25'E; UQ F30495 l1819, western cliff of Bungewogorai Creek, Doncaster Member, 26°36'S 148°42'E; UQ F61084, 61086-7, 200 yards from the southern side of Warrego Highway, 100 yards west of Bungeworgorai Creek, Doncaster Member, 26°36'S, 148°42.5'E; QM F2030 Maranoa River, Mitchell, 26°28'S, 147°58'E; JCU L912 (2 specimens) Flinders River, east of Glendower homestead, Jones Valley Member, 20°41'S, 144°34'E; JCU L909 (5 specimens) Glendower Station, Flinders River, Doncaster Member 20°41'S, 144°33'E.

Southern Eromanga Basin, South Australia: SAM P3023 Lake Eyre, 28°14°S, 136°35'E; SAM P19612 (2 specimens) and P21362, `the shelly patch', Cooper Pedy, 28°56°S, 134°45'E. AM F9214-15, 9926-7, F10004, White Cliffs, western N.S.W, 30°50'S, 143°05'E.

Carpentaria Basin, Queensland: QGS F8431, east Bank of Walsh River, 0.6 mls north of Boomers Hole, Wallumbilla Formation, 16°32'S, 143°47'E; JCU F8109 L169, Boomers Hole, Wrotham Park Station, Wallumbilla Formation, 16°40'S, 144°00'E.

Carnarvon Basin, Western Australia: WAM 62.194 (approximately 50 specimens), Murchison River district, Windalia Radiolarite, 27°36'S, 114°12'E; WAM 65.1159 (approximately 50 specimens), 20 miles west of Binnu via Geralton, Windalia Radiolarite, 28°02'S, 114°40'E; WAM 68.470, surface rock 10 miles East of Kalbarri, Windalia Radiolarite, 27°47'S, 114°21'E; WAM 69.25 (approximately 15 specimens), 11 miles from Kalbarri on road to Ajana, undifferentiated Windalia Radiolarite and Birdrong Sandstone, 27°37'S, 114°10'E; WAM 79.3104 (approximately 20 specimens), West Binnu, near junction of West Binnu Road and Yerina Springs Road, Windalia

Radiolarite, 28°02'S, 114°36'E; WAM 81.1946, Twelve Mill Hill, east of Kalbarri, Windalia Radiolarite 27°41'S, 114°12'E; WAM 83.633/9 (7 specimens),scree at base of west side of Windalia Hill, Windalia Radiolarite 23°16'S, 114°48'E; UWA F92.6 Ajana, track heading south from Yuna, Windalia Radiolarite, 27°57'S, 114°36'E; GSWA Barrabiddy 1, see Appendix A. 1, undifferentiated Windalia Radiolarite, 23°49′57″S, 114°20′E; GSWA Boologooro 1, see Appendix A. 2, Windalia Radiolarite, 24°19′27.3″S, 113°53.3″E; GSWA Edaggee 1, see Appendix A. 3, Windalia Radiolarite, 25°21′27.0″S, 114°14′04.9″E; GSWA Yinni 1, see Appendix A. 4, Windalia Radiolarite, 26°03′22.8″S, 114°48′58.5″E.

Money Shoals Basin, Northern Territory: JCU F1297-13001, 13003-13022,13024-13025,13027-13030, 13036, Imaluk Beach, Cox Peninsula, Darwin Formation, 12°26.5'S, 130°46'E.

Other: UQ F35511, F35606 Minmi Shell Bed Gully, 1/4 mile NE of Minmi crossing, Minmi Member, Surat Basin, N.S.W., 16°29'S, 143°50'E.

Diagnosis: Medium sized, moderately slender, slightly hastate *Peratobelus* with long ventro-lateral grooves that extend onto the apical region and are initially straight but dorsally deflected in the stem region.

Description: Guard of medium size, reaching lengths of about 10 cm, elongate and slender with the length some eight times the maximum width. Outline and profile cylindroconical to weakly hastate, profile symmetrical. Cross-section subcircular to very slightly oval and depressed (Figures B. 4. 7 and B. 4. 8) with the axis of maximum width located at the base of the stem region. Apical region typically attenuated, almost conical and sharply pointed with an apical angle of 12-20°; may be less sharply pointed with curved margins seen in profile with apical angles ranging to 30°; apex central or slightly offset towards the venter. Ventro-lateral grooves long, narrow, deeply incised but becoming less so towards the posterior. They extend from the anterior margin to the anterior part of the apical region. They are straight and subparallel on the alveolar region and anterior part of the stem, where they mark the edge of the venter. On the posterior stem and apical region they weaken and are deflected dorsally. Axial line is subcentral and commonly excavated as a canal.

Alveolus penetrates about one third of the guard length; phragmocone conical, slightly offset towards the dorsum with the siphuncle at its ventral margin.

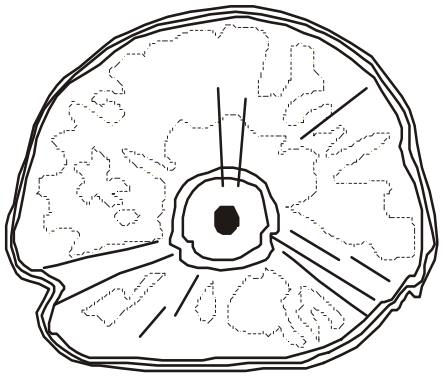

Figure B. 4. 7 *Peratobelus bauhinianus* Skwarko. WAM 65.1159, Windalia Radiolarite, Carnarvon Basin. Transverse view shows ventro-lateral grooves and ventrally offset apical canal. The guard section is elliptical with a slightly flattened ventral surface. Internal microstructure and growth lines lost due to diagenetic overprint. Dl_{max}: 9.6 mm; Dv_{max}: 7.9 mm. Magnification x 5.5.

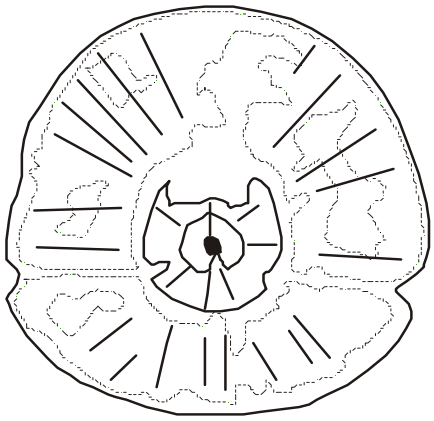

Figure B. 4. 8 *Peratobelus bauhinianus* Skwarko. WAM 62.194, Windalia Radiolarite, Carnarvon Basin. Subcircular transverse section of juvenile specimen showing clear ventro-lateral grooves and of the apical canal slightly offset towards the venter. Internal microstructure and growth lines lost due to diagenetic overprint. Dl_{max}: 9.2 mm; Dv_{max}: 9.0 mm. Magnification x 6.

Dimensions: in millimetres (mm)

	L	**X**	**Dl_{max}**	**Dv_{max}**
JCU F13002	25.5	10.0	-	7.5
WAM 65.1159d	33.7	24.2	8.1	7.4
UQ F35511	36.2	19.7	9.5	10.1
WAM 65.1159c	39.1	18.1	9.8	8.6
WAM 62.194c	39.8	16.1	7.2	6.8
JCU F13025	40.0	15.0	11.5	11.0
WAM 62.194h	40.0	13.4	8.0	6.8
WAM 65.1159b	40.9	17.9	8.5	7.1
WAM 62.194e	43.0	17.9	8.2	7.4
WAM 65.1159a	44.9	26.9	11.8	9.3
WAM 62.194b	44.6	17.9	8.3	8.2
WAM 62.194 g	45.0	18.0	8.3	7.0
WAM 62.194d	45.2	15.9	9.3	7.2
WAM 69.25d	46.0	26.2	9.9	9.2
WAM 62.194f	46.6	19.1	8.3	8.0
WAM 62.194i	47.2	19.0	9.4	7.9
QGS F8431	47.2	27.3	8.9	8.8
WAM 62.194a	48.1	21.2	8.8	8.1

WAM 69.25c	50.6	33.3	11.0	8.5
AM F10004	59.0	26.8	11.1	11.0
UQ F30495	59.4	50.9	15.9	14.9
WAM 83.638	60.8	23.2	10.0	9.7
WAM 69.25b	60.9	40.6	10.9	10.5
SAM P3023	63.2	38.1	20.9	18.7

Discussion: This species of *Peratobelus* has been much confused with *P. oxys* as discussed above. There has been a long history of collection of distinctively slender Aptian belemnites from the Walumbilla Formation and correlative units of the Eromanga Basin but the first available specific name that can be utilised is *P. bauhinianus* which was applied by Skwarko (1966) to a small collection from a single locality near Borroloola in the eastern Northern Territory. Its morphology is clearly represented by a suite of well preserved moulds from the Darwin Formation of the Bathurst Island Group exposed around Darwin Harbour, Northern Territory, where it occurs prolifically in a belemnite bed within a thin Aptian interval as reported by Henderson (1998). The poorly preserved moulds described by Skwarko (1966) as *Peratobelus* (?) *bauhinianus* are from an Aptian horizon within his `coastal suite' of the Mulliman Beds. Strata of this suite are best considered as an inland extension of the Bathurst Island Group (Henderson, 1998). Thus the type series of *Peratobelus* (?) *bauhinianus* is from a stratigraphic horizon that is close to that of the belemnite bed at Darwin Harbour from which much better material is available. The poorly preserved moulds also from the Mulliman Beds assigned as *Dimitobelus* (?) *youngensis* by Skwarko (1966) are likely to be conspecific with *B. bauhinianus*. They have the same slender form, cross-sectional shape and grooves but the apex is unusually blunt. *P. bauhinianus* is extensively represented by collections from the Windalia Radiolarite (Aptian) of the Carnarvon Basin but preservation is generally poor.

The species shows variation in guard inflation, cross-sectional shape (Dl_{max}:Dv_{max} 1.1-1.3), the shape of the apical area, and the degree to which hastation is developed. Even so, it is a distinctive taxon. It is closely related to *P. foersteri*, described from the Aptian of southern Mozambique by Doyle (1987b). The Mozambique species however has a subquadrate cross-section, with a flattened venter, whereas *P. bauhinianus* has a more rounded cross-sectional outline.

Distribution and Age: This species is widely represented in the late Aptian Wallumbilla Formation of the northern Eromanga and Carpentaria basins. It also occurs in Aptian strata of the south-western Eromanga Basin; only old collections are available but these are likely to have come from the Bulldog Shale. It the characteristic macrofossil of the Windalia Radiolarite which is assigned an Aptian age. A single fragmentary guard from the underlying Munderong Shale (late Barremian) probably represents *B. bauhinianus* but is too incomplete for reliable identification. The species is common in the lower, Aptian, part of the Darwin Formation of the Money Shoals Basin in the Northern Territory and is also known from correlative horizons of the Mulliman Beds.

EXPLANATION OF PLATE 1

Each numbered group illustrates from left to right: ventral outline, profile and dorsal outlines, unless otherwise stated.

Figures 1-5. *Peratobelus bauhinianus* (Skwarko). 1, QGS F8431 x 1, Blackdown Formation, Aptian, Laura Basin. 2, UQ F35606 x 1, Minmi Member, early Aptian, Carpentaria Basin. 3, UQ F61086 x (.75), Doncaster Member, Aptian, north-eastern Eromanga Basin. 4, WAM 62.194 x 1, Windalia Radiolarite, Aptian, Carnarvon Basin. 5, UQ L240 x 1, mould of profile, Maryborough Formation, Aptian, Maryborough Basin.

Figures. 6-7. *Peratobelus oxys* (Tenison-Woods). 6, UQ F12980 x (.75), Doncaster Member, Aptian, north-eastern Eromanga Basin. 7, internal mould, UQ F64860 x (.75), Doncaster Member, north-eastern Eromanga Basin.

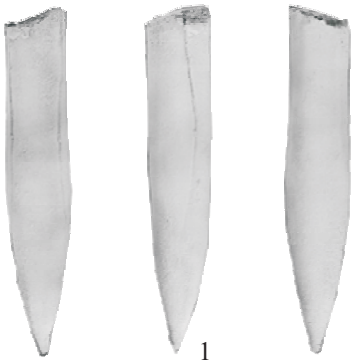

1

2

3

4

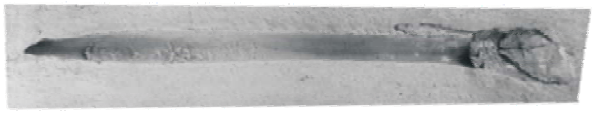

5

6

7

EXPLANATION OF PLATE 2

Each numbered group illustrates from left to right: ventral outline, profile and dorsal outlines, unless otherwise stated.

Figures 1-9. *Peratobelus oxys* (Tenison-Woods). 1, GSSA M2470 x (.75), Bulldog Shale, Aptian, southern Eromanga Basin. 2, longitudinal section, QM F43847 x (.75), Doncaster Member, Aptian, north-eastern Eromanga Basin. 3, Lectotype UQ F35523 x (.75), Doncaster Member, Aptian, north-eastern Eromanga Basin. 4, UQ F61087 x (.75), Doncaster Member, Aptian, north-eastern Eromanga Basin. 5, longitudinal section, QGS F1374 x (.5), Doncaster Member, Aptian, north-eastern Eromanga Basin. 6, lateral and inner profile, QM F16432 x (.5), locality unknown, Aptian, north-eastern Queensland. 7, phragmocone only, QM F5757 x (.5), Doncaster Member, Aptian, north-eastern Eromanga Basin. 8, phragmocone only, QGS F8324 x (.5), Blackdown Formation, Aptian, Laura Basin. 9, QM F33176 x (.5), Blackdown Formation, Aptian, Laura Basin.

1

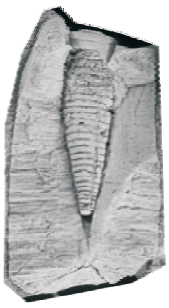

2

3

4

5

6

7

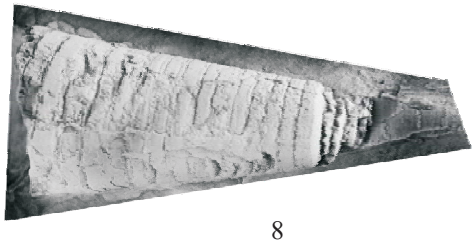

8

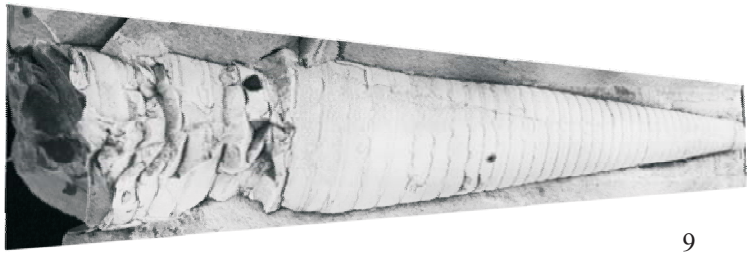

9

SECTION C

Strontium-isotope stratigraphy of the Aptian – Cenomanian in Australia

Section C. Strontium-isotope stratigraphy of the Aptian - Cenomanian in Australia

C. 1 Abstract

$^{87}Sr/^{86}Sr$ analyses are presented for a suite of belemnite guards from the Aptian-Albian sequence of the northern Eromanga Basin and the Barremian-Cenomanian sequence of the Carnarvon Basin. Additional analyses were obtained for selected Aptian and Albian stratigraphic horizons in the southern Eromanga, Carpentaria and Laura Basins. Cathodoluminescence and trace element geochemical protocols were employed to ensure that the samples selected for analysis were free of diagenetic modification. Strontium-isotope ratios plotted for the Carnarvon Basin and a composite curve for the east Australian platform permit close correlation of their lithostratigraphic successions. These are then calibrated against the international Cretaceous time scale by comparison to the previously established global strontium curve. The calibration confirms disconformities in both successions across the Aptian-Albian boundary as has been recognised from biostratigraphic research. It indicates that some adjustments are required to the ages of some dinocyst biozones of importance in the Australian Early Cretaceous timescale. The *Muderongia australis*/*Odontochitina operculata* boundary is late Barremian, the *Odontochitina operculata*/*Diconodinium davidii* boundary is diachronous, being early Aptian in the succession of the Carnarvon Basin and late Aptian in that of the Eromanga Basin. The *Pseudoceratium ludbrookiae* Zone is long ranging, extending across the late Albian and into the Cenomanian. A small but persistent offset in Albian strontium-isotope ratio values for samples from the east Australian platform relative to those from the Carnarvon Basin is attributed to the influence of siliceous volcanism along the east Australian margin. Eustatic trends for the epeiric sea related to the east Australian platform succession and the western continental shelf, represented by the Carnarvon Basin succession, are closely matched in time. The negative excursion shown by Aptian strontium-isotope values is correlative with transgressive marine inundation of the Australian continent, consistent with the enhanced generation of new ocean floor as the driving mechanism for both sea-level rise and the isotopic trend. A positive excursion for the Albian, also associated with transgression, is attributed to global warming and an enhanced continental strontium flux due to weathering.

C. 2 Introduction

Since the pioneering work of DePaolo and Ingram (1985), Elderfield (1986), Veizer (1989) and McArthur (1994), Sr-isotope stratigraphy has been widely applied to chronostratigraphic correlation in the Phanerozoic and is well documented for most of the Cenozoic (Hodell et al., 1989; Hodell et al., 1990) and Late Cretaceous (DePaolo and Ingram, 1985; Hess et al., 1986; Richter and DePaolo, 1988; McArthur et al., 1993).

The main reasons for the variability of marine-carbonate Sr-isotope ratios over geological time are well understood (Hedge and Walthall, 1963; Veizer and Compston, 1974; Palmer and Elderfield, 1985; Elderfield, 1986; Hess et al., 1986). Secular variation in $^{87}Sr/^{86}Sr$ of seawater may be caused by a change in input from riverine (continental fluxes; $^{87}Sr/^{86}Sr$ ~ 0.712) and/or hydrothermal activity (mantle fluxes; $^{87}Sr/^{86}Sr$ ~ 0.703). Fluxes are dependent on a range of factors such as; continental erosion, isotopic composition of eroding continental rocks, configuration and topographic relief of continents, extent of continental inundation by epeiric seas, and variations in both climate and palaeo-oceanographic conditions, volcanic activity, rate of seafloor spreading, and the hydrothermal flux from mid-ocean ridges. During the Jurassic and Cretaceous isotopic trends appear to have been strongly influenced by plate tectonics and sea floor spreading (Berner and Rye, 1992) when variations in hydrothermal flux controlled the overall trends of the curve (Ingram et al., 1994; Jones et al., 1994a).

Strontium-isotope stratigraphy depends on three premises: (1) the residence time of Sr in the oceans is long compared to the mixing time of the oceans, so the isotopic composition of Sr in the oceans is uniform at any given time; (2) when marine carbonates precipitate, they incorporate Sr from coexisting seawater without isotopic fractionation; and (3) once incorporated into marine carbonates, providing the primary mineralogy is unchanged the Sr isotopic contents are tightly bound and retained with the low Rb/Sr ratio of these minerals thereby prohibiting significant change in their Sr isotopic composition over geological time.

This paper examines the Sr-isotope record of Australian Early Cretaceous sequences with the intent of improving their correlation to the international timescale standard (Ogg et al., 2004). It is based on isotopic signatures in belemnite guards that provide an excellent basis for such study due to their abundance, extensive stratigraphic representation, and pristine mineralogy. Jones et al. (1994b) and Jones and Jenkyns (1994b; 2001) successfully used belemnites to determine the detailed evolution of Sr-isotopes for Northern Hemisphere Jurassic and Cretaceous seawater. Previous Sr-isotope analyses undertaken on Early Cretaceous biogenic carbonate from

high latitudes in the Southern Hemisphere include the studies of Price and Grocke (2002) and McArthur et al. (2004). Data is presented, analysed and interpreted in this the first Sr-isotope study on the Early Cretaceous System of Australia.

This study presents data on Sr isotopic trends from two large-scale elements of the Early Cretaceous System in Australia: the epeiric stratigraphic assemblage of eastern Australia and the continental margin stratigraphic succession of Western Australia. It seeks to employ Sr-isotope stratigraphy to evaluate continent-wide correlation of the Early Cretaceous Australian timescale based on biostratigraphy and also to evaluate correlation of the Australian biostratigraphic zonation with the international Early Cretaceous timescale.

C. 3 Stratigraphic context of the Australian Cretaceous System

The Cretaceous System is extensively represented in Australia, occupying much of the continent and providing an important palaeoenvironmental record for the mid to high southern latitudes in the Early Cretaceous. The Cretaceous break-up of Gondwana resulted in the general development of passive margin assemblages on the borderlands of continental Australia. In addition, a very extensive basinal system of epeiric character developed in response to general subsidence of the eastern continental sector (Gurnis et al., 1998). During this time Australia was located in mid to high palaeo-latitudes of 35-68°S (Li and Powell, 2001).

The Cretaceous System represented by Australian passive margins is best known from the Carnarvon Basin, especially its onshore southern part (Figure C. 3. 1). Development of this margin is related to the separation of India from Western Australia in the Valanginian at 132.5 Ma (Veevers et al., 1991). The rapid development of the Indian Ocean was accompanied by a series of marine transgressions on the continental borderlands, which culminated in major marine flooding during the Aptian-Albian.

Figure C. 3. 1 Map with present coast line of Australia showing locations of Cretaceous epi-continental basins referred to in this paper: (A) Carnarvon, (B) Carpentaria, (C) Laura and (D) Eromanga.

The southern Carnarvon Basin (Hocking et al., 1994) formed a stable platform during the Cretaceous, overlying Paleozoic sedimentary successions and on-lapping the Precambrian craton to the west. Its succession (see Figure C. 8. 2) is best known from a suite of stratigraphic wells drilled in the last decade by the Geological Survey of Western Australia (GSWA) and collaborators (Figure C. 3. 2). A marine transgression across the platform during the Barremian-Aptian interval deposited units that have since undergone very little burial and remain largely undeformed (Taylor and Haig, 2001). The succession includes a basal sand unit, the Birdrong Sandstone (less than 10 metres thick) lying unconformably on older rocks; an argillaceous unit, the lower Munderong Shale (12-38 metres thick) representing maximum marine flooding for the initial transgressive cycle; and an upper sand unit, (10-32 metres thick, Windalia Sand Member of the Munderong Shale). During the late Aptian, the Windalia Radiolarite (30-47 metres thick), a distinctive siliceous radiolarian-rich siltstone, was deposited as a low stand systems tract. It is overlain by the Gearle Siltstone (early Albian to late Cenomanian and between 20 and 95 metres thick), consisting of laminated pyritic mudstone and siltstone with abundant belemnites, indicative of renewed transgression.

On the eastern part of the continent a vast Jurassic–Early Cretaceous epeiric system, generally termed the Great Artesian Basin, flooded in the Early Cretaceous. Inundation may have begun as early as the Barremian (~125 Ma) and terminated with a latest Albian-Cenomanian regression, out-of-phase with the global sea-level curve (Frakes et al., 1987; Haq et al., 1988). The marine episode represents a depositional cycle extending over 30 m.y., with peak flooding recognized during the early late Albian (Frakes et al., 1987; Haig and Lynch, 1993; Henderson, 2004).

The system represents a little disturbed intracratonic sedimentary assemblage. Basement structural highs separate four basinal subdivisions of the platform: the Laura, Eromanga, Carpentaria and Surat Basins (Palfreyman, 1984; Veevers, 1984: see Figure C. 2. 1). Although each of the basins has a discrete lithostratigraphic framework many of the stratigraphic units are remarkably continuous.

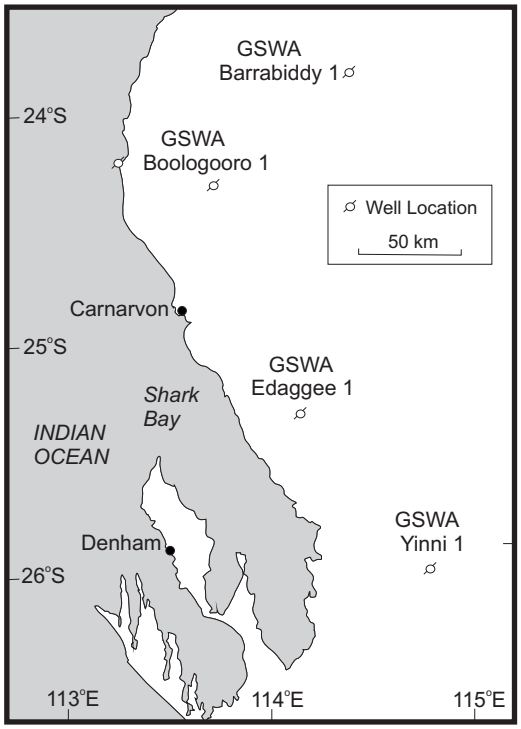

Figure C. 3. 2 Map showing the location of stratigraphic wells GSWA Barrabiddy 1, GSWA Boologooro 1, GSWA Edaggee 1 and GSWA Yinni 1 within the onshore Carnarvon Basin that furnished belemnites used in strontium-isotope analysis (modified from Haig et al., 2004).

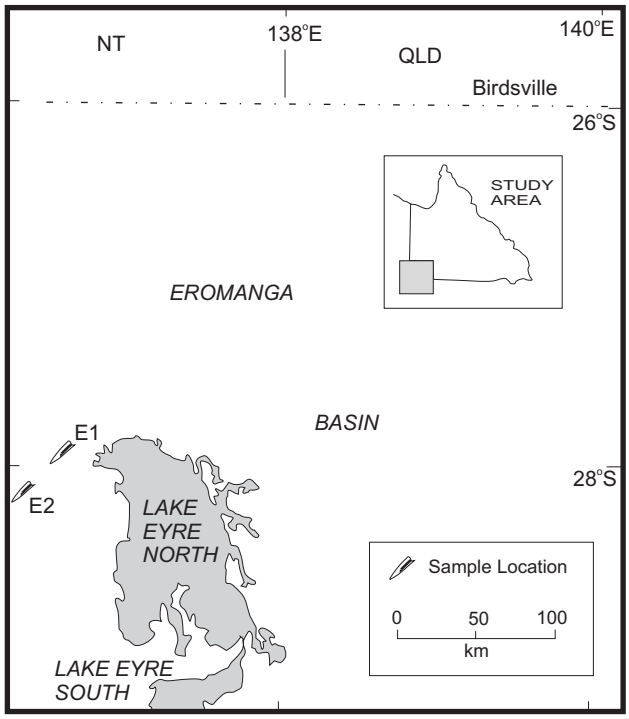

Figure C. 3. 4 Location of surface belemnite samples used for Sr-isotope analysis in the southern Eromanga Basin (modified from Kreig et al., 1995).

The lithostratigraphic succession of the Eromanga Basin (Figure C. 3. 3) is extensively expressed by surface outcrop as documented by regional mapping. Cretaceous strata from the southern Eromanga Basin are documented from surface outcrops (Figure C. 3. 4) with the basal unit represented by the Cadna-owie Formation. This is overlain by the Bulldog Shale, Coorikiana Sandstone and the Oodnadatta Formation.

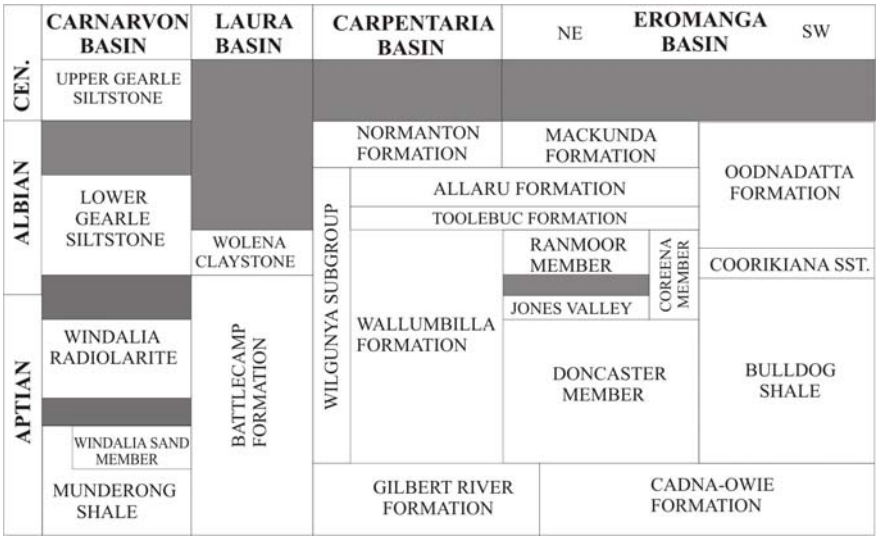

Figure C. 3. 3 Aptian-Albian lithostratigraphic units recognised in Cretaceous onshore basins of Australia (modified from Haig and Lynch, 1993). Correlations are based on global and Austral biostratigraphic ammonite and microfossil zonations (see also Figure C. 9. 2).

Detail of the succession from the northern Eromanga Basin is best provided by stratigraphic core holes, and a useful composite section is also provided by outcrop along the Flinders River east of Hughenden (Figure C. 3. 5 B).

For the northern part of the basin the Cretaceous section begins with sandstone of the Gilbert River and Cadna-owie Formations (15-110 metres thick) which have been assigned as Neocomian on the basis of palynology (Burger and Shafik, 1996). The Wallumbilla Formation, some 185-253 metres thick, follows with its lower part, a thick mudstone unit, comprising the Doncaster Member (120-150 metres thick). This is succeeded by a distinctive glauconitic sandstone interval 5-8 metres in thickness, the Jones Valley Member. These units have been assigned to the Aptian based on diverse biostratigraphic evidence (Henderson et al., 2000) and were deposited during a

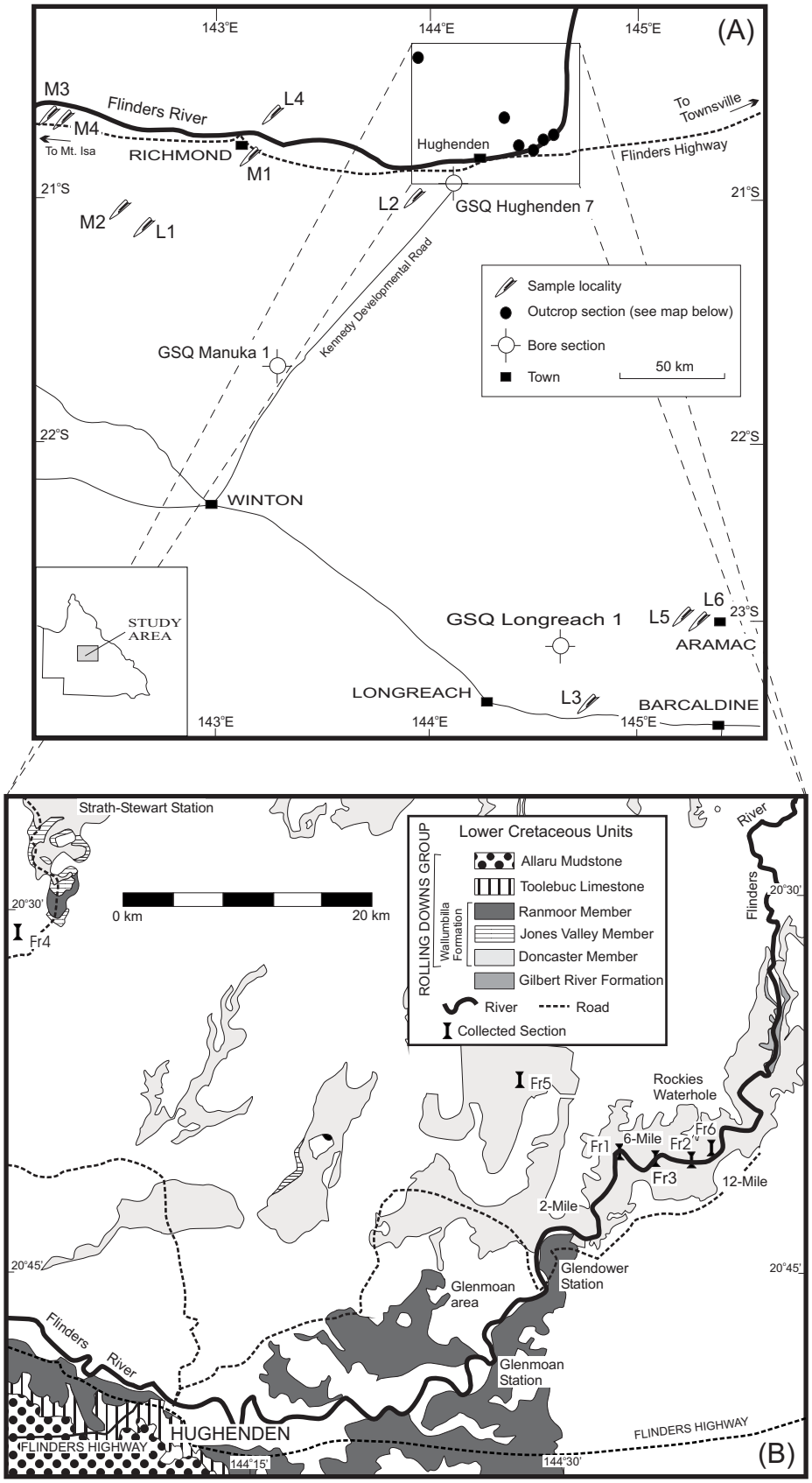

Figure C. 3. 5 (A) North-eastern Eromanga Basin showing locations of reference stratigraphic wells plus key sections and localities that furnished belemnites for strontium-isotope analysis. (B) Detail of the Hughenden/Flinders River area showing Early Cretaceous rock units and key sections (modified from Campbell and Haig, 1993).

transgressive regime (Day, 1969; Frakes et al., 1987). The upper part of the Wallumbilla Formation, the Ranmoor Member (60-95 metres thick), marks a significant late early Albian transgressive pulse, also represented by the lower Gearle Siltstone of the Western Australian Carnarvon Basin (Haig et al., 1996).

The Toolebuc Formation (6-25 metres thick) follows and is succeeded by mudstone of the Allaru Formation (45-120 metres thick). For the southern Eromanga Basin, as represented in South Australia, the Bulldog Shale and Oodnadatta Formation are considered to be correlative with the Wallumbilla Formation and Toolebuc Formations plus the Allaru Formations respectively (Krieg, 1995). The Toolebuc-Allaru interval has been assigned to the late Albian based on diverse biostratigraphic evidence (Henderson et al., 2000; Henderson and Kennedy, 2002). A poorly fossiliferous unit, the Mackunda Formation (90-275 metres thick) follows and is considered to be of latest Albian age. During the Cenomanian, non-marine deposition prevailed in the eastern Australian platform as represented by the Winton Formation.

The Cretaceous successions for the northern part of the east Australian platform are poorly known. For the Carpentaria Basin, the Walsh River exposes the lower part of the succession and stratigraphic drilling has provided the best overall documentation of the total sequence. Marine Cretaceous strata of the Laura Basin are poorly known and are documented from a few isolated outcrops from the Laura district (Figure C. 3. 6). The basal unit in the Carpentaria Basin, the Gilbert River Formation, is succeeded by the Wallumbilla, Toolebuc, Allaru and Normanton Formations, largely mirroring the succession of the northern Eromanga basin. For the Laura Basin, the Wolena Claystone succeeds the Battlecamp Formation.

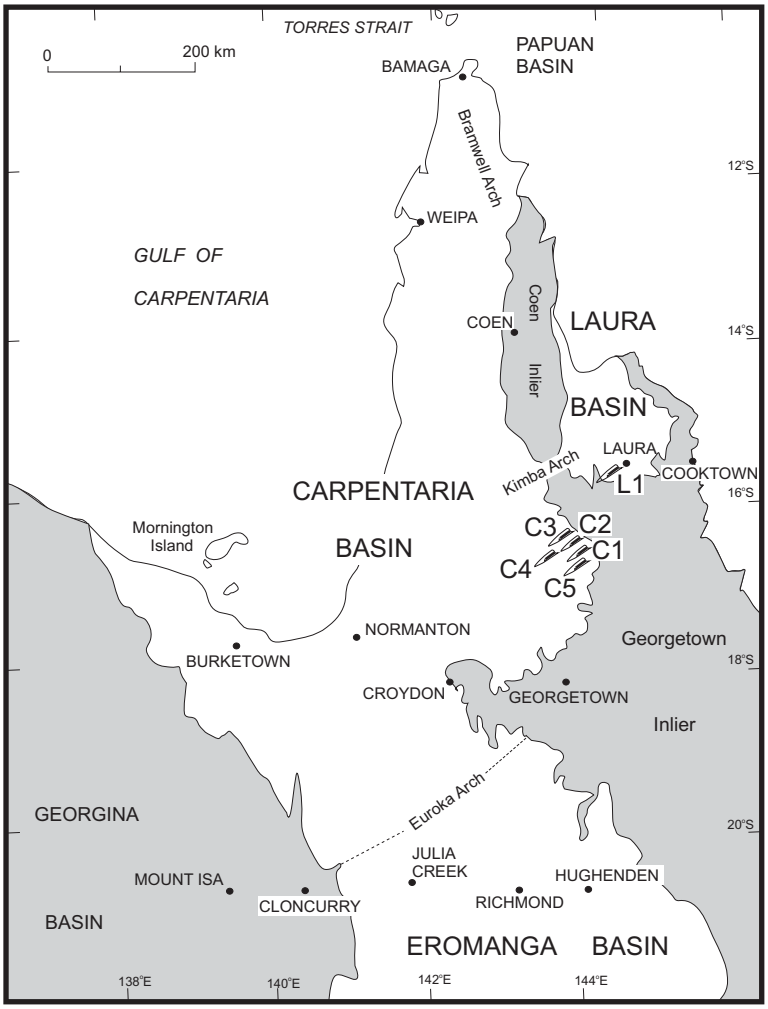

Figure C. 3. 6 Regional setting of the Carpentaria Basin and Laura Basin relative to pre-Mesozoic basement (grey tone) (modified from Smart and Senior, 1980) showing surface sample localities.

C. 3. 1 Biostratigraphic zonation of the Australian Lower Cretaceous System

Molluscan macrofossils are widespread within Australian Cretaceous strata. Ammonites are the most significant macrofossil group but belemnites are also prevalent, as are bivalves. However, no comprehensive biostratigraphic zonation for this group has been developed for Early Cretaceous time.

Macroinvertebrates from the east Australian platform have traditionally been assigned to two Early Cretaceous assemblages, the Roma and Tambo faunas of Whitehouse (1926) with the boundary marked by the top of the Jones Valley Member. A detailed examination of the stratigraphic distribution of shelly faunas by Day (1969) still failed to produce a more detailed zonation. Faunas of the Eromanga Basin are largely endemic but also contain some Tethyan elements (Day, 1969; 1974; McNamara, 1980; McKenzie, 1999).

Northern Territory faunas described by Skwarko (1966; 1983) maybe correlated with these above faunal divisions. Wright (1963) and Henderson (1990) described younger faunas from the Bathurst Island Group as late Albian-Turonian that can be correlated with established Tethyan ammonite zonations. Molluscan fauna of the Early Cretaceous are poorly known from Western Australia.

Drawing on earlier studies from the east Australian platform (Morgan, 1980; Burger, 1982a) and western margin (Backhouse, 1978; Wiseman, 1979; Backhouse, 1987, 1988), Helby et al. (1987) proposed a comprehensive microfloral zonation of the Australian Early Cretaceous which incorporates both palynomorphs and some dinoflagellates. Subsequent investigations suggest that the Helby zonation is robust; it was largely constructed using borehole records from the submerged continental margin and the east Australian platform.

Foraminifera of the Early Cretaceous are dominated by benthic taxa which are largely facies controlled yet may be used for biostratigraphic zonation within specific facies (Haig, 1979b; Haig and Lynch, 1993; Haig et al., 1996). Recognised planktonic

zones are based on *Hedbergella* as documented by Haig (1979b) for assemblages of Aptian-Albian age from the northern Eromanga Basin.

Shafik (1985; 1990; 1994) proposed a nannofossil zonation based mainly on core records from basins marginal to Western Australia including the Rowley and Carnarvon Terraces, and from the epeiric Eromanga Basin. Albian nannofossils from drilled offshore Cretaceous sections are known from the west Australian margin (Bralower and Siesser, 1992; Mutterlose, 1992). In the Eromanga Basin, Albian nannofossil assemblages are sparse. The Tethyan *Prediscosphaera columnata* zone of the middle Albian is represented in the Toolebuc Formation and lowermost Allaru Mudstone (Shafik, 1985).

To date, application of the global Early Cretaceous timescale with respect to Australian sequences has been entirely dependent on biostratigraphic correlation. Palaeobiogeographic provincialism applied to the Australian region during much of the interval (Henderson et al., 2000). As a result, secure correlation of the Australian Cretaceous System to the global reference succession of the Anglo-Paris Basin on which the timescale is based (see Ogg et al., 2004) using ammonites, planktonic foraminifera and nannoplankton has yet to be achieved.

C. 4 Existing chronostratigraphic controls

Stage assignments within the Australian Early Cretaceous System have been achieved through application of the range of biostratigraphic zonation schemes reviewed above. Neocomian stages have been identified largely from dinocysts and palynomorphs. Aptian and Albian stage assignments have been largely made on defined on the basis of molluscs, foraminifera, and dinocysts.

C. 4. 1 Macrofossil age determinations

Bivalves include numerous cosmopolitan genera but many species are endemic and of little use for international correlation. Belemnites belong to the Austral Family Dimitobelidae, unknown from the Northern Hemisphere. Ammonites are dominated by the Family Labeceratidae, which are also restricted to an Austral distribution.

Australiceras, *Tropaeum*, and *Lithancyclus*, part of the `Roma Fauna', occur both in the Doncaster Member (Day, 1969; Day, 1974) of the northern Eromanga succession and Aptian strata of the Anglo-Paris Basin and elsewhere in Europe (Casey, 1960). McKenzie (1999) recognised a distinctive ammonite fauna from the Coreena Member of this succession. It includes members of the Family Hamitidae also represented in the Anglo-Paris Basin where they are of early Albian age.

The Tambo fauna includes *Beudanticeras*, which first appears in the basal beds of the Ranmoor Member (Vine and Day, 1965) of the northern Eromanga Basin succession and is widely regarded as an Albian indicator (Casey, 1961; Wright, 1963; Wright and Kennedy, 1987). The Austral ammonites *Myloceras* and *Labeceras* first appear in the Toolebuc Formation of the northern Eromanga Basin (Day, 1968) and also the more southerly Oodnadatta Formation (Reyment, 1964). Both genera first appear in the ammonite succession of Madagascar (Besaire and Collignon, 1959), East Africa (Spath, 1925; Venzo, 1936) and South Africa (Klinger, 1976) in association with Albian ammonites known from the Anglo Paris Basin.

Henderson and Kennedy (2002) recognised *Mortoniceras (Goodhallites) goodhalli* as providing a secure correlation tie between the Eromanga basinal succession and the global reference ammonite zonation. This species occurs in both the Allaru Formation and in the late Albian *Mortoniceras inflatum* zone of the Anglo-Paris Basin zonal scheme. A number of characteristics Anglo-Paris Basin ammonites of latest Albian (Vraconian), Cenomanian and Turonian ages are represented in the Bathurst Island Group of the Money Shoals Basin, Northern Territory (Wright, 1963; Henderson, 1990).

C. 4. 2 Nannofossil age determinations

The middle and late Albian *Prediscosphaera columnata* zone, widely recognised in Cretaceous successions, is also represented in Australia. Its indicator species *Sollasites falklandensis* is abundant in the Ranmoor Member, Toolebuc and Allaru Formations from the Eromanga Basin (Shafik, 1985) and is uncommon in the basal Gearle assemblages from the Carnarvon Basin (Haig et al., 1996). The European type middle Albian `Argiles tegulines' of northeastern France contains a rich assemblage representing the *P. columnata* Zone (Sissingh, 1978). The earliest appearance level of the late Albian index *Eiffellithus turriseiffeli* in the type upper Albian `Marnes de Brienne' (northeastern France) has not been precisely documented but other European occurrences suggests it is restricted to the late Albian. Nannofossil distributions in the Gault beds I-V at Copt Point, England (early Albian) and in the Col de Palluel section, south-eastern France (Thierstein, 1976), support the conclusion that that *P. columnata* Zone extends into the upper Albian (see Shafik, 1985).

C. 4. 3 Foraminiferal age determinations

International planktonic foraminiferal zonation allows recognition of the Albian on the basis of *Hedbergella* species (Haig, 1979a). The early Albian *H. planispira* zone is recognised from the Laura Basin Wolena Claystone and the Eromanga Basin Ranmoor Member. The mid-Albian *H. infracetacea* zone is represented in the Toolebuc Formation of the Eromanga Basin (Haig, 1979b). The late Albian *H. delrioensis* zone is known from the Allaru Mudstone of the Carpentaria and Eromanga basins (Haig and Lynch, 1993).

For the Carnarvon Basin only the *H. planispira* Zone is recognised and occurs in the basal Gearle Siltstone (Haig et al., 1996).

C. 4. 4 Dinoflagellate age determinations

For the Early Cretaceous, Helby et al. (1987) and Helby and Partridge (2004) defined five successive zones in both the Aptian and Albian, in ascending order: *Muderongia testudinaria* Zone, *Muderongia australis* Zone, *Ovoidinium cinctum* Zone, *Odontochitina operculata* Zone, *Diconodinium davidii* Zone, *Munderongia tetracantha* Zone, *Canninginopsis denticulata* Zone, *Pseudoceratium ludbrookiae* Zone, *Diconodinium multispinum* Zone and *Palaeohystrichophora infusorioides* Zone. They noted strong facies dependence for the *O. cinctum* Zone and observed that in many sequences the *O. operculata* Zone directly overlies the *M. australis* Zone. Parts of the Austral dinocyst zonation scheme can be correlated to well-dated sequences in Europe (Oosting et al., in press.). Based on diagnostic dinoflagellate events, the *M. testudinaria, M. australis* and *O. operculata* zones were recognised in both a fully cored section (DSDP site 263) from the Australian Northwest Shelf and the type early Aptian sequence at Angles, France. The correlation of these two sequences indicates that the *M. testudinaria* Zone extends to late Barremian (Oosting et al., in press.) instead of being entirely Hauterivian as suggested by Helby et al. (1987) and Helby and Partridge (2004) and the *M. australis* Zone extends across the Barremian/Aptian stage into the earliest Aptian. The *O. cinctum* Acme Zone of Helby et al. (1987), located between the *M. australis* and *O. operculata* zones, was not recognised by Oosting et al. (in press.) who assigned it to within the upper part of the *M. australis* Zone. The *O. operculata* Zone is considerably younger in Australia (early Aptian) than in Europe where its co-occurrence with index ammonites shows that it is Barremian.

Aptian dinoflagellates *Odontochitina operculata* and *Disconodinium davidii* (late Aptian), along with *Muderongia tetracantha*, *Canninginopsis denticulata* and the bottom of the *Pseudoceratium ludbrookiae* zones are known from the Bulldog Shale and assigned as early to early late Albian in the biostratigraphic schemes of both Helby et al. (1987), Helby and Partridge (2004) and Oosting et al. (in press.). The upper part of the *Pseudoceratium ludbrookiae* Zone has been recognised from the Toolebuc and Oodnadatta formations (Morgan, 1980). *Odontochitina operculata* has also been

recorded from the Aptian Windalia Radiolarite of the Carnarvon Basin (Helby et al., 1987).

C. 5 Stratigraphic distribution of belemnites

Belemnite guards are widespread in the Cretaceous System of Australia and, due to their abundance, excellent preservation and tight stratigraphic control on their distribution, provide an ideal medium for Sr isotopic stratigraphy. This study compliments a detailed biostratigraphic analysis of the Family Dimitobelidae (see Sections A & B) based on assemblages from the Eromanga and Carnarvon Basins.

Drawing on the extensive collections of belemnites available in museums and other repositories, and new field and core collections, a suite of specimens were selected to represent stratigraphic distribution of the group from the Carnarvon Basin and the east Australian platform (see Figures C. 3. 2 to C. 3. 6). Employing visual inspection and analytical screening, this suite was reduced to 75 specimens for Sr-isotope analysis. Most represented whole guards but some fragmentary guards were included to achieve more complete stratigraphic coverage. The location and stratigraphic positions of samples are given in Table C. 1-4, along with analytical data and taxonomic identification, generally to the species level.

The Western Australian sample set was largely derived from a single core-hole, GSWA Boologooro 1. Sampling embraced 89 metres of continuously cored section through the upper Windalia Radiolarite and Gearle Siltstone, considered on biostratigraphic grounds to range in age from late Aptian to early Cenomanian. Correlation of Boologooro 1 with other core holes, Barrabiddy 1, Edaggee 1, and Yinni 1 enabled sampling to be extended into the lower Windalia Radiolarite and Munderong Shale (Figure C. 8. 2) intervals considered to be of the late Barremian and early Aptian.

Stratigraphic succession for the east Australian platform is best known from the northern Eromanga Basin. Sampling here was based on an exposed composite section measured along the banks of the Flinders River with close stratigraphic control

through the Wallumbilla Formation (Figure C. 3. 5), considered on biostratigraphic grounds to span the early late Aptian to middle Albian. However, the majority of the available Eromanga Basin belemnite collections are from scattered individual localities. These may be placed in the stratigraphic succession on the basis of location relative to the distribution of lithostratigraphic units established from regional mapping. A superpositional composite for these scattered localities may be constructed with reference to GSQ Manuka 1 and Longreach 1, fully cored drill holes from the northern Eromanga region (Figure C. 8. 1).

Sampling from the southern Eromanga, Carpentaria and Laura Basins is based on collections from individual localities. Samples may be placed in superpositional relationships based on their localities relative to the stratigraphic framework available from regional mapping that closely relates to that of the Eromanga Basin (Figure C. 8. 1).

C. 6 Sample selection and preparation

The major limitation in strontium stratigraphy relates to preservation of biogenic carbonate such that the original seawater signature is retained. Without careful selection procedures, samples that have experienced significant diagenetic alteration may go undetected, prejudicing analytical results. It is thus essential to develop proxies that screen preservation of the sample materials. In many studies, the Sr-isotope ratio ($^{87}Sr/^{86}Sr$) has itself been used as the primary indicator of diagenesis (Veizer and Compston, 1974; Burke et al., 1982; Derry and Jacobsen, 1988; Derry et al., 1989). Samples from individual stratigraphic horizons that give the same $^{87}Sr/^{86}Sr$ are likely to have recorded an original $^{87}Sr/^{86}Sr$ value (McArthur, 1994; Jones et al., 1994a), retaining the original elemental and isotopic contents. Likewise, a well-defined trend in $^{87}Sr/^{86}Sr$ throughout a stratigraphic sequence is consistent with good sample preservation.

Belemnites have been a favoured macrofossil for Sr isotopic analysis (Veizer et al., 1999) and have been used exclusively in this study. Belemnites secrete massive skeletons made of the most stable biogenic carbonate mineral, calcite (Ditchfield et al., 1994). Diagenetic alteration is typically reflected by substitution for calcium in the calcite lattice by iron, manganese and magnesium. The presence of Fe and Mn is reflected in luminescence properties and the contents of all three elements can be determined by trace element analysis.

In the present study, guards were cleaned in acetic acid to dissolve any secondary diagenetic calcite and then washed in an ultrasonic bath. Each guard was then cut perpendicular to its length at the point of maximum inflation (Figure C. 6. 1). Transverse polished thin sections (~ 100 μm thick) were made from most of the guards and detailed petrographic investigation by standard light microscopy and cathodoluminescence (CL) using a JEOL JSM-5410LV Scanning Electron Microscope in back-scatter mode were employed to distinguish primary biogenic carbonate from diagenetically altered material (see Figures C. 6. 3, C. 6. 4). Guards with significant diagenetic alteration, as revealed by these techniques, were not analysed.

Cross-sections were sampled by microdrilling using a handheld rotary drill and 0.25 mm drill bits that were washed between samples in acetone and ethanol. Samples were taken from non-luminescent zones inside each guard and away from the exterior surface and axial canal which may represent sites of diagenetic alteration. The internal structure of the guards shows clear, concentric growth lamellae with light calcite-rich domains separated by dark domains where organic matrix is concentrated. Where possible, sampling was restricted to individual light domains, either by following a growth zone in the plane of section or normal to the plane of section, parallel to its elongation (Podlaha et al., 1998). This procedure could not be applied to the four youngest guards from GSWA Boologooro 1 (B1- B4), which were very small. Visual inspection of these samples indicated excellent preservation with the external surface still lustrous. These samples were prepared using an agate mortar and pestle crushing technique with equipment rinsed between samples in acetone and ethanol. All powders were screened for diagenetic modification using geochemical trace element protocols.

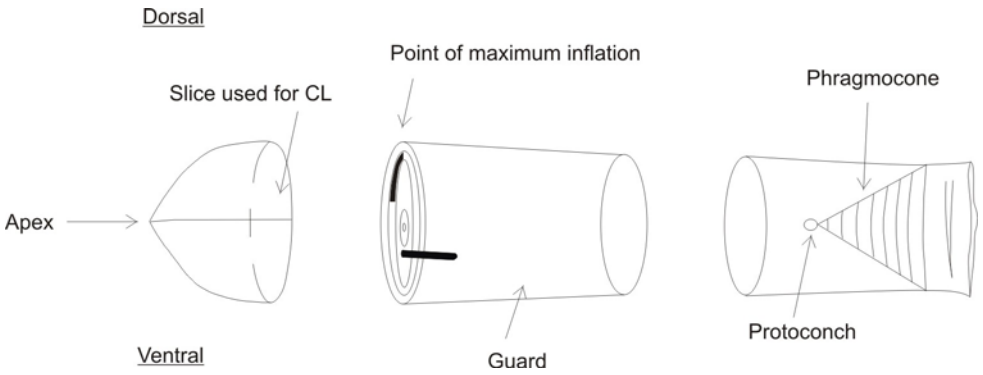

Figure C. 6. 1 Schematic representation of sample preparation for optical and geochemical studies. Microdrilling sample sites shown in black.

Sample aliquots were used to determine trace elemental concentrations, with duplicates used in strontium analysis. Ca, Fe, Mg, Mn and Sr concentrations were determined using a Varian Liberty Series II Inductively Coupled Plasma Atomic Emission Spectrometer (ICPAES) and the multi-element standard ICP-200.7. A weighed sample was dissolved in 1 ml of 10 % HNO_3. Concentrations of trace elements were measured following dilution with distilled water to 10 ml. Due to its high concentration the Ca content of the samples was determined after a further 10-fold dilution. All values for Mg and Sr were recalculated assuming a Ca value equivalent to that of pure calcite (3.95×10^5 ppm). This procedure eliminated inaccuracies that may have arisen in weighing minute sample masses.

The majority of belemnites sampled are visually well-preserved, with isotopic and elemental compositions that replicate well, and low concentrations of Fe and Mn (≤ 100) consistent with good preservation of primary calcite (Veizer and Compston, 1974). Low concentrations of Sr and Mg are also typical of well-preserved belemnites (see Saelen and Karstang, 1989; McArthur et al., 2000). The ICP results were used to further screen samples for preservational quality. Selection was made on the basis of relatively high strontium contents (Sr > 800 ppm) and negligible trace element content, i.e. Mn < 100 ppm, Fe < 100 ppm, Mg > 500 ppm (see Tables C. 1-4). Jones et al. (1994b) considered that belemnites containing more than 150 ppm Fe are likely to yield unreliable Sr-isotope results. The belemnite calcite used in this study contained very little Mn substitution due to diagenesis.

A comparison of the trace element contents of the belemnite guards with values published for modern low magnesium calcite (LMC) marine shells shows a good level of comparability (Figure C. 6. 2), suggesting that most of the belemnite guards retain near pristine geochemistry. Given that Sr concentrations as low as 200 ppm have been reported for modern brachiopod shells (Morrison and Brand, 1986; Brand, 1989) samples with Sr contents above this value and with low concentrations of other trace elements, are likely to be unaffected by diagenetic modification. Veizer et al. (1999) suggested the low Sr concentrations in fossil shells might be in part due to inclusion of small domains of secondary calcite, as distinct from partial recrystallization, leaving the bulk of the shell unaltered. The presence of such secondary calcites are likely to be revealed by cathodoluminescence due to distinctive trace element chemistry (Bruhn et al., 1995; Bruckschen et al., 1995a). Samples with such luminescent domains were eliminated from analysis (Figures C. 6. 3 and C. 6. 4).

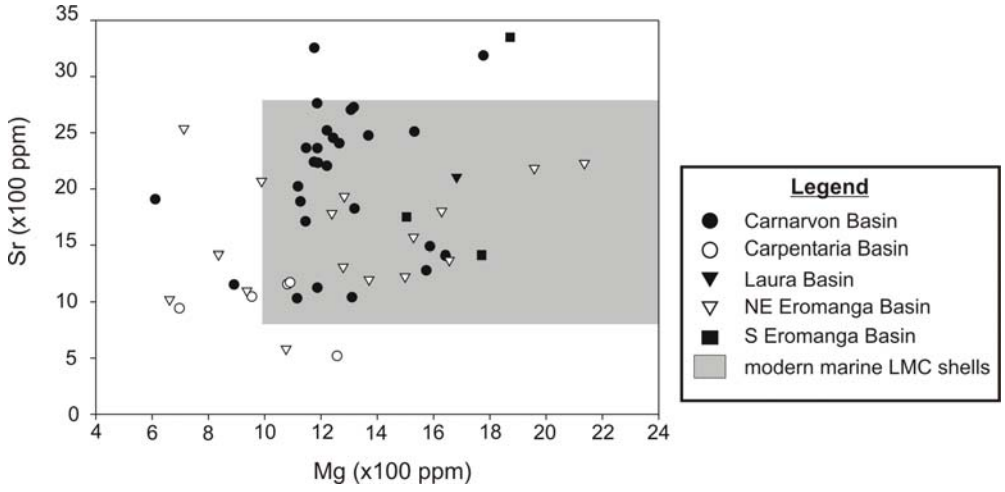

Figure C. 6. 2 Scatter diagram of Sr and Mg trace element concentrations in studied Cretaceous belemnite guards (Tables C. 1-4). The field of typical concentrations for modern marine low magnesium calcite shells is from Milliman (1974) and Morrison and Brand (1986).

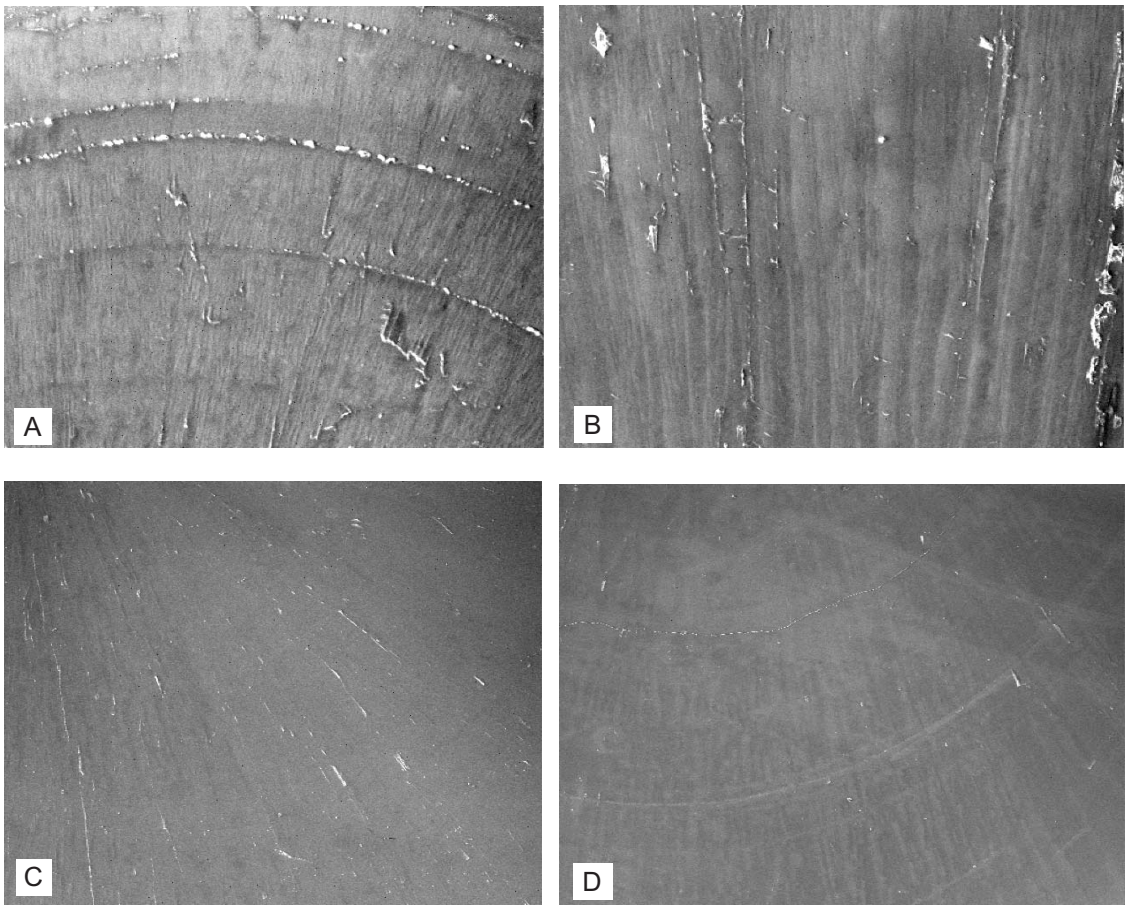

Figure C. 6. 3 Cathodoluminescence images of well-preserved belemnite guard cross-sections showing growth-laminae comprised of calcite prisms. None are luminescent, indicating that diagenetic alteration has not occurred. In black and white images intrinsic fluorescence shows as a strong tone contrast. The guards contain areas enriched in organic matter alternating with zones that are not, which represent `seasonal growth rings' that vary from one specimen to another and is not species specific (Podlaha et al., 1998). A. JCU F11632 L913, Ranmoor Member, early Albian, width 1.76 mm; B. JCU F11654 L916, basal Ranmoor Member, width 1.76 mm; C. QM F36160, Ranmoor Member, Albian, width 1.32 mm; D, QGS L813, Ranmoor Member, Albian, width 3.77 mm.

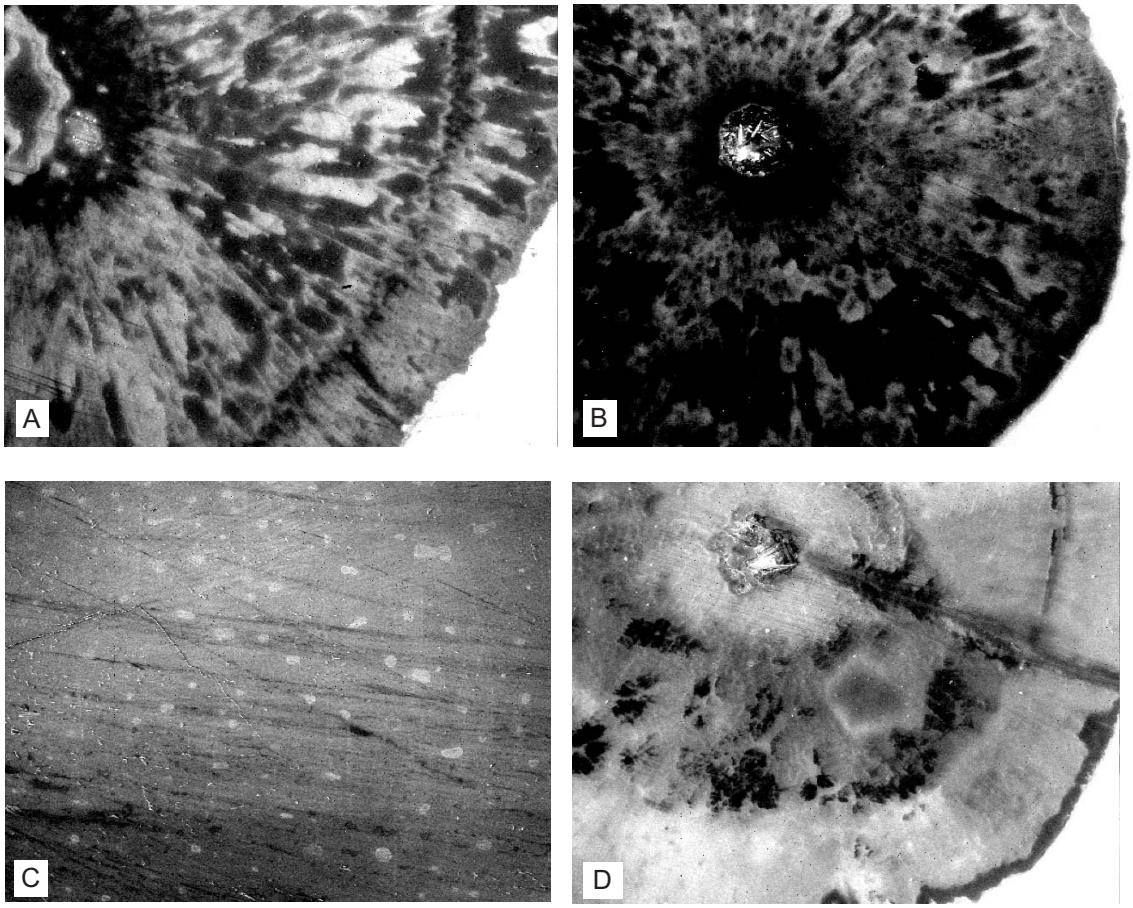

Figure C. 6. 4 Cathodoluminescence images of poorly-preserved belemnite guard cross-sections. Domains affected by diagenetic alteration are shown by dark tones and a mottled appearance is characteristic of specimens that have suffered extensive diagenetic overprint. Note the enhanced diagenetic signature of domains adjoining the apical canal for images (A) and (B). A. WAM 69.25, Windalia Radiolarite, Aptian, width 3.77 mm; B. WAM 91.839, Windalia Radiolarite, Aptian, width 3.77 mm; C. WAM 65.1159, Windalia Radiolarite, Aptian, width 1.76 mm; D. UWA 2/11/99-16, Upper Gearle Siltstone, Cenomanian, width 3.77 mm.

C. 7 Strontium-isotope analysis

Analyses of powder aliquots were conducted at the ACQUIRE laboratory, University of Queensland, in two stages: dissolution and separation of the Sr contents followed by isotopic analysis by mass spectrometry. Analytical procedures were performed under sterile conditions and at a stable temperature of 26°C. Results were derived, and their reproducibility monitored, using the SRM-987 and EN-1 standards (Ludwig et al., 1988).

C. 7. 1 Sample dissolution and separation of strontium

Between 45 and 55 mg of powder was weighed into a polypropylene centrifuge tube and 4 ml of 1N hot distilled acetic was added. Following the reaction samples were centrifuged at 2000 rpm for 10 minutes. Three millilitres of leachate was transferred by pipette to a 10 ml teflon beaker and evaporated to dryness on a hot plate. The residue was dissolved in 2 ml quartz distilled 6N HCl and again, evaporated to dryness. The resulting residue was then dissolved in 3 ml of quartz distilled 1N HCl. One millilitre of this solution was taken up in a pasteur pipette and loaded onto the top of a pre-conditioned cation (AG50W-X8 resin) exchange column. Following elution with 62 ml of 1N HCl and 21 ml of 2.5N HCl, Sr was collected in 7 ml 2.5N HCl in a 10 ml Teflon beaker and dried on a teflon coated hotplate in a vented HEPA filtered enclosure for 5-6 hours. Once dried 30 ml of concentrated HNO_3 was added to the beaker to remove any remaining organic residues. Preparations were then sealed prior to mass spectrometry.

C. 7. 2 Mass spectrometry

Strontium samples were loaded onto single tantalum (Ta) filaments with 1M H_3PO_4 and heated until the sample glowed red for approximately 5 seconds. This reaction produced tantalum oxide which enhances sample ionization. Isotopic ratios

were measured on a Fisons VG54-30 thermal ionization mass spectrometer using a static acquisition routine.

In static multi-collection the magnetic field is fixed and the isotopes to be determined are measured synchronously in the appropriate Faraday Cup. In this analytical mode the gains of the individual amplifiers must be accurately known and be very stable. The static analysis procedure used the following Faraday Cup configuration: L2 - ^{84}Sr; L1-^{85}Rb; Axial-^{86}Sr; H1-^{87}Sr; H2-^{88}Sr.

All samples were analysed with a 4 x 10^{-11} to 4.5 x 10^{-11} Å ^{88}Sr beam. Between 7 and 10 blocks of 20 ratios were collected for each sample. Background readings were taken at 0.5 mass units from each peak with an integration time of 20 seconds. Peaks were counted for a period of 5 seconds. Amplifier gains were calibrated using a 10 volt signal varied by < 5 ppm over the 30 days during which the analyses were completed. Sr-isotope ratios were corrected for mass fractionation using the $^{86}Sr/^{88}Sr$ value of 0.1194. ^{85}Rb was measured during analyses to monitor the possible isobaric interference of ^{87}Rb on ^{87}Sr. As the measured $^{87}Rb^{+}/^{86}Sr^{+}$ ratio was $<10^{-5}$ in all analyses the isobar $^{87}Rb^{+}$ did not have any effect on $^{87}Sr/^{86}Sr$.

C. 7. 3 Analytical reproducibility

Replicate samples were analysed through the course of this study allowing for quantitative estimate of the analytical reproducibility before and after the barrel-by-barrel normalization. The replicate analyses involved reloads from the same Sr separation and were only performed when the initial value was undeniably out of character and spectrum. Long-term analytical system variance was calculated from replicate determinations of $^{87}Sr/^{86}Sr$ from the standards SRM-987 and EN-1 (Ludwig et al., 1988).

In theory, there can be an uncertainty in the `real' $^{87}Sr/^{86}Sr$ measurements from samples, since standards and samples may differ in Sr concentration and matrix composition. Matrix differences may cause fractionation during mass spectrometry if Sr is not cleanly separated by ion-exchange chromatography (Howarth and McArthur, 1997). $^{87}Sr/^{86}Sr$ in a real sample will, unlike a reference material, differ between sub-

samples. However, in practice the reproducibility of $^{87}Sr/^{86}Sr$ determinations on standards and samples are close (Hodell et al., 1990). Estimates of variance based on replicated long-term measurements of samples is preferred (Howarth and McArthur, 1997); in this study the analytical procedure was replicated typically between 1-4 times (n =1-4) per sample.

The determination of a seawater Sr-isotope curve allows a second method of monitoring analytical reproducibility. Not only should seawater be isotopically homogeneous at any given time, but the Sr-isotope curve should also evolve at a relatively slow and smooth rate, with no sudden excursions. Samples of similar age, analysed at different times throughout the study should give nearly identical $^{87}Sr/^{86}Sr$ ratios. In this study samples of a variety of ages were loaded together in each barrel such that it was uncommon for adjacent data points in the final Strontium-isotope curve to have been derived from analyses in the same barrel. In this way, any systematic variation in analytical results related to batching in individual barrel runs would be readily recognisable.

Non-radiogenic $^{84}Sr/^{88}Sr$ and $^{84}Sr/^{86}Sr$ ratios were measured for each sample to evaluate instrument performance and reproducibility of ion beam focus conditions. Results were excellent with 188 measurements of non-radiogenic ratios determined during analysis of the belemnites yielding $^{84}Sr/^{88}Sr$ ratios of 0.006750 ± 0.000002 (2σ) and $^{84}Sr/^{86}Sr$ ratios of 0.056532 ± 0.000014 (2σ). A total of 40 static analyses of NBS $SrCO_3$ standard SRM-987 were undertaken during the period of this study with mean ratio results of $^{84}Sr/^{88}Sr$ at 0.006749 ± 0.000002 (2σ), $^{84}Sr/^{86}Sr$ at 0.056525 ± 0.000020 (2σ) and $^{87}Sr/^{86}Sr$ at 0.710252±0.000024 (2σ).

A more realistic estimate of the external reproducibility of analyses that explains the chemical scatter, is provided by data for EN-1, a modern clam from Enewetak Atoll (Ludwig et al., 1988). Twenty-eight static analyses of EN-1 obtained during analysis of the carbonate sample suite yield mean ratios for $^{87}Sr/^{86}Sr$ as 0.709180±0.000038 (2σ), $^{84}Sr/^{88}Sr$=0.006749 ± 0.000002 (2σ) and $^{84}Sr/^{86}Sr$=0.056527 ± 0.000020 (2σ). Excellent agreement between the $^{87}Sr/^{86}Sr$, $^{84}Sr/^{88}Sr$ and $^{84}Sr/^{86}Sr$, for this

standard reflects the instrument stability and quality of the static data. Ratio values for $^{87}Sr/^{86}Sr$ for this standard obtained in the present study are almost identical with a mean value of 0.709176 ± 0.000032 (2σ). This is identical to the mean of 576 isotopic analyses of EN-1 obtained at The University of Queensland using static procedures between 1996 and December 2003. Weighted means are not used in this report as they result in a biased estimate of the external precision. Both EN-1 and SRM-987 data sets are provided in Appendix C.

The final strontium results were normalised to values of EN-1 (0.709173) and $^{87}Sr/^{86}Sr$ (0.1194). SRM-987 gave a standard value of 0.710249 (n=1) with a standard deviation (±11) for n=2. Mean $^{87}Sr/^{86}Sr$ values are reported in Tables C. 1-4, along with the maximum and minimum deviations from the mean of replicate analyses and the number (*n)* of replicates for each sample. Concentrations of Rb were too low to require correction for radiogenic ^{87}Sr.

C. 8 Strontium-isotope curve construction and its significance

Based on the analytical data (Tables C. 1-4), Sr-isotope curves may be constructed for Early Cretaceous successions from both the east Australian platform (Figure C. 8. 1) and the Carnarvon Basin (Figure C. 8. 2). $^{87}Sr/^{86}Sr$ values range between 0.7074485 and 0.7071845 for samples from the platform and 0.707484 and 0.707183 for samples from the Carnarvon Basin, and compare well with values obtained in previous Sr-isotope studies of Early Cretaceous biogenic carbonate.

For the east Australian succession, superposition of samples is based on regional-scale lithostratigraphic sequences. Most of the data is from the northern Eromanga Basin where a common lithostratigraphic framework applies. Samples are distributed through a 500 metres sequence extending from the Doncaster Member of the Wallumbilla Formation to the Mackunda Formation (Figure C. 8. 1). The isotope curve derived from this succession shows smooth trends with a

Table C. 1

Isotopic and chemical data for belemnites from the Aptian-to-Albian strata of the north-eastern Eromanga Basin, Queensland.

Stage	Lithological No.	Isotope Sample No.	Specimen No.	Locality	Latitude	Longitude	Basin	Lithostratigraphic Position	Biostratigraphic Position: *AMMOBACULITES* Benthic Association	Biostratigraphic Position: *HEDBERGELLA* Planktonic association	Macrofauna	Species	$^{87}Sr/^{86}Sr$ Means	Range Pos.	Range Neg.	*n*	Ca ppm	Mg ppm	Sr ppm	Mg/Ca ppm	Sr/Ca ppm	recalculated Mg ppm	recalculated Sr ppm
Latest Albian	L1	TW-03-5297-21	QM F27918	Winchester Downs 80km SW of Richmond, Qld	21°11'S	142°37'E	Eromanga	Lower Mackunda Formation	*Eomarssonella crespinae* Zone	*Hedbergella delrioensis*	Tambo	*D. diptychus*	0.707415			1	$2.44x10^5$	1350	1210	$5.53x10^{-3}$	$4.96x10^{-3}$	2184	1958
Late Albian	L2	TW-03-LA2	JCU 1987	Longreach, Qld	c. 23°15'S	c. 144°34'E	Eromanga	Upper Allaru Mudstone	*Eomarssonella crespinae* Zone	*Hedbergella delrioensis*	Tambo	*D.diptychus*	0.707392			1	$3.45x10^5$	509	940	$1.48x10^{-3}$	$2.72x10^{-3}$	582	1076
Late Albian	L3	TW-03-LA1	UQ F16922	Currane Station, 14.5km N of Dartmouth, central Qld.	23°24'S	144°45'E	Eromanga	Upper Allaru Mudstone	*Eomarssonella crespinae* Zone	*Hedbergella delrioensis*	Tambo	*D.liversidgei*	0.707441			1	$4.31x10^5$	2110	1400	$4.89x10^{-3}$	$3.25x10^{-3}$	1933	1283
Early late Albian	L4	TW-03-5297-19	QGS F1369	Cambridge Downs Run, Flinders River, 13km from Richmond Downs Station	20°35'S	143°18'E	Eromanga	Toolebuc Limestone	*Eomarssonella crespinae* Zone	Zone of dwarf *Hedbergella*	Tambo	*D.diptychus*	0.707414	0.5	0.5	2	$2.79x10^5$	969	1170	$3.47x10^{-3}$	$4.19x10^{-3}$	1371	1656
Early Albian	L5	TW-03-5297-24	QGS F1759	Aramac Well	22°58'S	145°14'E	Eromanga	Upper Coreena Member	*Eomarssonella crespinae* Zone	*Hedbergella planispira* Zone	Tambo	*D.diptychus*	0.707366	5.5	5.5	2	$2.79x10^5$	1110	1080	$3.98x10^{-3}$	$3.87x10^{-3}$	1571	1529
Early Albian	L6	TW-03-LC1	QGS F1370	Aramac Well at 72.54m, Aramac Town, Qld	22°59'S	145°15'E	Eromanga	Upper Coreena Member	*Eomarssonella crespinae* Zone	*Hedbergella planispira* Zone	Tambo	*D.diptychus*	0.707449	21.5	21.5	2	$4.55x10^5$	1380	1580	$3.03x10^{-3}$	$3.47x10^{-3}$	1198	1371
Late Albian	M1	TW-03-20	QM F27742	Richmond, Qld	20°44'S	143°08'E	Eromanga	Allaru Mudstone	*Eomarssonella crespinae* Zone	*Hedbergella delrioensis*	Tambo	*D.diptychus*	0.707427	11.5	11.5	2	$2.57x10^5$	1450	1390	$5.64x10^{-3}$	$5.4x10^{-3}$	2228	2136
Late Albian	M2	TW-03-FRA1	QM F2105	Tarbrax Station, near Maxwellton	21°06' S	142°26'E	Eromanga	Lower Mackunda Formation	*Eomarssonella crespinae* Zone	*Hedbergella delrioensis*	Tambo	*D.diptychus*	0.707392			1	$4.34x10^5$	1980	1790	$4.56x10^{-3}$	$4.12x10^{-3}$	1802	1629
Early late Albian	M3	TW-03-T2	JCU 11616	Quarry 15km E of Julia Creek	20°38' S	141°54'E	Eromanga	Toolebuc Limestone	*Eomarssonella crespinae* Zone	Zone of dwarf *Hedbergella*	Tambo	*D.diptychus*	0.707464			1	$4.61x10^5$	1430	1750	$3.1x10^{-3}$	$3.79x10^{-3}$	1225	1499
Late early Albian	M4	TW-03-T1	JCU 11615	Quarry 15km E of Julia Creek	20°38' S	141°54'E	Eromanga	Toolebuc Limestone	*Eomarssonella crespinae* Zone	Zone of dwarf *Hedbergella*	Tambo	*D. stimulus*	0.707383			1	$4.97x10^5$	1650	1610	$3.3x10^{-3}$	$3.2x10^{-3}$	1311	1279
Early Albian	FR1	TW-03-5297-39	JCU F11633 L910	Flinders River, Prairie, Grid Ref: 430 120	20°40'S	144°32'E	Eromanga	Ranmoor Member	*Eomarssonella crespinae* Zone	*Hedbergella planispira* Zone	Tambo	*D. stimulus*	0.707371	18.0	20.0	3	$2.97x10^5$	1340	932	$4.5x10^{-3}$	$3.1x10^{-3}$	1782	1239
Late Aptian	FR2	TW-03-5297-38	JCU F11636 L908	Flinders River, Prairie, Grid Ref: 506 113	20°40'S	144°36'E	Eromanga	Upper Doncaster Member	*A. pitmani-T. cushmani* Zone	no planktics	Roma	*P. oxys*	0.707185	1.5	1.5	2	$2.92x10^5$	813	693	$2.78x10^{-3}$	$2.37x10^{-3}$	1099	937
Late Aptian	FR3	TW-03-5297-45	JCU F11637 L912	Flinders River, Prairie, Grid Ref: 493 100	20°41'S	144°34'E	Eromanga	Jones Valley Member	*Aaptotoichus pitmani* Zone	no planktics	Boundary Roma/Tambo	*P. oxys*	0.707196			1	$3.21x10^5$	830	538	$2.58x10^{-3}$	$1.67x10^{-3}$	1021	662
Late Aptian	FR4	TW-03-5297-34	JCU F11638 L916	Flinders River, Marathon, Grid Ref: 096 275	20°32'S	143°58'E	Eromanga	Jones Valley Member	*Aaptotoichus pitmani* Zone	no planktics	Boundary Roma/Tambo	*P. oxys*	0.707287	10.0	10.0	2	$2.07x10^5$	1330	374	$6.4x10^{-3}$	$1.8x10^{-3}$	2537	713
Early Albian	FR5	TW-03-5297-32	JCU F11634 L914	Flinders River, Hughenden, Grid Ref: 368 167	20°37'S	144°28'E	Eromanga	Upper Ranmoor Member	*Eomarssonella crespinae* Zone	no planktics	Tambo	*D. stimulus*	0.707374	0.5	0.5	2	$2.56x10^5$	921	542	$3.5x10^{-3}$	$2.11x10^{-3}$	1421	836
Early Aptian	FR6	TW-03-FR1	JCU F11639 L907	Flinders River, Prairie, Grid Ref: 535 137	20°39'S	144°38'E	Eromanga	Lower Doncaster Member	*A. pitmani-T. cushmani* Zone	no planktics	Roma	*P. oxys*	0.707269			1	$4.39x10^5$	2300	1100	$5.2x10^{-3}$	$2.5x10^{-3}$	2069	989

Table C. 2

Isotopic and chemical data for belemnites from the Aptian-to-Albian strata of the southern Eromanga Basin, South Australia.

N.B. Formaniniferal and dinoflagellate zones adapted from Kreig, 1995.

Stage	Lithological No.	Isotope Sample No.	Specimen No.	Locality	Latitude	Longitude	Basin	Lithostratigraphic Position	Biostratigraphic Position			Species	$^{87}Sr/^{86}Sr$	Range			Ca	Mg	Sr	Mg/Ca	Sr/Ca	recalculated Mg	recalculated Sr
									Palynology Zone	Foraminiferal Zone	Dinoflagellate Zone		Means	Pos.	Neg.	*n*	ppm	ppm	ppm	ppm	ppm	ppm	ppm
Late Albian	E1	TW-03-5297-12	NMV 310468	Woodduck Creek, Peake Station, S.A.	27°56'S	136°13'E	Eromanga	Oodnadatta Formation	*Philmopollenites pannosus*	*Eomarssonella crespinae*	*Pseudoceratium lubrookiae*	*D. diptychus*	0.707421	5.5	5.5	2	$3.10x10^5$	1110	1390	$3.58x10^{-3}$	$4.48x10^{-3}$	1414	1771
Late Albian	E2	TW-03-5297-11	NMV 310431	From cliffs on banks of River Neales, 22.5km SE of Algebuckinna, S.A.	28°08'S	135°59'E	Eromanga	Oodnadatta Formation	*Philmopollenites pannosus*	*Eomarssonella crespinae*	*Pseudoceratium lubrookiae*	*D. stimulus*	0.707427	9.0	16.0	3	$3.36x10^5$	1490	1280	$4.4x10^{-3}$	$3.8x10^{-3}$	1751	1504

Table C. 3

Isotopic and chemical data for belemnites from the Aptian-to-Albian strata of the Carpentaria and Laura Basin, north Queensland.

Stage	Lithological No.	Isotope Sample No.	Specimen No.	Locality	Latitude	Longitude	Basin	Lithostratigraphic Position	Biostratigraphic Position			Species	$^{87}Sr/^{86}Sr$	Range			Ca	Mg	Sr	Mg/Ca	Sr/Ca	recalculated Mg	recalculated Sr
									Palynological Unit	Foraminiferal Zone	Dinoflagellate Zones		Means	Pos.	Neg.	*n*	ppm	ppm	ppm	ppm	ppm	ppm	ppm
Early late Aptian	C1	TW-03-EC1	QGS 8430 W10	East bank of Walsh River, 1km N of Boomers Hole	16°40'S	143°59'E	Carpentaria	Lower Wallumbilla Formation	K2a	*A. pitmani-T. cushmani* Zone	*Odontochitina operculata*	*P. oxys*	0.707237			1	$4.71x10^5$	1400	1300	$2.97x10^{-3}$	$2.76x10^{-3}$	1174	1090
Late Aptian	C2	TW-03-5297-26	QGS F8773	North bank of Elizabeth Creek, 0.3km W of crossing of Wrotham Park; Walsh Telegraph Station Track	16°39'S	143°58'S	Carpentaria	Upper Wallumbilla Formation	K1d	*A. pitmani-T. cushmani* Zone	*Odontochitina operculata*	*P. oxys*	0.707195			1	$2.66x10^5$	636	470	$2.39x10^{-3}$	$1.76x10^{-3}$	944	697
Early Aptian	C3	TW-03-WR1	JCU F81234	Boomers Hole Walsh River	16°32'S	143°47'E	Carpentaria	Lower Wallumbilla Formation	K1b-c	*Textulariopsis cushmani*	*Odontochitina operculata*	*P. oxys*	0.707206	5.0	5.0	2	$4.53x10^5$	1330	1240	$2.93x10^{-3}$	$2.73x10^{-3}$	1159	1081
Early Aptian	C4	TW-03-WR3	QM F33252 L681	Boomers Hole Walsh River	16°32'S	143°47'E	Carpentaria	Lower Wallumbilla Formation	K1b-c	*Textulariopsis cushmani*	*Odontochitina operculata*	*P. oxys*	0.707244			1	$4.22x10^5$	1120	1020	$2.65x10^{-3}$	$2.41x10^{-3}$	1048	954
Early late Aptian	C5	TW-03-WR2	JCU F5171	1.6km N of Boomers Hole, Walsh River	16°49'S	143°58'E	Carpentaria	Lower Wallumbilla Formation	K1b-c	*A. pitmani-T. cushmani* Zone	*Odontochitina operculata*	*P. oxys*	0.707246	14.5	14.5	2	$4.24x10^5$	1350	559	$3.18x10^{-3}$	$1.3x10^{-3}$	520	1257
Early Albian	La1	TW-03-5297-01	JCU 11618	Laura, Tablelands	15°56'S	144°10'E	Laura	Wolena Claystone	K2a	*Eomarssonella crespinae*	*Canninginopsis denticulata*	*D. dayi*	0.707393			1	$3.64x10^5$	1940	1550	$5.3x10^{-3}$	$4.2x10^{-3}$	2105	1682

Table C. 4

Isotopic and chemical data for belemnites from the Aptian-to-Cenomanian strata of the Carnarvon Basin, Western Australia.

Stage	Lithological No.	Isotope Sample No.	Specimen No.	Well Name-Depth (m)	Latitude	Longitude	Basin	Lithostratigraphic Position	Biostratigraphic Position: Benthic Association	Biostratigraphic Position: *HEDBERGELLA* Planktonic association	Biostratigraphic Position: Dinoflagellate Zones	Species	$^{87}Sr/^{86}Sr$ Means	Range Pos.	Range Neg.	Range *n*	Ca ppm	Mg ppm	Sr ppm	Mg/Ca ppm	Sr/Ca ppm	recalculated Mg ppm	recalculated Sr ppm
Early late Cenomanian	B1	TW-03-2	UWA B1	Boologooro 1 (293.1)	24°19'S	113°54'E	Carnarvon	Upper Gearle Siltstone	*Textulariopsis spp.* Zone	*Hedbergella delrioensis*	*Diconodinium multispinum* Zone	*Dimitobelus sp.*	0.707410	3.5	3.5	2	$3.98x10^5$	1840	1330	$4.62x10^{-3}$	$3.34x10^{-3}$	1826	1319
Early late Cenomanian	B2	TW-03-4	UWA B2	Boologooro 1 (297.95)	24°19'S	113°54'E	Carnarvon	Upper Gearle Siltstone	*Textulariopsis spp.* Zone	*Hedbergella delrioensis*	*Diconodinium multispinum* Zone	*Dimitobelus sp.*	0.707406	13.0	13.0	2	$4.01x10^5$	2240	1240	$5.58x10^{-3}$	$3.09x10^{-3}$	2206	1221
Early late Cenomanian	B3	TW-03-9	UWA B3	Boologooro 1 (301.55)	24°19'S	113°54'E	Carnarvon	Upper Gearle Siltstone	*Textulariopsis spp.* Zone	*Hedbergella delrioensis*	*Diconodinium multispinum* Zone	*Dimitobelus sp.*	0.707407	8.5	8.5	2	$3.93x10^5$	1900	608	$4.83x10^{-3}$	$1.54x10^{-3}$	1909	611
Late early Cenomanian	B4	TW-03-12	UWA B4	Boologooro 1 (305.15)	24°19'S	113°54'E	Carnarvon	Upper Gearle Siltstone	*Textulariopsis spp.*	*Hedbergella delrioensis*	*Diconodinium multispinum* Zone	*Dimitobelus sp.*	0.707411	13.3	21.7	4	$4.01x10^5$	2560	1240	$6.38x10^{-3}$	$3.09x10^{-3}$	2521	1221
Late early Cenomanian	B5	TW-03-16	UWA B5	Boologooro 1 (308.8)	24°19'S	113°54'E	Carnarvon	Upper Gearle Siltstone	*Textulariopsis spp.*	*Hedbergella delrioensis*	*Diconodinium multispinum* Zone	*D. stimulus*	0.707421			1	$4.17x10^5$	1220	941	$2.9x10^{-3}$	$2.25x10^{-3}$	1155	891
Early Cenomanian	B6	TW-03-18	UWA B6	Boologooro 1 (311.6)	24°19'S	113°54'E	Carnarvon	Lower Upper Gearle Siltstone	*Textulariopsis spp.*	*Hedbergella delrioensis*	*Diconodinium multispinum* Zone	*D.diptychus*	0.707443	2.5	2.5	2	$3.68x10^5$	1760	1050	$4.78x10^{-3}$	$2.85x10^{-3}$	1889	1127
Late Albian	B7	TW-03-19	UWA B7	Boologooro 1 (326.6)	24°19'S	113°54'E	Carnarvon	Lower Upper Gearle Siltstone	*Textulariopsis spp.*	*Hedbergella delrioensis*	*Diconodinium multispinum* Zone	*Dimitobelus sp.*	0.707461	4.0	4.0	2	$3.76x10^5$	3100	1120	$8.24x10^{-3}$	$2.97x10^{-3}$	3256	1176
Late Albian	B8	TW-03-20	UWA B8	Boologooro 1 (330.7)	24°19'S	113°54'E	Carnarvon	Lower Upper Gearle Siltstone	*Textulariopsis spp.*	*Hedbergella delrioensis*	*Diconodinium multispinum* Zone	*Dimitobelus sp.*	0.707484	5.0	5.0	2	$3.76x10^5$	2250	1130	$5.98x10^{-3}$	$3.0x10^{-3}$	2363	1187
Late Albian	B9	TW-03-22	UWA B9	Boologooro 1 (339.14)	24°19'S	113°54'E	Carnarvon	Lower Upper Gearle Siltstone	*Textulariopsis spp.*	*Hedbergella delrioensis*	*Diconodinium multispinum* Zone	*Dimitobelus sp.*	0.707454	14.0	13.0	3	$3.93x10^5$	2750	1180	$6.99x10^{-3}$	$3.0x10^{-3}$	2763	1186
Late Albian	B10	TW-03-26	UWA B10	Boologooro 1 (345.35)	24°19'S	113°54'E	Carnarvon	Lower Upper Gearle Siltstone	*Textulariopsis spp.*	*Hedbergella delrioensis*	*Diconodinium multispinum* Zone	*Dimitobelus sp.*	0.707445	6.0	6.0	2	$3.72x10^5$	2570	1240	$6.9x10^{-3}$	$3.33x10^{-3}$	2728	1316
Late Albian	B11	TW-03-29	UWA B11	Boologooro 1 (346.9)	24°19'S	113°54'E	Carnarvon	Basal Upper Gearle Siltstone	*Textulariopsis spp.*	*Hedbergella delrioensis*	*Diconodinium multispinum* Zone	*Dimitobelus sp.*	0.707461	3.0	3.0	2	$3.89x10^5$	2330	1130	$5.9x10^{-3}$	$2.9x10^{-3}$	2365	1147
Early late Albian	B12	TW-03-30	UWA B12	Boologooro 1 (347.4)	24°19'S	113°54'E	Carnarvon	Upper Lower Gearle Siltstone	*Eomarssonella crespinae*	*Hedbergella delrioensis*	*Pseudoceratium ludbrookiae* Zone	*Dimitobelus sp.*	0.707442	9.0	9.0	2	$3.84x10^5$	2340	1230	$6.09x10^{-3}$	$3.2x10^{-3}$	2407	1265
Early late Albian	B13	TW-03-33	UWA B13	Boologooro 1 (350.65)	24°19'S	113°54'E	Carnarvon	Upper Lower Gearle Siltstone	*Eomarssonella crespinae*	*Hedbergella delrioensis*	*Pseudoceratium ludbrookiae* Zone	*D. stimulus*	0.707480	2.5	2.5	2	$3.78x10^5$	2350	1190	$6.2x10^{-3}$	$3.14x10^{-3}$	2455	1243
Early late Albian	B14	TW-03-35	UWA B14	Boologooro 1 (351.42)	24°19'S	113°54'E	Carnarvon	Upper Lower Gearle Siltstone	*Eomarssonella crespinae*	Zone of dwarf *Hedbergella*	*Pseudoceratium ludbrookiae* Zone	*Dimitobelus sp.*	0.707509	3.0	6.0	3	$3.79x10^5$	2410	1470	$6.3x10^{-3}$	$3.87x10^{-3}$	2511	1532
Early late Albian	B15	TW-03-41	UWA B15	Boologooro 1 (352.95)	24°19'S	113°54'E	Carnarvon	Upper Lower Gearle Siltstone	*Eomarssonella crespinae*	Zone of dwarf *Hedbergella*	*Pseudoceratium ludbrookiae* Zone	*Dimitobelus sp.*	0.707457			1	$3.84x10^5$	2630	1270	$6.84x10^{-3}$	$3.3x10^{-3}$	2705	1306
Late early Albian	B16	TW-03-42	UWA B16	Boologooro 1 (357)	24°19'S	113°54'E	Carnarvon	Lower Gearle Siltstone	*Eomarssonella crespinae*	Zone of dwarf *Hedbergella*	*Pseudoceratium ludbrookiae* Zone	*Dimitobelus sp.*	0.707446			1	$3.78x10^5$	2370	1310	$6.26x10^{-3}$	$3.46x10^{-3}$	2476	1368
Late early Albian	B17	TW-03-45	UWA B17	Boologooro 1 (359.9)	24°19'S	113°54'E	Carnarvon	Lower Gearle Siltstone	*Eomarssonella crespinae*	Zone of dwarf *Hedbergella*	*Pseudoceratium ludbrookiae* Zone	*D.diptychus*	0.707408	12.7	13.3	3	$3.82x10^5$	2160	1150	$5.65x10^{-3}$	$3.01x10^{-3}$	2233	1189
Late early Albian	B18	TW-03-48	UWA B18	Boologooro 1 (361.05)	24°19'S	113°54'E	Carnarvon	Lower Gearle Siltstone	*Eomarssonella crespinae*	*Hedbergella planispira*	*Canninginopsis denticulata* Z one	*D. stimulus*	0.707476	8.5	8.5	2	$3.93x10^5$	2230	1170	$5.67x10^{-3}$	$2.97x10^{-3}$	2241	1175
Late early Albian	B19	TW-03-52	UWA B19	Boologooro 1 (365.63)	24°19'S	113°54'E	Carnarvon	Lower Gearle Siltstone	*Eomarssonella crespinae*	*Hedbergella planispira*	*Canninginopsis denticulata* Z one	*D. stimulus*	0.707446	1.0	1.0	2	$3.96x10^5$	1130	1190	$2.85x10^{-3}$	$3.0x10^{-3}$	1127	1187
Early Albian	B20	TW-03-54	UWA B20	Boologooro 1 (374)	24°19'S	113°54'E	Carnarvon	Lower Gearle Siltstone	*Eomarssonella crespinae*	*Hedbergella planispira*	*Canninginopsis denticulata* Z one	*D. stimulus*	0.707396	3.0	8.0	3	$4.08x10^5$	1540	1640	$3.7x10^{-3}$	$4.01x10^{-3}$	1490	1587
Early Albian	B21	TW-03-57	UWA B21	Boologooro 1 (377.65)	24°19'S	113°54'E	Carnarvon	Lower Gearle Siltstone	*Eomarssonella crespinae*	*Hedbergella planispira*	*Canninginopsis denticulata* Z one	*P. australis*	0.707379	1.0	1.0	2	$4.06x10^5$	2080	1150	$5.12x10^{-3}$	$2.83x10^{-3}$	2023	1118
Late early Aptian	B22	TW-03-59	UWA B22	Boologooro 1 (378.42)	24°19'S	113°54'E	Carnarvon	Windalia Radiolarite	*A. pitmani*	not zoned	*Muderongia tetracantha* Zone	*P. oxys*	0.707183	4.0	4.0	2	$4.28x10^5$	1130	1420	$2.64x10^{-3}$	$3.3x10^{-3}$	1042	1310
Early Aptian	B23	TW-03-62	UWA B23	Boologooro 1 (382.7)	24°19'S	113°54'E	Carnarvon	Windalia Radiolarite	*A. pitmani*	not zoned	*Diconodinium davidii* Zone	*Dimitobelus sp.*	0.707258	2.0	4.0	3	$3.76x10^5$	1630	1090	$4.33x10^{-3}$	$2.89x10^{-3}$	1712	1145
Early late Albian	Ba1	TW-03-66	UWA Ba1	Barrabiddy 1 (84.1)	23°50'S	114°20'E	Carnarvon	Lower Gearle Siltstone	*Eomarssonella crespinae*	Zone of dwarf *Hedbergella*	*Pseudoceratium ludbrookiae* Zone	*D. stimulus*	0.707453	2.5	2.5	2	$4.45x10^5$	1590	1850	$3.57x10^{-3}$	$4.15x10^{-3}$	1411	1642
Early Aptian	Ba2	TW-03-69	UWA Ba2	Barrabiddy 1 (150.75)	23°50'S	114°20'E	Carnarvon	Munderong Shale	not zoned	not zoned	*Muderongia australis* Zone	*P. oxys*	0.707496	27.0	26.0	3	$4.20x10^5$	3390	1890	$8.07x10^{-3}$	$4.5x10^{-3}$	3188	1777
Early Albian	E1	TW-03-65	UWA E1	Edaggee 1 (264.85)	25°21'S	114°14'E	Carnarvon	Basal Lower Gearle Siltstone	*E. crespinae-A. pitmani*	*Hedbergella planispira*	*Muderongia tetracantha* Zone	*Dimitobelus sp.*	0.707369	3.0	5.0	3	$4.44x10^5$	1440	1770	$3.2x10^{-3}$	$3.98x10^{-3}$	1281	1574
Early Aptian	Y1	TW-03-68	UWA Y1	Yinni 1 (59.03)	26°03'S	114°49'E	Carnarvon	Windalia Radiolarite	*T. cushmani - A. pitmani* Zone	not zoned	*O. operculata-D. Davidii* Zone	*P. australis*	0.707208	12.8	28.2	4	$4.32x10^5$	1130	1220	$2.6x10^{-3}$	$2.82x10^{-3}$	1033	1115

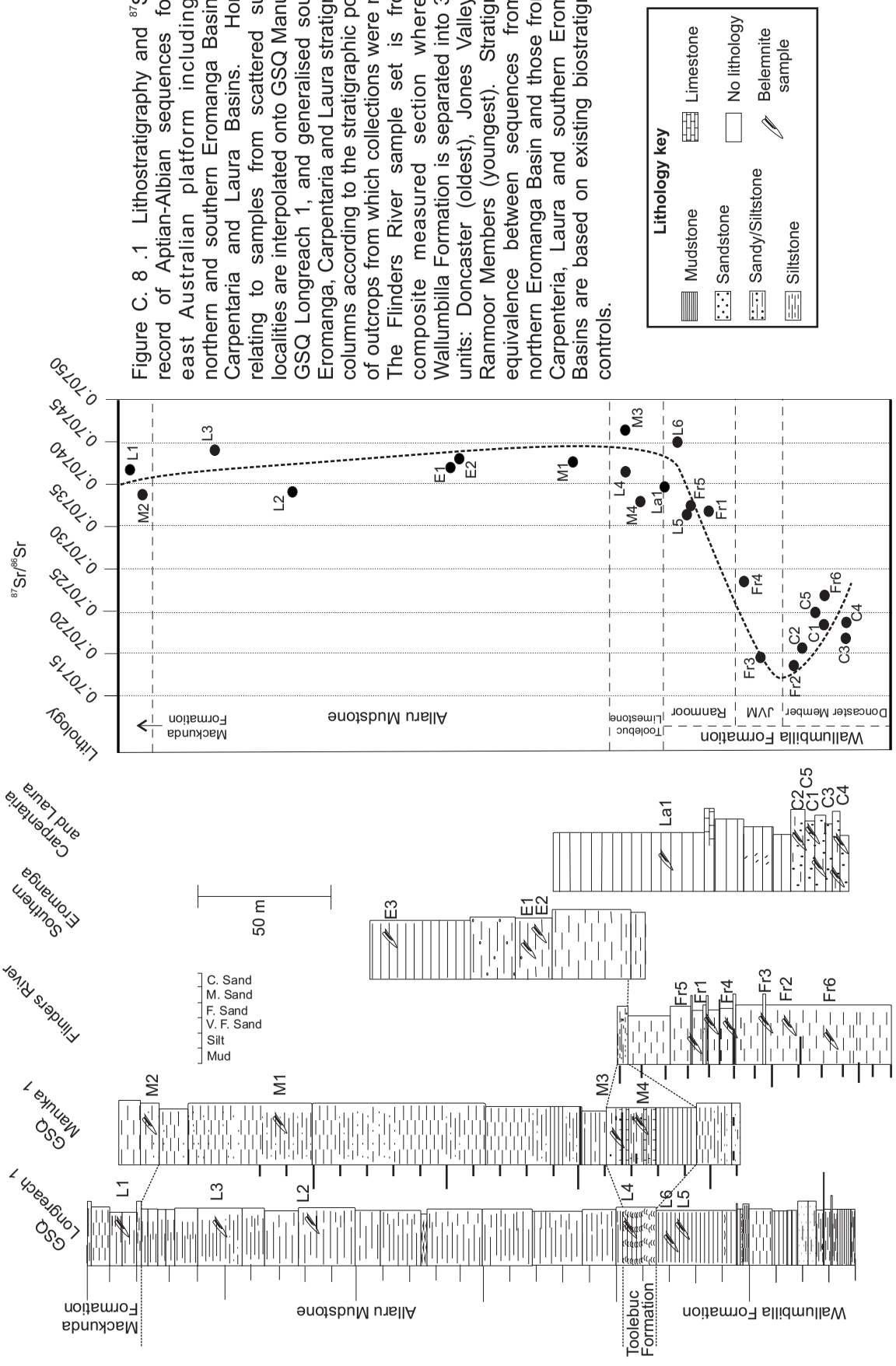
Lithology key
Mudstone
Limestone
Sandstone
No lithology
Sandy/Siltstone
Belemnite sample
Siltstone
Lithology
87Sr/86Sr
0.70715
0.70720
0.70725
0.70730
0.70735
0.70740
0.70745
0.70750
Mackunda Formation
Allaru Mudstone
Toolebuc Limestone
Wallumbilla Formation
Ranmoor
JVM
Doncaster Member
L1
L2
L3
M1
M2
M3
M4
L4
L5
L6
La1
E1
E2
Fr1
Fr2
Fr3
Fr4
Fr5
Fr6
C1
C2
C3
C4
C5
Figure C. 8 .1 Lithostratigraphy and 87Sr/86Sr record of Aptian-Albian sequences for the east Australian platform including the northern and southern Eromanga Basin, and Carpentaria and Laura Basins. Horizons relating to samples from scattered surface localities are interpolated onto GSQ Manuka 1, GSQ Longreach 1, and generalised southern Eromanga, Carpentaria and Laura stratigraphic columns according to the stratigraphic position of outcrops from which collections were made. The Flinders River sample set is from a composite measured section where the Wallumbilla Formation is separated into 3 sub-units: Doncaster (oldest), Jones Valley and Ranmoor Members (youngest). Stratigraphic equivalence between sequences from the northern Eromanga Basin and those from the Carpenteria, Laura and southern Eromanga Basins are based on existing biostratigraphic controls.
GSQ Longreach 1
GSQ Manuka 1
Flinders River
Southern Eromanga
Carpentaria and Laura
50 m
C. Sand
M. Sand
F. Sand
V. F. Sand
Silt
Mud
Mackunda Formation
Allaru Mudstone
Toolebuc Formation
Wallumbilla Formation

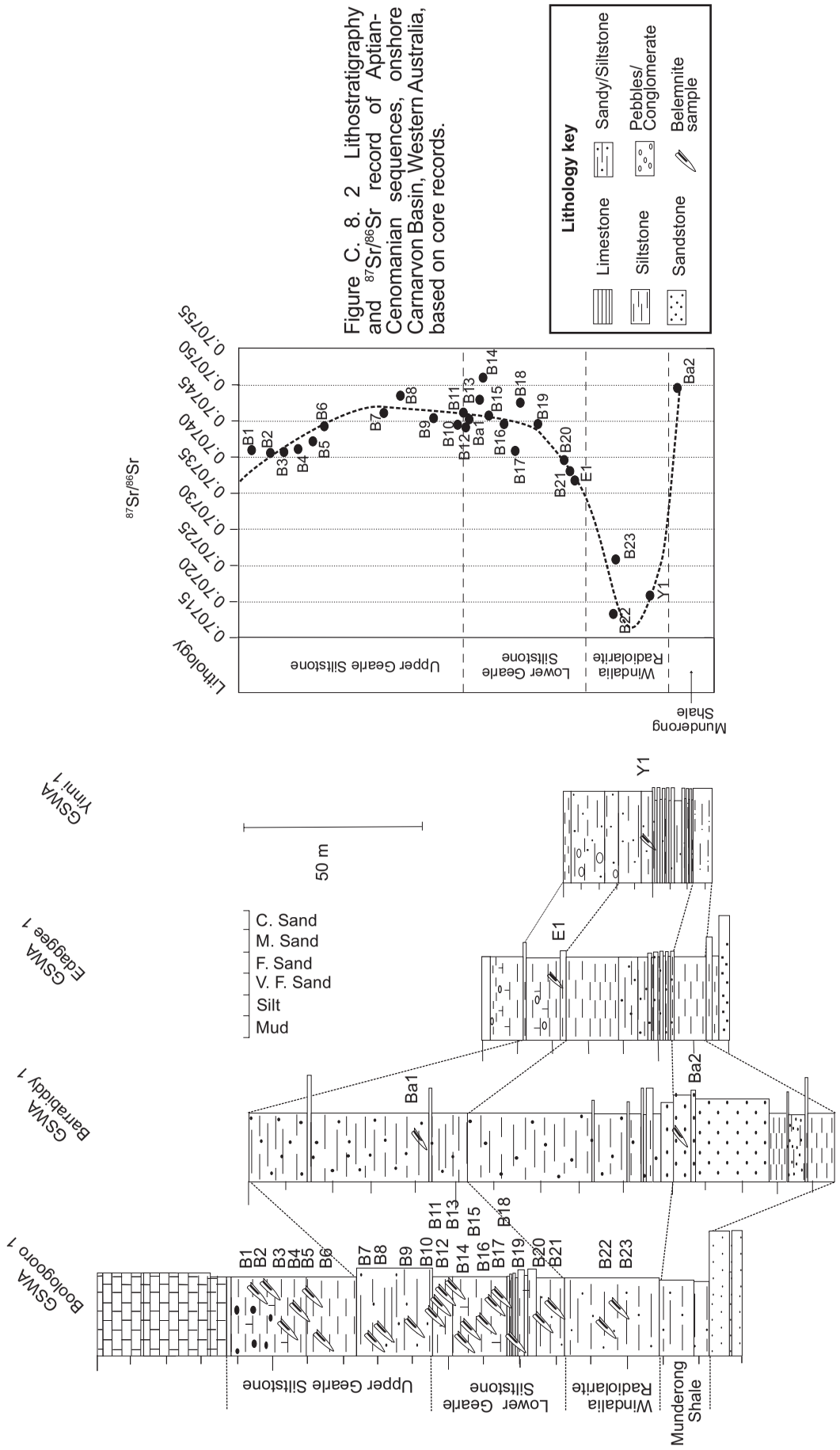

Figure C. 8. 2 Lithostratigraphy and $^{87}Sr/^{86}Sr$ record of Aptian-Cenomanian sequences, onshore Carnarvon Basin, Western Australia, based on core records.

prominent negative excursion in its lower part culminating in a $^{87}Sr/^{86}Sr$ value of 0.7071845. This culmination is followed by a relatively steep positive excursion reaching a $^{87}Sr/^{86}Sr$ value of 0.707464. The curve continues with little change in values and terminates at a $^{87}Sr/^{86}Sr$ value of 0.707415.

Samples from northern divisions of the east Australian platform, the Carpentaria and Laura Basins fit remarkably well when interpolated onto the Sr-isotope curve on the basis of stratigraphic correlation. The Carpentaria Basin data fits the prominent negative excursion plotted from the Eromanga data and is supported by superpositional relationships for the samples involved. Samples C3 and C4 are from the basal beds of the Wallumbilla Formation exposed along Walsh River and located very close to the contact with the underlying Gilbert River Formation. Samples C1 and C2 are from Wallumbilla Formation exposed by Elizabeth Creek. Ammonites found in these strata include aconiceratids that are not represented in the Wallumbilla Formation exposed in the Walsh River where exposures are considered to represent older horizons. The biostratigraphic age assigned to the Wolena Claystone, from which the Laura Basin sample was collected, is interpreted as being equivalent to that of the Ranmoor Formation of the Eromanga Basin (Haig and Lynch, 1993).

For the Western Australian samples superposition is based on lithostratigraphic succession apparent in stratigraphic boreholes. All of the data is from the southern Carnarvon Basin where a uniform lithostratigraphic framework applies. Samples are distributed through some 150 metres of sequence extending from the Munderong Shale to the upper Gearle Siltstone (Figure C. 8. 2). The Sr-isotope trend apparent from the data matches that for the eastern Australian succession. The southern Carnarvon Basin isotope curve likewise shows smooth trends with a prominent negative excursion in its lower part reaching a minimum Sr value of 0.707183. This negative culmination is followed by a positive excursion to a maximum $^{87}Sr/^{86}Sr$ value of 0.707509, with a sharp inflection in trend. Data points following the positive excursion show significant scatter, but the youngest group of analysed samples defines a smooth trend with ratios of approximately 0.70740.

Three discrete segments can be recognised in each of the two Sr-isotope curves. The first of these is characterised by a marked negative trend with $^{87}Sr/^{86}Sr$ values shifting progressively from 0.70750 to values below 0.70720. An equally marked positive trend follows with values moving progressively from less than 0.70720 to close to 0.70747. Thereafter values fall within a band between 0.70738 and 0.70748. Each segment may be used as a means of recognising synchronicity in the eastern and western successions.

The oldest segment displaying the negative trend is representative of samples from the Doncaster and Jones Valley Members of the Wallumbilla Formation of the northern Eromanga Basin. Samples from the lower part of the Wallumbilla Formation of the Carpentaria Basin also fit this trend. The southern Carnarvon Basin is represented by samples from the upper part of the Munderong Shale and Windalia Radiolarite.

A marked positive trend follows. For the northern Eromanga Basin, this trend corresponds with the deposition of the upper part of the Wallumbilla Formation, the Ranmoor Member, and the succeeding Toolebuc Formation. A sample from the Wolena Claystone of the Laura Basin also fits this trend. Such relationships accord with correlation of these units, based on biostratigraphic data.

With respect to the Carnarvon Basin succession, this trend is reflected in samples from lower part of the lower Gearle Siltstone but samples with isotopic values representing its early part are missing from the data set. This suggests that the Gearle Siltstone/Windalia Radiolarite boundary may represent a paracomformity. Palynological data (Dixon et al., 2003a) also suggests that this contact is an omission surface. Sample B18 from within the lower Gearle Siltstone marks the culmination of the trend. Its isotopic ratio of 0.7074755 is close to that of sample M3 which marks the culmination of the positive trend for the northern Eromanga Basin curve, measured at 0.707464.

Carnarvon Basin samples obtained from the upper part of the lower Gearle Siltstone show rapid changes in values between 0.70740 and 0.70750, perhaps reflecting a short interval of unusual tectonic activity of global scale. The period of

these changes is very short and definition of the curve depends on close stratigraphic sampling. For the northern Eromanga Basin this interval is represented by the lower part of the Allaru Formation for which Sr isotopic data is presently lacking.

The third and final segment to the Sr-isotope curve is representative of samples from the Allaru and Mackunda Formations of the northern Eromanga Basin. Ratios of samples from the Allaru Mudstone and its southern Eromanga equivalent, the Oodnadatta Formation, show near-stable Sr-isotope values, within the range 0.70738-0.70743. In the southern Carnarvon Basin this segment of the curve is represented by samples that span the lower Gearle Siltstone/upper Gearle Siltstone boundary and are closely matched at approximately 0.70745. A similar value is shown by the lowest sample from the Allaru Formation of the northern Eromanga Basin. For the youngest part of this Carnarvon Basin segment values range from 0.70741 to 0.70748 with the uppermost six samples defining a smooth curve descending from a value of 0.70744 to that of 0.70741. There is no match for the late upper Gearle in the east Australian platform, where non-marine deposition prevailed.

C. 9 Correlation of Australian sequences to the global Early Cretaceous timescale using strontium-isotope stratigraphy

A global Sr-isotope curve for the Early Cretaceous along with Sr-curves for the Australian sequences derived in this study is presented in Figure C. 9. 1. The global curve has been complied from Northern Hemisphere successions which have been calibrated against absolute time using the time scale of Gradstein et al. (1994) which employed Boreal ammonite zones and subzones under the assumption that they are of equal duration.

The Early-mid Cretaceous Sr-isotope record has been developed largely by data from belemnites and oysters from England (Jones et al., 1994a), foraminifera from 12 widely scattered deep sea drill sites (Bralower et al., 1997), bulk chalks from

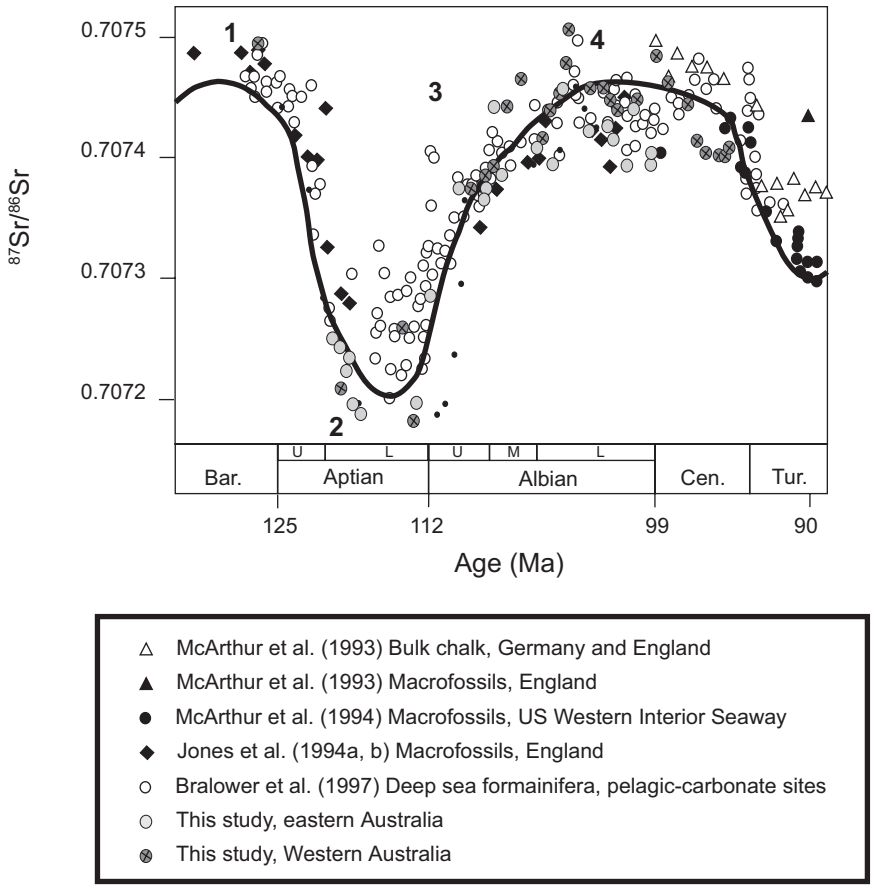

Figure C. 9. 1 Compilation of strontium isotopic data from published work including the data obtained in this study. The line of best fit is from Jones et al. (2001b), based on all data available at that time. Ages of stage boundaries are from Gradstein et al. (2004).

Germany and England (McArthur et al., 1993), and macrofossils from the United States Western Interior Seaway (McArthur et al., 1994).

The Neocomian to Albian sections of the curve are accurately correlated to the timescale of Ogg et al. (2004) on the basis of biostratigraphic control. Correlation of the data points from the English succession is based on the Boreal ammonite zonation of the Anglo-Paris Basin (Jones et al., 1994b). Correlation of the data points based on foraminifera employs the standard planktic foraminiferal and nannofossil biozonations as applied to the Early Cretaceous (Bralower et al., 1997).

As noted by Ogg et al. (2004) in their comprehensive review of the Cretaceous timescale, subdivision of the Aptian and Albian stages still awaits formal resolution and agreed stratotype definition. Subunits are treated here as informal. Following these authors, the Aptian is partitioned into early and late divisions corresponding to the European `Bedoulian' and `Gargasian' plus `Clansaysian' substages respectively. The boundary is placed at 124 Ma by Ogg et al. (2004) so that the subdivisions are of unequal duration. A threefold (lower, middle and upper) division of the Albian, based on the Tethyan ammonite zonation applied in Europe, is widely used and is utilised in the discussion below. The boundaries are set at 109 Ma and 106 Ma as suggested by Ogg et al. (2004).

The composite global curve (Figure C. 9. 1) shows several clear segments. The first of these is a major negative trend where $^{87}Sr/^{86}Sr$ values decline from 0.70745 to 0.70725 and extends from the latest Barremian through to the early Aptian. This excursion is almost exactly mirrored by the Australian data and permits correlation to the Carnarvon Basin sequence (see Figure C. 9. 2). The upper Muderong Shale is placed in the late Barremian, as indicated by a $^{87}Sr/^{86}Sr$ value of 0.70750 for sample Ba2, located 5 metres below the upper contact of this unit in Barrabiddy 1 where it has a thickness of 45 metres.

The second segment of the global curve is a trough that identifies the late Aptian where $^{87}Sr/^{86}Sr$ values are below 0.70725. This trough culminates at 0.707185 and represents the upper Windalia Radiolarite, which, in its entirety, is assigned as early to early late Aptian. Values for samples from the Doncaster Member in the northern Eromanga Basin and Wallumbilla Formation *sensu lato* of the Carpentaria Basin are closely comparable and are assigned as the late Aptian. The Wallumbilla Formation outcropping along the Walsh River and nearby in Elizabeth Creek, represents the most extensive exposure of the formation in the Carpentaria Basin; based on isotope data it is correlative with the Doncaster Member of the northern Eromanga Basin. Sampling through the Doncaster Member exposed in the Flinders River section does not cover the lowest 20 metres in a complete section of some 90 metres. Even so, the entirety of this unit is best assigned as late Aptian because the $^{87}Sr/^{86}Sr$ value of the stratigraphically lowest data-point is well separated from the early Aptian range. Samples C3 and C4 represent the base of the Wallumbilla Formation in the sequence exposed along the Walsh River and show that this unit in the Carpentaria Basin is wholly within the late Aptian.

Values for samples from the Jones Valley Member and the basal Ranmoor Member of the Flinders River Section are widely disparate, indicative of a considerable age span, although representing a narrow lithostratigraphic interval of only 15 metres. The Jones Valley Member is a thin (5-8 metres) unit of latest Aptian age; it represents a condensed interval consistent with its glauconitic lithology. A substantial difference between the highest Jones Valley Member value and that of the lowest sample from the Ranmoor Member, obtained 10 metres above its lower contact, suggests that the boundary between these units represents a disconformity, as previously suggested by Haig and Lynch (1993) based on biostratigraphic considerations, approximating to 2 m.y. (see Figure C. 9. 2). Although the glauconitic interval represented by the Jones Valley Member is absent from the Carnarvon Basin succession, an extended hiatus is identified from incongruent values within the upper Windalia Radiolarite and basal Gearle Siltstone. As sampling was detailed through the top of the Windalia Radiolarite and into the basal lower Gearle Siltstone, this interval must represent a disconformity at the Windalia-Gearle contact, as previously

reported by Mory et al. (1999) and Dixon et al. (2003a) based on biostratigraphic considerations, approximating to 5 m.y.

The third segment of the isotope curve is marked by a positive trend in $^{87}Sr/^{86}Sr$ towards 0.7074 which characterises the early and middle Albian. Samples in this study register values from only the upper part of this range and indicate ages close to the middle-late Albian boundary for the base of the Gearle Siltstone and Toolebuc Formation.

A fourth segment of the global curve is represented by a crest with Sr-isotope values ranging slightly above 0.7074. Its inception is in the mid-Albian and corresponds to Sr isotopic values from the Ranmoor Member of the Eromanga Basin succession. Sr-isotope values for samples of the Toolebuc-Mackunda interval are not age diagnostic in any detail because of the small range exhibited by the global curve through the middle and late Albian. The data are consistent with the middle-late Albian assignment for this part of the Eromanga Basin sequence, inclusive of the Oodnadatta Formation in its southern part, on biostratigraphic grounds. It is clear from the Sr-isotope record that the lower Gearle Siltstone correlates with an extended sequence in the eastern Australian succession that includes the Ranmoor Member, the Toolebuc Formation and part of the Allaru Mudstone.

Based on biostratigraphic assessment, Mory et al. (1999) and Dixon et al. (2003a) suggested that the hiatus between the lower and upper Gearle Siltstone spanned much of the late Albian. Although there is a decline in Sr isotopic values for the upper Gearle Siltstone samples the Sr-isotope data do not accurately identify the Albian-Cenomanian boundary and the analyses to hand are not informative on the nature of the hiatus. Strontium-isotope values for the upper Gearle Siltstone are consistent with a Cenomanian age, as indicated by biostratigraphic correlation.

C. 9. 1 Implications for the Australian Cretaceous timescale

Biozones for stratigraphically useful fossil groups in relation to the Sr-isotope curve are summarised in Figure C. 9. 2. Strontium-isotope stratigraphy indicates that some adjustments to the positions of Australian biozones relative to the international Early Cretaceous timescale are required. The Aptian-Albian boundary lies at a diagnostic point in the composite curve, at the termination of the second segment, described above and marked by a $^{87}Sr/^{86}Sr$ value of 0.70725, but is unconformable in both the sequences considered here.

Dinocysts are well represented in the successions for which strontium data is now available. The oldest unit of the Carnarvon Basin succession considered here, the Munderong Shale, generally contains dinocysts indicative of the *Munderongia australis* Zone (Taylor and Haig, 2001). However taxa indicative of the succeeding *Odontochitina operculata* Zone have been recognised from the upper part of the unit. This is the case for core samples from Edaggee 1 (Dixon et al., 2003a) and also appears to apply in core from Yinni 1 (Dixon et al., 2003b). For the Munderong Shale intersection in Barrabiddy 1, a sample with *O. operculata* was obtained 0.8 metres from the top of a 45.5 metre full section of this formation and *M. australis* was recognised in samples from 2.4 metres below the upper contact and throughout the remainder of the unit (Mory et al., 1999). This places the *M. australis* / *O. operculata* zonal boundary immediately above a belemnite sample from 5.75 metres below the upper contact in this core that returned a Barremian Sr-isotope value. Accordingly this zonal boundary is likely to lie within the late Barremian rather than the early Aptian position assigned to it by Oosting et al. (in press.) based on inter-regional biostratigraphic correlation.

Windalia Radiolarite intersected in Boologooro 1 and 1A contains dinocysts of the *Diconodinium davidii* Zone (Mory and Dixon, 2002) as is also the case for the intersection of this unit in Barrabiddy 1 (Mory et al., 1999). However, the *O. operculata* / *D. davidii* zonal boundary occurs within the lowest 10 metres of a 22 metre intersection in of Windalia Radiolarite in Yinni 1 (Dixon et al., 2003b). Poor representation of the *O. operculata* Zone in Carnarvon Basin cores suggests that the Munderong Shale–Windalia Radiolarite contact is a variably developed omission

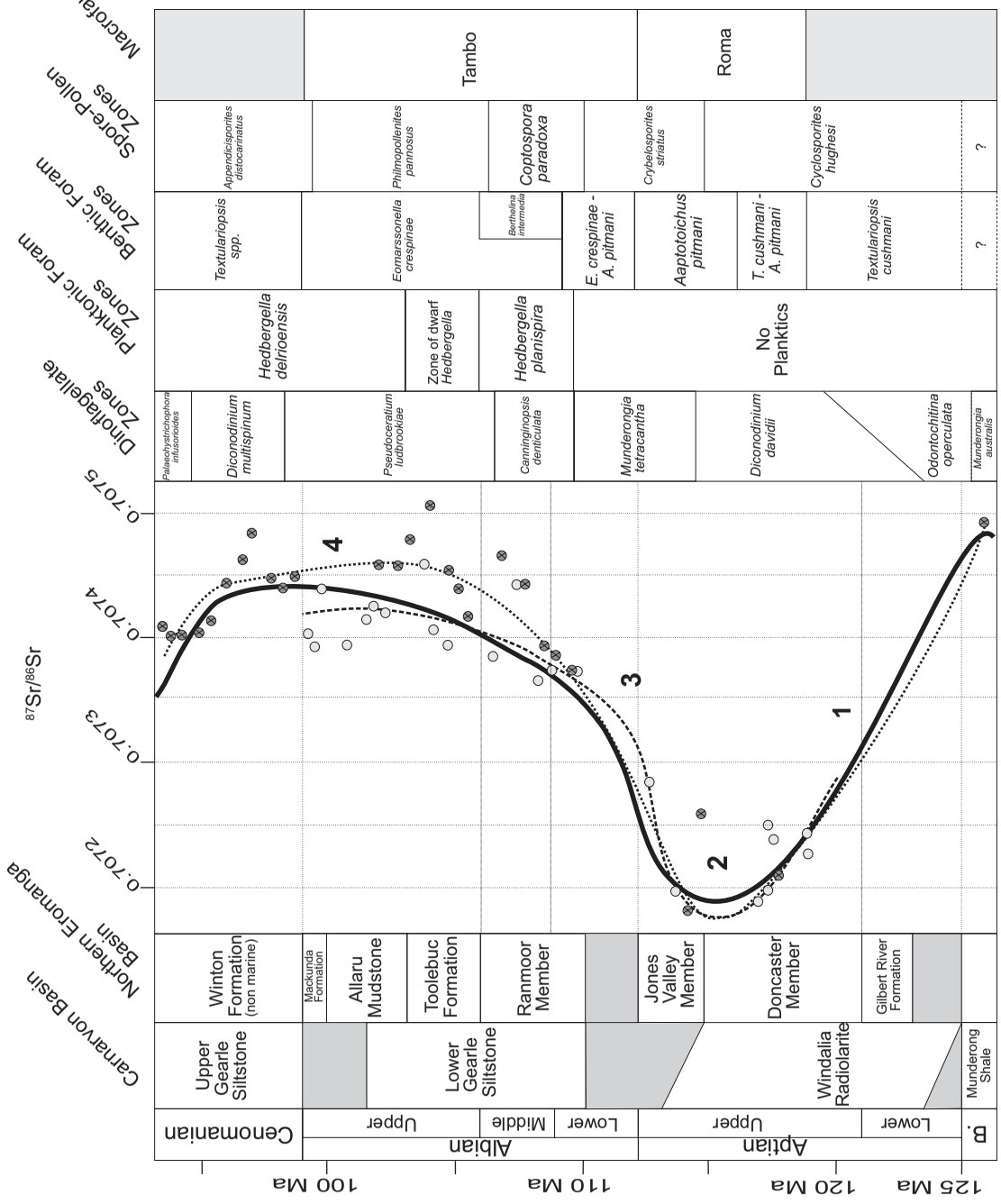

Figure C. 9. 2 Strontium-isotope curves for the east Australian platform ·····○····· and the Carnarvon Basin ----⊗---- sequences together with the reference curve for the Early Cretaceous provided by Jones et al. (2001b), plotted on the time scale of Ogg et al. (2004). Also shown are the biostratigraphic zonations that are based on faunal and floral successions for the two successions complied from Haig and Barnbaum (1978), Haig (1979), Haig and Lynch (1993), Dixon et al. (1996), Haig et al. (1996), Helby et al. (1987), Burger (1985), Campbell and Haig (1999), Haig, 2005 and Oosting et al. (2006).

surface which registers the *O. operculata* / *D. davidii* zonal boundary in some sections. Strontium isotopic values from the top 4.7 metres of the 38 metre intersection of Windalia Radiolarite in Boologooro 1 and 1A suggest that this formation spans much of the early and early late Aptian. Accordingly the *O. operculata* / *D. davidii* zonal boundary is best assigned to the early Aptian.

In Boologooro 1 the basal lower Gearle Siltstone contains the *Canninginopsis denticulata* dinocyst zone with the *Munderongia tetracantha* Zone completely missing (Mory and Dixon, 2002) probably due to disconformity at the Windalia-Gearle contact, The *Munderongia tetracantha* Zone is represented at the very top of the Windalia Radiolarite in Boologooroo 1 (Haig et al. , 2004) and in Edaggee 1 (Dixon et al., 2003a), and a sample from the lower part of the lower Gearle registers the *Canninginopsis denticulata* Zone in Edaggee 1. In Barrabiddy 1 the zones of *Munderongia tetracantha* and *Canninginopsis denticulata* succeed each other in the basal part of the lower Gearle Siltstone. Based on these relationships, and Sr-isotope calibration of the succession, the *D. davidii* / *M. tetracantha* zonal boundary is assigned to the late Aptian whereas the boundary separating the *M. tetracantha* and *Canninginopsis denticulata* zones lies close to the early-middle Albian boundary.

For the succession of the northern Eromanga Basin, the *Odontochitina operculata/Diconodinium davidii* zonal boundary was documented by Oosting (2004) as being within the basal interval of the Wallumbilla Formation (equivalent to the lower Doncaster Member) from a number of wells including Hughenden 7 and Manuka 1. This was also the case for Wallumbilla Formation intersected by Mossman 1 in the Carpentaria Basin, above the level of the lowest samples for which Sr-isotope data is available. The zonal boundary here appears to be within the late Aptian, somewhat higher than its position in the Carnarvon Basin.

The top of the Doncaster Member and the entire Jones Valley Member equivalents for samples from Hughenden 7 and other cores were placed within the *Diconodinium davidii* Zone by Oosting (2004) whereas the Ranmoor Member equivalents contain successive *Munderongia tetracantha* / *Canninginopsis denticulata* and *Canninginopsis denticulata* / *Pseudoceratium ludbrookiae* zonal boundaries. The same age

assignments as apply in the Carnarvon Basin succession are indicated by the Sr-isotope data.

The base of the *P. ludbrookiae* Zone occurs in the lower Gearle Siltstone in Boologooro 1 (Mory and Dixon, 2002) as is also the case for Barrabiddy 1 (Mory et al., 1999), in strata of middle Albian age. However, the zone extends into the upper Gearle Siltstone in Boologooro 1. Here the five uppermost samples analysed for Sr-isotopes have values of ~ 0.7074 and are within the Cenomanian. The stratigraphically lowest of these is from just 2 metres above the range of *P. ludbrookiae* in core from this hole. The middle Albian–early Cenomanian is indicated for the zone of *P. ludbrookiae* which extends somewhat higher than previously thought. Oosting (2004) found *P. ludbrookiae* to range through the Allaru and Mackunda Formations of the Eromanga Basin, right to the top of the marine section. The *Xenascus asperatus* Zone has not been recorded from the Carnarvon Basin succession, bringing into question its utility. The *Diconodinium multispinum* Zone is known from the upper Gearle Siltstone of Boologooro 1, from within the interval known to be Cenomanian from the Sr-isotope data. The uppermost interval of the formation is probably within the *Palaeohystrichophora infusorioides* Zone (Mory and Dixon, 2002). Both of these zones have been recorded for the upper Gearle Siltstone intersected by Edaggee 1 (Dixon et al., 2003a).

The spore-pollen zonal scheme of Helby et al. (1987) can be related to the Sr-isotope curve for the northern Eromanga Basin, based on the study of Hughenden 7 by Burger (1982b) and augmented by the broadscale study of Great Artesian Basin cores reported by Burger (1986). The *Cyclosporites hughseii* Zone (=*Osmundacidites dubius* Zone of Burger) is represented through the Doncaster Member (late Aptian). The *Crybelosporites striatus* Zone ranges through the Jones Valley Member equivalent and into the basal part of the Ranmoor Member, straddling the Aptian-Albian boundary. Most of the latter member is assigned to the *Coptospora paradoxa* Zone which is essentially of middle Albian age. The *Philmopollenites pannusus* Zone is represented by the uppermost interval of the Ranmoor Member in Hughenden 7 and

generally ranges through the Toolebuc, Allaru and Mackunda Formations for the Eromanga Basin. It is best assigned to the late middle and late Albian.

The ages assigned to key ammonites based on biostratigraphic correlation are supported by the strontium stratigraphy, with the Aptian/Albian boundary within the disconformity between the Jones Valley and Ranmoor Members in the succession of the northern Eromanga Basin and marked by the distinction between Roma and Tambo faunas. The appearance of *Tropeum* at the base of the late Aptian (Gargasian `substage') in Europe (Ogg et al., 2004) is consistent with its occurrence at the base of the Doncaster Member in the Flinders River section (R. Henderson, pers. comm.) and its occurrence in the Windalia Radiolarite (Ellis, 1993). Henderson and Kennedy (2002), assign the Allaru Mudstone to the early late Albian based on the occurrence of *Goodhallites goodhalli*, also represented in the Albian faunal succession of Anglo-Paris Basin as is consistent with the Sr-isotope data.

The benthic foraminiferal zonation for northeastern Australia proposed by Haig (1979b) and Haig and Lynch (1993) was recognised in the Flinders River section and the in core from Hughenden 7 and Manuka 1 by Campbell and Haig (1999). The *Aaptotoichus pitmani/A.pitmani–Eomarsonella crespinae* zonal boundary approximates to the contact between Jones Valley and Ranmoor Members and marks the Aptian-Albian division. The *A. pitmani* Zone is represented in the Doncaster and Jones Valley Members and is therefore late Aptian. The occurrence of this zone in the upper Windalia Radiolarite of the Carnarvon Basin succession reported by Dixon et al. (2003b) is also late Aptian. Representation of the *Eomarssonella crespinae* plus *Berthelina intermedia* Zone in the lower Gearle Siltstone and *Textulariopsis* Zone in the upper Gearle Siltstone respectively as reported in Dixon et al. (2003a) are of the middle-late Albian and Cenomanian.

Calcareous plankton are not well represented in either basinal succession. However occurrences of planktic foraminifera reported by Haig and Lynch (1993), Campbell and Haig (1999), Mory et al. (1999) and Dixon et al. (2003a) and nannoplankton recorded by Shafik (1985) and Dixon et al. (2003b), when related to the Sr-isotope curves presented here, give the same ages as those assigned to the zones they represent in global compilations (e.g. Bolli and Saunders, 1985; Ogg et al., 2004).

Biostratigraphic correlation of plankton in the basal lower Gearle Siltstone place it as lower Albian but offset from the Aptian/Albian boundary (Haig et al., 1996) and this age is also supported by the Sr-isotope data.

C. 10 Discussion

There is variation within the global data set and Sr-isotope values of equivalent age including those from the present study. However, the Australian data sits well within the spread of Sr-isotope values from other global records (Figure C. 9. 1). The current study used two unrelated successions of comparable age and is confident in the analytical results as they were obtained through a single laboratory employing a common procedure. A small but significant difference is apparent between the Albian values for the Carnarvon Basin and those of the east Australian platform. The source of sediment to the east Australian platform offers a potential explanation. It is considered to be dominantly pyroclastic in origin (Smart and Senior, 1982) derived from a large-scale silicic volcanic province located along the continental borderland to the east (Bryan et al., 2000). This circumstance may have moderated the Sr-isotope signature in waters of the Albian epeiric sea. $^{87}Sr/^{86}Sr$ ratios are depleted for acid volcanic rocks relative to oceanic values (see Leeman, 1982); either runoff from an extensive landscape of such rocks, or isotopic exchange between hydrating volcanic glass and seawater may well have resulted in slightly lower seawater values within a restricted, epicontinental water body.

Correlation between the sequences of the Carnarvon and northern Eromanga Basins based on the strontium ratio curve invites a comparison in eustatic history between eastern and western sectors of the Australian continent. A good level of comparability is evident for the Aptian and early to middle Albian, throughout this interval with the combined eustatic record corresponding to major excursions in the Sr-isotope curve (Figure C. 9. 3).

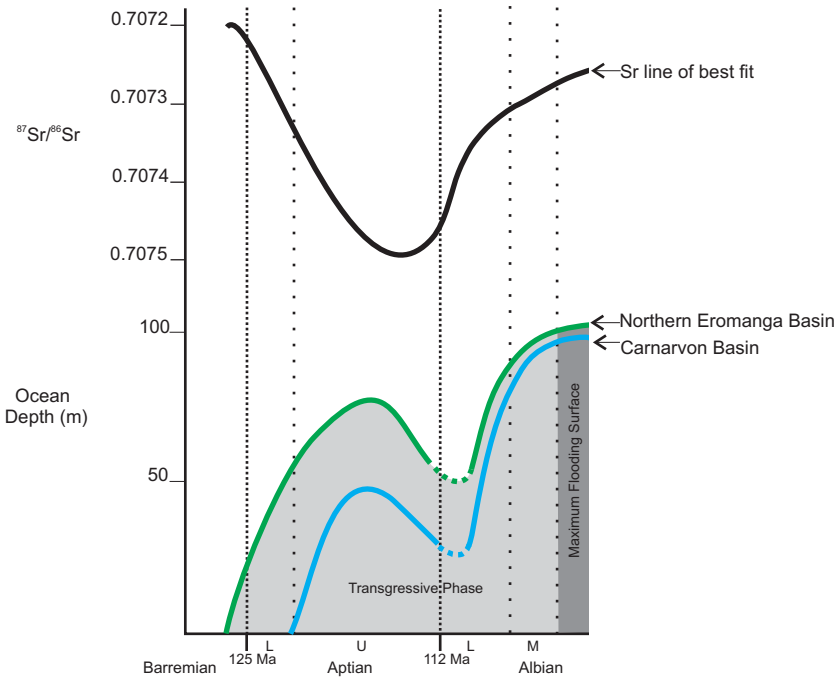

Figure C. 9. 3 Eustatic curves for the northern Eromanga Basin and Carnarvon Basin utilising water depths estimated from microfossils by Haig and Lynch (1993), Haig et al. (1996), Campbell and Haig (1999) and Taylor and Haig (2001). Strontium line of best fit from Jones et al. (2001b).

For the northern Eromanga Basin, Aptian transgression is marked by the littoral Gilbert River Formation, basal in the Cretaceous section, and succeeded by the Doncaster Member for which benthic foraminiferal assemblages record an initial deepening trend followed by shallowing in the upper Doncaster and continuing into the Jones Valley Member (Campbell and Haig, 1999). The disconformity, recognised as the contact between the Jones Valley and Ranmoor Members, represents a shallowing culmination and sediment bypass. For the Carnarvon Basin, inundation occurred earlier, conditioned in part by flexure of the western continental margin following its separation from India in the Valanginian. The Munderong Shale is the oldest marine unit in the southern Carnarvon Basin and its foraminiferal assemblages show a deepening trend (Taylor and Haig, 2001) which continued into the Windalia Radiolarite. The disconformity at the contact between the Windalia Radiolarite and the lower Gearle Siltstone represents shallowing and sediment bypass coeval with the corresponding eustatic episode registered for the northern Eromanga Basin. Aptian transgression resulted in the maximum inundation of continental Australia during the Mesozoic (Frakes et al., 1987). This eustatic cycle corresponds to the substantial negative excursion in strontium. As outlined by Jones and Jenkyns (2001) this coincidence may be explained by a major pulse of oceanic crust formation, simultaneously driving down the strontium-isotope ratio and inducing sea-level rise.

However, no such explanation pertains to the early-mid Albian positive excursion, which coincides with renewed transgression registered by microfaunas in the Ranmoor Member and the lower Gearle Siltstone (Haig and Lynch, 1993; Haig et al., 1996; Campbell and Haig, 1999). For the northern Eromanga Basin the deepening culmination is represented by the euxinic facies of the Toolebuc Formation (Henderson, 1998, 2004) for which values mark the termination of the positive Sr-isotope excursion. This transgressive episode corresponds to a eustatic rise that is clearly registered in the sedimentary record at global scale (Hancock and Kauffman, 1979; Haq et al., 1988). During this interval, the generation of new seafloor remained at a high level (see Jones and Jenkyns, 2001) but the flux of strontium from this source failed to maintain low $^{87}Sr/^{86}Sr$ values. However, a significant rising trend in oceanic temperature, registered by the oxygen isotope record, for the Carnarvon Basin and

elsewhere (Section D) corresponds to this excursion. A global climatic shift through this interval, sponsoring enhanced chemical weathering and a more substantial flux of strontium from continental sources, provides a rationale for the progressive rise in $^{87}Sr/^{86}Sr$ values.

SECTION D

Australian mid to high palaeolatitude Aptian - Cenomanian sea surface palaeotemperature estimates based on oxygen-isotope records from belemnite guards

Section D. Australian mid to high palaeolatitude Aptian - Cenomanian sea surface palaeotemperature estimates based on oxygen-isotope records from belemnite guards

D.1 Abstract

Measurements of oxygen-isotopes from belemnite guards are presented for specimen suites of the late Aptian-Albian from the Great Artesian Basin of eastern Australia and the late Barremian- Cenomanian from the Carnarvon Basin of Western Australia. Specimens used in the study were carefully screened for diagenetic overprint by means of luminescence and trace element protocols. Analyses of successive growth-laminae were undertaken for ten specimens of diverse provenance and age. Results generally indicate variation in palaeotemperature across a range of less than 4°C. Mean values for the range typically lie within 1°C of palaeotemperatures indicated by `bulk' single analyses obtained from the same specimens, thereby substantiating the veracity of single analyses for determining palaeotemperature trends through time. Within-specimen variation is best explained by belemnite migration during life. Data from the Carnarvon Basin, providing sea surface temperature estimates for palaeolatitudes of 40 – 45°S, show a long-term warming trend from 8-9°C to ~ 13°C through the Aptian and Albian. Shorter period (2-3 Ma) fluctuations of 4.5 and 2.5°C, in the mid Albian and the Cenomanian respectively, are also indicated as well as an abrupt cooling from ~13°C in the late Barremian to ~8°C in the late early Aptian across an interval of some 5 Ma. Data from the Great Artesian Basin, representing palaeolatitudes of 40 – 45°S, show a wide scatter which is attributed to the epeiric sea context of this sample set. The scatter reflects a combination of variable fresh water dilution, seasonal temperature regime fluctuations and isotopic exchange between seawater and pyroclastic sediment within the epeiric sea which invaded continental Australia in the Early Cretaceous. The lowest indicated palaeotemperature values derived from this data set and its Aptian-Albian trend are comparable to those obtained for the Carnarvon Basin. The lower range (Aptian) palaeotemperature estimates obtained in this study are consistent with a global temperature regime similar to the present; they are also compatible with cold continental winter minima as indicated by the occurrence of dropstones and glendonite in the southern inboard perimeter of the east Australian epeiric sea. The upper range (late Barremian, Albian and Cenomanian) palaeotemperatures suggest elevated global temperature regimes as indicated by a number of previous studies.

D. 2 Introduction

The Cretaceous has long been considered a greenhouse period, experiencing warm, equable global climatic conditions, with low latitudinal temperature gradients and ice-free polar-regions. This conclusion was originally based on floral and faunal distributions (Hallam, 1985; Frakes and Francis, 1988) and palaeotemperature estimates based on O-isotopes obtained from middle to low palaeolatitude marine biogenic carbonate (Barron et al., 1981). Contemporary documentation of high latitude floras shows that forests were present at palaeolatitudes as high as 80°

(Vakrameev, 1978; Douglas and Williams, 1982; Mutterlose, 1992; Henderson et al., 2000). Pronounced seasonality at higher latitudes, as expected from seasonal variation in solar energy, is apparent in the tree ring record (Vakrameev, 1978; Dettmann, 1994). More recent O-isotope palaeotemperature work (e.g. Huber et al., 2002) has provided estimates of sea temperatures from high palaeolatitudes; crucial for accurate modelling of the global Cretaceous climate. These studies also suggest high latitude sea temperatures were significantly higher in the Cretaceous than now.

Recently, views on the palaeogeographic position of Australia during the Early Cretaceous have changed considerably. Previous authors placed the southern margin of Australia at approximately 80°S during the Aptian (Henderson et al., 2000; Veevers, 2000) placing dinosaur localities in Victoria in a polar context (e.g. Rich and Rich, 1988). A recent compilation of palaeomagnetic data sets by Li and Powell (2001) has re-positioned the Early Cretaceous southern margin at approximately 65°S, placing the Australian continent in a somewhat different palaeogeographic context.

Evidence that moderate palaeotemperatures prevailed in high latitudes is broadly supported by previous Australian isotopic studies on belemnite guards from Aptian and Albian strata of Lake Eyre district, Central Australia, and the Roma district, Queensland (Dorman and Gill, 1959) and from early Albian strata from Western Australia (Pirrie et al., 1995). Palaeolatitudinal estimates by Li and Powell (2001) and Schettino and Scotese (2005), based on palaeomagnetic data, place much of Australia south of 45°S at these times (Figure D. 1. 1). Palaeotemperature records from higher Cretaceous Southern Hemisphere palaeolatitudes, based on isotopic studies of belemnites from the Albian-Maastrichtian of New Zealand (Stevens and Clayton, 1971), the Antarctic Peninsula (Pirrie and Marshall, 1990b) and Argentina (Pirrie et al., 2004) also indicate sea temperatures considerably higher than those of the present day. Palaeolatitudes exceeding 50°S prevailed for these locations with New Zealand lying within the polar circle (Li and Powell, 2001; Schettino and Scotese, 2005).

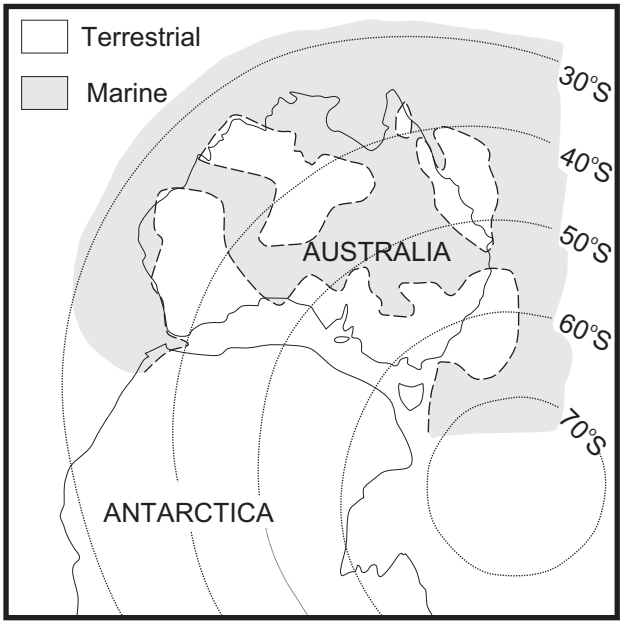

Figure D. 1. 1 Aptian - Albian palaeogeographic reconstruction of Australia and Antarctica. Aptian strata deposited in the southeastern extremity of the epicontinental seaway contains glendonites and ice-rafted dropstones (e.g. Frakes et al., 1995, Alley and Frakes, 2003). Solid lines represent the modern continental boundaries of Australia and Antarctica. Dashed lines represent the inferred continental boundaries during the Aptian - Albian. Palaeolatitudes from Li and Powell (2001); diagram modified after Veevers et al. (1991).

There is compelling evidence of seasonal sea ice development from the stratigraphic record of the southern Eromanga Basin, based on ice-rafted dropstones (Frakes and Francis, 1988; Alley and Frakes, 2003) and the occurrence of glendonites in the Bulldog Shale (Sheard, 1990; Frakes et al., 1995) near the southern inboard extremity of the Aptian epicontinental sea at a palaeolatitude of some 54°S (Figure D. 1. 1). Glendonites are unique calcite pseudomorphs after metastable ikaite ($CaCO_3.6H_20$) which form at the Earth's surface only at temperatures between -1.9°C and 7°C for marine and continental waters (De Lurio and Frakes, 1999). High latitude Valanginian-late Aptian glendonites also occur in the Sverdrup Basin in the Canadian Artic (Kemper, 1975; Frakes and Francis, 1988; Frakes et al., 1995; De Lurio and Frakes, 1999), and in the Valanginian of eastern Siberia and at Spitsbergen (Kemper, 1975). All of these occurrences indicate low temperature environments and have been associated with possible ice-rafted clasts (Francis and Frakes, 1993). In addition, Gregory et al. (1989) argued that mean annual temperatures of <5°C prevailed for southern Australia based on isotopic studies of Aptian-Albian carbonate concretions obtained from the terrestrial Otway and Strzelecki Groups, Victoria, Australia. The presence of seasonal snow and the possibility of permanent ice at high elevation at a palaeolatitude of approximately 65°S (Li and Powell, 2001) is implied by such data.

These contrasting palaeoenvironmental indicators raise questions of the Cretaceous climate. Was it warm and equable or was it sufficiently cold to develop polar ice? This has been subject to ongoing speculation (see Barron et al., 1981; Barron, 1983; Frakes and Francis, 1988; Huber et al., 1995; Huber et al., 2002) and is still open to debate.

This paper sets out to examine sea temperatures that prevailed in the Australian region during the Early Cretaceous based on O isotopic proxies using biogenic carbonate from belemnites. Part of the data set is from samples of the Aptian-Albian from the Great Artesian Basin, located between palaeolatitudes 40°S - 55°S during this time interval (Figure D. 1. 2). Palaeotemperature trends recorded by samples from the Eromanga, Carpentaria and Laura subdivisions of the Great Artesian Basin are of particular interest because they relate to a very extensive,

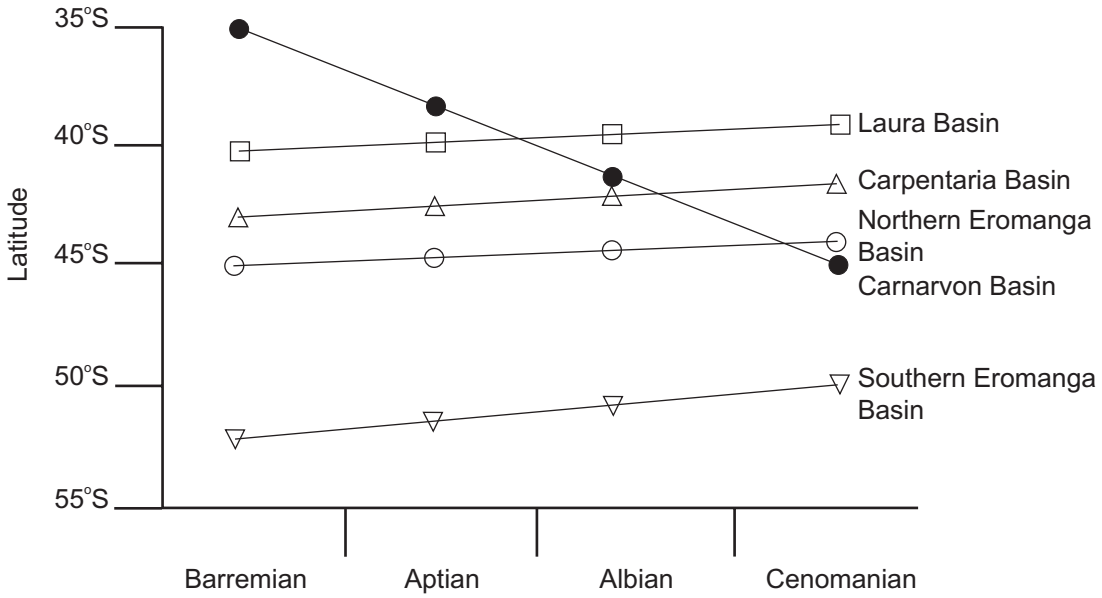

Figure D. 1. 2 Indicative palaeolatitudinal trends for sampling sites, based on palaeo-latitudinal estimates for the Early Cretaceous (ca. 130 Ma) and mid-Cretaceous (ca. 96 Ma) time provided by Li and Powell (2001). The northern and southern Eromanga Basin as well as subjacent sectors of the Carpentaria and Laura Basin show little change in palaeo-latitude from the Early to mid Cretaceous. The palaeolatitudinal trend for the Carnarvon Basin, Western Australia, is southerly due to anticlockwise rotation of continental Australia.

shallow epeiric sea that was widely developed across the Australian continent in the Early Cretaceous. Most of the data reported here is for the northern Eromanga Basin and subjacent Carpentaria and Laura Basins, located at a palaeolatitude of approximately 45°S during these times. Part of the study is based on samples of Barremian-Cenomanian age from the onshore Carnarvon Basin which is considered to have accumulated a sedimentary record of neritic association (Hocking et al., 1994; Dixon et al., 2003a) at a palaeolatitude of approximately 45°S during the Albian (Figure D. 1. 2).

Estimates of oceanic palaeotemperature based on O isotopic data obtained from biogenic carbonate are entirely dependent on salinity. Dilution caused by runoff is well recognised as a strong influence of O-isotope signatures (Pirrie and Marshall, 1990b; McArthur et al., 2004; Pirrie et al., 2004). Where brackish water conditions prevailed, isotopic values may simply reflect the influence of fresh water dilution which induced a negative shift in $\delta^{18}O$. This has proven to be the case for the Western Interior Seaway of North America where Cochran et al. (2003) found that abnormal salinities were characteristic, rendering palaeotemperature estimates based on O-isotopes impractical. Given that the main element of the Australian Cretaceous System, the Great Artesian Basin, represents an extensive epicontinental sea a similar situation might be expected. Indeed Frakes and Francis (1988) regarded the palaeotemperature estimates of Dorman and Gill (1959), based on isotopic evidence from the Great Artesian Basin, to be prejudiced by a fresh water influence.

Work on the western North American epeiric sea shows that these epicontinental seaways may have been depleted in $\delta^{18}O$ by several per mille relative to global ocean due to dilution (Tourtelot and Rye, 1969; Kyser et al., 1993; Pangani and Arthur, 1998). A freshwater influence for the Australian epicontinental seaway would result in low salinity waters with ^{18}O depletion, shifting indicated palaeotemperature estimates to erroneously high values (Frakes et al., 1995; De Lurio and Frakes, 1999). However, substantial freshwater dilution should be reflected in Sr-isotopes as fresh water runoff is enriched in $^{87}Sr/^{86}Sr$, and gives a different signature compared to normal marine circumstances as documented by Cochran et al. (2003). Indeed the

influence of the continental flux through fresh water runoff is considered to be a major factor in the change of Sr isotopic composition of seawater through time (Jones et al., 1994b; Veizer et al., 1999; Jones and Jenkyns, 2001).

Investigation of Sr isotopic ratios for samples from the Australian epeiric sea (Section C) shows:

(1) They match values for samples of the same age from the Carnarvon Basin which represents an open ocean, shelf setting; and

(2) They match ratios measured globally for open ocean carbonates of equivalent age.

Strontium-isotopic data for the Australian Early Cretaceous shows that comparable signatures prevailed in the Great Artesian Basin and the Carnarvon Basins, indistinguishable from the global signature for $^{87}Sr/^{86}Sr$, indicating that the marine waters of these basins was comprehensively mixed with the waters of the global ocean. Salinity variation caused by terrestrial runoff was no more than a minor influence, but even so, has the potential to prejudice palaeotemperature estimates in the epeiric Great Artesian Basin.

D. 2. 1 Belemnite guards as a basis for palaeotemperature estimates

Belemnite guards have been used widely in palaeotemperature studies (Dorman and Gill, 1959; Naydin et al., 1966; Stevens and Clayton, 1971; Pirrie and Marshall, 1990b; Ditchfield et al., 1994; Pirrie et al., 1995; Pirrie et al., 2004) because they are robust skeletal elements constructed of low-Mg calcite; a relatively stable mineral phase under diagenetic conditions. They are widespread throughout the Cretaceous System of Australia where they are well preserved and subject to close temporal control within well-established stratigraphic frameworks involving sedimentary rock units deposited in shallow marine (neritic) environments (see Section C).

New O-isotope palaeotemperature data obtained from Australian belemnites of Aptian, Albian and Cenomanian ages facilitate compilation of temperature curves for the Great Artesian (see Section C, Figures C. 3. 4 - C. 3. 6) and Carnarvon Basins

(see Section C, Figure C. 3. 2). The 56 guards employed in this study also provided Sr isotopic data (Section C) through which their accretion in normal marine salinities can be substantiated. Nine guards were subjected to analyses of multiple samples from different concentric growth rings to evaluate ontogenetic palaeotemperature trends.

D. 2. 2 Palaeobiology of belemnites in relation to palaeotemperature estimates

Belemnites showed tripartite palaeogeographic distribution during the Early Cretaceous (Christensen, 1997b). The Family Belemnopseidae had a Tethyan distribution, whereas the Family Belemnitellidae was restricted to the Boreal Realm and the Family Dimitobelidae inhabited the southern temperate Austral Realm. Palaeoecological interpretation of belemnites, based on their occurrence and palaeobiology, suggests that they were probably nektonic shelf dwellers with habitats ranging from surface waters and nearshore environments (Jarvis, 1980; Saelen et al., 1996) to deeper shelf-sea environments (Christensen, 1976; Anderson et al., 1994; Price et al., 2000). Palaeogeographical studies of the Dimitobelidae suggest that this family was predominantly restricted to shelf settings (Doyle and Pirrie, 1999). Fragmentary and abraded specimens have been identified from deep marine slope apron and submarine fan complexes in the James Ross Basin, Antarctica (Doyle, 1987c; Ineson, 1989) but these may have been transported from a shelf origin.

However, detail of the life habitats and depth range of belemnites in open ocean environments is speculative. Similar uncertainty applies to their geographical range and individuals are likely to have been only partly restricted by temperature. Doyle (1988) concluded that belemnites showed eurythermal tendencies and rare endemism.

The nearest living relatives of Early Cretaceous belemnites are the coleoids which have been documented as very mobile in their environment, both laterally and vertically (Hanlon and Messenger, 1996). Just like their living relatives, belemnites are likely to have migrated on a seasonal basis. The nature of such migration is obscure, but was probably dependant on a host of factors such as food, predators, currents, turbidity, temperature, and salinity as is the case for modern squid. Of these factors,

salinity is of greatest importance, as cephalopods cannot survive in brackish or highly saline waters (Hanlon and Messenger, 1996; Doyle, 1997; Cochran et al., 2003). Although squid are found in marine waters from equatorial to polar regions, temperature is considered a limiting factor in some living cephalopod distributions. However, as documented by Clarke (1966) and Hanlon and Messenger (1996), most oceanic squid can tolerate a relatively wide temperature range and even some small variations in salinities for brief periods. Given a predatory lifestyle, food supply is a prime control on cephalopod distribution and abundance, with members of the group favouring shelf seas where crustaceans and other food sources are plentiful.

Belemnite guards are constructed of incremental growth-laminae which record the ontogeny of individual animals. The growth banding is preserved as successive dark and light increments, which chart the palaeoenvironmental history of each specimen. Isotopic analyses of successive growth bands in individual belemnite guards show significant differences in $\delta^{18}O$. For example Stevens and Clayton (1971) found that $\delta^{18}O$ values ranged from -3.47 to +0.01 across the succession of laminae in an individual guard and that clear palaeotemperature trends are apparent in the succession of laminae for a number of specimens. This evidence is consistent with individual belemnites showing migratory behaviour, and experiencing different oceanic temperature regimes during their life. Such patterns may reflect either latitudinal migration of individual belemnites during their life history or could reflect bathymetric migration for individuals inhabiting different depth zones during ontogeny at much the same location.

There is also evidence from the $\delta^{18}O$ records of some guards of seasonality, with an alternation of palaeotemperatures indicated by successive growth bands. Indeed the laminated record is itself interpreted as reflecting seasonal fluctuations, with dark bands representing winter months and the lighter bands deposited during summer (Naydin et al., 1966; Longinelli, 1969; Stevens and Clayton, 1971). However, such variations could also reflect latitudinal migration from cold water to warm water, or from deeper, colder water to shallower, warmer water (Stevens and Clayton, 1971).

The migratory behaviour of belemnites suggested by these considerations is of direct relevance in interpreting the palaeotemperature records obtained in this study. All of the specimens subjected to analysis are of neritic association, where wave mixing should have generated a surface oceanic layer of relatively uniform temperature (Pickard and Emery, 1982). Water depths for the epeiric sea represented by strata of the Great Artesian Basin, are estimated to have been no more than 200 metres (Frakes et al., 1987) and palaeoenvironments represented by strata of the onshore Carnarvon Basin are considered to be of shelf association on both sedimentological and palaeontological grounds (Hocking et al., 1994). However, there is no guarantee that individual belemnites were exclusively associated with the palaeoenvironmental setting in which they last lived. Palaeotemperature records obtained from them may not necessarily reflect conditions in the oceanic surface layer at the location from which they were collected.

D. 3 Geological setting and sample selection

Palaeogeographic context for the Australian continent during the Cretaceous Period have been provided by Li and Powell (2001), based on a review of the available palaeomagnetic data. Their conclusions are closely matched by a global palaeomagnetic synthesis of palaeogeography recently complied by Schetteno and Scotese (2005). During the Early Cretaceous the Australian continent moved palaeolatitudinal position but mainly by rotation such that its eastern perimeter shifted very little. The western margin is considered by Li and Powell (2001) to have migrated in a southern trajectory by approximately 10° (Figure D. 1. 2). The separation of Australia along its western margin from India in the Valanginian (Veevers et al., 1991) led to the formation of the Carnarvon Basin as a passive margin assemblage facing the nascent Indian Ocean. The Southern Ocean separating Australia and Antarctica began to form at about 96 Ma (Cenomanian), with the opening of the Tasman Sea separating New Zealand occurring slightly later at 85 Ma (Santonian) (Li and Powell, 2001). Cretaceous ocean currents in the Australasian

region were constrained by the narrow seaways between the Gondwanan fragments, with the main elements of general circulation restricted to the palaeo-Pacific and Tethyan seaways (e.g. Henderson, 1990; Hay, 1995)(see Figure D. 6. 1).

Inundation of eastern Australia by an epeiric sea occurred during Barremian-Albian time, as recorded by Cretaceous strata of the Carpentaria, Laura, Surat and Eromanga subdivisions of the Great Artesian Basin. Ephemeral sedimentary remnants in central Australia suggest that shallow seaways may have extended across the continent during the Aptian linking the Great Artesian and Carnarvon basins (Frakes et al., 1987)(see Figure D. 1. 1).

Drawing on the extensive collections of belemnites available in museums and other repositories, and new field and core collections, a suite of specimens were selected to represent stratigraphic distribution of the group from the Carnarvon Basin and the Great Artesian Basin. Employing visual inspection and analytical screening (see Section C), this suite was reduced to 75 specimens selected for both O- and Sr-isotope analysis. Most represented whole guards but some fragmentary guards were included to achieve a more complete stratigraphic coverage. The location and stratigraphic positions of samples are given in Tables D. 1-4, along with analytical data and taxonomic identification, generally to species level.

The Carnarvon Basin sample set was largely derived from a single core-hole, GSWA Boologooro 1. Sampling embraced 89 metres of continuously cored section through the upper Windalia Radiolarite and Gearle Siltstone, considered on the basis of Sr-isotope stratigraphy and biostratigraphic grounds to range in age from late Aptian to Early Cenomanian. Correlation of Boologooro 1 with Barrabiddy 1, enabled sampling to be extended into the late Barremian Munderong Shale and early Aptian lower Windalia Radiolarite represented in that corehole (Figure D. 3. 1). In addition, four specimens obtained from surface exposures were sampled, analysed, and interpolated into the overall succession based on lithostratigraphic and biostratigraphic considerations.

Figure D. 3. 1 Lithostratigraphy and palaeotemperature record of Aptian - Cenomanian sequences, Carnarvon Basin, Western Australia, based on core records. Samples W1 to W4 ( ) have been interpolated into the sequences using palaeotemperture determinations and the sample's lithostratigraphic position in relation to other specimens. The plotted palaeotemperatures are the mean values determined using seasonal measurements.

Stratigraphic succession for the Great Artesian Basin is best known from the northern Eromanga sub-basin (Figure D. 3. 2). Sampling here was based on a composite exposed section measured along the banks of the Flinders River, in the northern sub-basinal sector, with close stratigraphic control through the Wallumbilla Formation, now known to extend through the Aptian stage (Section C). However, the majority of the available Eromanga sub-basin belemnite collections are from scattered, individual localities. These may be placed in the stratigraphic succession of the basin on the basis of their location relative to the distribution of lithostratigraphic units established from regional mapping. A superpositional composite for selected belemnite specimens scattered localities may be constructed with reference to GSQ Manuka 1 and GSQ Longreach 1, fully cored drill holes from the northern Eromanga sub-basin (Figure D. 3. 2).

Sampling from the southern Eromanga, Carpentaria and Laura sub-basins is based on belemnite collections from individual localities. These may be placed in superpositional relationships based on location relative to the distribution of lithostratigraphic units determined by regional geological mapping combined with biostratigraphic controls.

Local age assignments for the sequence of samples from the Great Artesian and the Carnarvon basins are based on biostratigraphic control of the lithostratigraphic units from which they were collected. In the Great Artesian Basin, macrofossils and palynology provide most of the control whereas for the Carnarvon Basin biostratigraphy is largely based on calcareous microfossils and palynology. Correlation to the international timescale (Gradstein et al., 1994; Ogg et al., 2004) is based largely on Sr-isotope stratigraphy across the Barremian to Aptian interval (see Section C) and index fossils for the Albian to Cenomanian interval.

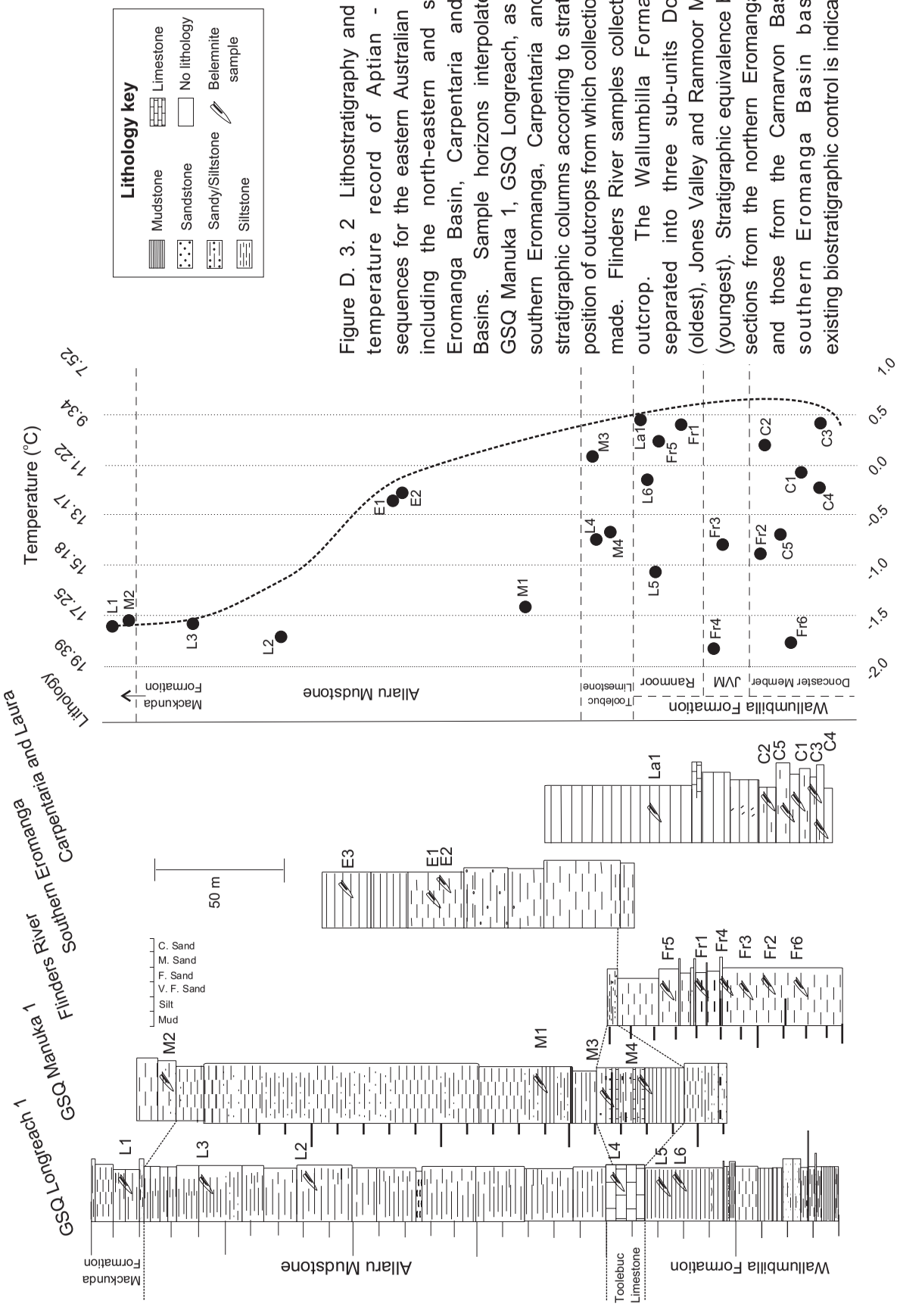

Figure D. 3. 2 Lithostratigraphy and palaeo-temperature record of Aptian - Albian sequences for the eastern Australian platform including the north-eastern and southern Eromanga Basin, Carpentaria and Laura Basins. Sample horizons interpolated onto GSQ Manuka 1, GSQ Longreach, as well as southern Eromanga, Carpentaria and Laura stratigraphic columns according to stratigraphic position of outcrops from which collections were made. Flinders River samples collected from outcrop. The Wallumbilla Formation is separated into three sub-units Doncaster (oldest), Jones Valley and Ranmoor Members (youngest). Stratigraphic equivalence between sections from the northern Eromanga Basin and those from the Carnarvon Basin and southern Eromanga Basin based on existing biostratigraphic control is indicated.

D. 4 Analytical methods

D. 4. 1 Sample preparation and evaluation

The guards used for sampling were within the set selected for Sr-isotope analysis on the basis of visual inspection, luminescence properties, and elemental analysis (see Section C). Powder samples, approximately 150-200 μg in weight, were extracted via drilling of individual growth bands displayed by guard cross-sections which were prepared as thin slices to show internal fabrics. Sampling was restricted to pale growth bands where organic content of the skeletal fabric is minimized. Areas of calcite alteration within the guard, typically observed adjoining the axial canal and as alteration selvedges to microfractures, are avoided using such methods of selection as luminescence imaging and visual inspection via microscopy.

Diagenetic alteration is typically reflected by substitution for calcium in the calcite lattice by iron, manganese and magnesium. The presence of Fe and Mn is reflected in luminescence properties, and the contents of all three elements have been determined by trace element analysis for the complete sample set (see Section C).

Sub-samples of the drilled powders were investigated by elemental analysis using a Varian Liberty Series II Inductively Coupled Plasma Atomic Emission Spectrometer (ICPAES) and the multi-element standard ICP-200.7 in a similar routine to that employed in Sr-isotope analysis. The trace element geochemistry of the sub-samples shows Mn and Fe values less than 100 ppm. Sr values vary from 316 to 2136 ppm, with Mg ranging from 10 to 3350 ppm (Tables D. 1-4). The trace element data is consistent with the interpretation that the belemnite guards are unaltered (Marshall, 1992)(see Section C).

To sample for ontogenetic variations, drilled powders was taken from cross-sectional discs of the guards by sampling successive light calcite-rich growth bands from the central apical canal to the outer surface (Figures D. 4. 1 and D. 4. 2). Thin growth bands were omitted from sampling to avoid contamination from more than

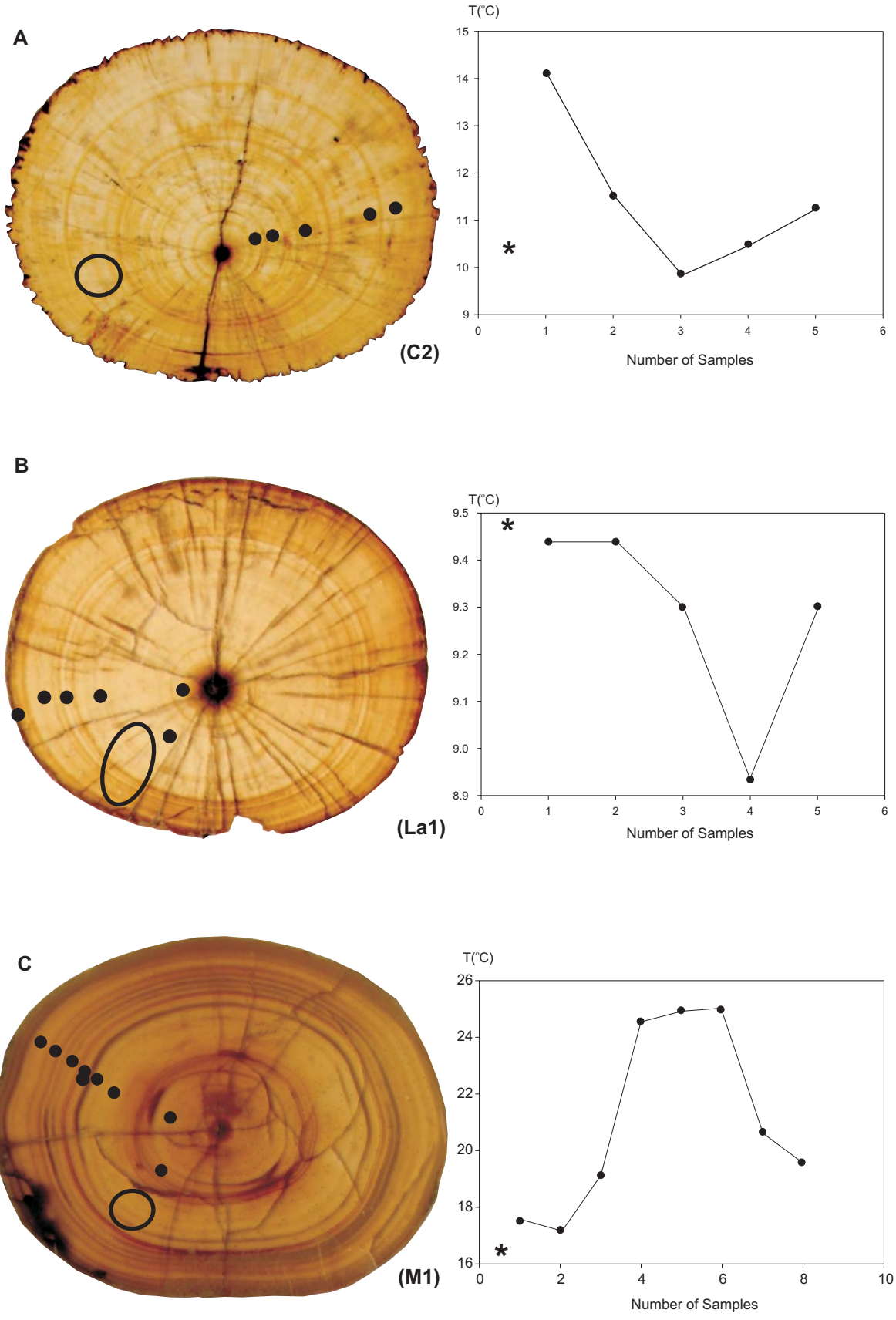

Figure D. 4. 1 *continue overleaf*

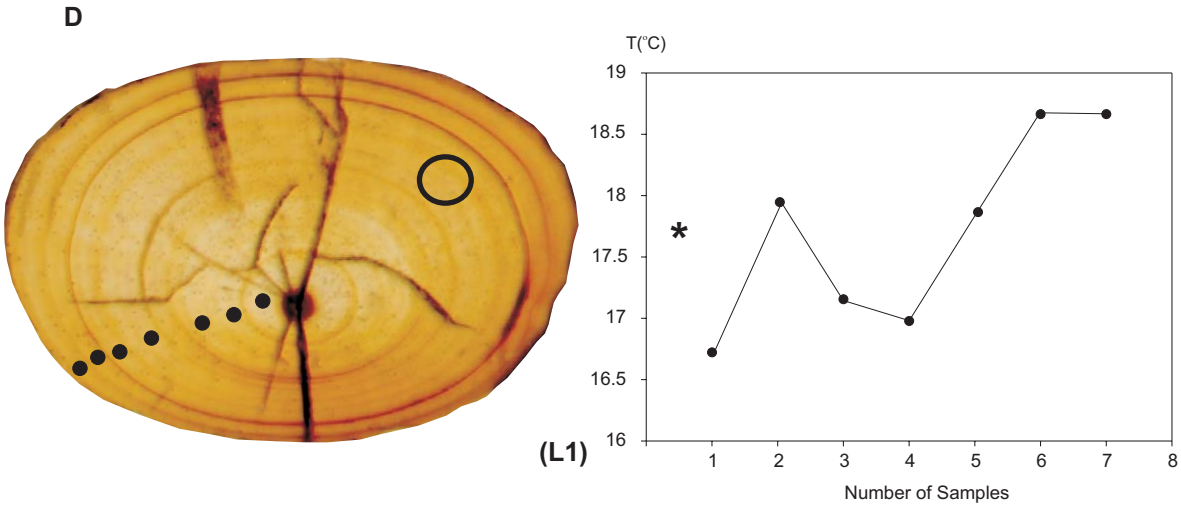

Figure D. 4. 1 A-D Multiple sample locations on transverse sections of belemnite guards from eastern Australia and corresponding analytical results plotted as palaeotemperatures. Sample numbers are in the order of growth-laminae with sample 1 nearest the apical canal and representing the most juvenile growth-laminae. Also shown by open circles are the sites of `bulk' samples taken from several laminae and the palaeotemperature resulting from the `bulk' analysis *. Cross-section illustrations are magnified as shown. A, specimen C2, Wallumbilla Formation, latest Aptian (x3.4); B, specimen La1, Wolena Claystone, late early Albian (x4); C, specimen M1, Allaru Mudstone, late Albian (x4.3); D, specimen L1, Mackunda Formation, latest Albian (x4.2).

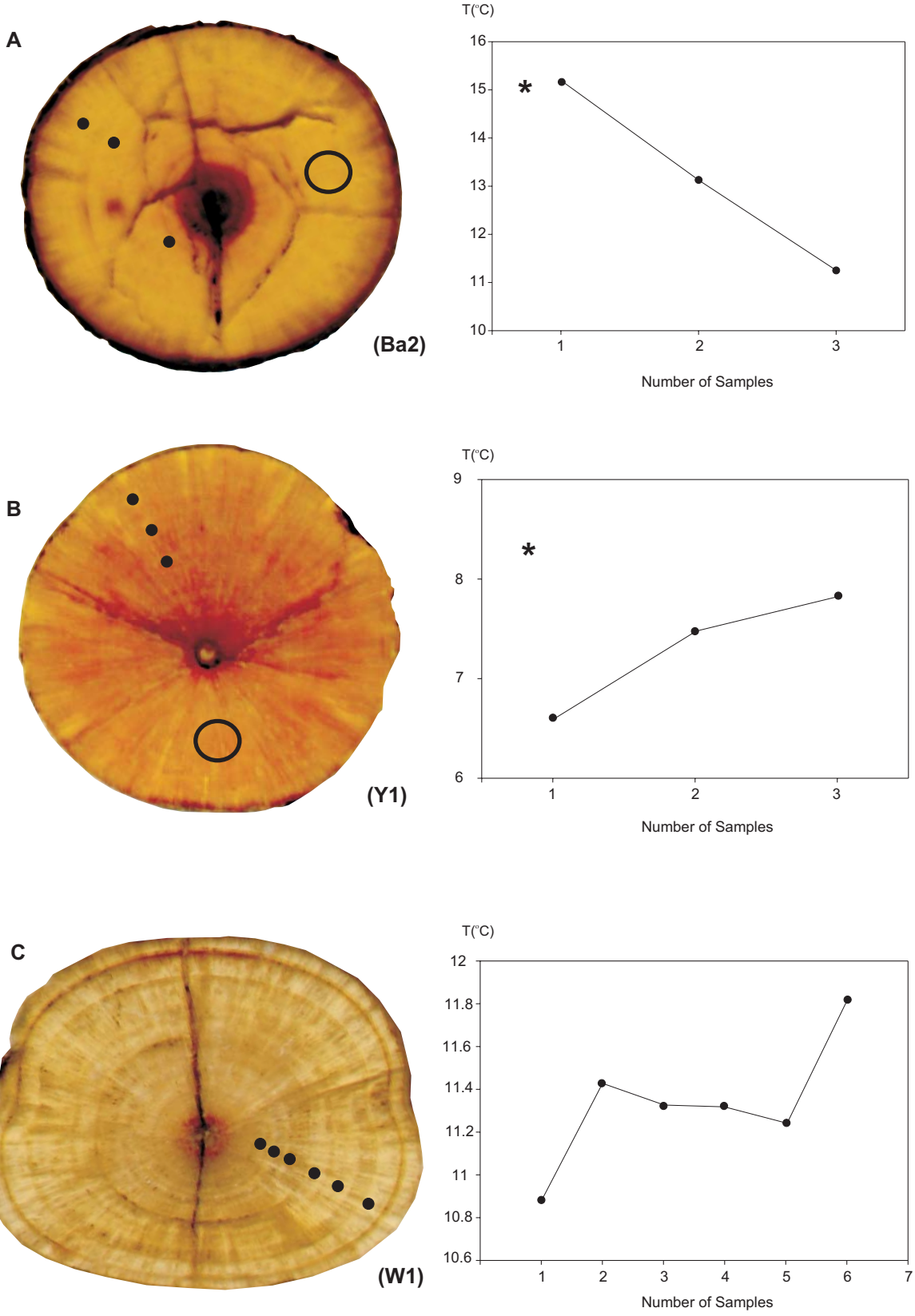

Figure D. 4. 2 *continue overleaf*

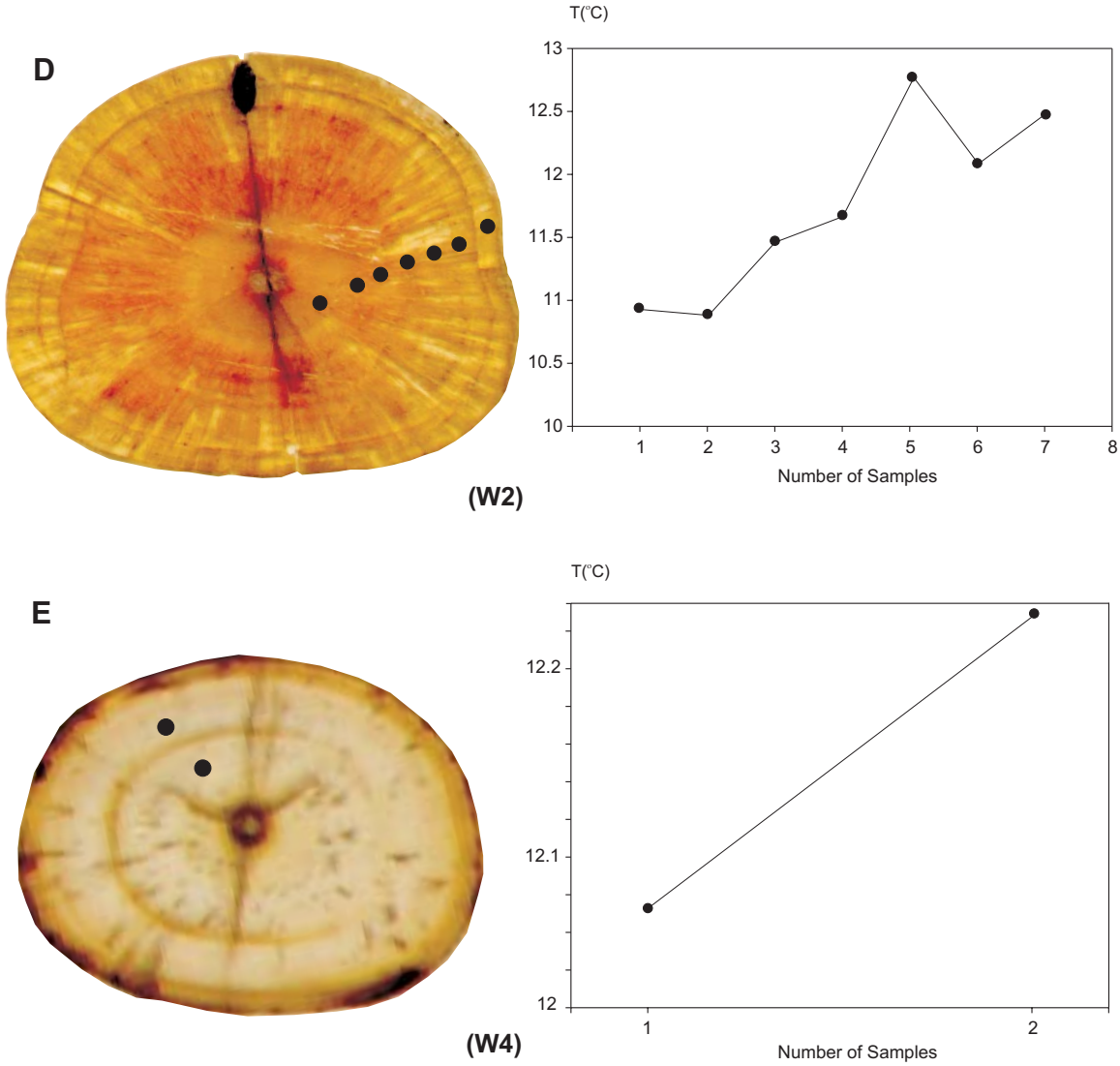

Figure D. 4. 2 A-E Multiple sample locations on transverse sections of belemnite guards from western Australia and corresponding analytical results plotted as palaeotemperatures. Sample numbers are in the order of growth-laminae with sample 1 nearest the apical canal and representing the most juvenile growth-laminae analysed. Also shown by open circles are the sites of `bulk' samples taken from several laminae and the palaeotemperature resulting from the `bulk' analysis *. Samples W1, W2 and W4 do not have `bulk' results. Magnification of diagrams as specified. A, specimen Ba2, Munderong Sandstone, earliest Aptian (x6.6); B, specimen Y1, Windalia Radiolarite, early Aptian (x7.9); C, specimen W1, Windalia Radiolarite, late Aptian (x5); D, specimen W2, Alinga Formation, late Albian (x4.2); E, specimen W4, upper Gearle Siltstone, Cenomanian (x12.3).

one band. Dark bands were avoided, as these are rich in organic material that may prejudice O-isotope analysis.

A 150-200 μg portion of each homogenised sample was used for stable O-isotope analysis. The remainder of the pooled sample aliquots (3.9 mg-16.0 mg) were utilized to determine trace elemental concentrations and in Sr-isotope analysis (see Section C).

D. 4. 2 Analytical techniques

Isotopic analyses were obtained by reacting the calcite with 3 drops of 107 % H_3PO_4 at 90°C in an automated individual-carbonate reaction (Kiel) device coupled with a Finnigan MAT 251 mass spectrometer operated by the Research School of Earth Sciences, Australian National University. Samples were not pre-treated prior to mass spectrometric measurement as it has been shown that cleaning protocols involving vacuum roasting, hydrogen peroxide, or oxygen plasma cleaning do not improve sample reproducibility (McConnaughey, 1989). The isotope ratios are reported as per mille (‰) deviations relative to PDB and were calibrated via the NBS-19 calcite standard ($\delta^{18}O$ = -2.20B‰, $\delta^{13}C$ = 1.95‰). Average internal precision is ±0.05‰ for $\delta^{18}O$ and ± 0.03‰ for $\delta^{13}C$ on a typical 150-μg sample.

D. 5 Results

Measured $\delta^{18}O$ values range between -3.22 and 1.34‰ and $\delta^{13}C$ values range between -0.78 and 5.13‰ (Tables D. 1-4).

Table D. 1

Isotopic and chemical data for belemnites from the Aptian-to-Albian strata of the north-eastern Eromanga Basin, Queensland.

Stage	Lithological No.	Isotope Sample No.	Specimen No.	Locality	Latitude	Longitude	Basin	Lithostratigraphic Position	Species	$^{87}Sr/^{86}Sr$ Means	Ca ppm	recalculated Mg ppm	recalculated Sr ppm	$d^{13}C_{PDB}$	$d^{18}O_{PDB}$	T(°C)
Latest Albian	L1	5297-21	QM F27918	Wincester Downs 80km SW of Richmond, Qld	21°11'S	142°37'E	Eromanga	Lower Mackunda Formation	*D. diptychus*	0.707415	$2.44x10^5$	2184	1958	missing	missing	17.7
Multiple Analysis	"	1 of 7	"	"	"	"	"	"	"	"	"	"	"	0.60	-1.33	16.5
Multiple Analysis	"	2 of 7	"	"	"	"	"	"	"	"	"	"	"	0.22	-1.66	17.9
Multiple Analysis	"	3 of 7	"	"	"	"	"	"	"	"	"	"	"	0.12	-1.47	17.1
Multiple Analysis	"	4 of 7	"	"	"	"	"	"	"	"	"	"	"	0.46	-1.43	17.0
Multiple Analysis	"	5 of 7	"	"	"	"	"	"	"	"	"	"	"	0.40	-1.64	17.8
Multiple Analysis	"	6 of 7	"	"	"	"	"	"	"	"	"	"	"	0.20	-1.84	18.7
Multiple Analysis	"	7 of 7	"	"	"	"	"	"	"	"	"	"	"	0.74	-1.84	18.7
Late Albian	L2	LA2	JCU 1987	Longreach, Qld	c.23°15'S	c.144°34'E	Eromanga	Upper Allaru Mudstone	*D.diptychus*	0.707392	$3.45x10^5$	582	1076	0.12	-1.70	18.1
Late Albian	L3	LA1	UQ F16922	Currane Station, 14.5km N of Dartmouth, central Qld.	23°24'S	144°45'E	Eromanga	Upper Allaru Mudstone	*D.liversidgei*	0.707441	$4.31x10^5$	1933	1283	-0.32	-1.57	17.5
Early late Albian	L4	5297-19	QGS F1369	Cambridge Downs Run, Flinders River, 13km from Richmond Downs Station	20°35'S	143°18'E	Eromanga	Toolebuc Limestone	*D.diptychus*	0.707414	$2.79x10^5$	1371	1656	2.42	-0.74	14.1
Early Albian	L5	5297-24	QGS F1759	Aramac Well	22°58'S	145°14'E	Eromanga	Upper Coreena Member	*D.diptychus*	0.707366	$2.79x10^5$	1571	1529	2.58	-1.06	15.4
Early Albian	L6	LC1	QGS F1370	Aramac Well at 72.54m, Aramac Town, Qld	22°59'S	145°15'E	Eromanga	Upper Coreena Member	*D.diptychus*	0.707449	$4.55x10^5$	1198	1371	2.10	-0.09	11.6
Late Albian	M1	5297-20	QM F27742	Richmond, Qld	20°44'S	143°08'E	Eromanga	Allaru Mudstone	*D.diptychus*	0.707427	$2.57x10^5$	2228	2136	0.30	-1.41	16.9
Multiple Analysis	"	1 of 8	"	"	"	"	"	"	"	"	"	"	"	-0.69	-1.55	17.5
Multiple Analysis	"	2 of 8	"	"	"	"	"	"	"	"	"	"	"	0.27	-1.48	17.2
Multiple Analysis	"	3 of 8	"	"	"	"	"	"	"	"	"	"	"	0.42	-1.96	19.2
Multiple Analysis	"	4 of 8	"	"	"	"	"	"	"	"	"	"	"	-0.91	-3.14	24.5
Multiple Analysis	"	5 of 8	"	"	"	"	"	"	"	"	"	"	"	-0.36	-3.22	24.9
Multiple Analysis	"	6 of 8	"	"	"	"	"	"	"	"	"	"	"	-0.05	-3.22	24.9
Multiple Analysis	"	7 of 8	"	"	"	"	"	"	"	"	"	"	"	0.83	-2.32	20.8
Multiple Analysis	"	8 of 8	"	"	"	"	"	"	"	"	"	"	"	0.94	-2.07	19.7
Late Albian	M2	FRA1	QM F2105	Tarbrax Stn, near Maxwellton	21°06' S	142°26'E	Eromanga	Lower Mackunda Formation	*D.diptychus*	0.707392	$4.34x10^5$	1802	1629	0.69	-1.54	17.4
Early late Albian	M3	T2	JCU 11616	Quarry 15km E of Julia Creek	20°38' S	141°54'E	Eromanga	Toolebuc Limestone	*D.diptychus*	0.707464	$4.61x10^5$	1225	1499	1.51	0.10	10.8
Late early Albian	M4	T1	JCU 11615	Quarry 15km E of Julia Creek	20°38' S	141°54'E	Eromanga	Toolebuc Limestone	*D. stimulus*	0.707383	$4.97x10^5$	1311	1279	1.39	-0.66	13.8
Early Albian	FR1	5297-39	JCU F11633 L910	Flinders River, Prairie, Grid Ref: 430 120	20°40'S	144°32'E	Eromanga	Ranmoor Member	*D.stimulus*	0.707371	$2.97x10^5$	1782	1239	1.15	0.45	9.5
Late Aptian	FR2	5297-38	JCU F11636 L908	Flinders River, Prairie, Grid Ref: 506 113	20°40'S	144°36'E	Eromanga	Upper Doncaster Member	*P. oxys*	0.707185	$2.92x10^5$	1099	937	4.41	-0.88	14.7
Late Aptian	FR3	5297-45	JCU F11637 L912	Flinders River, Prairie, Grid Ref: 493 100	20°41'S	144°34'E	Eromanga	Jones Valley Member	*P. oxys*	0.707196	$3.21x10^5$	1021	662	2.54	-0.77	14.2
Late Aptian	FR4	5297-34	JCU F11638 L916	Flinders River, Marathon, Grid Ref: 096 275	20°32'S	143°58'E	Eromanga	Jones Valley Member	*P. oxys*	0.707287	$2.07x10^5$	2537	713	2.45	-1.82	18.6
Early Albian	FR5	5297-32	JCU F11634 L914	Flinders River, Hughenden, Grid Ref: 368 167	20°37'S	144°28'E	Eromanga	Upper Ranmoor Member	*D. stimulus*	0.707374	$2.56x10^5$	1421	836	0.73	0.27	10.2
Early Aptian	FR6	FR1	JCU F11639 L907	Flinders River, Prairie, Grid Ref: 535 137	20°39'S	144°38'E	Eromanga	Lower Doncaster Member	*P. oxys*	0.707269	$4.39x10^5$	2069	989	2.40	-1.77	18.4

Table D. 2

Isotopic and chemical data for belemnites from the Aptian-to-Albian strata of the southern Eromanga Basin, South Australia.

N.B. Formaniniferal and dinoflagellate zones adapted from Kreig *et. al .,* 1995.

Stage	Lithological No.	Isotope Sample No.	Specimen No.	Locality	Latitude	Longitude	Basin	Lithostratigraphic Position	Species	$^{87}Sr/^{86}Sr$ Means	Ca ppm	recalculated Mg ppm	recalculated Sr ppm	$d^{13}C_{PDB}$	$d^{18}O_{PDB}$	T(°C)
Late Albian	E1	5297-12	NMV 310468	Woodduck Creek, Peake Station, S.A.	27°56'S	136°13'E	Eromanga	Oodnadatta Formation	*D. diptychus*	0.707421	$3.10x10^5$	1414	1771	1.09	-0.28	12.30
Late Albian	E2	5297-11	NMV 310431	From cliffs on banks of River Neales, 22.5km SE of Algebuckinna, S.A.	28°08'S	135°59'E	Eromanga	Oodnadatta Formation	*D. stimulus*	0.707427	$3.36x10^5$	1751	1504	0.69	-0.24	12.15

Table D. 3

Isotopic and chemical data for belemnites from the Aptian-to-Albian strata of the Carpentaria and Laura Basin, north Queensland.

Stage	Lithological No.	Isotope Sample No.	Specimen No.	Locality	Latitude	Longitude	Basin	Lithostratigraphic Position	Species	$^{87}Sr/^{86}Sr$ Means	Ca ppm	recalculated Mg ppm	recalculated Sr ppm	$d^{13}C_{PDB}$	$d^{18}O_{PDB}$	T(°C)
Early late Aptian	C1	EC1	QGS 8430 W10	East bank of Walsh River, 1km N of Boomers Hole	16°40'S	143°59'E	Carpentaria	Lower Wallumbilla Formation	*P. oxys*	0.707237	$4.71x10^5$	1174	1090	2.48	-0.04	11.4
Late Aptian	C2	5297-26	QGS F8773	North bank of Elizabeth Creek, 0.3km W of crossing of Wrotham Park; Walsh Telegraph Station Track	16°39'S	143°58'E	Carpentaria	Upper Wallumbilla Formation	*P. oxys*	0.707195	$2.66x10^5$	944	697	3.30	0.22	10.4
Multiple Analysis	"	1 of 5	"	"	"	"	"	"	"	"	"	"	"	2.71	-0.74	14.1
Multiple Analysis	"	2 of 5	"	"	"	"	"	"	"	"	"	"	"	3.14	-0.05	11.4
Multiple Analysis	"	3 of 5	"	"	"	"	"	"	"	"	"	"	"	3.16	0.44	9.6
Multiple Analysis	"	4 of 5	"	"	"	"	"	"	"	"	"	"	"	3.66	0.20	10.5
Multiple Analysis	"	5 of 5	"	"	"	"	"	"	"	"	"	"	"	5.13	0.00	11.2
Early Aptian	C3	WR1	JCU F81234	Boomers Hole Walsh River	16°32'S	143°47'E	Carpentaria	Lower Wallumbilla Formation	*P. oxys*	0.707206	$4.53x10^5$	1159	1081	3.14	0.46	9.5
Early Aptian	C4	WR3	QM F33252 L681	Boomers Hole Walsh River	16°32'S	143°47'E	Carpentaria	Lower Wallumbilla Formation	*P. oxys*	0.707244	$4.22x10^5$	1048	954	2.04	-0.25	12.2
Early late Aptian	C5	WR2	JCU F5171	1.6km N of Boomers Hole, Walsh River	16°49'S	143°58'E	Carpentaria	Lower Wallumbilla Formation	*P. oxys*	0.707246	$4.24x10^5$	520	1257	3.40	-0.68	13.9
Early Albian	La1	5297-01	JCU F11618	Laura, Tablelands	15°56'S	144°10'E	Laura	Wolena Claystone	*D. dayi*	0.707393	$3.64x10^5$	2105	1682	0.54	0.46	9.5
Multiple Analysis	"	1 of 5	"	"	"	"	"	"	"	"	"	"	"	0.81	0.47	9.4
Multiple Analysis	"	2 of 5	"	"	"	"	"	"	"	"	"	"	"	0.47	0.47	9.4
Multiple Analysis	"	3 of 5	"	"	"	"	"	"	"	"	"	"	"	0.04	0.51	9.3
Multiple Analysis	"	4 of 5	"	"	"	"	"	"	"	"	"	"	"	0.82	0.61	8.9
Multiple Analysis	"	5 of 5	"	"	"	"	"	"	"	"	"	"	"	1.01	0.51	9.3

Table D. 4

Isotopic and chemical data for belemnites from the Aptian-to-Cenomanian strata of the Carnarvon Basin, Western Australia.

Stage	Lithological No.	Isotope Sample No.	Specimen No.	Well Name-Depth (m)	Latitude	Longitude	Basin	Lithostratigraphic Position	Species	$^{87}Sr/^{86}Sr$ Means	Ca ppm	recalculated Mg ppm	recalculated Sr ppm	$d^{13}C_{PDB}$	$d^{18}O_{PDB}$	T(°C)
Early late Cenomanian	B1	2	UWA B1	Boologooro 1 (293.10)	24°19'S	113°54'E	Carnarvon	Upper Gearle Siltstone	*Dimitobelus sp.*	0.707410	$3.98x10^5$	1826	1319	-0.37	-0.74	12.7
Early late Cenomanian	B2	4	UWA B2	Boologooro 1 (297.95)	24°19'S	113°54'E	Carnarvon	Upper Gearle Siltstone	*Dimitobelus sp.*	0.707406	$4.01x10^5$	2206	1221	0.74	-0.63	13.7
Early late Cenomanian	B3	9	UWA B3	Boologooro 1 (301.55)	24°19'S	113°54'E	Carnarvon	Upper Gearle Siltstone	*Dimitobelus sp.*	0.707407	$3.93x10^5$	1909	611	0.14	-0.52	13.2
Late early Cenomanian	B4	12	UWA B4	Boologooro 1 (305.15)	24°19'S	113°54'E	Carnarvon	Upper Gearle Siltstone	*Dimitobelus sp.*	0.707411	$4.01x10^5$	2521	1221	0.06	-0.53	13.3
Late early Cenomanian	B5	16	UWA B5	Boologooro 1 (308.80)	24°19'S	113°54'E	Carnarvon	Upper Gearle Siltstone	*D. stimulus*	0.707421	$4.17x10^5$	1155	891	-0.78	-0.49	13.1
Early Cenomanian	B6	18	UWA B6	Boologooro 1 (311.60)	24°19'S	113°54'E	Carnarvon	Lower Upper Gearle Siltstone	*D.diptychus*	0.707443	$3.68x10^5$	1889	1127	0.51	-0.32	12.5
Late Albian	B7	19	UWA B7	Boologooro 1 (326.60)	24°19'S	113°54'E	Carnarvon	Lower Upper Gearle Siltstone	*Dimitobelus sp.*	0.707461	$3.76x10^5$	3256	1176	0.55	-0.41	12.8
Late Albian	B8	20	UWA B8	Boologooro 1 (330.70)	24°19'S	113°54'E	Carnarvon	Lower Upper Gearle Siltstone	*Dimitobelus sp.*	0.707484	$3.76x10^5$	2363	1187	0.15	-0.55	13.4
Late Albian	B9	22	UWA B9	Boologooro 1 (339.14)	24°19'S	113°54'E	Carnarvon	Lower Upper Gearle Siltstone	*Dimitobelus sp.*	0.707454	$3.93x10^5$	2763	1186	-0.03	-0.51	13.2
Late Albian	B10	26	UWA B10	Boologooro 1 (345.35)	24°19'S	113°54'E	Carnarvon	Lower Upper Gearle Siltstone	*Dimitobelus sp.*	0.707445	$3.72x10^5$	2728	1316	-0.15	-0.39	12.7
Late Albian	B11	29	UWA B11	Boologooro 1 (346.90)	24°19'S	113°54'E	Carnarvon	Basal Upper Gearle Siltstone	*Dimitobelus sp.*	0.707461	$3.89x10^5$	2365	1147	0.83	-0.29	12.3
Early late Albian	B12	30	UWA B12	Boologooro 1 (347.40)	24°19'S	113°54'E	Carnarvon	Upper Lower Gearle Siltstone	*Dimitobelus sp.*	0.707442	$3.84x10^5$	2407	1265	0.29	-0.39	12.7
Early late Albian	B13	33	UWA B13	Boologooro 1 (350.65)	24°19'S	113°54'E	Carnarvon	Upper Lower Gearle Siltstone	*D. stimulus*	0.707480	$3.78x10^5$	2455	1243	0.20	-0.50	13.2
Early late Albian	B14	35	UWA B14	Boologooro 1 (351.42)	24°19'S	113°54'E	Carnarvon	Upper Lower Gearle Siltstone	*Dimitobelus sp.*	0.707509	$3.79x10^5$	2511	1532	0.37	-0.31	12.4
Early late Albian	B15	41	UWA B15	Boologooro 1 (352.95)	24°19'S	113°54'E	Carnarvon	Upper Lower Gearle Siltstone	*Dimitobelus sp.*	0.707457	$3.84x10^5$	2705	1306	1.44	-0.33	12.5
Late early Albian	B16	42	UWA B16	Boologooro 1 (357.00)	24°19'S	113°54'E	Carnarvon	Lower Gearle Siltstone	*Dimitobelus sp.*	0.707446	$3.78x10^5$	2476	1368	0.93	-0.32	12.5
Late early Albian	B17	45	UWA B17	Boologooro 1 (359.90)	24°19'S	113°54'E	Carnarvon	Lower Gearle Siltstone	*D.diptychus*	0.707408	$3.82x10^5$	2233	1189	0.48	0.16	10.6
Late early Albian	B18	48	UWA B18	Boologooro 1 (361.05)	24°19'S	113°54'E	Carnarvon	Lower Gearle Siltstone	*D. stimulus*	0.707476	$3.93x10^5$	2241	1175	0.78	-0.13	11.7
Late early Albian	B19	52	UWA B19	Boologooro 1 (365.63)	24°19'S	113°54'E	Carnarvon	Lower Gearle Siltstone	*D. stimulus*	0.707446	$3.96x10^5$	1127	1187	0.87	0.43	9.6
Early Albian	B20	54	UWA B20	Boologooro 1 (374.00)	24°19'S	113°54'E	Carnarvon	Lower Gearle Siltstone	*D. stimulus*	0.707396	$4.08x10^5$	1490	1587	1.15	0.74	7.0
Early Albian	B21	57	UWA B21	Boologooro 1 (377.65)	24°19'S	113°54'E	Carnarvon	Lower Gearle Siltstone	*P. bauhinianus*	0.707379	$4.06x10^5$	2023	1118	1.71	0.17	10.6
Late early Aptian	B22	59	UWA B22	Boologooro 1 (378.42)	24°19'S	113°54'E	Carnarvon	Windalia Radiolarite	*P. bauhinianus*	0.707183	$4.28x10^5$	1042	1310	2.16	0.27	10.2
Early Aptian	B23	62	UWA B23	Boologooro 1 (382.70)	24°19'S	113°54'E	Carnarvon	Windalia Radiolarite	*Dimitobelus sp.*	0.707258	$3.76x10^5$	1712	1145	1.29	0.60	9.0
Early late Albian	Ba1	66	UWA Ba1	Barrabiddy 1 (84.10)	23°50'S	114°20'E	Carnarvon	Lower Gearle Siltstone	*D. stimulus*	0.707453	$4.45x10^5$	1411	1642	0.70	0.16	10.6
Late Barremian	Ba2	69	UWA Ba2	Barrabiddy 1 (150.75)	23°50'S	114°20'E	Carnarvon	Munderong Shale	*P. bauhinianus*	0.707496	$4.20x10^5$	3188	1777	-0.15	-1.00	15.2
Multiple Analysis	"	1 of 3	"	"	"	"	"	"	"	"	"	"	"	0.13	-1.03	15.3
Multiple Analysis	"	2 of 3	"	"	"	"	"	"	"	"	"	"	"	-0.25	-0.55	13.4
Multiple Analysis	"	3 of 3	"	"	"	"	"	"	"	"	"	"	"	1.50	-0.01	11.3
Early Albian	E1	65	UWA E1	Edaggee 1 (264.85)	25°21'S	114°14'E	Carnarvon	Basal Lower Gearle Siltstone	*Dimitobelus sp.*	0.707369	$4.44x10^5$	1281	1574	2.16	0.69	8.6
Early Aptian	Y1	68	UWA Y1	Yinni 1 (59.03)	26°03'S	114°49'E	Carnarvon	Windalia Radiolarite	*P. bauhinianus*	0.707208	$4.32x10^5$	1033	1115	2.18	0.79	8.3
Multiple Analysis	Y1	1 of 3	"	"	"	"	"	"	"	"	"	"	"	2.19	1.34	6.3
Multiple Analysis		2 of 3	"	"	"	"	"	"	"	"	"	"	"	2.52	1.02	7.4
Multiple Analysis		3 of 3	"	"	"	"	"	"	"	"	"	"	"	2.34	0.96	7.7

cont' **Table D. 4**

cont' Isotopic and chemical data for belemnites from the Aptian-to-Cenomanian strata of the Carnarvon Basin, Western Australia.

Stage	Lithological No.	Isotope Sample No.	Specimen No.	Location	Latitude	Longitude	Basin	Lithostratigraphic Position	Species	$^{87}Sr/^{86}Sr$ Means	Ca ppm	recalculated Mg ppm	recalculated Sr ppm	$d^{13}C_{PDB}$	$d^{18}O_{PDB}$	T(°C)
Early Albian	W1	WAM 23	WAM 91.839	6.5km NW of Murchinson House, White Cliff	27°36'S	114°12'E	Carnarvon	Basal Gerale Siltstone	*D. diptychus*							
Multiple Analysis	"	1 of 6	"	"	"	"	"	"	"	n/a	$2.83x10^5$	1070	959	1.15	0.09	10.9
Multiple Analysis	"	2 of 6	"	"	"	"	"	"	"	n/a	"	"	"	1.32	-0.05	11.4
Multiple Analysis	"	3 of 6	"	"	"	"	"	"	"	n/a	"	"	"	1.14	-0.03	11.3
Multiple Analysis	"	4 of 6	"	"	"	"	"	"	"	n/a	"	"	"	1.57	-0.03	11.3
Multiple Analysis	"	5 of 6	"	"	"	"	"	"	"	n/a	"	"	"	1.87	0.01	11.3
Multiple Analysis	"	6 of 6	"	"	"	"	"	"	"	n/a	"	"	"	1.35	-0.16	11.8
Late Albian	W2	WAM 34	WAM 97.705	Alinga Point	27°37'S	114°10'E	Carnarvon	Alinga Formation	*D. diptychus*							
Multiple Analysis	"	1 of 7	"	"	"	"	"	"	"	n/a	$3.2x10^5$	1280	1050	1.52	0.08	10.9
Multiple Analysis	"	2 of 7	"	"	"	"	"	"	"	n/a	"	"	"	2.06	0.09	10.9
Multiple Analysis	"	3 of 7	"	"	"	"	"	"	"	n/a	"	"	"	1.32	-0.07	11.5
Multiple Analysis	"	4 of 7	"	"	"	"	"	"	"	n/a	"	"	"	1.16	-0.12	11.7
Multiple Analysis	"	5 of 7	"	"	"	"	"	"	"	n/a	"	"	"	0.86	-0.40	12.8
Multiple Analysis	"	6 of 7	"	"	"	"	"	"	"	n/a	"	"	"	0.83	-0.22	12.1
Multiple Analysis	"	7 of 7	"	"	"	"	"	"		n/a	"	"	"	0.79	-0.33	12.5
Cenomanian	W3	Ceno UWAb	UWA 2/11/99-16-1	East of Thirdine Point, Pillawarra Plateau	24°10'E	114°29'E	Carnarvon	Upper Gearle Siltstone	*Microbelus haigi*							
Multiple Analysis	"	1 of 2	"	"	"	"	"	"	"	n/a	$2.55x10^5$	190	280	none	none	none
Multiple Analysis	"	2 of 2	"	"	"	"	"	"	"	n/a	"	"	"	-0.01	-0.38	11.3
Cenomanian	W4	Ceno UWAg	UWA 2/11/99-16-2	East of Thirdine Point, Pillawarra Plateau	24°10'E	114°29'E	Carnarvon	Upper Gearle Siltstone	*Microbelus haigi*							
Multiple Analysis	"	1 of 2	"	"	"	"	"	"	"	n/a	$2.01x10^5$	10	316	0.44	-0.22	12.1
Multiple Analysis	"	2 of 2	"	"	"	"	"	"	"	n/a	"	"	"	0.89	-0.26	12.2

D. 5. 1 Palaeotemperature calculations

O-isotope values are interpreted to be primary: there is no covariance in the data set between $\delta^{18}O$ and known diagenetic indicators such as Mn and Fe. Nor is there covariance of other trace elements with isotope values, a pattern consistent with the calcite mineralogy reflecting seawater isotope compositions of typical marine waters, and temperatures of biogenic accretion, rather than overprinting diagenetic signatures.

O-isotope composition of carbonates is reported in conventional `δ' notation as `parts per thousand' (‰) difference in ^{18}O between the isotopic contents of a sample compared to that of an international standard.

$$\delta = \frac{(\text{sample } ^{18}O - \text{standard } ^{18}O)}{(\text{sample } ^{16}O - \text{standard } ^{16}O)} \times 1000$$

Carbon and oxygen isotopic values are generally both measured in relation to the PDB carbonate standard but water compositions and some carbonate oxygen values are reported with respect to standard mean ocean water (SMOW). Values obtained using the two standards are related by a simple equation (Friedman and O'Neil, 1977) such that:

$$\delta^{18}O_{calcite} \text{ (vs SMOW)} = 1.03086\ \delta^{18}O_{calcite} \text{ (vs PDB)} + 30.86$$

Isotopic compositions of natural materials vary in response to a wide range of environmental reactions such as evaporation, condensation, photosynthesis, organic metabolism and mineral precipitation, each of which leads to isotope fractionation with changes in the proportion of isotope species due to slight differences in the reactivity of the different isotopes. The precipitation of a carbonate mineral from solution may involve significant O isotopic fractionation but in many circumstances the process is assumed to take place in isotopic equilibrium such that the composition

of the precipitated mineral is related to the composition of the fluid from which it precipitated by a temperature-dependent fractionation factor (α).

The O isotopic composition of a carbonate mineral precipitated in equilibrium with its environment is determined by the O isotopic composition of the fluid from which the mineral precipitated and fractionation due to the temperature of precipitation. The fractionation effects are relatively large, with precipitated carbonates having isotopic compositions typically around 25-30‰ greater than the waters from which they formed (Marshall, 1992). Different carbonate minerals show slight differences in fractionation and palaeotemperature equations are accordingly different for each mineral.

Palaeotemperature values for calcite samples can be calculated using a formula derived from measurements of the isotopic composition of the shells of calcareous organisms grown under different temperature conditions (Epstein and Lowenstam, 1953; Craig, 1965). The equation used here is from Anderson and Arthur (1983) as modified from that originally proposed by Craig (1965).

$$T\,^{\circ}\mathrm{C} = 16.0 - 4.14\,(\delta_c - \delta_w) + 0.13\,(\delta_c - \delta_w)^2$$

Where $\delta_c = \delta^{18}O$ of the analysed calcite with respect to the PDB international standard, and $\delta_w = \delta^{18}O$ (SMOW) of the water in which the calcite was precipitated relative to the `SMOW' international standard. Whereas δ_c is measured, δ_w has to be estimated. This can be problematic because δ_w varies in the present oceans and average δ_w has varied throughout geological time (Hudson and Anderson, 1989). It is important to note that temperature decrease and global ice-volume build-up (and consequent oceanic ^{18}O enrichment) will have a similar effect on δ_c.

Temporal variations in the O isotopic composition of ocean water have been caused by major changes in balance between the different global oxygen reservoirs. During glaciation, the trapping of large volumes of isotopically lighter water in continental icecaps affects the isotopic composition of the oceans. Calculations suggest that the total difference between glacial and interglacial conditions would

lead to a $\delta^{18}O$ shift of approximately 1.2‰. Shackleton and Kennett (1975) estimated the oceanic value of $\delta^{18}O$ to be -1.0‰ SMOW, equivalent to -1.2 PDB, for an ice-free global Mesozoic palaeoenvironment.

In geological systems it is only possible to measure the isotopic composition of the carbonate and interpretation in terms of either temperatures or water compositions relies on careful assumptions about the other variable. As both fluid compositions and palaeotemperature may be affected by changes in the natural environment it is often necessary to consider both factors when interpreting the isotopic signal from the rock record (Hudson and Anderson, 1989). The Cretaceous Period is regarded as having been ice-free and complications due to glacial influences do not apply. Thus relative changes in temperature can be determined by analysing primary changes in the isotopic composition of well-preserved fossils and by comparing results from organisms from different habitats and from different latitudes (Pirrie and Marshall, 1990b; 1990a).

Vital effects are known to induce isotopic fractionation in some instances. For example, isotopic values obtained from the calcitic bivalve *Inoceramus* sp. are known to be spurious as palaeotemperature proxies (Voigt et al., 2003). Very little is known about kinetic or vital fractionation effects during skeleton precipitation of extinct belemnites. Coleoids are considered to be their closest extant relatives (Stevens, 1973) and stable isotopic studies on the living genera *Spirula* and *Sepia* suggests O isotopic equilibrium precipitation (Voigt et al., 2003). A study by Landman et al. (1994) on contemporary nautiloids, a distant group of shelled cephalopods, also suggests temperature-dependent equilibrium precipitation of the argonitic shells.

Voigt and Wilmsen (2003) noted an offset between the O isotopic composition of belemnites, typically with heavier values, and the shells of associated benthic organisms from the same sections and suggested that vital effects have influenced the belemnite records. However, other studies (Urey et al., 1951; Morrison and Brand, 1986; Saelen et al., 1996) do not support this conclusion and there are no compelling reasons supporting the operation of significant vital effects during calcification of the belemnite guard. The observations made by Voigt and Wilmsen (2003) are most likely related to belemnite palaeoecology.

In general, O-isotope equilibrium fractionation for belemnites is considered to be exclusively due to temperature effects so members of the group have been very widely used in palaeotemperature assessment based on O-isotope analyses.

D. 5. 2 Palaeotemperature estimates from $\delta^{18}O$ analyses

Estimates of palaeotemperatures were derived from O-isotope proxies to track sea temperature trends through the Barremian-Aptian interval of the Great Artesian Basin and the Aptian-Cenomanian interval of the Carnarvon Basin. The complete sets of analyses are detailed in Tables D. 1-4.

D. 5. 2. 1 Single analyses from individual specimens

The representativeness of individual analyses in tracking general palaeotemperature trends is a question at issue, given the known propensity of belemnites to record palaeotemperature variability within individual specimens. This question was evaluated through reference to multiple analyses obtained from successive growth-laminae of individual guards, in comparison to single `bulk' analyses from the same guards obtained in the same way as `bulk' analyses were obtained across the entire specimen set. A comparison of such data is provided in Figure D. 5. 1. Successive growth-laminae of individual guards generally show isotopic variation indicative of a palaeotemperature range of no more than about 4°C. In just one specimen (M1) the range is more extreme with indicated palaeotemperatures spanning more than 8°C. The data indicate that individual guards reflect different `bulk' palaeotemperature regimes, in spite of internal variation, best expressed as a mean of that range. `Bulk' analyses of individual guards, with the exception of specimen M1, depart by little more than 1°C from the mean values obtained from analysis of successive growth-laminae. Even in the case of the non-conforming data set for specimen M1, the `bulk' palaeotemperature value indicates growth under conditions of high sea temperatures near the upper limit of

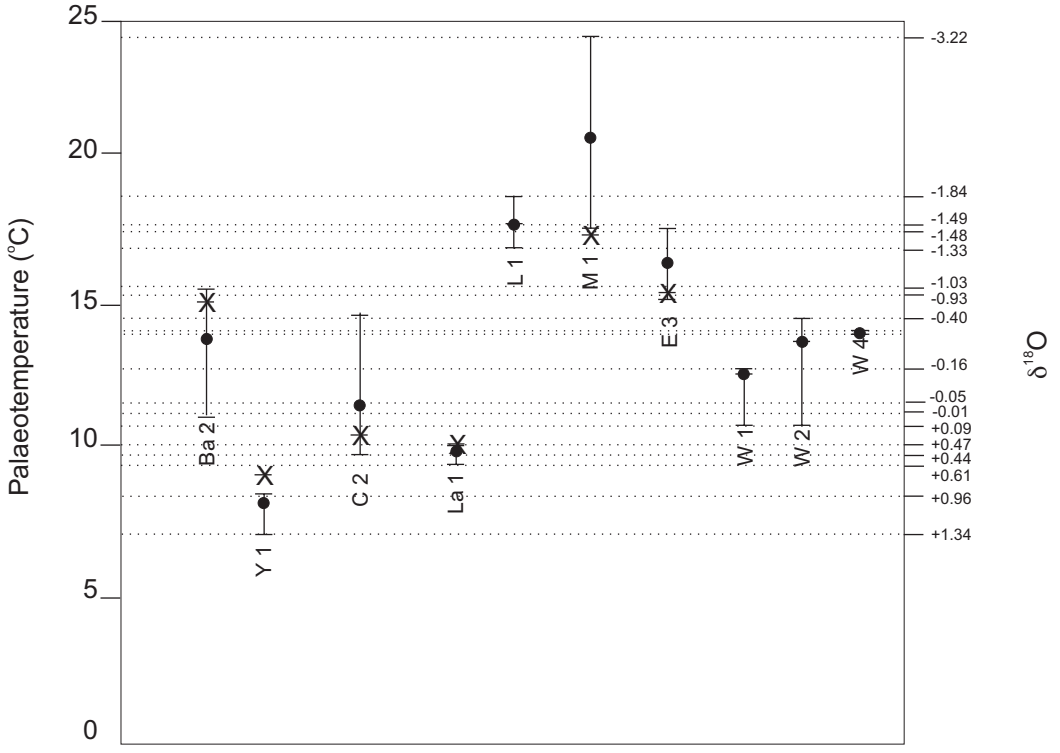

Figure D. 5. 1 Plot of $\delta^{18}O$ and the inferred palaeotemperatures for specimens from which multiple analyses have been obtained (see Figures D. 4. 1 and D. 4. 2). Results obtained from 'bulk' (X) analyses in relation to the range of values and the mean (●) obtained from analyses of successive growth-laminae are compared. Specimens L1, W1, W2 and W4 were not analysed for `bulk' results.

the sea temperature range indicated by the total data set, and in that sense is consistent with palaeotemperatures indicated by analyses of individual growth-laminae. It is therefore considered that `bulk' analyses can be taken as a reliable indicator of the broad scale palaeotemperature regime in which individual belemnites grew. As such, they should provide a useful indicator of palaeotemperature trends through time.

Results for the Carnarvon Basin show good levels of comparability between analyses for sequential samples. A clear first order trend is apparent with $\delta^{18}O$ values ranging between 0.79 and -1.03 and equating to a broadscale palaeotemperature rise of approximately 8°C during the Aptian to 14°C in the Cenomanian (Figures D. 3. 1 and D. 5. 2). In addition, a pronounced $\delta^{18}O$ shift from
-1.0 to 0.6 across the Barremian-Aptian boundary interval indicates a temperature decline from 15 to 8°C. However, this trend depends on a single late Barremian data point and therefore is not strongly substantiated.

Sequential samples from Boologooro 1 indicate several second order trends in the data sets (Figure D. 5. 2). An abrupt trend of rising palaeotemperatures from 7 to 13°C through the mid Albian is based on nine sequential analyses from the Boologooro core. A slow progressive increase in palaeotemperature from approximately 11 to 14°C occurs within the Cenomanian. In addition, short period temperature shifts of up to 2°C are indicated in the early Albian and early Cenomanian, but these are based on few data points and their veracity is somewhat questionable. The early Albian and Cenomanian palaeotemperature shifts supported by multiple sequential samples indicate that significant changes in climatic regimes across intervals of about 4 m.y. occurred during the Early Cretaceous. The indicated changes are equivalent in scale to the mid-latitude sea-surface temperature fluctuations that applied in the Pleistocene (see CLIMAP, 1981).

The Great Artesian Basin data shows considerable scatter with samples of closely comparable age differing in $\delta^{18}O$ values by as much as 1.5‰, equivalent to a

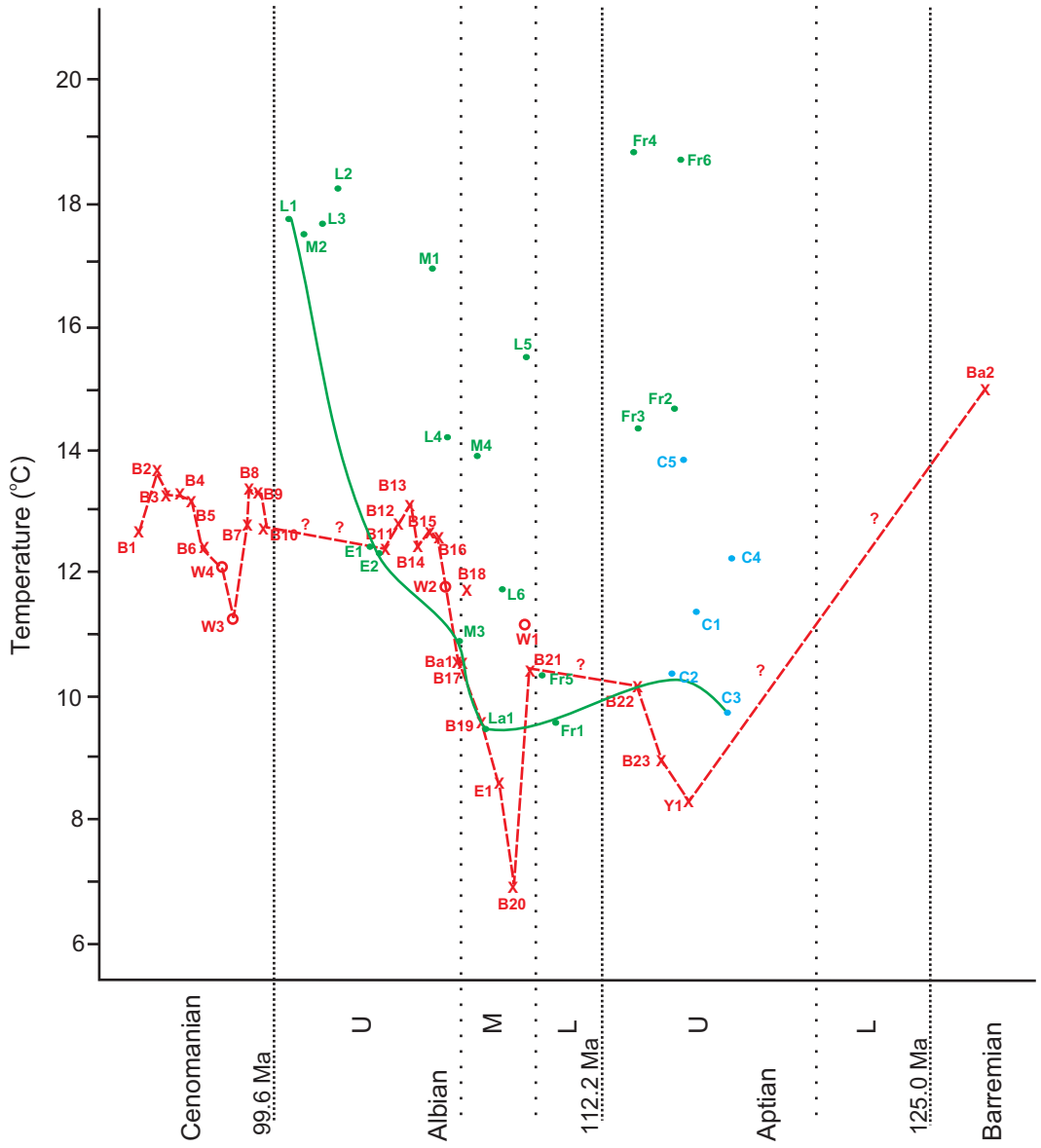

Figure D. 5. 2 Palaeotemperature trends through the Early Cretaceous from the Western Australian Carnarvon Basin (----------) and the eastern Australian platform (———) where values at the lower end of the range are used.

disparity of almost 10°C in palaeotemperature estimates. Two aspects of the Great Artesian Basin data set require explanation.

Firstly, the overall palaeotemperature estimates are higher by 1 to 10°C than those of age equivalent samples from the Carnarvon Basin, something of a paradox considering palaeolatitudes suggest the reverse should apply. Early Cretaceous palaeogeographic location of the Carnarvon Basin places it at a lower palaeolatitude than the Great Artesian Basin (Figures D. 1. 1 and D. 1. 2) which should result in a higher temperature regime. This paradox reflects the epeiric nature of the sea to which the Great Artesian Basin is related. All of the isotopic analyses relate to light growth bands that represent summer conditions. Shallow epeiric seas can be expected to warm more effectively than continental borderland shelf seas connected to open ocean as applied in the palaeogeographic circumstance of the Carnarvon Basin. Extensive, shallow seas that are poorly connected to the open ocean, such as that associated with the Great Artesian Basin, are affected by local circumstances of thermal capacity, conditioned by solar insolation, turbidity and convective circulation. In addition, reconstruction of Early Cretaceous global palaeogeography and surface ocean currents (see Figure D. 6. 3) suggests that the east Australian epeiric sea may have connected to warm ocean in the north whereas the Carnarvon Basin is likely to have been influenced by cool waters circulated from the south along the narrow seaway separating India and Australia.

Secondly, the wide disparities in palaeotemperature estimates provided by samples of very similar age are anomalous. For example, two early Aptian samples from a single horizon of the Carpentaria Basin succession have palaeotemperature estimates differing by some 2°C, and samples of the same early Albian horizon from Aramac Well, Eromanga Basin, differ by about 4°C. This circumstance is also certain to reflect the epeiric nature of the Great Artesian Basin and peculiarities of its water mass related to its palaeogeographic context.

Three possible explanations may apply, either singly or in combination:

(1) Scatter due to the influence of dilution from freshwater runoff. In high latitudes where precipitation generally exceeds evaporation, it can be anticipated that land-locked marine water bodies tend to be isotopically lighter than the global ocean. Because of the semi-enclosed nature of the epeiric during the Early Cretaceous, the influence of runoff and precipitation is likely to induce isotopically lighter seawater compositions. The palaeobotanical record (Henderson et al., 2000) suggests a pluvial regime for the Australian landmass in the Early Cretaceous. Modelling by Marshall (1992) indicates that 10% dilution of normal marine waters will induce a one per mille negative shift in O-isotope value, equivalent to a shift of approximately 4°C degrees in palaeotemperature estimate. Cochran et al. (2003) argued that salinity influenced O-isotope records from Maastrichtian molluscs from the mid to high latitude epeiric Western Interior Seaway of North America with $^{18}O/^{16}O$ values ranging by as much as 1‰ due to freshwater dilution. These authors also found appreciable scatter in $^{87}Sr/^{86}Sr$ values obtained for the same sample set, substantiating a fresh-water influence. He et al. (2005) described variation in $^{18}O/^{16}O$ values for Campanian-Maastrichtian Western Interior ammonites of Campanian-Maastrichtian age, with variation by up to 2‰ for samples from the same ammonite zone and thus closely comparable in age. Although these authors ascribed the scatter in their results to other agencies, brackish influence offers a likely explanation. However, for the Great Artesian Basin data presented here salinity variation must be considered as no more than a minor influence because Sr isotopic values obtained for the same sample set (Section C) are unaffected (see Section C).

(2) Modification of the composition for waters of the epeiric sea due to isotopic exchange with sediment. The provenance of sediment supplied to the Great Artesian Basin during the Early Cretaceous is unusual, being dominated by smectitic muds that are considered to be largely hydrated glass of pyroclastic origin (Smart and Senior, 1980), derived from a large silicic volcanic province located to the east (Bryan et al., 2000). Cuadros et al. (1999) have recently shown that hydrothermal reaction of

volcanic tuff with water, accompanied by the growth of new smectite from glass, results in O isotopic fractionation by the solid phase. Broadscale, longer term hydration of volcanic glass at ambient temperatures in a shallow, very extensive water body may therefore be expected to modify its O-isotope composition.

(3) The palaeotemperature signatures of individual guards could reflect short-term temperature regimes that prevailed in the epeiric sea due to the vagaries of seasonal heating, as discussed above, rather than being indicative of long term temperature trends.

Based on these considerations, the lowest values in the range of indicated palaeotemperatures for the Great Artesian data set are likely to be the most reliable estimates. Working on this basis, a similar first-order trend is apparent for the Great Artesian Basin as that shown by the Carnarvon Basin with a warming trend through the late Aptian-Albian interval from 10 to 18°C (Figure D. 5. 2).

D. 5. 2. 2 Multiple analyses from single specimens

Palaeotemperature fluctuations are recorded in the succession of growth-laminae built in belemnite guards during life span and reflect seasonal water temperature changes and/or migratory patterns either laterally or vertically within the water column.

In the first study of this kind, Urey et al. (1951) measured the isotopic compositions of successive growth-laminae within Late Cretaceous guards and found variability for individual specimens; interpreted as seasonal variations in ocean temperature that prevailed during the life of the organism. These authors considered the isotopic variation in single specimens as consistent with seasonal variations displayed in modern calcareous marine shells, with the mean of palaeotemperature estimates providing a plausible value for the general sea temperature in which the belemnites lived, assuming that Late Cretaceous oceans had the same O isotopic composition as those of the present. However, many subsequent authors, such as Stevens and Clayton (1971) and Doyle (1992), found that isotopic variation in

individual belemnites could not be rationalised in this way and invoked belemnite migration as an explanation.

Several authors have reviewed problems associated with the use of stable isotopes to infer depth habitats among belemnites (Wefer and Berger, 1991; D'Hondt and Arthur, 1995; Huber et al., 1995). In addition to depth, interspecies differences in $\delta^{18}O$ and $\delta^{13}C$ may potentially be influenced by (1) the kinetic effects of different calcification rates for different species and changes in calcification rates during ontogeny, (2) shell growth during different seasons, (3) accuracy of isotopic analysis (generally ± 0.1‰), and (4) differential preservation. The approach taken in this study is to examine isotopic trends within individual specimens to evaluate the cause of variability. No systematic differences in isotope values between taxa are apparent in the data.

In this study, nine belemnites from different basins and of different ages were investigated for isotopic variability with samples taken from 2-8 growth-laminae. Samples where taken wholly from within individual light-coloured growth bands, carefully avoiding dark margins to minimise contamination with interskeletal organic matter. The sampled bands are regarded as representing summer growth.

Results are displayed as graphical plots showing palaeotemperature trends during ontogeny together with the location of the sampled growth-laminae (Figures D. 4. 1 and D. 4. 2). Details of sample localities and stratigraphic position are provided in Tables D. 1-4.

Patterns of variation are similar for specimens of different ages and for specimens from the Great Artesian and Carnarvon basins. This comparability suggests that changes in salinity, isotopic change due to seawater-sediment interaction or decade-scale temperature variability of the east Australian epeiric sea are unlikely to have underpinned the patterns exhibited by Great Artesian Basin specimens. Some specimens (e.g. L1, Y1, W2 and W4) show consistency of trend, mostly with progressively warmer palaeotemperatures registered through ontogeny but the reverse applies in the case of specimen Ba2. Others (C2, La1, M1 and W1)

show significant trend reversals with no matching trend between palaeotemperature and ontogenetic growth stage.

Palaeotemperature variation amongst specimens is constrained within a 4°C temperature range for all but one specimen. Such a temperature range experienced during the lifetime of an individual belemnite in an epeiric sea or shelf system may be explained in terms of changing depth habitats. Due to the occurrence of seasonal thermoclines, differences between surface and bottom temperatures span this range (see Church and Forbes, 1983). However, lateral migration by individuals throughout life is an equally viable alternative explanation.

An exception to the general palaeotemperature variation of 4°C is apparent. Specimen M1 of the Albian, from the northern Eromanga Basin, experiences a range of 9°C. Such variability could only have been achieved by large-scale lateral migration through perhaps 12°, or more of palaeolatitude based on the estimates of global sea temperatures for the Cretaceous (Barron et al., 1981; Huber et al., 1995; Bralower et al., 1999; Larson and Erba, 1999; Pirrie et al., 2004). Given the migrational behaviour known for modern squid (Hanlon and Messenger, 1996) locomotion over such a geographic range is certainly plausible. This palaeotemperature range could not be accounted for by a thermal gradient in the water column, given that the east Australian epeiric sea is considered to have never exceeded 200 metres in depth (Campbell and Haig, 1999).

Given that the pre-mortality palaeotemperatures of the most advanced growth stages represent association with the epeiric sea, and are low in the ontogenetic palaeotemperature range, the pattern displayed by this specimen cannot be explained by migration from the shallows to the deeper waters off the east Australian continental margin. Rather, the pattern must represent a high latitudinal juvenile growth stage, large-scale migration towards the equator and subsequent return to high latitude late in the life history.

This evidence of life history migration for Australian belemnites is consistent with their palaeobiogeographic pattern with the same taxa inhibiting both the Early

Cretaceous epeiric sea and open shelves of the continental borderland (see Sections A and B). This pattern contrasts strongly with that of ammonites, a group less well equipped for effective locomotion, which shows strong partitioning between the epeiric sea and the continental margins (Henderson et al., 2000).

D. 6 Discussion

D. 6. 1 Australian Early Cretaceous palaeotemperature estimates and trends

The general palaeotemperature trend through the Early Cretaceous for both eastern and western Australian sequences, accepting the lower range of values from the Eromanga Basin as more reliable long-term trend indicators, show rising temperatures through the Aptian to Cenomanian, from lower ranges of 8 to 9°C through a warmer regime of 13 to 18°C. The lower values of each range are from the Carnarvon Basin and represent open ocean neritic temperatures, whereas higher values are associated with epeiric sea conditions.

$\delta^{18}O$ analyses from published work on Australasian belemnites (Lowenstam and Epstein, 1954; Dorman and Gill, 1959; Bowen, 1961; Dorman, 1968; Stevens and Clayton, 1971; Pirrie et al., 1995) together with those of the present study, are summarised in Figure D. 6. 1. Previous studies of Great Artesian Basin belemnites, none of which employed protocols to recognise diagenetic alteration, also show a wide scatter in $\delta^{18}O$ values. Their range is mirrored by values obtained in the present study.

Previous results for the late Albian *Dimitobelus* from the Carnarvon Basin are discrepant from those presented here. Bowen (1961) analysed 19 specimens from the Albian and Cenomanian with a sample from Albian giving a maximum palaeotemperature estimate of 30.1°C, and the remainder of the sample set providing a mean of 19.4°C during the Albian. However, no protocols were employed in this study to determine diagenetic overprint and the upper part of the palaeotemperature

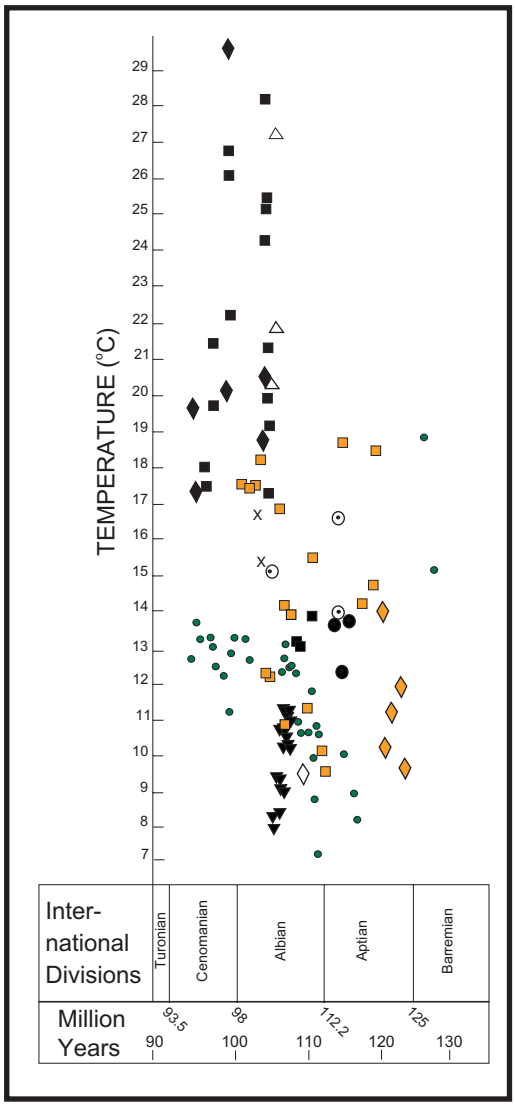

Figure D. 6. 1 Cretaceous palaeo-temperature determinations from Australasian belemnites. Note that the ages attributed to data points from previous studies are not necessarily subject to tight age control. Values from the Carnarvon Basin study by Bowen (1961) are represented as average palaeotemperature estimates and not as individual records.

range indicated by this dataset may be an artefact. Based on the analysis of 17 specimens from the basal Gearle Siltstone, Pirrie and Marshall (1995) estimated late Albian palaeotemperatures to be some 10°C. These values are consistent with results obtained for the present study, which have a 10 to 13°C range through the late Albian.

It is useful to compare palaeotemperature estimates for the Albian-Aptian from both eastern and western Australia obtained in this study with graphs of mean sea-level atmosphere temperatures versus latitude inferred from the sedimentary record by Fairbridge (1964), based on the distribution of climate sensitive sedimentary rocks and annual average sea surface temperatures for the current Earth (Locarnini et al., 2006) relative to those estimated for the last glacial from CLIMAP (1981). For mid to high latitudes the non-glacial curve of Fairbridge approximates to a crude average of the warmest and coldest estimates of Cretaceous sea-level atmospheric temperatures provided by Barron et al. (1983) and Barron and Washington (1984).

Late Albian values for the east Australian platform register temperatures of approximately 18°C, consistent with a non-glacial globe but minimum values for the late Aptian-middle Albian of 10 to 11°C; these palaeotemperatures differ from sea surface temperatures at mid latitudes for the present Earth (Figure D. 6. 2). However, as discussed above, these values may be prejudiced as general indicators of mid latitude surface sea temperatures by their epeiric context, so values for the Carnarvon Basin are a more useful basis for discussion. The latter suggest that mid latitude surface sea temperatures were somewhat cooler than those of the present and may have applied in the Aptian whereas values for the Albian–Cenomanian interval, rising from 12 to 18°C approach conditions which presently prevail.

The Aptian-Aptian palaeotemperatures obtained in the present study are remarkably consistent with those obtained by Clarke and Jenkyns (1999) from $^{18}O/^{16}O$

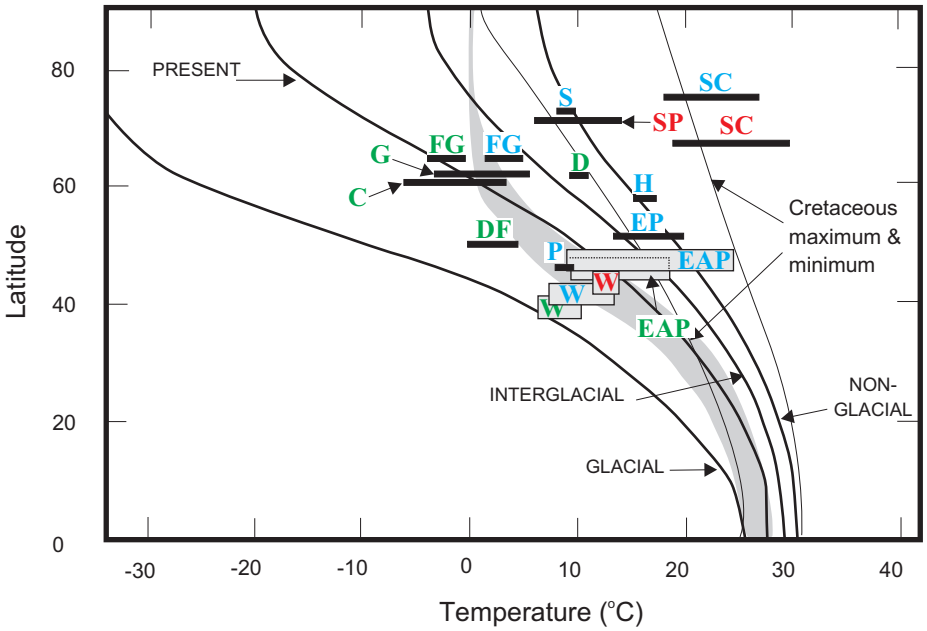

Figure D. 6. 2 Relationship diagram for global temperature regimes and Early Cretaceous palaeotemperature estimates. Curves represent sea level air temperatures under different Quaternary regimes from Fairbridge (1964) and Cretaceous regimes inferred by Barron et al. (1983). Shaded area represents the generalised range of modern annual average surface sea temperatures (Locarnini et al., 2006) and those of the last glaciation from CLIMAP (1981). Palaeotemperature estimates from this study shown for the Western Australia Carnarvon Basin, **W**, and east Australian platform, **EAP**. Data from previous studies: **SC**, Stevens and Clayton (1971); **D**, Ditchfield et al. (1994); **H**, Huber et al. (1995); **EP**, Clarke and Jenkyns (1999); **P**, Pirrie et al. (2004); **SP**, Spicer and Parrish (1986; 1990); **S**, Spicer and Corfield (1992); **DF**, De Lurio and Frakes (1997); **G**, Gregory et al. (1989), **C**, Constantine et al. (1998) and **FG**, Ferguson et al. (1999). Aptian records are in green, Albian, blue and Cenomanian, red.

analyses of pelagic carbonate sampled by deep sea drilling on the Exmouth Plateau on the north-western Australian margin and proximal to the southern Carnarvon Basin. A rising temperature trend from 12.3°C in the late Aptian to 17.4°C in the late Albian was obtained in this study, as compared to 8 and 13°C, respectively, in the present study. Remarkably, the Exmouth record also shows second order, short period (2-3 m.y.) rising temperature trends in the mid Albian and Cenomanian that match those recognised in the present study, substantiating the authenticity of these features.

An O-isotope study of European belemnites and inceramids by Arthur et al. (1985) also recognised Aptian–Cenomanian warming trend. Albian-Cenomanian palaeotemperatures of 14 to 16°C obtained from pelagic carbonate in deep sea core from the Falklands Plateau (Huber et al., 1995) at a palaeolatitude of 60°S appear to be anomalously high. Estimates of about 10°C from the Aptian-Albian of the Antarctic Peninsula by Ditchfield et al. (1994) and 9°C from the Albian of southern Argentina derived from analyses of belemnites, representing similar palaeolatitudes, sit more comfortably with the results presented here (Figure D. 6. 2). Similarly, O-isotope results obtained by Stevens and Clayton (1971) for late Albian-Cenomanian belemnites from New Zealand are anomalous, indicating temperatures ranging between 17 and 28°C at very high palaeolatitudes.

Although the late Barremian palaeotemperature estimate in this study is based on a single sample, indicating a substantially higher value than those registered for the Aptian, it is consistent with the results from other studies. Podlaha et al. (1998) and McArthur et al. (2004) recorded palaeotemperatures estimated from mid-palaeolatitude European belemnite rostra at 12°C and 16°C respectively and Price and Grocke (2002) obtained a palaeotemperature of 16°C for high palaeolatitude belemnites from the Falkland Plateau.

Frakes and Francis (1988) maintained that the Southern Hemisphere pole was not ice-free during the Early Cretaceous on the basis of ice-rafted dropstones and glendonites found in the Aptian Bulldog Shale of the southern Eromanga Basin. Although transport in tree roots could be invoked as an explanation for the drop stones, the circumstance of glendonite occurrence is incontrovertible as this mineral pseudomorphs ikaite which forms only in sea temperatures below 7°C. It could be

expected that winter minimum temperatures in the southern reach of the east Australian epeiric sea reached very low values due to the land-locked palaeogeographic setting and because the substantial pre-breakup Australian-Antarctic landmass will have encouraged a continental rather than maritime climatic regime. Summer temperatures, as indicated by the belemnite data, reached a minimum of 9°C. A mean seasonal temperature fluctuation exceeding 15°C, with standing winter ice in the landscape, is plausible in the context of a global climatic regime similar to the present. This is currently the case for the high latitude somewhat epeiric Baltic Sea (Church and Forbes, 1983).

Based on O-isotope analyses of non-marine carbonate concretions of the Aptian-Albian from coastal Victoria, on the southern margin of Australia, Gregory et al. (1989) argued that meteoric waters had mean annual temperatures near freezing, at -2 ± 5°C. In a comparable but more detailed study from the same region, with age control provided by palynology, Ferguson and Gregory (1999) obtained mean annual temperatures for meteoric waters of ~ -5°C for the Aptian rising to ~5°C in the late Albian. Plots for these data on the relationship diagram (Figure D. 6. 2) are somewhat anomalous in relation to the palaeotemperature estimates obtained in the present study. They also conflict with the palaeobotanical record; Douglas and Williams (1982) inferred an ice-free, warm- to cool-temperate climatic context for Early Cretaceous floras of Victoria. Although cool Aptian conditions prevailed for Australia, sea surface temperatures above 10°C are incompatible with permafrost for any part of the Australian continent through this interval. The degree to which such analyses reflect the isotopic composition of surface waters, an assumption made in deriving the palaeotemperature measurements, is questionable. Concretions result from diagenetic processes involving formation waters, the isotopic composition of which is unconstrained. This is especially the case given that the sedimentary hosts of the concretions are volcaniclastic with potential for isotopic exchange with groundwater during alteration, weathering and early diagenesis (see Cuadros et al., 1999). It must also be noted that the polar palaeolatitude applied by these authors to their sample set no longer applies (see Li and Powell, 2001).

The results presented here may be evaluated against high latitude palaeotemperature estimates from the Northern Hemisphere based on palaeobotanical studies. Mean annual temperatures on the order of 10°C at approximately 70°N have been inferred on the basis of fossil plant leaf morphology (Spicer, 1987; Parrish and Spicer, 1988) which support the possibility of polar peri-glacial and possibly limited glacial conditions during the Cretaceous (Barron et al., 1981; Frakes and Francis, 1988; Pirrie and Marshall, 1990b). These palaeotemperature estimates plot anomalously high on the relational diagram (Figure D. 6. 2).

The gradual warming of oceans from the Albian through to the Cenomanian recognised in sequences from this study is also documented in sequences from Europe and the south-eastern United States (Lowenstam and Epstein, 1954), northwest Germany (Spaeth et al., 1971), New Zealand (Stevens and Clayton, 1971), as well as the Russian Platform and adjacent areas (Naydin et al., 1966). Several ocean drilling programs have also recognised the rise in palaeotemperatures through the Albian-Cenomanian, from the Shatsky Rise, North Pacific Ocean (Douglas and Savin, 1975) and Exmouth Plateau (Thomas et al., 1992; Clarke and Jenkyns, 1999).

D. 6. 2 Physical oceanography of the Australian Cretaceous epeiric sea

The Cretaceous Period was characterised by the existence of broad continental seaways that linked the world oceans. The Cretaceous trans-Australian seaway was the product of extensive flooding of the Australasian continent during the mid-Cretaceous. Like the trans-Asian (Vinogradov, 1968), trans-African (Reyment, 1980) and the trans-American (Hay et al., 1993) seaways of the Cretaceous, it provided a relatively shallow connection between oceanic areas in different climatic regimes.

Detail of the palaeogeography of the Australian seaway are not well constrained and the preserved distribution of marine Cretaceous strata may not accurately reflect the Cretaceous palaeogeography. The Mesozoic seaways were fundamentally different from Late Cenozoic to modern marginal epeiric seas, which have either a single opening (e. g. the Baltic Sea, northern Europe and the Western Interior Seaway, North America), or are widely connected to the deep ocean (the Gulf

Interior Seaway, North America), or are widely connected to the deep ocean (the Gulf of Carpentaria, northern Australia). Because these epeiric seas have no modern analogs in terms of magnitude or setting, knowledge of their oceanography is limited. In particular, distributions of water mass as defined by temperature and salinity variations are poorly characterised.

Evaluation of inferred early-mid Cretaceous ocean currents suggests that global circulation differed substantially from that of the present due to differences in palaeogeography and climate. Close association of the African and European continental blocks with those of the Americas impeded low latitude marine linkages (Figure D. 6. 3). Barron et al. (1990) suggested that a major south easterly sea surface current swept the borderland of contiguous Australasia and Antarctica.

The Great Artesian Basin covers some one million km^2 and its related epeiric seaway extended over 3000 kilometres from west to east. It had separate openings with broad connections to the Indo-Pacific Ocean to the north and narrow, poorly defined opening(s) to the east connecting to the Pacific Ocean (Figures D. 1. 1 and D. 6. 3). Open oceanic connection of the continental margin represented by the Carnarvon Basin is apparent but the main current system sweeping this sector may have been related to opening of ocean floor between Antarctica, India and Western Australia (Figure D. 6. 3). Such a current would have been north directed and cool, relative to a southerly directed, warm arm of the oceanic gyre operating along the northern and eastern margins of Australia. It is therefore possible that the effect in gross palaeotemperature regimes between the eastern Australia epeiric sea and the Western Australia marginal sea was due to broadscale oceanic circulation patterns.

The North America Western Interior Seaway represents a comparable Cretaceous oceanic system where inferred brackish water conditions as suggested by Hay et al. (1993) have been supported by O and Sr-isotope analyses (Cochran et al., 2003) and the nature of benthic assemblages which lack sponges, bryozoans, brachiopods, corals and echinoderms. It is noteworthy that belemnites are also lacking from the faunal record. Recently, He et al. (2005) presented O-isotope data for the Maastrichtian Bearpaw Formation of the Western Interior Seaway which also

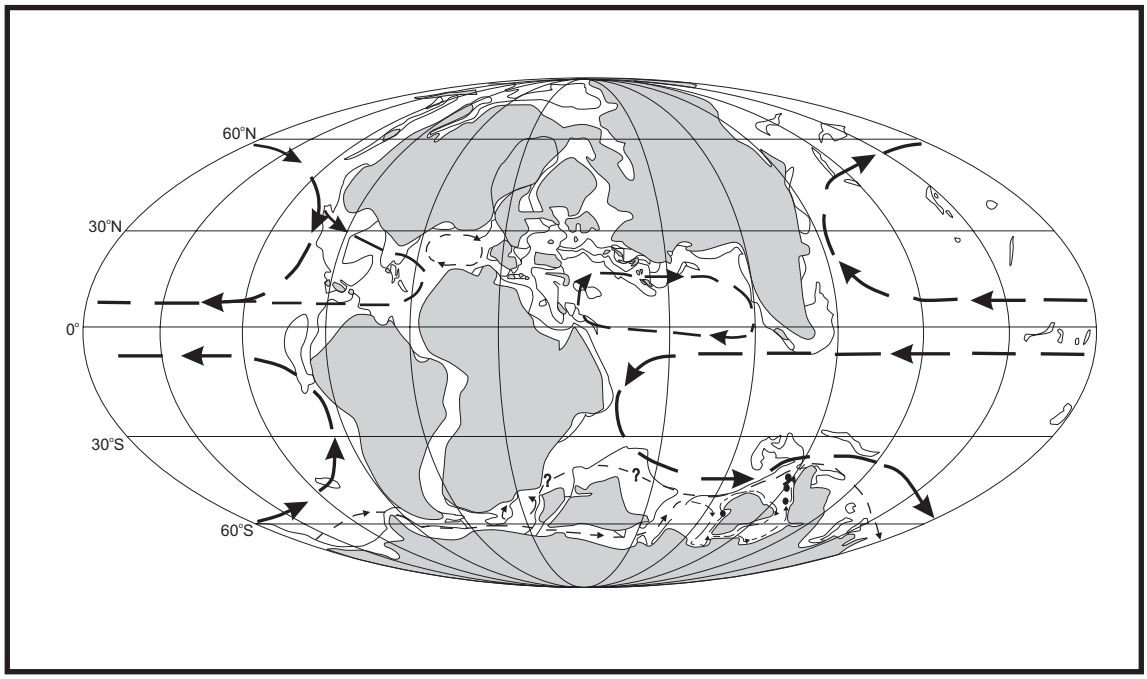

Figure D. 6. 3 Palaeogeographic map for the Barremian-Aptian interval showing the inferred palaeocurrent circulation that influenced the Antarctic-Australian landmass. Modified from Oosting (2004).

indicated a very wide scatter of approximately 1‰ palaeotemperature estimates ranging by as much as 4°C for samples for the same stratigraphic level. These authors argued for other mechanisms of isotopic partitioning in the Western Interior Seaway to explain their results involving intrusion of oceanic deep waters and oxygen depletion due to biological activity. However, fresh water dilution remains the most plausible explanation for the results as reported.

O-isotope analyses reported here support the contention that the Australian epicontinental seaway experienced brackish water conditions, as is the case for modern seas of comparable palaeogeographic context (see Hay et al., 1993). Brackish conditions are also indicated by benthic foraminiferal assemblages (Haig and Barnbaum, 1978; Haig, 1979b; 2006). Applying the relationship between freshwater dilution and ^{18}O suggested by Marshall (1992) the scatter in isotopic values across a range of 1‰ is consistent with salinity ranging to a 10% dilution below the global oceanic average. However, fresh water dilution was insufficient to deter ammonites and belemnites that are consistently represented in the sedimentary record of the Great Artesian Basin and are regarded as essentially stenohaline organisms (Stevens, 1965; Doyle, 1992; Hanlon and Messenger, 1996). It must also be noted that fresh water dilution on a substantial scale should be reflected in scatter $^{86}Sr/^{87}Sr$ values obtained from belemnite rostra and this is not the case (Section C).

SECTION E

The carbon-isotope record for Australian Aptian – Cenomanian sequences in relation to palaeoceanographic events

Section E. The carbon-isotope record for Australian Aptian - Cenomanian sequences in relation to palaeoceanographic events

E.1 Abstract

Carbon-isotope data obtained from belemnite guards is presented for Early - mid Cretaceous sequences of the Great Artesian Basin (Aptian-Albian) and Carnarvon (late Barremian-Cenomanian) Basin. The Great Artesian Basin dataset largely reflects its epeiric context and does not generally register patterns of isotopic partitioning of global significance. Albian and Cenomanian $\delta^{13}C_{carb}$ values for the Carnarvon Basin succession are lower than those which have been measured elsewhere and this offset is considered to reflect low productivity. A broadscale reduction in $\delta^{13}C_{carb}$ values through the Albian-Cenomanian corresponds with a warming trend through this interval and is attributed to enhanced atmospheric levels of CO_2. Due to gaps in the records, Oceanic Anoxic Events of early Aptian age and those within the late Aptian – early Albian interval are not registered. The Toolebuc organic-rich facies, recognised as representing OAE 1c, is characterised by a positive $\delta^{13}C_{carb}$ excursion also apparent in the record from the Carnarvon Basin. Timing of this event in Australia is early late Albian and its global significance remains uncertain. A prominent negative $\delta^{13}C_{org}$ excursion which marks the Toolebuc interval is attributed to the influence of organic matter of terrestrial source.

E. 2 Introduction

The early and mid Cretaceous (Aptian-Cenomanian) is known for the deposition of organic-rich marine sediments, both on the deep ocean floor and on the continental borderlands (Schlanger and Cita, 1982), which have been long regarded as symptomatic of unusual palaeoceanographic circumstances variously considered as due to sluggish circulation ("stagnation") of the ocean basins (Ryan and Cita, 1977), Fischer and Arthur, 1977; Arthur and Natland, 1979), expansion of the oxygen minimum layer (Schlanger and Jenkyns 1976; Thiede and van Andel, 1977; Tyson, 1995) or enhanced productivity (Erba and Premoli Silva, 1994; Parrish, 1995; Erbacher et al., 1996). Because of their special significance, episodes of carbon-rich sedimentary deposition have been labelled as oceanic anoxic events (OAEs).

In more recent research, it has become apparent that the sequestering of organic matter in the Cretaceous sedimentary record has perturbed the balance of carbon-isotopes in the atmosphere and oceans. Because photosynthesis fractionates

carbon-isotopes by selectively utilising ^{12}C, the burial of large volumes of organic matter in the sedimentary record results in ^{13}C enrichment for the contemporaneous atmospheric and oceanic reservoirs. As a result, the carbon isotopic contents of biogenic carbonate deposited in equilibrium with ocean waters provides a proxy for carbon cycling between the sedimentary and Earth surface systems. Trends in $\delta^{13}C_{carb}$ are considered to reflect global palaeoceanographic conditions, with positive excursions identifying OAEs (Scholle and Arthur, 1980; Arthur et al., 1990; Bralower et al., 1994). It has also been demonstrated that the isotopic composition of marine organic matter, mapped as $\delta^{13}C_{org}$, also registers OAE events (e.g. Erbacher, 1994; Menegatti et al., 1998; Bralower et al., 1999) and it appears that terrestrial organic matter may show matching $\delta^{13}C_{wood}$ signatures (e.g. Grocke et al., 1999).

As summarised by Leckie et al. (2002), current OAE nomenclature labels the general episode of organic carbon sequesterisation within the Aptian and Albian Stages as OAE 1, with short lived events of less than 1 Ma registered as OAE 1a (Selli, early Aptian), OAE1b (with three discrete phases; Jacob, late Aptian, Paquier, early early Albian, Urbino, late early Albian), OAE1c (Toolebuc, late Albian) and OAE 1d (Breistroffer, latest Albian). The subsequent episode, labelled as OAE 2 (Bonarelli), marks the Cenomanian – Turonian boundary.

This paper provides $\delta^{13}C_{carb}$ trends for the Aptian – Albian sequence of the Great Artesian Basin and for the late Barremian – Cenomanian Carnarvon Basin succession obtained from analyses of belemnite guards. Given that carbon-isotopes are relatively stable in biogenic carbonate, that belemnites guards generally provide the best geochemical record for biogenic calcite in the Jurassic and Cretaceous because of their size and calcite mineralogy, and that the guards utilised in this study have been screened for diagenetic overprint (Sections C and D), their record should be a reliable proxy for isotopic trends for the water bodies in which they were accreted. However, relative to studies based on bulk carbonate analyses from pelagic sediment obtained from deep sea cores or carbonate-rich sequences exposed on land, sample spacing is coarse and the resolution of short period events therefore somewhat prejudiced. A $\delta^{13}C_{org}$ record recently obtained from cores for the Aptian-Albian

sequence of the northern Eromanga Basin (Henderson, 2004; Oosting, 2004) provides a useful comparison.

E.3 Carbon-isotope stratigraphy relative to the OAE events

Close temporal resolution for both the Great Artesian Basin and Carnarvon Basin successions reported here as provided by strontium-isotope stratigraphy (section C) shows that substantial disconformities exist in both successions and that the temporal registration obtained from belemnites is also incomplete. Thus an early Aptian record through the OAE 1a (Selli) event is unavailable. This is also the case for OAE 1b (Jacob, Paquier and Urbino events) which lie within the Aptian-Albian boundary unconformity that is represented in both successions. Registration of the latest Albian (Vraconian) OAE 1d (Breistroffer) event is suspect due to unconformity in the Carnarvon Basin succession and marine sequence in the Great Artesian Basin is unlikely to extend this high in the Albian. OAE 1c (Toolebuc) should be registered in both successions and indeed the name of this event comes from the euxinic facies of the Toolebuc Formation of the northern Eromanga Basin.

E.4 Methodology and results

Carbon-isotope analyses were made in parallel with oxygen-isotope analyses reported in Section D, using the same samples and analytical methodologies, and the same sample screening protocols as applied in Section C. Results are reported as $\delta^{13}C_{carb}$ relative to the PDB standard and are summarised in Table D 1-4. $\delta^{13}C$ values show a considerable range, -0.3 to 4.4 for the Great Artesian Basin succession (Figure E. 4. 1) and -0.7 to 2.3 for the Carnarvon Basin succession (Figure E. 4. 2).

Figure E. 4 .1 Lithostratigraphy and $\delta^{13}C$ record of Aptian-Albian sequences for the eastern Australian platform including the north-eastern and southern Eromanga Basin, and Carpentaria and Laura Basins. Horizons relating to samples from scattered surface localities are interpolated onto GSQ Manuka 1, GSQ Longreach 1, and generalised southern Eromanga, Carpentaria and Laura stratigraphic columns according to the stratigraphic position of outcrops from which collections were made. The Flinders River sample set are from a composite measured section where the Wallumbilla Formation is separated into 3 sub-units Doncaster (oldest), Jones Valley and Ranmoor Members (youngest). Stratigraphic equivalence between sequences from the northern Eromanga Basin and those from the Carpenteria, Laura and southern Eromanga Basin are based on existing biostratigraphic controls.

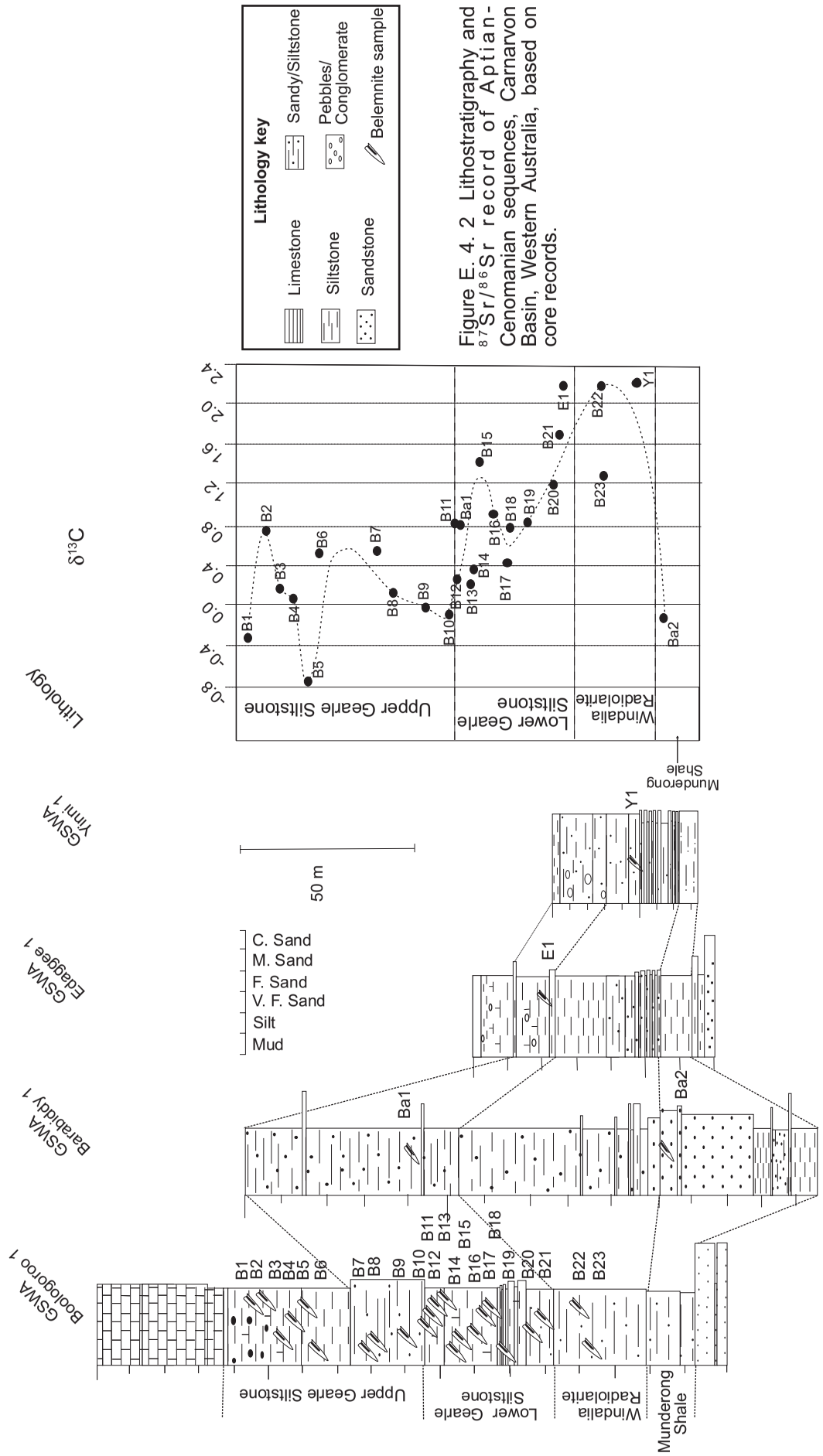

Figure E. 4. 2 Lithostratigraphy and $^{87}Sr/^{86}Sr$ record of Aptian-Cenomanian sequences, Carnarvon Basin, Western Australia, based on core records.

E.5 Discussion

The range of $\delta^{13}C$ values, and the trends through time (Figure E. 5. 1) for the two basinal successions are clearly quite different, indicating that different isotopic compositions applied in the water masses of the east Australian epeiric sea and the marginal sea to which the Carnarvon Basin related. A similarly clear distinction also applied in oxygen-isotope compositions (section D). In the same way, the difference in carbon isotopic signatures doubtless reflects the unusual character of the epeiric context of the Great Artesian Basin relative to the global ocean. It must relate to internal carbon cycling within the epeiric water mass, acting as a partially closed system, involving its biota and seafloor sediment. As reviewed by Holster (1997) productivity, the burial potential of organic material (sea bottom oxygen levels and sedimentation rate) and the supply of both organic and inorganic carbon from riverine sources are all potential influences. The nature of organic recycling can also be added, given that anaerobic bacterial communities are known to strongly partition carbon-isotopes in their metabolic processes (De Leeuw et al., 1995). It is noteworthy that OAE events have been rarely identified in records obtained from epeiric sedimentary systems and that Cochran et al. (2003) and He et al. (2005) reported wide variation in $\delta^{13}C_{carb}$ values obtained from Campanian and Mastrichtian samples from the epeiric Western Interior Seaway of North America that post-date an OAE influence. However no such complications pertain to the Carnarvon Basin record which has the added advantage of superpositional integrity provided by the single core (Boologooro 1) from which most the samples were obtained.

Albian and Cenomanian $\delta^{13}C_{carb}$ values for the Carnarvon Basin succession are generally < 1 per mil (Figure E. 4. 2) and occupy a lower range than values measured for most other successions of equivalent age which are generally within the range of 2-3 per mil (see Leckie et al., 2002, fig. 11). This offset is likely to reflect productivity of the neritic waters which supported the belemnite population from which the analyses were obtained. The influence of surface water productivity on the carbon-isotope systematics of the water column are well recognised (Kump, 1991; Holtser, 1997). Enhanced photosynthetic activity in the upper layer of the water column will draw

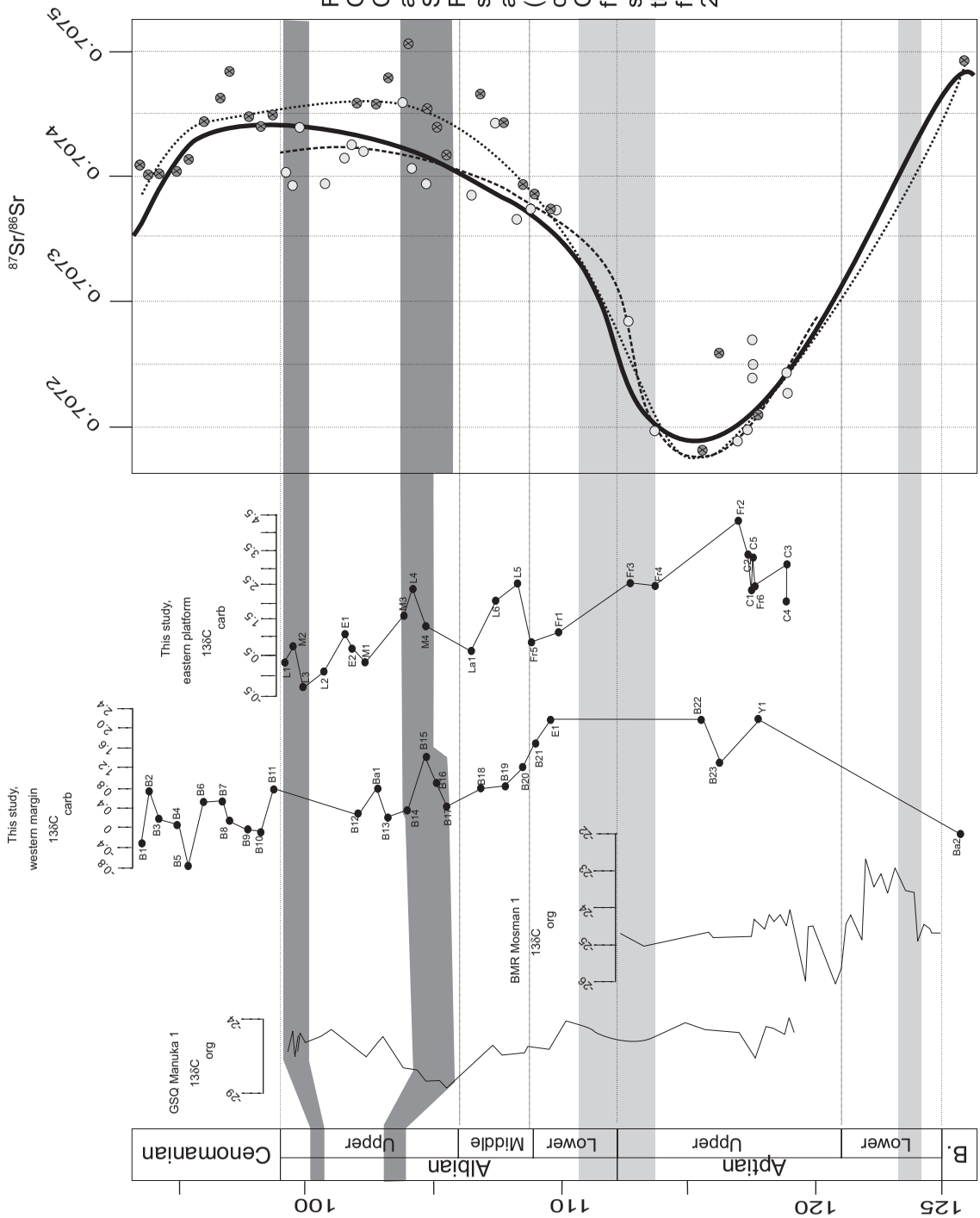

Figure E. 5. 1 $\delta^{13}C_{carb}$ curves for the Great Artesian ·····○····· and the Carnarvon ----⊗---- basins plotted against the Sr-isotope curve (see Section C) for timescale control. Recognized OAEs are represented by shaded bands with their age assignments taken from Ogg et al. (2004). Also shown are the $\delta^{13}C_{org}$ curves for two coreholes from the Great Artesian Basin: QGS Manuka 1 from the northern Eromanga sub-basin and BMR Mosman 1 from the Carpentaria sub-basin (compiled from Oosting, 2004; Henderson, 2004).

down ^{12}C relative to ^{13}C, due to biological fractionation. Differences in isotopic ratios ($\Delta\delta^{13}C_{carb}$) between calcareous plankton and benthic shell-forming organisms are widely employed in palaeoceanography as a productivity proxy. The data thus suggest that productivity in the shelf waters above the seafloor on which the Carnarvon Basin succession accumulated was characterised by lower productivity than that of the world ocean in general. Higher values, and greater surface water productivity, are registered by the Windalia Radiolarite which is rich in siliceous plankton and also the basal interval of the lower Gearle Siltstone which is also rich in plankton (Haig et al., 1996).

The Carnarvon Basin dataset shows a broad first-order trend of declining $\delta^{13}C$ values from the late Aptian through to the Cenomanian. The same broad trend is apparent for the Great Artesian Basin dataset, even though no reliability can be placed on the detail of it in terms of a global signature. Other broadscale datasets compiled for the same interval also show this trend (Price and Gröcke, 2002; Leckie et al., 2002). It corresponds with a broadscale warming across the same interval registered in palaeotemperatures obtained from oxygen-isotope analyses (Section D).

This trend is most likely due to atmospheric concentration of CO_2 which is known to accurately track global temperatures and which is also depleted relative to ocean waters with $\delta^{13}C$ for the modern atmosphere registering -7 (Ruddiman, 2001). Given atmospheric–ocean exchange of CO_2, general global warming should be accompanied by a reduction in $\delta^{13}C$ values expressed by surface waters of the global ocean. It is noteworthy that the mid Cretaceous was characterised by a significant upsurge of volcanic activity and associated outgassing, with estimates of pCO_2 ranging between 2 and 6 times modern levels (see Poulsen et al., 2001).

The Toolebuc interval in the northern Eromanga Basin is characterised by a positive $\delta^{13}C$ excursion which can be matched to a similar isotope event of early Late Albian age registered for the Carnarvon Basin succession (Figure E. 4. 1). This excursion marks OAE1c. Although noted in a number of OAE review papers and compilations (Arthur et al. 1990; Bralower et al., 1993; Leckie et al., 2002) the Toolebuc event (OAE 1c) has been subject to very little specific investigation. Some commentators place the event as of short duration (e.g. Leckie et al, 2002), but others

(Brawlower et al., 1993; Galeotti et al. 2003) consider that it spanned an enduring period. It has generally been assigned on biostratigraphic grounds to the *Bicinella breggiensis* planktic foraminiferal zone which spans the late Albian. The data presented here suggest that the event was confined to the early late Albian. The extent to which it had global expression is presently uncertain and awaits further research.

The positive $\delta^{13}C_{carb}$ excursion for the Toolebuc anoxic event recorded in the Eromanga Basin reported here is matched by an equally marked negative excursion in $\delta^{13}C_{org}$ (Henderson, 2004) which is now known from a number of core records (Oosting, 2004) and is a basin-wide feature of the Toolebuc interval. This is best explained by a significant terrestrial contribution to organic matter within the Toolebuc Formation. Interestingly Galeotti et al. (2003) also found that carbon of terrestrial origin to be a significant component in black shales representing OAE 1c in the Amadeus interval of central Italy.

REFERENCE LIST

Reference List

Avias, J. V., 1953, Contribution a l'Etude Stratigraphique et Paleontologique de la Nouvelle-Caledonie Centrale: Science Terre, v. 1.

Alley, N. F., and Frakes, L. A., 2003, First known Cretaceous glaciation; Livingston Tillite of the Cadna-owie Formation, South Australia: Australian Journal of Earth Sciences, v. 50, p. 139-144.

Anderson, T. F., and Arthur, M. A., 1983, Stable isotopes of oxygen and carbon and their application to sedimentological and palaeoenvironmental problems, in Arthur, M. A., Anderson, T. F., Kaplan, I. R., Veizer, J., and Land, L. S., eds., Stable Isotopes in Sedimentary Geochemistry, SEPM, Short Course Notes 10, p. 1-151.

Anderson, T. F., Popp, B. N., Williams, A. C., Ho, L.-Z., and Hudson, J. D., 1994, The stable isotopic record of fossils from the Peterborough Member, Oxford Clay Formation (Jurassic), U. K.: palaeoenvironmental implications: Journal of the Geological Society London, v. 151, p. 125-138.

Arthur, M. A., Dean, W. E., Pollastro, R. M., Claypool, G. E., and Scholle, P. A., 1985, Comparative geochemical and mineralogical studies of two cyclic transgressive pelagic limestone units, Cretaceous Western Interior Basin, in Pratt, L. M., Kauffmann, E. G., and Zelt, F. B., eds., Fine-grained Deposits and Biofacies of the Cretaceous Western Interior Seaway: Evidence of Cyclic Sedimentary Processes: Colorado, Society of Economic Paleontologists and Mineralogists, p. 16-27.

Arthur, M. A., Jenkyns, H. C., Brumsack, H. –J., and Schlanger, S. O., 1990, Stratigraphy, geochemistry and paleoceanography of organic carbon-rich Cretaceous sequences, in Ginsburg, R. N., and Beaudoin, B., eds., Cretaceous resource events and rhythms: Kluwer Academic, Massachusetts, p.75-119.

Backhouse, J., 1978, Palynological zonation of the Late Jurassic and Early Cretaceous sediments of the Yarrangadee Formation, central Perth Basin, Western Australia: Geological Survey of Western Australia Report, v. 7, p. 52.

Backhouse, J., 1987, Microplankton zonation of the Lower Cretaceous Warnbro Group, Perth Basin, Western Australia: Association of Australasian Palaeontologists Memoir, v. 4, p. 205-226.

Backhouse, J., 1988, Late Jurassic and Early Cretaceous palynology of the Perth Basin, Western Australia: Geological Survey of Western Australia Bulletin, v. 135, 233 p.

Barron, E. J., 1983, A warm equable Cretaceous: the nature of the problem: Earth Science Reviews, v. 19, p. 305-338.

Barron, E. J., and Peterson, W. H., 1990, Mid-Cretaceous ocean circulation: results from model sensitivity studies: Paleoceanography, v. 5, p. 319-337.

Barron, E. J., Thompson, S. L., and Scheneider, S. H., 1981, An ice free Cretaceous? Results from climate model simulations: Science, v. 212, p. 501-508.

Barron, E. J., and Washington, W. M., 1984, The role of geographic variables in explaining paleoclimate: results from Cretaceous climate model sensitivity studies: Journal of Geophysical Research, v. 89, p. 1267-1279.

Bather, F. A., 1888, Shell-growth in Cephalopoda (Siphonopoda): Annuals and Magazine of Natural History, v. 6, p. 298-310.

Berner, R. A., and Rye, D. M., 1992, Calculations of the Phanerozoic strontium isotope record of the oceans from a carbon cycle model: American Journal of Science, v. 292, p. 136-148.

Besaire, H., and Collignon, M., 1959, Le Systeme Cretace a Madagascar, El Sistema Cretacico, 11: Mexico, p. 135-198.

Birkelund, T., 1957, Upper Cretaceous belemnites from Denmark: Copenhagen, Biologiske Skrifter udgivet af det Kongelige Danske Videnskabernes Selskab, v. 9, p. 1-69.

Blanford, H. F., and Stoliczka, F., 1861, The fossil Cephalopoda of the Cretaceous rocks of southern India: Palaeontological Indica, v. 1.

Bolli, H. M., and Saunders, J. B., 1985, Oligocene to Holocene low latitude planktic Foraminifera, in Bolli, H. M., Saunders, J. B., and Perch-Nielson, K., eds., Plankton Stratigraphy: Cambridge, Cambridge University Press, p. 155-262.

Bowen, R., 1961, Palaeotemperature analyses of Mesozoic Belemnoidea from Australia and New Guinea: Bulletin of Geological Society of America, v. 72, p. 769-774.

Bralower, T. J., Arthur, M. A., Leckie, R. M., Sliter, W. V., Allard, D., and Schlanger, S.O., 1994, Timing and paleoceanography of oceanic and dysoxia/anoxia in the Late Barremian to Early Aptian (Early Cretaceous): Palaios, v. 9, p.335-369.

Bralower, T. J., CoBabe, E., Clement, B., Sliter, W. V., Osburn, C. L., and Longoria, J., 1999, The record of global change in mid-Cretaceous (Barremian-Albian) sections from the Sierra Madre, northeastern Mexico: Journal of Foraminiferal Research, v. 29, p. 418-437.

Bralower, T. J., Fullagar, P. D., Paull, C. K., Dwyer, G. S., and Leckie, R. M., 1997, Mid-Cretaceous strontium-isotope stratigraphy of deep-sea sections: Geological Society of America Bulletin, p. 1421-1442.

Bralower, T. J., and Siesser, W. G., 1992, Cretaceous calcareous nannofossil biostratigraphy of sites 761, 762 and 763, Exmouth and Wombat Plateaus, north-western Australia: Proceedings of the Ocean Drilling Program, Scientific Results, v. 122, p. 529-556.

Bralower, T. J., Sliter, W. V., Arthur, M. A., Leckie, R. M., Allard, D., and Schlanger, S. O., 1993, Dysoxic/anoxic episodes in the Aptian-Albian (Early Cretaceous), in Pringle, M. S., et al., ed., The Mesozoic Pacific: Geology, Tectonics and Volcanism, Series 77: Washington, D. C., Geophysical Monograph, AGU.

Brand, U., 1989, Biogeochemistry of late Paleozoic North American brachiopods and secular variation of seawater composition: Biogeochemistry, v. 7, p. 159-193.

Brown, D. A., Campbell, K. S. W., and Crook, K. A. W., 1968, The geological evolution of Australia and New Zealand: London, Pergamon Press, 409 p.

Bruckschen, P., Bruhn, F., Veizer, J., and Buhl, D., 1995a, Diagenetic alteration of calcitic fossil shells: proton microprobe (PIXE) as a trace element tool: Nuclear Instruments and Methods of Physical Research, v. B, p. 427-431.

Bruhn, F., Bruckschen, P., Richter, D. K., Meijer, J., Stephan, A., and Veizer, J., 1995, Diagenetic history of sedimentary carbonates: constraints from combined cathodoluminescence and trace element analyses by micro-PIXE: Nuclear Instruments and Methods of Physical Research, v. B, p. 409-414.

Bryan, S. E., Ewart, A., Stephens, C. J., Parianos, J., and Downes, P. J., 2000, The Whitsunday Volcanic Province, Central Queensland, Australia: lithological and stratigraphic investigations of a silicic-dominated large igneous province: Journal of Volcanology and Geothermal Research, v. 99, p. 55-78.

Bryan, W. H., and Jones, O. A., 1946, The geological history of Queensland. A stratigraphical outline: University of Queensland, Department of Geology Original Paper, v. 2.

Burger, D., 1973, Spore zonation and sedimentary history of the Neocomian, Great Artesian Basin, Queensland: Geological Society of Australia Special Publication, v. 4, p. 87-118.

Burger, D., 1980, Palynological studies in the Lower Cretaceous of the Surat Basin, Australia: Bureau of Mineral Resources Geology and Geophysics Bulletin, v. 189, p. 106.

Burger, D., 1982a, A basal Cretaceous dinoflagellate suite from north-eastern Australia: Palynology, v. 6, p. 161-192.

Burger, D., 1982b, Palynological examination of Late Mesozoic sediments in QGS Hughenden 7, and notes on geological events in the Northern Eromanga Basin: Brisbane, Queensland Geological Survey, 22 p.

Burger, D., 1986, Palynology, cyclic sedimentation, and palaeoenvironments in the Late Mesozoic of the Eromanga Basin: Geological Society of Australia Special Publication, v. 12, p. 53-70.

Burger, D., and Shafik, S., 1996, Cretaceous (Charts 10 and 11), in Young, G. C., and Laurie, J. R., eds., An Australian Phanerozoic Timescale: Melbourne, Oxford University Press, p. 160-174.

Burke, W. H., Denison, R. E., Hetherington, E. A., Koepnick, R. B., Nelson, H. F., and Otto, J. B., 1982, Variations of seawater 87Sr/86Sr throughout Phanerozoic time: Geology, v. 10, p. 516-519.

Campbell, R. J., and Haig, D. W., 1999, Bathymetric change during Early Cretaceous intracratonic marine transgression across the northeastern Eromanga Basin, Australia: Cretaceous Research, v. 20, p. 403-446.

Casey, R., 1960, A monograph of the Ammonoidea of the Lower Greensand: Palaeontological Society Monograph, v. 36, p. 1-44, pl. 1-10.

Casey, R., 1961, A monograph of the Ammonoidea of the Lower Greensand: Palaeontographical Society Monograph, v. 36, p. 45-118, pl. 11-25.

Challinor, A. B., 1990, A belemnite biozonation for the Jurassic-Cretaceous of Papua New Guinea and a faunal comparison with eastern Indonesia: BMR Journal of Geology and Geophysics, v. 11, p. 429-427.

Challinor, A. B., 1991, Belemnite successions and faunal provinces in the southwest Pacific and the belemnites of Gondwana: BMR Journal of Geology and Geophysics, v. 12, p. 301-325.

Challinor, A. B., Doyle, P., Howlett, P. J., and Nal'nyaeva, T. I., 1992, Belemnites of the Circum-Pacific region, in Westermann, G. E. G., ed., The Jurassic of the Circum-Pacific, World and regional geology, 3, p. 334-341.

Christensen, E., 1925, Neue Beitrage zum Bau der Belemniten: Neues Jahrbuch fuer Geologie und Palaeontologie, v. 51, p. 118-58.

Christensen, W. K., 1976, Palaeobiogeography of Late Cretaceous belemnites of Europe: Palaontol. Zeit., v. 50, p. 113-129.

Christensen, W. K., 1997a, The Late Cretaceous belemnite family Belemnitellidae; taxonomy and evolutionary history: Bulletin of the Geological Society of Denmark, v. 44, p. 59-88.

Christensen, W. K., 1997b, Palaeobiogeography and migration in the Late Cretaceous belemnite family Belemnitellidae: Acta Palaeontologica Polonica, v. 42, p. 457-495.

Church, J. A., and Forbes, A. M. G., 1983, Circulation in the Gulf of Carpentaria. I: Direct Observations of Currents in the Southeast Corner of the Gulf of Carpentaria, in Imberger, J., ed., Physical Oceanography in Australia, 34: Melbourne, CSIRO Australian Journal of Marine and Freshwater Research, p. 1-10.

Clarke, L. J., and Jenkyns, H. C., 1999, New oxygen isotope evidence for long-term Cretaceous climatic change in the Southern Hemisphere: Geology, v. 27, p. 699-702.

Clarke, M. R., 1966, A review of the systematics and ecology of oceanic squids, Advances in Marine Biology, 4, p. 91-300.

Clarke, W. B., 1862, On the occurrence of Mesozoic and Permian faunae in eastern Australia: Quarterly Journal of Geology, Society of London, v. 18, p. 244-247.

CLIMAP, 1981, Seasonal Reconstructions of the Earth's Surface at the Last Glacial Maximum, Technical Report, Map and Chart Series 36: Boulder, Colorado, Geological Society of America, 18 p.

Cochran, J. K., Landman, N. H., Turekian, K. K., Michard, A., and Schrag, D. P., 2003, Paleoceanography of the Late Cretaceous (Maastrichtian) Western Interior Seaway of North America: evidence from Sr- and O-isotopes: Palaeogeography, Palaeoclimatology, Palaeoecology, v. 191, p. 45-64.

Craig, H., 1965, The Measurement of Oxygen Isotope Palaeotemperatures, in Tongiorgi, E., ed., Stable Isotopes in Oceanographic Studies and Palaeotemperatures: Pisa, Consiglio Nazionale delle Richerche, Laboratorio di Geologia Nucleare.

Cuadros, J., Caballero, E., Javier Huertas, F., Huertas, F., and Linares, J., 1999, Experimental alteration of volcanic tuff; smectitie formation and effect on ^{18}O isotope composition: Clays and Clay Minerals, v. 47, p. 769-776.

Cuvier, G., 1795, Second Memoire sur l'organisation et les rapports des Animaux a sang blanc, dans lequel on traite de la structure des Mollusques et de leur division en orders: Magasin Encyclopedique ou Journal des Sciences, des Lettres et des Arts, v. 2, p. 433-449.

David, T. W. E., 1950, The Geology of the Commonwealth of Australia: London, Arnold.

Day, R. W., 1964, Stratigraphy of the Roma-Wallumbilla area: Geological Survey of Queensland, v. 318, p. 1-23.

Day, R. W., 1965, Nomenclature of the Rolling Downs Group, northern Eromanga Basin, Queensland, in Vine, R. R., and Day, R. W., eds., Queensland Government Mining Journal, 66, p. 416-421.

Day, R. W., 1967a, Marine Lower Cretaceous fossils from the Minmi Member, Blythesdale Formation, Roma- Wallumbilla area: Geological Survey of Queensland, no. 335, v. 9, p. 1-30.

Day, R. W., 1967b, A mixed Roma-Tambo fauna from the Tambo area: Queensland Government Mining Journal, v. 68, p. 10-12.

Day, R. A., 1968, Biostratigraphy and Taxonomy of Lower Cretaceous Molluscan Faunas from the Queensland portion of the Great Artesian Basin: Unpub. PhD thesis, Australian National University, 585 p.

Day, R. A., 1969, The lower Cretaceous of the Great Artesian Basin, in Campbell, K. W. S., ed., Stratigraphy and Palaeontology. Essays in honour of Dorothy Hill: Canberra, Australian National University Press, p. 140-173.

Day, R. W., 1974, Aptian ammonites from the Eromanga and Surat basins, Queensland: Geological Survey of Queensland Publication, v. 360, p. 19.

De Leeuw, J. W., Frewin, N. L., Van Bergen, P. F., Sinninghe Damste, J. S., and Collinson, M. E., 1995, Organic carbon as a palaeoenvironmental indicator in the marine realm: in Bosence, D. W. J. and Allison, P.A. eds., Marine Palaeoenvironmental Analysis From Fossils: Geological Society of London Special Publication, v. 83, p. 43-73.

De Lurio, J., and Frakes, L. A., 1999, Glendonites as a paleoenvironmental tool: Implications for early Cretaceous high latitude climates in Australia: Geochemica et Cosmochimica Acta, v. 63, p. 1039-1048.

DePaolo, D. J., and Ingram, B. L., 1985, High-resolution stratigraphy with strontium isotopes: Science, v. 227, p. 938-941.

Derry, L. A., and Jacobsen, S. B., 1988, The Nd and Sr isotopic evolution of Proterozoic seawater: Geophysical Resources Letters, v. 15, p. 397-400.

Derry, L. A., Keto, L. S., Jacobsen, S. B., Knoll, A. H., and Swett, K., 1989, Sr isotopic variations in Upper Proterozoic carbonates from Svalbard and East Greenland: Geochemica et Cosmochimica Acta, v. 53, p. 2331-2339.

Dettmann, M., 1963, Upper Mesozoic microfloras from south-eastern Australia: Proceedings of the Royal Society of Victoria, v. 77, p. 1-138.

Dettmann, M., 1986, Early Cretaceous palynoflora of subsurface strata correlative with the Koonwarra Fossil Bed, Victoria: Association of Australasian Palaeontologists Memoir, v. 3, p. 79-110.

Dettmann, M. E., 1994, Cretaceous vegetation: the microfossil record, in Hill, R. S., ed., History of the Australian Vegetation: Cretaceous to Recent: Cambridge, Cambridge University Press, p. 143-170.

Dettmann, M., and Playford, G., 1969, Palynology of the Australian Cretaceous: a review, in Campbell, K. W. S., ed., Stratigraphy and Palaeontology. Essays in honour of Dorothy Hill: Canberra, Australian National University Press, p. 174-210.

D'Hondt, S., and Arthur, M. A., 1995, Interspecific variation in stable isotope signals of Maastrichtian planktonic foraminifera: Paleoceanography, v. 10, p. 125-135.

Ditchfield, P. W., Marshall, J. D., and Pirrie, D., 1994, High latitude palaeotemperature variation: New data from the Tithonian to Eocene of James Ross Island, Antarctica: Palaeogeography, Palaeoclimatology, Palaeoecology, v. 107, p. 79-101.

Dixon, M., Haig, D. W., Mory, A. J., Backhouse, J., Ghori, K. A. R., Howe, R., and Morris, P. A., 2003a, GSWA Edaggee 1 Well Completion Report, Gascoyne Platform, Southern Carnarvon Basin Western Australia, 8: Perth, Geological Survey of Western Australia.

Dixon, M., Haig, D. W., Mory, A. J., Backhouse, J., Ghori, K. A. R., and Morris, P. A., 2003b, GSWA Yinni 1 well completion report (interpretative) Gascoyne Platform Southern Carnarvon Basin, Western Australia, 7: Perth, Geological Survey of Western Australia.

Dorman, F. H., 1968, Some Australian oxygen isotope temperatures and a theory for a 30-million-year world-temperature cycle: Journal of Geology, v. 76, p. 297-313.

Dorman, F. H., and Gill, E. D., 1959, Oxygen-isotope palaeotemperature measurements on Australian fossils: Proceedings of the Royal Society of Victoria, v. 71, p. 73-98.

Douglas, J. G., and Savin, S. M., 1975, Oxygen and carbon isotope analyses of Tertiary and Cretaceous microfossils from Shatsky Rise and other sites in the North Pacific Ocean: Initial Reports of the Deep Sea Drilling Project, v. 35, p. 509-521.

Douglas, R. G., and Williams, G. E., 1982, Southern polar forests: the early Cretaceous floras of Victoria and their palaeoclimatic significance: Palaeogeography, Palaeoclimatology, Palaeoecology, v. 39, p. 171-185.

Doyle, P., 1985, Indian belemnites from the Albian (Lower Cretaceous) of James Ross Island Antarctica: British Antarctic Survey Bulletin, v. 69, p. 23-34.

Doyle, P., 1987a, The Cretaceous Dimitobelidae (Belemnitida) of the Antarctic Peninsula region: Palaeontology, v. 30, p. 147-177.

Doyle, P., 1987b, Early Cretaceous belemnites from southern Mozambique: Palaeontology, v. 30, p. 311-317.

Doyle, P., 1987c, Lower Jurassic-lower Cretaceous belemnite biogeography and the development of the Mesozoic Boreal realm: Palaeogeography, Palaeoclimatology, Palaeoecology, v. 61, p. 237-254.

Doyle, P., 1988, The belemnite family Dimitobelidae in the Cretaceous of Gondwana, in Wiedmann, I., and Kullman, J., eds., Cephalopods Past and Present: Stuttgart, Schweizerbart'sche Verlagsbuchandlung, p. 539-552.

Doyle, P., 1992, A review of the biogeography of Cretaceous belemnites: Palaeogeography, Palaeoclimatology, Palaeoecology, v. 92, p. 207-221.

Doyle, P., 1997, 9: Molluscs: Cephalopods, Understanding Fossils: An introduction to Invertebrate Palaeontology: England, Wiley, p. 159-181.

Doyle, P., and Pirrie, D., 1999, Belemnite distribution patterns: implications of new data from Argentina, in Oloriz, F., and Rodriguez-Tovar, F. J., eds., Advancing Research on Living and Fossil Cephalopods: New York, Kluwer Academy, p. 419-436.

Elderfield, H., 1986, Strontium Isotope Stratigraphy: Palaeogeography, Palaeoclimatology, Palaeoecology, v. 57, p. 71-90.

Ellis, G., 1993, Late Aptian-early Albian Radiolaria of the Windalia Radiolarite (type section), Carnarvon Basin: Eclogae Geologicae Helvetiae, v. 86, p. 943-995.

Epstein, S., and Lowenstam, H. A., 1953, Temperature-shell growth relations of Recent and interglacial Pleistocene shoal-water biota from Bermuda: Journal of Geology, v. 61, p. 424-438.

Erba, E., 1996, The Aptian stage: Bulletin de l'Institut Royal des Sciences Naturelles de Belgique, Sciences de la Terre, v. 66-supplement, p. 31-43.

Erba, E., Channell, J. E. T., Claps, M., Jones, C., Larson, R., Opdyke, B., Premoli Silva, I., Riva, A., Salvani, G., and Toricelli, S., 1999, Integrated stratigraphy of Cismon Apticore (southern Alps, Italy): A "reference section" for the Barremian-Aptian interval at low latitudes: Journal of Foraminiferal Research, v. 29, p. 371-391.

Erba, E., and Larson, R., 1991, Nannofossils and superplumes: EOS, v. 72.

Erba, E., and Premoli Silva, I., 1994, Orbitually driven cycles in trace-fossil distribution from the Piobbico core (late Albian, central Italy): Special Publication International Association of Sedimentologists, v. 19, p. 211-225.

Erbacher, J., and Thurow, J., 1997, Influences of oceanic anoxic events on the evolution of mid-Cretaceous radiolaria in the north Atlantic and western Tethys: Micropalaeontology, v. 30, p. 139-158.

Erbacher, J., Thurow, J., and Littke, R., 1996, Evolution patterns of radiolarian and organic matter variations: a new approach to identify sea-level changes in mid-Cretaceous pelagic environments: Geology, v. 24, p. 499-502.

Etheridge, R. J., 1878, Catalogue of Australian fossils: Cambridge.

Etheridge, R. J., 1880, On the identification of the first secondary fossil found in Australia: Proceedings of the Royal Society of Tasmania.

Etheridge, R. J., 1892, The geology and paleontology of Queensland and New Guinea, Geological Survey of Queensland.

Etheridge, R. J., 1902a, The Cretaceous mollusca of South Australia and the Northern Territory: Memoirs of the Royal Society South Australia, v. 2, p. 1-54.

Etheridge, R. J., 1902b, A monograph on the Cretaceous invertebrate fauna of New South Wales: Memoirs of the Geological Survey of New South Wales, v. 11, p. 1-98.

Etheridge, R. J., and Dun, W. S., 1902, Catalogue of the Cretaceous fossils of Australia. Appendix I p. 51-84, in Etheridge, R. J., ed., A monograph of the Cretaceous invertebrate fauna of New South Wales, 11, Memorial Geological Survey N.S.W., p. i-xiii, 1-98, pl. 1-11.

Evans, P. R., 1966, Mesozoic stratigraphic palynology in Australia: Australian Oil and Gas Journal, v. 12, p. 58-63.

Exon, N. F., and Senior, B. R., 1976, The Cretaceous of the Eromanga and Surat basins: BMR Journal of Australian Geology and Geophysics, v. 1, p. 33-50.

Fairbridge, R. W., 1964, The importance of limestone and its Ca/Mg content to palaeoclimatology, in Nairn, A. E. M., ed., Problems in Palaeoclimatology: London, Wiley Interscience, p. 431-478.

Ferguson, K. M., Gregory, R. T., and Constantine, A., 1999, Lower Cretaceous (Aptian-Albian) secular changes in the oxygen and carbon isotope record from high paleolatitude, fluvial sediments, southeast Australia: Comparisons to the marine record: Geological Society of America Special Paper, v. 332, p. 59-72.

Fisher, A. G., and Arthur, M. A., 1977, Secular variations in the pelagic realm, in deep water carbonate environments: in Cook, H. E. and Enos, P., eds., Society of Economic Palaeontologists and Mineralogists Special Publications 25: Tulsa, Oklahoma, p. 19-50.

Frakes, L. A., Alley, N. F., and Deynoux, M., 1995, Early Cretaceous ice rafting and climate zonation in Australia: International Geology Review, v. 37, p. 567-583.

Frakes, L. A., Burger, D., Anthrope, M., Wiseman, J., Dettmann, M., Alley, N., Flint, R., Gravestock, D., Ludbrooke, N., Backhouse, J., Skwarko, S., Scheibnerova, V., McMinn, A., Moore, P. S., Bolton, B. R., Douglas, J. G., Christ, R., Wade, M., Molnar, R. E., McGowran, B., Balme, B. E., and Day, R. A., 1987, Australian Cretaceous shorelines, stage by stage: Palaeogeography, Palaeoclimatology, Palaeoecology, v. 59, p. 31-48.

Frakes, L. A., and Francis, J. E., 1988, A guide to Phanerozoic cold polar climates from high-altitude ice-rafting in the Cretaceous: Nature, v. 333, p. 547-549.

Francis, J. E., and Frakes, L. A., 1993, Cretaceous climates: Sedimentary Review, v. 1, p. 17-30.

Friedman, I., and O'Neil, J. R., 1977, Compilation of stable isotope fractionation factors of geochemical interest, in Fleicher, M., ed., Data of Geochemistry, Paper 440-KK, Geological Survey Professional, p. KK1-KK12 + figs.

Galeotti, S., Sprovieri, M., Coccioni, R., Bellanca, A., and Neri, R., 2003, Orbitually modulated black shale deposition in the upper Albian Amadeus Segment (Central Italy): a multi proxy reconstruction: Palaeogeography, Palaeoclimatology, Palaeoecology, v. 190, p.441-458.

Glaessner, M. F., 1945, Mesozoic fossils from the central highlands of New Guinea: Proceedings of the Royal Society of Victoria, v. 56, p. 151-168.

Glaessner, M. F., 1957, Cretaceous belemnites from Australia, New Zealand, and New Guinea: Australian Journal of Science, v. 20, p. 88-89.

Glaessner, M. F., 1958, New Cretaceous fossils from New Guinea: Records of the South Australian Museum, v. 13, p. 199-226, pl. 24-26.

Gradstein, F. M., Agterberg, F. P., Ogg, J. G., Hardenbol, J., van Veen, P., Thierry, J., and Huang, Z., 1994, A Mesozoic time scale: Journal of Geophysical Research, v. 99, p. 24051-24074.

Gradstein, F. M., Lourens, L. J., Ogg, J. G., Smith, A. G., and Bleeker, W., 2004, A new Geological Time Scale, with special reference to Precambrian and Neogene: Episodes, v. 27, p. 83-100.

Gregory, R. T., Douthitt, C. B., Duddy, I. R., Rich, P. V., and Rich, T. H., 1989, Oxygen isotope composition of carbonate concretions from the Lower Cretaceous of Victoria, Australia: Implications of the evolution of meteoric waters of the Australian continent in a paleopolar environment: Earth and Planetary Science Letters, v. 92, p. 27-42.

Gröcke, D. H., Hesselbo, S. P., and Jenkyns, H. C., 1999, Carbon-isotope composition of Lower Cretaceous fossil wood: Ocean-atmosphere chemistry and relation to sea –level change: Geology, v. 27, p. 155-158.

Gürich, G., 1901, Jura- und Devon- Fossilien von White Cliffs Australien: Neues Jarbuch fuer Geologie und Palaeontologie Beil. Bd., v. 14, p. 484-518.

Gurnis, M., Mueller, R. D., and Moresi, L., 1998, Dynamics of Cretaceous vertical motion of Australia and the Australian-Antarctic discordance: Science, v. 279, p. 1499-1504.

Haig, D. W., 1979a, Global distributions patterns for mid-Cretaceous foraminiferids: Journal of Foraminiferal Research, v. 9, p. 29-40.

Haig, D. W., 1979b, Cretaceous foraminiferal biostratigraphy of Queensland: Alcheringa, v. 3, p. 171-187.

Haig, D. W., 2006, Gondwana-Australian Permian to Cretaceous agglutinated foraminifera as indicators of bottom-water conditions in epeiric seas: Australian Earth Sciences Convention 2006, Melbourne Convention and Exhibition Centre, 2-6 July, 2006.

Haig, D. W., 2005, Foraminiferal evidence for inner neritic deposition of Lower Cretaceous (Upper Aptian) radiolarian-rich black shales on the Western Australian margin Journal of Micropalaeontology, v. 24, p. 55-75, Part 1.

Haig, D. W., 2004, Comparison of foraminifera and habitats from Australian Permian and Cretaceous Interior Seas: Memoirs of the Association of Australasian Palaeontologists, v. 29, p. 31-46.

Haig, D. W., and Barnbaum, D., 1978, Early Cretaceous microfossils from the type Wallumbilla Formation, Surat Basin, Queensland: Alcheringa, v. 2, p. 159-178.

Haig, D. W., and Lynch, D. A., 1993, A late early Albian transgressive pulse over northeastern Australia, precursor to epeiric basin anoxia: foraminiferal evidence: Marine Micropalaeontology, v. 22, p. 311-362.

Haig, D. W., Watkins, D. K., and Ellis, G., 1996, Mid-Cretaceous calcareous and siliceous microfossils from the basal Gearle Siltstone, Giralia Anticline, Southern Carnarvon Basin: Alcheringa, v. 20, p. 41-68.

Hallam, A., 1985, A review of Mesozoic climates: Geological Society of London Journal, v. 142, p. 433-445.

Hanai, T., 1953, Lower Cretaceous belemnites from Miyako district, Japan: Japanese Journal of Geology and Geography, v. 23, p. 63-80.

Hancock, J. M., and Kauffman, E. G., 1979, The great transgression of the Cretaceous: Journal of Geological Society of London, v. 136, p. 175-186.

Hanlon, R. T., and Messenger, J. B., 1996, Cephalopod Behaviour: Cambridge, Cambridge University Press, 248 p.

Haq, B. U., Hardenbol, J., and Vail, P. R., 1988, Chronology of fluctuating sea levels since Triassic: Science, v. 235, p. 1156-1167.

Hay, W. W., 1995, Cretaceous paleoceanography: Geologica Carpathica, v. 46, p. 257-266.

Hay, W. W., Eicher, D. L., and Diner, R., 1993, Physical oceanography and water masses in the Cretaceous Western Interior Seaway, in Caldwell, W. G. E., and Kauffmann, E. G., eds., Evolution of the Western Interior Basin, Special Paper 39, Geological Association of Canada, p. 297-318.

He, S., Kyser, T. K., and Caldwell, W. G. E., 2005, Paleoenvironment of the Western Interior Seaway inferred from d18O and d13C values of molluscs from the Cretaceous Bearpaw marine cyclotherm: Palaeogeography, Palaeoclimatology, Palaeoecology, v. 217, p. 67-85.

Hedge, C. E., and Walthall, F. G., 1963, Radiogenic strontium-87 as an index of geological processes: Science, v. 140, p. 1214-1217.

Helby, R. J., Morgan, R., and Partridge, A. D., 1987, A palynological zonation of the Australian Mesozoic: Association of Australasian Palaeontologists Memoir, v. 4, p. 1-94.

Helby, R. J., and Partridge, A. D., 2004, Updated Jurassic-Early Cretaceous dinocyst zonation NWS Australia: Geoscience Australia Publication.

Henderson, R. A., 1990, Late Albian ammonites from the Northern Territory, Australia: Alcheringa, v. 14, p. 109-148.

Henderson, R. A., 1998a, Palaeoenvironmental and eustatic record of the mid-Cretaceous Bathurst Island group, Money Shoals Platform, northern Australia: Palaeogeography, Palaeoclimatology, Palaeoecology, v. 138, p. 115-138.

Henderson, R. A., 1998b, Eustatic and palaeoenvironmental assessment of the mid-Cretaceous Bathurst Island Group of the Money Shoals Platform, northern Australia: Palaeogeography, Palaeoclimatology, Palaeoecology, v. 138, p. 115-138.

Henderson, R. A., 2004, A mid-Cretaceous association of shell beds and organic-rich shale: bivalve exploitation of a nutrient rich, anoxic sea-floor environment: Sedimentary Geology, v. 19, p. 156-169.

Henderson, R. A., Crampton, J. S., Dettmann, M., Douglas, J. G., Haig, D. W., Shafik, S., Stilwell, J. D., and Thulborn, R. A., 2000, Biogeographical observations on the Cretaceous biota of Australasia: Memoir of the Association of Australasian Palaeontologists, v. 23, p. 355-404.

Henderson, R. A., and Kennedy, W. J., 2002, Occurrence of Goodhallites goodhalli J. Sowerby (Ammonoidea) in the Eromanga Basin: an index species for the late Albian (Cretaceous): Alcheringa, v. 26, p. 223-237.

Hess, J., Bender, M. L., and Schilling, J. G., 1986, Evolution of the ratio strontium-87 to strontium -86 from Cretaceous to present: Science, v. 231, p. 979-984.

Hill, D., Playford, G., and Woods, J. T., 1968, Cretaceous fossils of Queensland: Brisbane, Queensland Palaeontographical Society, 35 p.

Hocking, R. M., Moors, H. T., and Van De Graaff, W. J. E., 1987, Geology of the Carnarvon Basin, Western Australia: Geological Survey of Western Australia Bulletin., v. 133, p. 1-289.

Hocking, R., Mory, A. J., and Williams, I. R., 1994, An atlas of Neoproterozoic and Phanerozoic basins of Western Australia, in Purcell, P. G., and Purcell, R. R., eds., The Sedimentary Basins of Western Australia: Perth, Proceedings of Petroleum Exploration Society of Australia Symposium, p. 21-43.

Hodell, D. A., Mead, G. A., and Mueller, P. A., 1990, Variation in the strontium isotopic composition of seawater (8 Ma to present): Implications for chemical weathering rates and dissolved fluxes to the oceans: Chemical Geology, v. 80, p. 291-307.

Hodell, D. A., Mueller, P. A., McKenzie, J., and Mead, G. A., 1989, Strontium isotope stratigraphy and geochemistry of the late Neogene ocean: Earth and Planetary Science Letters, v. 92, p. 165-178.

Holster, W. T., 1997, Geochemical events documented in inorganic carbon isotopes, Palaeogeography, Palaeoclimatology, Palaeoecology, v. 132, p. 173-182.

Howarth, R. J., and McArthur, J. M., 1997, Statistics for strontium isotope stratigraphy: A robust LOWESS fit to the marine Sr-isotope curve for 0 to 206 Ma, with look-up table for derivation of numerical age: Journal of Geology, v. 105, p. 441-456.

Huber, B. T., Hodell, D. A., and Hamilton, C. P., 1995, Middle-Late Cretaceous climate of the southern high latitudes: Stable isotopic evidence for minimal equator-to-pole thermal gradients: Geological Society of America Bulletin, v. 107, p. 1164-1191.

Huber, B. T., Norris, R. D., and MacLeod, K. G., 2002, Deep-sea paleotemperature record of extreme warmth during the Cretaceous: Geology, v. 30, p. 123-126.

Hudson, J. D., and Anderson, T. F., 1989, Ocean temperatures and isotopic compositions through time: Transactions of the Royal Society of Edinburgh, v. 80, p. 183-192.

Ineson, J. R., 1989, Coarse-grained submarine fan and slope apron deposits in a Cretaceous back-arc basin, Antarctica: Sedimentology, v. 36, p. 793-819.

Ingram, B. L., Coccioni, R., Montanari, A., and Richter, F. M., 1994, Strontium isotope composition of mid-Cretaceous seawater: Science, v. 264, p. 546-550.

Jarvis, I., 1980, Palaeobiology of Upper Cretaceous belemnites from the phosphatic chalk of the Anglo-Paris basin: Palaeontology, v. 23, p. 889-914.

Jeletzky, J. A., 1965, Late Upper Jurassic and early Lower Cretaceous fossil zones of the Canadian western Cordillera, British Columbia: Geological Survey of Canada Bulletin, v. 103, i-x, p. 1-70, pl. 1-22.

Jones, C. E., and Jenkyns, H. C., 2001, Seawater Strontium isotopes, oceanic anoxic events, and seafloor hydrothermal activity in the Jurassic and Cretaceous: American Journal of Science, v. 301, p. 112-149.

Jones, C. E., Jenkyns, H. C., and Hesselbo, S. P., 1994a, Strontium isotopes in the Early Jurassic seawater: Geochemica et Cosmochimica Acta, v. 58, p. 1285-1301.

Jones, C. E., Jenkyns, H. C., Coe, A. L., and Hesselbo, S. P., 1994b, Strontium isotopic variations in Jurassic and Cretaceous seawater: Geochemica et Cosmochimica Acta, v. 58, p. 3061-3074.

Kemper, E., 1975, Deer Bay Formation (Berriasian-Valanginian) of Sverdrup Basin and biostratigraphy of the Arctic Valanginian: Geological Survey of Canada Paper, v. 75-1B, p. 245-254.

Klinger, H. C., 1976, Cretaceous heteromorph ammonites from Zululand: Memoirs of the Geological Survey of South Africa, v. 69, p. 142.

Krieg, G. W., 1995, Mesozoic, in Drexel, J. F., and Preiss, W. V., eds., The Geology of South Australia. The Phanerozoic, 2, South Australian Geological Survey: Bulletin 54, p. 93-149.

Kump, L. R., 1991, Interpreting carbon-isotope excursions: Strangelove oceans: Geology, v. 19, p. 299-302.

Kuypers, M. M. M., 2001, Mechanisms and biochemical implications of the mid Cretaceous global organic burial events: Unpub. PhD thesis, Utrecht University.

Kyser, T. K., Caldwell, W. G. E., Whittaker, S. G., and Cadrin, A. J., 1993, Paleoenvironment and geochemistry of the northern portion of the Western Interior Seaway during the

Cretaceous time, in Caldwell, W. G. E., and Kauffman, E. G., eds., Evolution of the Western Interior Basin, 39, Geological Association of Canada Special Paper, p. 355-375.

Landman, N. H., Cochran, J. K., Rye, D. M., Tanabe, K., and Arnold, J. M., 1994, Early life of Nautilus: evidence from isotopic analyses of aquarium-reared specimens: Paleobiology, v. 20, p. 40-51.

Larson, R. L., and Erba, E., 1999, Onset of the mid-Cretaceous greenhouse in the Barremian - Aptian: Igneous events and the biological, sedimentary, and geochemical responses: Paleoceanography, v. 14, p. 663-678.

Leckie, R. M., 1985, Foraminifera of the Cenomanian-Turnonian boundary interval, Greenhorn Formations, Rock Canyon Anticline, Pueblo Colorado, in Pratt, L. M., Kauffman, E. G., and Zelt, F. B., eds., Fine-Grained Deposits and Biofacies of the Cretaceous Interior Seaway: evidence of Cyclic Sedimentary Processes, Field Trip Guidebook 4: Tulsa, OK, Society of Economic Palaeontologists and Mineralogists, p.139-149.

Leckie, R. M., Bralower, T. J., and Cashman, R., 2002, Oceanic anoxic events and plankton evolution: Biotic response to tectonic forcing during the mid-Cretaceous: Paleoceanography, v. 17, p. 13-1; 13-29.

Leeman, W. P., 1982, Tectonic and magmatic significance of strontium isotopic variations in Cenozoic volcanic rocks from the western United States: Geological Society of America Bulletin, v. 93, p. 487-503.

Li, Z. X., and Powell, C. M., 2001, An outline of the palaeogeography evolution of the Australasian region since the beginning of the Neoproterozoic: Earth Science Reviews, v. 53, p. 237-277.

Locarnini, R. A., Mishonov, A., Antonov, J. A., Boyer, T. P., and Garcia, H. E., 2006, NOAA Atlas: Temperature, in Levitus, S., ed., World Ocean Atlas, 1. NOAA Atlas: Washington, D. C., National Oceanographic Data Centre.

Longinelli, A., 1969, Oxygen-18 Variations in Belemnite Guards: Earth and Planetary Science Letters, v. 7, p. 209-212.

Lowenstam, H. A., and Epstein, S., 1954, Paleotemperatures of the post-Aptian Cretaceous as determined by the Oxygen Isotope Method: The Journal of Geology, v. 62, p. 207-248.

Ludbrook, N. H., 1966, Cretaceous biostratigraphy of the Great Artesian Basin in South Australia: Bulletin of the Geological Survey of South Australia, v. 40, p. 1-223.

Ludwig, K. R., Halley, R. B., Simmons, K. R., and Peterman, Z. E., 1988, Strontium isotope stratigraphy of the Enewetak Atoll: Geology, v. 16, p. 173-177.

Marshall, J. D., 1992, Climatic and oceanographic signals from the carbonate rock record and their preservation: Geological Magazine, v. 129, p. 143-160.

Masse, J. –P., 1993, Valanginian-Early Aptian carbonate platforms from Provence, southeastern France, in Simo, T., Scott., R. W., and Masse, J. –P., eds., Cretaceous Carbonate Platforms, Memoir 56, American Association of Petroleum Geologists, p.363-374.

McArthur, J. M., 1994, Recent trends in strontium isotope stratigraphy: Terra Nova, v. 6, p. 331-358.

McArthur, J. M., Donovan, D. T., Thirlwall, M. F., Fouke, B. W., and Mattey, D., 2000, Strontium isotope profile of the Early Turonian (Jurassic) Ocean Anoxic Event, the duration of ammonite biozones, and belemnite palaeotemperatures: Earth and Planetary Science Letters, v. 179, p. 269-285.

McArthur, J. M., Kennedy, W. J., Chen, M., Thirlwall, M. F., and Gale, A. S., 1994, Strontium isotope stratigraphy for the Late Cretaceous: Direct numerical age calibration of the Sr-

isotope curve for the U.S.A Western Interior Seaway: Palaeogeography, Palaeoclimatology, Palaeoecology, v. 108, p. 95-119.

McArthur, J. M., Mutterlose, J., Price, G. D., Rawson, P. F., Ruffell, A. H., and Thirlwall, M. F., 2004, Belemnites of Valanginian, Hauterivian and Barremian age: Sr-isotope stratigraphy, composition (87Sr/86Sr, d13C, d18O, Na, Sr, Mg), and palaeo-oceanography: Palaeogeography, Palaeoclimatology, Palaeoecology, v. 202, p. 253-272.

McArthur, J. M., Thirlwall, M. F., Gale, A. S., Kennedy, W. J., Burnett, J. A., Mattey, D., and Lord, A. R., 1993, Strontium isotope stratigraphy for the Late Cretaceous: A new curve, based on the English Chalk, in Hailwood, E. A., and Kidd, R. B., eds., High Resolution Stratigraphy, 70, Geological Society of London Special Publication, p. 195-209.

McConnaughey, T. A., 1989, 13C and 18O isotopic disequilibria in biological carbonates, I. Patterns: Geochemica et Cosmochimica Acta, v. 53, p. 151-162.

McCoy, F., 1866, On the discovery of Cretaceous fossils in Australia: Transactions of the Royal Society of Victoria, v. 7, p. 49-51.

McCoy, F., 1867a, On the occurrence of Ichthyosaurus and Plesiosaurus in Australia: Annuals and Magazine of Natural History, Serial 3, v. 19, p. 355-356.

McCoy, F., 1867b, On the discovery of Enaliosauria and other Cretaceous fossils in Australia: Transactions of the Royal Society of Victoria, v. 8, p. 41-42.

McCoy, F., 1867c, On the recent zoology and paleontology of Victoria: Annuals and Magazine of Natural History, Serial 3, v. 20, p. 175-202.

McKenzie, E. D., 1999, A new early to middle Albian (Cretaceous) Ammonite fauna from the Great Artesian Basin, Australia: Proceedings of the Royal Society of Queensland, v. 108, p. 57-88.

McNamara, K. J., 1980, Heteromorph ammonites from the Albian of South Australia: Royal Society of South Australia, Transactions, v. 104, p. 145-159.

McWhae, J. R. H., Playford, P. E., Lindner, A. W., Glenister, B. F., and Balme, B. E., 1958, The stratigraphy of Western Auatralia: Journal of Geological Society of Australia, v. 4, p. 1-161.

Menegatti, A. P., Weissert, H., Brown, R. S., Tyson, R. V., Farrimond, P., Strasser, A., and Caron, M., 1998, High –resolution d13C stratigraphy through the Aptian "Livello Selli" of the Alpine Tethys: Paleoceanography, v. 13, p. 530-545.

Milliman, J. D., 1974, Marine Carbonates, in Springer, ed., Recent Sedimentary Carbonates, 1: Berlin, 375 p.

Moore, C., 1870, Australian Mesozoic geology and palaeontology: Quarterly Journal of the Geological Society of London, v. 26, p. 226-261, pl. 10-18.

Morgan, R., 1980, Palynostratigraphy of the Australian Early and Middle Cretaceous: Memoirs of the Geological Survey of New South Wales, v. Palaeontology 18, p. 153.

Morrison, J. O., and Brand, U., 1986, Geochemistry of recent marine invertebrates: Geoscience Canada, v. 13, p. 237-254.

Mory, A. J., and Dixon, M., 2002, GSWA Boologooro 1 well completion report (basic data), Gascoyne Platform, Southern Carnarvon Basin, Western Australia, 7: Perth, Geological Survey of Western Australia.

Mory, A. J., Yasin, A. R., and Backhouse, J., 1999, GSWA Barrabiddy 1 and 1a well completion report, Wandagee Ridge, Southern Carnarvon Basin, Western Australia, 3: Perth, Geological Survey of Western Australia.

Mutterlose, J., 1992, Lower Cretaceous nannofossil biostratigraphy off north-western Australia (Leg 123): Proceedings of the Ocean Drilling Program, Scientific Results, v. 123, p. 343-368.

Naydin, D. P., Teys, R. V., and Zadorozhnyy, I. K., 1966, Isotopic paleotemperatures of the Upper Cretaceous in the Russian Platform and other parts of the USSR: Geochemistry International, v. 3, p. 1038-1051.

Ogg, J. G., Agterberg, F. P., and Gradstein, F. M., 2004, The Cretaceous Period, in Gradstein, F. M., Ogg, J. G., and Smith, A., eds., A Geologic Time Scale, 19: Cambridge, Cambridge University Press, p. 344-383.

Oosting, A., 2004, Palaeoenvironmental and climatic changes in Australia during the Early Cretaceous: Unpub. PhD thesis, Utrecht University, 206 p.

Oosting, A., Leereveld, H., Dickens, G. R., Henderson, R. A., and Brinkhuis, H., in press., Correlation of Barremian-Aptian (mid-Cretaceous) dinoflagellate cyst assemblages between the Tethyan and Austral realms: Cretaceous Research, v. in press, p. 1-22.

Palfreyman, W. D., 1984, Guide to the geology of Australia, Geology and Geophysics Bulletin, 181, Bureau of Mineral Resources, 111 p.

Palmer, M. R., and Elderfield, H., 1985, Sr isotope composition of sea-water over the past 75 Myr: Nature, v. 314, p. 526-528.

Pangani, M., and Arthur, M. A., 1998, Stable isotopic studies of Cenomanian-Turonian proximal marina fauna from the U. S. Western Interior Seaway, in Dean, W. E., and Arthur, M. A., eds., Stratigraphy and paleoenvironment of the Cretaceous Western interior Seaway, U. S. A., 6, Society of Economic Paleontologists and Mineralogists (SEPM), Concepts of Sedimentology and Paleontology, p. 201-225.

Parrish, J. T., 1995, Palaeoceanography of C_{org}-rich rocks and the preservation versus production controversy, in Huc, A. –Y., ed., Palaeogeography and palaeoclimate and Source Rocks, 40, American Association of Petroleum Geologists, Studies in Geology, p. 1-20.

Parrish, J. T., and Curtis, T., 1982, Atmospheric circulation, up-welling and organic-rich rocks in the Mesozoic and Cenomanian eras: Palaeogeography, Palaeoclimatology, Palaeoecology, v. 40.

Parrish, J. T., and Spicer, R. A., 1988, Late Cretaceous terrestrial vegetation: a near-polar temperature curve: Geology, v. 16, p. 22-25.

Phillips, J., 1870, Australian belemnites, in Moore, C., ed., Australian Mesozoic geology and paleontology, 26, Quarterly Journal of the Geological Society of London, p. 226-261.

Pickard, and Emery, 1982, Descriptive Physical Oceanography: an introduction: New York, Pergamen Press.

Pirrie, D., Doyle, P., Marshall, J. D., and Ellis, G., 1995, Cool Cretaceous climates - new data from the Albian of Western Australia: Journal of the Geological Society London, v. 152, 139-142.

Pirrie, D., and Marshall, J. D., 1990a, Diagenesis of Inoceramus and late Cretaceous palaeoenvironmental geochemistry: a case study from James Ross Island, Antarctica: Palaios, v. 5, p. 336-45.

Pirrie, D., and Marshall, J. D., 1990b, High paleolatiude Late Cretaceous paleotemperatures; new data from James Ross Island, Antarctica: Geology, v. 18, p. 31-34.

Pirrie, D., Marshall, J. D., Doyle, P., and Riccardi, A. C., 2004, Cool early Albian climates; new data from Argentina: Cretaceous Research, v. 25, p. 27-33.

Playford, G., Haig, D. W., and Dettmann, M., 1975, A mid-Cretaceous microfossil assemblage from the Great Artesian Basin, north-western Queensland: Neues Jahrbuch fur Geologie und Palaontologie, Abhandlungen, v. 149, p. 333-362.

Podlaha, O. G., Mutterlose, J., and Veizer, J., 1998, Preservation of d18O and d13C in Belemnite Rostra from the Jurassic/Early Cretaceous Successions: American Journal of Science, v. 298, p. 324-347.

Poulsen, C. J., Barron, E. J., Arthur, M. A., and Peterson, W. H., 2001, Response to the mid-Cretaceous global oceanic circulation to tectonic and CO_2 forcings: Paleoceanography, v. 16, p. 1-17.

Price, G. D., and Grocke, D. R., 2002, Strontium-isotope stratigraphy and oxygen- and carbon-isotope variation during the Middle Jurassic-Early Cretaceous of the Falkland Plateau, South Atlantic: Palaeogeography, Palaeoclimatology, Palaeoecology, v. 183, p. 209-222.

Price, G. D., Ruffell, A. H., Jones, C. E., Kalin, R. M., and Mutterlose, J., 2000, Isotopic evidence for temperature variation during the early Cretaceous (late Ryazanian-mid Hauterivian): Journal of Geological Society of London, v. 157, p. 335-344.

Reyment, R. A., 1964, Albian Ammonites from Fossil Creek, Oodnadatta, South Australia: Transcripts of the Royal Society of South Australia, v. 88, p. 21-36, pls. 1-5, text figs. 1-9.

Reyment, R. A., 1980, Biogeography of the Saharan Cretaceous and Paleocene epicontinental transgressions: Cretaceous Research, v. 1, p. 299-327.

Rich, T. H. V., and Rich, P. V., 1988, Polar dinosaurs and biotas of the early Cretaceous of southeastern Australia: National Geographic Reserve, v. 5, p. 15-53.

Richter, F. M., and DePaolo, D. J., 1988, Diagenesis and Sr isotopic evolution of seawater using data from DSDP 590B and 575: Earth and Planetary Science Letters, v. 90, p. 382-394.

Ruddiman, W. F., 2001, Earth's Climate: Past and Future: Freeman, p. 242-253.

Ryan, W. B. F., Cita., M. B., 1977, Ignorance concerning episodes of ocean wide stagnation: Marine Geology, v. 23, p. 197-215.

Saelen, G., and Karstang, T. V., 1989, Chemical signatures in belemnites: Geologica et Palaeontologica, v. 177, p. 333-346.

Saelen, G., Doyle, P., and Talbot, M. R., 1996, Stable-isotope analyses of belemnite rostra from Whitby Mudstone Fm., England: surface water conditions during deposition of a marine black shale: Palaios, v. 11, p. 97-117.

Schettino, A., and Scotese, C. R., 2005, Apparent polar wander paths for the major continents (200 Ma to the present day); a palaeomagnetic reference frame for global plate tectonic reconstructions: Geophysical Journal International, v. 163, p. 727-759.

Schlanger, S. O., Arthur, M. A., Jenkyns, H. C., and Scholle, P. A., 1987, The Cenomanian-Turonian oceanic anoxic event, in Brooks, J., and Fleet, A. J., eds., Marine Petroleum Source Rocks, I. Stratigraphy and distribution of organic-rich beds and the marine δ13C excursion: London, Geological Society, Special Publication 26, p. 371-399.

Schlanger, S. O., and Cita, M. B., 1982, Nature and Origin of Cretaceous carbon-rich facies: Academic, 229 p.

Schlanger, S. O., and Jenkyns, H. C., 1976, Cretaceous anoxic events: Causes and consequences: Geologie en Mijnbouw, v. 55, p. 179-184.

Schlanger, S. O., Jenkyns, H. C., and Premoli Silva, I., 1981, Volcanism and vertical tectonics in the Pacific basin related to global Cretaceous transgressions: Earth and Planetary Science Letters, v. 52, p. 435-449.

Scholle, P. A., and Arthur, 1980, Carbon isotope fluctuations in the Cretaceous pelagic limestones: Potential stratigraphic and petroleum exploration tool: American Association of Petroleum Geologists Bulletin, v. 64, p. 67-87.

Senior, B. R., Mond, A., and Harrison, P. L., 1978, Geology of the Eromanga Basin: Bulletin of the Australian Bureau of Mineral Resources Geology and Geophysics, v. 167, 183 p.

Shackleton, N. J., and Kennett, J. P., 1975, Palaeotemperature history of the Cenozoic and the initiation of Antarctic glaciation: oxygen and carbon isotope analysis in DSDP sites 277-279, and 281: Initial Reports of the Deep Sea Drilling Project, v. 29, p. 743-755.

Shafik, S., 1985, Calcareous nannofossils from the Toolebuc Formation, Eromanga Basin, Australia: Bulletin Bureau of Mineral Resources Journal of Australian Geology and Geophysics, v. 9, p. 171-181.

Shafik, S., 1990, Late Cretaceous nannofossil biostratigraphy of the Australian western margin, Bulletin Bureau of Mineral Resources of Geology and Geophysics, 295, p. 164.

Shafik, S., 1994, Significance of calcareous nannofossil-bearing Jurassic and Cretaceous sediments on the Rowley Terrace, offshore northwest Australia: AGSO Journal of Australian Geology & Geophysics, v. 15, p. 71-88.

Sheard, M. J., 1990, Glendonites from the southern Eromanga Basin in South Australia: palaeoclimatic indicators for Cretaceous ice: Geological Survey of South Australia Quarterly Geological Notes, v. 114, p. 17-23.

Sissingh, W., 1978, Microfossil biostratigraphy and stage-stratotypes of the Cretaceous: Geologie en Mijinbouw, v. 57, p. 433-440.

Skwarko, S. K., 1966, Cretaceous stratigraphy and palaeontology of the Northern Territory: Bureau of Mineral Resources Geology and Geophysics Bulletin, v. 73, p. 135.

Skwarko, S. K., 1983, Cenomanian (Late Cretaceous) mollusca from Mount Norris Bay, Arnhem Land, northern Australia: Bureau of Mineral Resources Geology and Geophysics Bulletin, v. 217, p. 73-83.

Smart, J., and Senior, B. R., 1980, Jurassic-Cretaceous Basins of Northeastern Australia, in Henderson, R. A., and Stephenson, P. J., eds., The Geology and Geophysics of Northeastern Australia: Brisbane, Geological Society of Australia, Queensland Division, p. 315-328.

Spath, L. F., 1925, On upper Albian Ammonoidea from Portuguese East Africa, with an appendix on Upper Cretaceous ammonites from Maputoland: Ann. Transv. Mus, v. 11, p. 179-200.

Spaeth, C., Hoefs, J., and Vetter, U., 1971, Some aspects of isotopic composition of belemnites and related palaeotemperatures: Geological Society of American Bulletin, v. 82, p. 3139-3150.

Spicer, R. A., 1987, The significance of the Cretaceous flora of northern Alaska for the reconstruction of the climate of the Cretaceous: Geologisches Jahrbuch, v. A96, p. 265-291.

Spicer, R. A., and Corfield, R. M., 1992, A review of terrestrial and marine climates in the Cretaceous with implications for modelling the `Greenhouse Earth': Geology Magazine, v. 129, p. 169-180.

Spicer, R. A., and Parrish, J. T., 1986, Paleobotanical evidence for cool north polar climates in middle Cretaceous times (Albian-Cenomanian) time: Geology, v. 14, p. 703-706.

Stevens, G. R., 1965, The Jurassic and Cretaceous belemnites of the Indo-Pacific region, Palaeontological Bulletin of the Geological Survey of New Zealand, 36, p. 283.

Stevens, G. R., 1967, Upper Jurassic fossils from Ellsworth Land, West Antarctica, and notes on upper Jurassic biogeography of the South Pacific region: New Zealand Journal of Geology and Geophysics, v. 10, p. 345-393.

Stevens, G. R., 1973, Cretaceous belemnites, in Hallam, A., ed., Atlas of palaeobiogeography.: London, Elsevier, p. 385-401.

Stevens, G. R., and Clayton, R. N., 1971, Oxygen isotope studies on Jurassic and Cretaceous belemnites from New Zealand and their biogeographical significance: New Zealand Journal of Geology and Geophysics, v. 14, p. 829-897.

Stilwell, J. D., and Crampton, J. S., 2001, Unusual belemnite-inoceramid bivalve association from the Albian (Late Cretaceous) of Queensland, Australia: Alcheringa, v. 25, p. 391-394.

Stolley, E., 1911, Studien an den Belemniten der Unteren Kreide Norddeutschlands: Jber. Neidersachs. Geol. Ver., v. 4, p. 174-191, 211.

Swinnerton, H. H., 1955, A monograph of British Lower Cretaceous belemnites.

Tate, R., 1880, Description of a new species of belemnite from the Mesozoic strata of central Australia: Transactions and Proceedings of the Royal Society of South Australia, v. 3, p. 104-105.

Tate, R., 1889, The age of the Mesozoic rocks of the Lake Eyre Basin: Australasian Association for the Advancement of Science Report, v. 1, p. 228-230.

Taylor, B. A., and Haig, D. W., 2001, Barremian foraminifera from the Munderong Shale, oldest marine sequence in the Cretaceous of the Southern Carnarvon Basin, Western Australia: Micropalaeontology, v. 47, p. 125-143.

Tenison-Woods, J. E., 1883a, On some Mesozoic fossils from central Australia: Proceedings of the Linnean Society of New South Wales, v. 8, p. 235-242.

Tenison-Woods, J. E., 1883b, On some Mesozoic fossils from the Palmer River, Queensland: Journal and Proceedings of the Royal Society of New South Wales, v. 16, p. 147-154.

Thiede, J., and van Andel, T. H., 1977, The palaeoenvironment of anaerobic sediments in the late Mesozoic South Atlantic Ocean: Earth and Planetary Science Letterss, v. 33, p. 301-309.

Thierstein, H. R., 1976, Mesozoic calcareous nannoplankton biostratigraphy of marine sediments: Marine Micropalaeontology, v. 1, p. 325-362.

Thomas, E., Shackleton, N. J., and Hall, M. A., 1992, Carbon isotope stratigraphy of Paleogene bulk sediments, Hole 762C (Exmouth Plateau, eastern Indian Ocean), in von Rad, U., and Haq, B. U., eds., Proceedings of the Ocean Drilling Program, Scientific results, 122: College Station, Texas, p. 897-901.

Tourtelot, H. A., and Rye, R. O., 1969, Distributions of oxygen and carbon isotopes in fossils of Late Cretaceous age, western interior region of North America: Geological Society Of America Bulletin, v. 80, p. 1903-1922.

Tsikos, H., Jenkyns, H. C., Walsworth-Bell, B., Petrizzo, M. R., Forster, A., Kolonic, S., Erba, E., Premoli Silva, I., Baas, M., Wagner, T., and Sinninghe Damste, J.S., 2004, Carbon-isotope stratigraphy recorded by the Cenomanian-Turonian Oceanic Anoxic Event: correlations and implications based on three key-localities: Journal of Geological Society London, v. 161, p. 711-720.

Tyson, R. V., 1995, Sedimentary Organic Matter, in Chapman and Hall, eds., Organic Facies and Palynofacies: London, p. 615.

Urey, H. C., Lowenstam, H. A., Epstein, S., and McKinney, C. R., 1951, Measurement of palaeotemperatures and temperatures of the Upper Cretaceous of England, Denmark and the South-eastern United States: Bulletin of the Geological Society of America, v. 62, p. 399.

Vakrameev, V. A., 1978, The climates of the Northern Hemisphere in the Cretaceous in the light of palaeobotanical data: Palaeontology, v. 12, p. 143-154.

Vallance, H. B., and Packham, G. H., 1959, New South Wales: Lex. Stratigr. int., v. 6.

Veevers, J. J., 1984, Phanerozoic Earth history of Australia: Clarendon, Oxford, 418 p.

Veevers, J. J., 2000, Billion-year earth history of Australia and neighbours in Gondwana: Gemoc Press, 80 p.

Veevers, J. J., Powell, M. C., and Roots, S. R., 1991, Review of seafloor spreading around Australia. 1. Synthesis of the patterns of spreading: Australian Journal of Earth Science, v. 38, p. 373-389.

Veizer, J., 1989, Strontium isotopes in seawater through time: Annual Review of Earth Planetary Science, v. 17, p. 141-167.

Veizer, J., Ala, D., Azmy, K., Brunckschen, P., Buhl, D., Bruhn, F., Carden, G. A. F., Diener, A., Ebneth, S., Godderis, Y., Jasper, T., Korte, G., Pawellek, F., Podlaha, O. G., and Strauss, H., 1999, 87Sr/86Sr, $\delta^{13}C$ and $\delta^{18}O$ evolution of Phanerozoic seawater: Chemical Geology, v. 161, p. 59-88.

Veizer, J., and Compston, W., 1974, 87Sr/86Sr composition of seawater during the Phanerozoic: Geochemica et Cosmochimica Acta, v. 38, p. 1461-1484.

Venzo, S., 1936, Cefalopodi del Cretaceo medio-superiore dello Zululand: Palaeontographica italia, v. 36, p. 59-133.

Vine, R. R., and Day, R. A., 1965, Nomenclature of the Rolling Downs Group, Northern Eromanga Basin, Queensland: Queensland Government Mining Journal, v. 66, p. 416-421.

Vinogradov, A. P., 1968, Atlas of the Lithological-Palaeogeographic Maps of the USSR, Moscow, Triassic, Jurassic and Cretaceous, v. 3, 71 p.

Voigt, S., Wilmsen, M., Mortimore, R. N., and Voigt, T., 2003, Cenomanian palaeotemperatures derived from the oxygen isotopic composition of brachiopods and belemnites: evaluation of Cretaceous palaeotemperature proxies: International Journal of Earth Sciences, v. 92, p. 285-299.

Ward, P. D., 1979, The Natural History of Nautilus: Allen and Unwin, 267 p.

Wefer, G., and Berger, W. H., 1991, Isotope paleontology: Growth and composition of extant calcareous species: Marine Geology, v. 100, p. 207-248.

Whitehouse, F. W., 1924, Dimitobelidae. A new family of Cretaceous belemnites: Geological Magazine, v. 61, p. 410-416.

Whitehouse, F. W., 1925, On Rolling Downs fossils collected by Professor J. W. Gregory: Transactions of the Royal Society of South Australia, v. 49, p. 27-36.

Whitehouse, F. W., 1926, The Cretaceous Ammonoidea of Eastern Australia: Memoirs of the Queensland Museum, v. 8, p. 195-242, pl. 34-41.

Whitehouse, F. W., 1928, The correlation of the marine Cretaceous deposits of Australia: Australasian Association for the Advancement of Science Report, v. 18, p. 275-280.

Willey, L. E., 1972, Belemnites from south-eastern Alexander Island; I, The occurrence of the family Dimitobelidae in the lower Cretaceous: British Antarctic Survey Bulletin, v. 28, p. 29-42.

Wiseman, J. F., 1979, Neocomian eustatic changes-biostratigraphic evidence from the Carnarvon Basin: APEA Journal, v. 19, p. 66-73.

Wissler, L., Funk, H., and Weissert, H., 2003, Response of Early Cretaceous carbonate platformsto changes in atmospheric carbon dioxide levels: Palaeogeography, Palaeoclimatology, Palaeoecology, v. 200, p. 187-205.

Wissler, L. Weissert, H., Masse, J. –P., and Bulot, L., 2002, Chemostratigraphic correlation of Barremian and Lower Aptian ammonite zones and magnetic reversals: International Journal of Earth Sciences (Geologische Runschau), v. 91, p. 272-279.

Woods, H., 1917, The Cretaceous faunas of the north-eastern part of the south island of New Zealand: New Zealand Geological Survey Paleontological Bulletin, v. 4 (1).

Woods, J. T., 1961, Mesozoic and Cainozoic sediments of the Wrotham Park area: Publication - Geological Survey of Queensland, v. 304, p. 1-6.

Wright, C. W., 1963, Cretaceous ammonites from Bathurst Island, northern Australia: Palaeontology, v. 6, p. 597-614.

Wright, C. W., and Kennedy, W. J., 1987, The Ammonoidea of the Lower Chalk: Monographs of the Palaeontology Society of London, v. 2, p. 127-218.

Zittel, K. A. v., 1895, Grundzuge der Palaeontologie (Palaozoologie): Munich and Leipzig.

APPENDICES

Interval	Rock Type	Depth (m)	*Genus*	*Species*	Description
1.0-98.0 m	**Gearle Siltstone**				
		75.87	*Dimitobelus*	*hendersoni*	Same as at 76 m; cylindrical small, thin guard, apical canal centrally placed; symmetrical.
		76.00	*Dimitobelus*	*hendersoni*	Cylindrical small, thin guard, apical canal centrally placed; symmetrical.
		79.10	*Dimitobelus*	*diptychus*	Ventro-lateral furrows evident, lateral lines not clear, ventral surface slightly convex.
		79.45	*Dimitobelus*	*?*	Paired lateral lines evident; cylindrical, slender guard; cross-section round, apical canal slightly ventrally placed.
		80.00	*Dimitobelus*	*hendersoni*	Cylindrical stem region of guard; under microscope no lines or grooves evident.
		82.10	*Dimitobelus*	*stimulus(2), hendersoni(1), diptychus juvenile(2)*	New (1) cylindrical stem region of guard; diptychus juvenile (1), or introduction of new cenomanian diminutive species.
		82.35	*Dimitobelus*	*stimulus (1), diptychus (1), diptychus juvenile (2), ? (2)*	New (1) cylindrical, small guard; (2) diminuitive guard max diameter in apical region, apex pointed, tapering at alveolar region; tear drop shape.
		84.10	*Dimitobelus*	*stimulus(1), hendersoni (1), diptychus (2)*	Stimulus: larger specimen double lateral lines flattened ventral & dorsal surfaces; new (1): small, cylindrical symmentrical, spherical; new (2) dimnuitive guard, juvenile diptychus (??) in shape, ventro-lateral lines prominent and extend the length of guard or join up with lateral lines.
		86.47	*Dimitobelus*	*?*	Diminuitive *dimitobelus* same as at 82.35 and 96.90 m.
		89.50	*Dimitobelus*	*liversidgei ?*	Cigar shaped small guard; no visible lines/grooves.
		90.00	*Dimitobelus*	*stimulus*	Double lateral lines evident; elliptical cross-section, central apical canal; ventral surface slightly flattened.
		91.50	*Dimitobelus*	*?*	Cylindrical small, thin guard, apical canal centrally placed; symmetrical; 2 grooves shallowly run length of guard. Very cylindrical in stem region.
		94.45	*Dimitobelus*	*stimulus*	Slender guard lateral lines well developed.
		94.50	*Dimitobelus*	*diptychus (2)*	Alveolar region; attentuated apex, ellpitical in cross-section; slightly inflated guard.
		94.60			New (1) cylindrical species, diminuitive guard.
		95.75	*Dimitobelus*	*diptychus*	Apical region paired lateral lines slightly convex ventral surface, elliptical slightly depressed cross-section.
		96.12	*Dimitobelus*	*stimulus*	2 whole specimens.
		96.20	*Dimitobelus*		Attenuated apex, cigar shaped guard, hastate, apical canal ventrally placed, elliptical cross-section.
		96.22	*Dimitobelus*	*?*	2 ventro lateral grooves evident; cylindrical guard; cross-section slightly elliptical;ventral surface slighlty flattened; apical canal slightly ventrally placed; small in stature.
		96.30	*Dimitobelus*	*stimulus (2)*	stimulus: alveolar region, slender and cylinderical, round cross-section, faint lateral lines.
		96.70	*Dimitobelus*	*hendersoni*	No lines/grooves evident; cylindrical guard, apical region highly attentuated; larger form as at 91.5 m.

Interval	Rock Type	Depth (m)	*Genus*	*Species*	Description
		96.90	*D. hendersoni (3), Dimitobelus (1), D. liversidgei(?)*		(1) Cylindrical form; (2) diminuitive form as at 82.35 m.
98.0-145.0 m	**Windalia Radiolarite**				
		123.05			Not enough sample.
		130.30	*Peratobelus*	*australis*	
		136.30			Not enough sample.
		136.90	*Peratobelus*	*australis*	Cross-section circular-semi elliptical, apical canal ventrally placed; one specimen not enough to be identifiable.
		138.45	*Peratobelus?*	*australis?*	Very faint ventral groove, if one at all - unidentifiable.
		139.00	*Peratobelus*	*australis*	
		141.30			Not enough sample alveolar region only; small phragmocone.
		144.00	*Peratobelus*	*? australis*	Cross-section circular-semi elliptical, apical canal ventrally placed.
		144.10	*Peratobelus*		
		144.55	*Peratobelus*	*australis*	
		144.70	*Peratobelus*	*australis*	
145.0-190.5 m	**Munderong Shale**				
		150.75	*Peratobelus*		

Interval	Rock Type	Depth (m)	*Genus*	*Species*	Description
0-32 m	**Alluvium**				
32-? M	**Trealla Limestone**				
?-82.1 m	**Korojon Calcarenite**				
82.1-280.2 m	**Toolonga Calcilutite**				
280.2-283.3 m	**Unnamed Turonium unit**				
283.3-347.1 m	**Upper Gearle Siltstone**				
		289.00	*Dimitobelus*	sp. nov. ? *1*	Diminuitive, slender cylindrical guard, no markings visable, highly acute apex, juvenile.
		293.10	*Dimitobelus*	*?*	Double lateral lines faint (?). Specimen in pieces cannot by identify at species level.
		294.40	*Dimitobelus*	sp. nov. ? *1*	Ventral groove that extends the base of phragmocone. Dorsal furrows evident and broad extend mid stem. Ventral surface excessively flattened to a concave extent. Cross-section almost square; laterally guard is arched.
		297.95			No visible markings, cylindrical, apical canal slightly ventrally positioned. Stem region viewed.
		298.65	*Dimitobelus*	*stimulus*	Juvenile, flattened venter and dorsal, eccentric cross-section in alveolus and apical regions, more cylindrical in mid stem.
		"	*Dimitobelus*	*diptychus*	Juvenile, pinched alveolus, lateral lines, depressed ventral
		299.9			Too fragmentary to identify.
		300.47	*Dimitobelus*		Diminuitive guard, slight tapering towards alveolar region; faintly impressed lateral lines could be paired. Acute apex. Cross-section shows ventral grooves; almost centrally place apical canal.Ventral surface appears slightly flattened in contrast to dorsal. *diptychus* juvenile????
		300.7	*Dimitobelus*		Double lateral lines faint, cylindrical, cross-section, slightly elliptical, central canal. Specimen in pieces not cannot identified at species level. Possibly *stimulus.*
		301.55	*Dimitobelus*		Slender cylindrical, paired lateral lines.
		"	*Dimitobelus*	*diptychus*	Juvenile, double lateral lines, pinched alveolus acute apex, flattened venter. Specimen has pits gauged out of outer layer of guard.
		302.26	*Dimitobelus*	*stimulus*	(1) Adult, medium guard, extremely flattened dorsal and ventral surfaces, acute drawn out apex, paired lateral lines evident.(1) Juvenile sample not as flattened, still quite cylindrical and symmetrical.
		303.25	*Dimitobelus*	*stimulus*	Paired lateral lines from alveolus to apex. Slightly flattened ventro-dorso surfaces. Slight pinching in alveolar region. Apex absent.
		305.15	*Dimitobelus*	*hendersoni*	Paired lateral lines, elliptical cross-section. Same as at 339.14 and 345.35 m.
		306.15	*n/a*		Not enough sample - unidentifiable.
		307.65	*Dimitobelus*	*diptychus*	Ventrolateral furrows, max transverse diameter mid-stem, apical region, slightly flattened ventral surface.

Interval	Rock Type	Depth (m)	*Genus*	*Species*	Description
		308.30			Cylindrical, slender, diminutive guard, no markings evident, apical canal central.
		308.8	*Dimitobelus*	*stimulus*	Badly preserved specimen, double lateral lines, flattened ventral and dorsal, canal slightly ventrally placed.
		310.7			Not enough sample - unidentifiable.
		311.6	*Dimitobelus*	*diptychus*	Slender, small, cylindrical guard. Markings faint if visable at all. Highly acute, pointed apex, apical canal ventrally placed, slightly flattened ventral and dorsal surfaces.
		326.6			Not enough sample - unidentifiable.
		330.70	*Dimitobelus*		Paired lateral lines, cylindrical slender, small guard, apical canal centrally placed. Same as 339.14 m.
		337.50			Small guard, oval in cross-section, flattened ventral and dorsal, centrally placed apical canal, ventral grooves, no lateral lines evident, may be faint. No apical region viewed.
		339.14	*Dimitobelus*	*hendersoni*	Stem region only viewed, paired lateral lines evident, slender guard,cylindrical but slightly flattened ventrally and dorsally, centrally placed apical canal.
		339.25	*Dimitobelus*	*hendersoni*	Lateral lines paried attenuated apex signs of a pinched alveolus, intermediate age.
		339.30	*Dimitobelus*	*diptychus*	Dimiuitive guard; apex acute and constricted; paired lateral lines to apex.elliptical cross-section, flattened ventral and dorsal surfaces, apical canal central; alveolus pinched.
		339.65			Alveolar region only, not enough to identify. Cylindrical small guard, no visible markings.
		345.35	*Dimitobelus*	*hendersoni*	Paired lateral lines, elliptical cross-section. Same as at 339.14 and 300.14 m.
		346.50			Not enough to identify. No evident markings externally.
		346.7	*Dimitobelus*	*stimulus*	Cylindrical, slender, diminutive guard, double lateral lines evident, apical canal central.
		346.90			Slender, small, cylindrical guard, stem region only viewed. No markings evident.
347.1-378.0 m	**Lower Gearle Siltstone**				
		347.4	*Dimitobelus*		Slender small guard, cylindrical, apical centered, double lateral lines clear, not grooves though.
		348.42	*Dimitobelus*	*hendersoni*	Slender, cylindrical guard. No markings evident. Acute apex.
		348.9	*Dimitobelus*	*stimulus*	Slender, cylindrical guard. No markings evident. Only stem region viewed.
		350.65	*Dimitobelus*	*stimulus*	Slender small guard, cylindrical, apical centered, double lateral lines clear, not grooves though.
		350.1	*Dimitobelus*	*diptychus; hendersoni*	medium sized alveolus and stem regions; ventro-lateral lines evident. Also lots of slender cylindrical fragments.
		351.42	*Dimitobelus*	*hendersoni*	Slender cylindrical guard, no markings evident, ventral and dorsal surfaces flattened, apical canal slightly ventrally placed.
		352.2	*Dimitobelus*	*stimulus*	Faint lateral lines, thin slender small guard, pointed this apex. Same as 360.2 m.
		352.4	*Dimitobelus*		Guard small, acute and constricted apex, rounded guard, paired lateral lines evident, apical canal slightly ventrally placed, cross-section elliptical.
		352.4	*Dimitobelus*	*hendersoni*	Lateral lines paired; cigar shape guard, attenuated apex.
		"	*Dimitobelus*	*stimulus ?*	Fragments of guard, cylindrical and slightly off centre canal.
		352.75			No visible markings externally, cylindrical xsection, central apical canal. Not enough to identify.
		352.95	*Dimitobelus*	*hendersoni*	Slender, cylindrical, dimiuitive guard, no markings evident. Canal central.

Interval	Rock Type	Depth (m)	*Genus*	*Species*	Description
		352.95	*Dimitobelus*	*hendersoni*	Fragments of *diptychus and stimulus* , lateral lines evident but ventro-dorso lateral not so clear.
		357.00			Same as at 346.9 m. Slender, small cylindrical guard. No markings evident.
		357.98			Not enough to identify.
		358.15	*Dimitobelus*	*stimulus ?*	Not enough to identify; slender small guard, central apical canal, faint double lateral lines.
		359.9	*Dimitobelus*	*hendersoni*	Clindrical guard, atentuated apex, central canal.
		360.2	*Dimitobelus*	*diptychus*	Attentuated apex, eccentric cross-section, central canal, sligthly flattened ventral surface *juvenile.*
		"	*Dimitobelus*	*stimulus ?*	Cylindrical, slender, centrally placed canal, paired lateral lines to alveolar region.
		360.55	*Dimitobelus*	*stimulus ?*	Cylindrical, slender guards; no markings evident, shape resembles *stimulus* .
		361.05	*Dimitobelus*	*stimulus ?*	Cylindrical, slender, centrally placed canal, paired lateral lines faint.
				hendersoni	
		"			Attentuated apex, eccentric cross-section, canal ventrally placed, flattened ventral/dorsal surface; not markings evident; juvenile.
		361.35	*new*		Diminuitive cylindrical guard, highly acute apical region. No evident lines/grooves.
		361.4	*Dimitobelus*		Faint lateral lines, thin slender small guard, pointed this apex. Same as 360.2 m.
		362.16	*Dimitobelus*	*diptychus*	Medium guard, alveolar region missing, ventral grooves evident, faintly impressed paired lateral lines which extend from ventral grooves moving dorsally towards apex. Flattened ventral surface.
		"	*Dimitobelus*	*stimulus*	Flattened venter and dorsal, double lateral lines.
		"	*Dimitobelus*	*stimulus*	(3) apical regions acutely pointed, vnetral and dorsal slightly flattened.slightly ventrally placed canal.
		365.63	*Dimitobelus*	*stimulus*	(2) flattened ventral and dorsal surface. Cross-section elliptical, apical canal centrally placed; welll incised paired lateral lines evident. Slender guard.
		"			Highly acute apex, very pointed; conical slender guard; no markings. Apical canal central.
		"	*Dimitobelus*	*stimulus*	Juvenile stimulus, paried lateral lines in stem and apex well incised, faint in alveolar region. Apical canal central. Ventral and dorsal surfaces slightly flattened.
		367.39			Slender small guard, cylindrical, apical centered, no markings evident.
		374	*Dimitobelus*	*stimulus*	Paired lateral lines, cental apical canal, slender guard.
		375.4	*Dimitobelus*	*stimulus ?*	Paired lateral lines, cental apical canal, slender guard.
		377.18	*Dimitobelus*		Paired lateral lines evident, one well incised ventral furrow which terminates at stem region. Large deep phragmocone area! No idea!! Similar to Lower Alinga sample from Alinga pt.
		377.65	*Peratobelus*	*australis*	Juvenile diminuitive specimen. Ventral groove crurve and to just before apex.
		"	*Peratobelus*		Medium sized specimen, goorve to mid stem, attenuated apex, cross-section elliptical, ventrally placed apical canal.
		"	*Peratobelus*		Dorso lateral furrow, diminutive guard, attenuated apex. Cross-section rounded canal ventrally arched.
		377.97			Attentuated apical region, not enough to identify.

Interval	Rock Type	Depth (m)	*Genus*	*Species*	Description
378.0-?400 m	**Windalia Radiolarite**				
		378.42	*Peratobelus*		Apical line ventrally skewed; slender, long, guard, well indented ventral grooves in alveolar region.
		379.30	*Peratobelus*		Seemingly large phragmocone, but not a lot of specimen to identify, in situ.
		380.47			In situ cannot identify, cylindrical in cross-section.
		382.7			Slender, cylindrical, central canal, no distinguishable markings evident; outer surface consolidated.
400?-419 m	**Muderong Shale**				
419-428 m	**Birdrong Sandstone**				

Interval	Rock Type	Depth (m)	*Genus*	*Species*	Description
0.0-39.5 m	**Alluvium**				
39.5-238.1 m	**Toolonga Calcilutite**				
238.1-245.8 m	**Unnamed Turonian Unit**				
245.8-255.0 m	**Upper Gerale Siltstone**	245.9	*Dimitobelus*	sp. nov. ? *1*	Ventral groove that extends the base of phragmocone. Dorsal furrows evident and broad extend mid stem. Ventral surface excessively flattened to a concave extent. Cross-section almost square; laterally guard is arched.
		247.70	*Dimitobelus*	*diptychus*	Juvenile, convex ventral surface flattened dorsal; ventral lateral furrows evident; pinched in the alveolar region; double lateral lines to apex; slightly obtuse in apical region.
		249.33	*Dimitobelus*	*ditpychus*	Identified from apex only.
		249.80	*Microbelus*	*haigi*	Slender diminuitive cylindrical specimen, drawn out attenuated apex. Smaller specimen of 251.75 and 251.57 m.
		251.00	*Dimitobelus*	*diptychus*	Identified from alveolar only. Also with this specimen were cylindrical pieces of belemnite guard, too smaller fragments to identify, but most likely new species of cylindrical diminuitive belemnite as from 256.8 m.
		251.07	*Microbelus*	*haigi*	Diminutive guard, ventral surface flattened, ventral grooves run entire length of guard; obtuse apex, tapered alveolar reion, point of maximum inflection close to point of termination at apex.
		251.15	*Dimitobelus*	*ditpychus*	Maybe the beginnings of ventro-lateral grooves in alveolar region; iron staining on outside of guard; 2nd specimen shows double lateral lines length of guard, no ventro grooves tho, but does taper in alveolar region.
		251.57	*Microbelus*	*haigi*	Juvenile specimen, very diminuitve in size! Grooves evident!
		"	*Dimitobelus*	*?*	Slender guard attentuated apex, diptychus maybe, paired lateral lines evident same as 251.75 m.
		251.75	*Dimitobelus*	*diptychus*	Juvenile specimen, paired lateral lines, ventro lateral grooves not well indented in juvenile specimen. Attenuated apex, pinched alveolar region, Dvmax stem reion near apex. Same as 253.27 m.
		"	*Dimitobelus*		Long slender diminuitive cylindrical specimen.
		"	*Microbelus*	*haigi*	(2) same shape as juvenile diptychus in this stratum, but diminuitive, and not lateral lines. Only well inscribed ventral groove from alveolar to apex, with flattened ventral surface and slightly rounded dorsal.
		"	*Dimitobelus*	*?*	No grooves evident, or lateral lines, slender accenuated apex, drawn out, small stem region, small guard, max diameter mid way.elliptical in cross-section. Same as 251.57 m.
		251.87	*Dimitobelus*		Elliptical in cross-section apical canal central; outer shell of guard under gone diagenesis, cannot see grooves/lines ets.
		252.25	*Microbelus*	*?*	Diminuitive specimen, convex dorsal, flattened ventral surface; ventral grooves in alveolar region deflect minorly to meet lateral lines (do not appear to be paired) which run from alveolus to apex, Point of maximum inflation is centre stem region.

Interval	Rock Type	Depth (m)	*Genus*	*Species*	Description
		253.27	*Dimitobelus*	*diptychus*	Ventro lateral grooves evident, ventral surface falttened dorsal slightly convex.
		"	*Dimitobelus*	*diptychus ?*	Venter convex, dorso slightly less so, lateral sides convex; rounded, point of maximum inflation in lower region of stem near attenuated apex, alveolar region pinched and flattened; ventro-lateral grooves in alveolar region; apicanal central. Similar to juvenile diptychus of 251.75 m.
		"	*Dimitobelus*	*?*	Attenuated apical region, cylindrical, slender guard.
		253.65	*Dimitobelus*	*diptychus*	Alveolar region narrow, with stem widening in mid flank region. Cross-section semi elliptical with depressions.
255.0-266.0 m	**Lower Gerale Siltstone**				
		256.39	*Dimitobelus*	*diptychus ?*	Cross-section same as diptychus. Ventro lateral grooves in alveolar region, attentuated apex, flattened alveolar regions, cross-section elliptical.
		256.80	*Dimitobelus*	*stimulus ?*	Cylindrical, slender diminuitive guard; paired lateral lines evident in alveolar region.
		256.90	*Dimitobelus*	*?*	diminuitive guard; highly attenuated and constricted apex, with Dv_{max} in apical region of stem; lateral furrows in alveolar region extend entire length of guard to apex as lateral line on either side of specimen; ventral ? surface inflated and dorsal ? surface extremely flattened. *Microbelus* due to lateral lines extending entire length of specimen, although does resemble juvenuile *diptychus* .
		259.60	*Dimitobelus*	*hendersoni?*	(1) cylindrical, slender diminuitive guard; apical region only same; (1) slender guard, attenuated apex, outer shell abraded thus no markings evident; maybe same as 266.75 m.
		260.30	*Dimitobelus*	*?*	Small guard; highly attenuated apex, lateral lines evident, flattened dorsal surface, slghtly convex ventral; cross-section ellptical and depressed; apical canal dorsally placed. Like diptychus but too attuated in apex region. Same as at 256.9 m.
		264.85			Badly preserved sample.
		265.90	*Dimitobelus*	*?*	Not enough sample to identify at species level.
266.0-296.7 m	**Windalia Radiolarite**				
		266.75	*Dimitobelus*	*hendersoni ?*	Cylindrical specimens, small-medium, no external markings evident on guard, phragmocone small, attenuated apex; maybe same as 259.6 m.
		268.4			in situ specimen, x section at alveolar end circular
		274.85	*Peratobelus*	*australis*	Small portion of stem region id'd from well indented grooves and small stature of guard.
		278.6	*Peratobelus*	*australis*	Identified from stem, grooves arching towards dorsal surface, small guard; in situ: small phragmocone in relation to guard; not well preserved to identify from in situ.
		280.85	*Peratobelus*		(2) juveniles, dorsal furrow in stem region accompanied by well inscribed ventral grooves.
		281.3			In situ specimen, medium size guard.
		282.3	*Peratobelus*	*australis*	In situ specimen, looks cylindrical , long & slender, cross-section elliptical at apex, apical canal off centre; phragmocone infilled; ventral grooves only extend half way along stem, appear straight, then curve dorsally.

Interval	Rock Type	Depth (m)	*Genus*	*Species*	Description
		283.74	*Peratobelus*	*australis*	Ventral grooves prominent, terminating in apical region; acute apex; small-medim guard.
296.7-309.5 m	**Munderong Shale**				
309.5-311.9 m	**Birdrong Sandstone**				

Interval	Rock Type	Depth (m)	*Genus*	*Species*	Description
0-38.7 m	**Alluvium**				
38.7-52.3 m	**Lower Gearle Siltstone**				
		46.15			Intensely broken up - unidentifiable.
		50.55	*Dimitobelus*	*stimulus ?*	In situ, white hard cement; double lateral lines mould in rock. Perfectly elliptical in cross-section, apical canal centrally placed and well developed.
52.3-74.2 m	**Windalia Radiolarite**				
		53.09	*Peratobelus*		Acute apex, elliptical, ventrally place apical canal.
		53.11	*Peratobelus*		Ventrally curved apical line; elliptical and flattened cross-section.
		53.20			Diminuitive no markings evident, cylindrical guard, pinched alveolar section; acute, could be juvenile diptychus??
		54.39	*Peratobelus*	*australis*	Subcentral apical line,cross-section cylindrical; well developed straight in alveolar grooves.
		54.70	*Peratobelus*	*australis*	Slender, small, guard, incised grooves terminate in apical region, after turning dorsally.
		56.59	*Peratobelus*		Cross-section, ventrally placed apical line.
		57.30	*Peratobelus*		Apical line curved, semi-acute apex.
		57.46	*Peratobelus*	*australis*	In situ, cross-section 2 specimens.
		59.03	*Peratobelus*	*australis*	
		66.15	*Peratobelus*	*australis*	2 specimens; 1 unidentifiable.
74.2-81.7 m	**Muderong Shale**				

Sample No	Lab No	Well	Formation	Depth (m)	ZBias	$^{84}Sr/^{86}Sr$	Error %sem	$^{84}Sr/^{88}Sr$	Error %sem	$^{87}Sr/^{86}Srm$	Error %sem	$^{87}Sr/^{86}Srm$ N = 0.710249	$^{84}Sr/^{88}Sr$ 0.710235	ΔSW 0.709168	$^{87}Sr/^{86}Srm$ 0.710248
B1	TW-03-2	Boologooro 1	Upper Gearle Siltstone	293.10	99	0.0565273	3.16553E-06	0.0067494	3.77966E-07	0.7074355	3.53707E-06	0.707414	0.707399772	-176.8228231	0.707413
B1	TW-03-2RLG	Boologooro 1	Upper Gearle Siltstone	293.10	61	0.0565249	3.27844E-06	0.0067491	3.91448E-07	0.7074287	4.24444E-06	0.707407	0.707392972	-177.5027888	0.707406
B2	TW-03-4	Boologooro 1	Upper Gearle Siltstone	297.95	72	0.0565143	3.05177E-06	0.0067478	3.64381E-07	0.7074162	3.53697E-06	0.707394	0.707380473	-178.7527257	0.707393
B2	TW-03-4R	Boologooro 1	Upper Gearle Siltstone	297.95	68	0.0565263	3.27853E-06	0.0067492	3.91454E-07	0.707442	3.5371E-06	0.707420	0.707406271	-176.172856	0.707419
B3	TW-03-9	Boologooro 1	Upper Gearle Siltstone	301.55	64	0.0565233	3.50444E-06	0.0067489	4.18432E-07	0.7074208	3.537E-06	0.707399	0.707385073	-178.2927489	0.707398
B3	TW-03-9R	Boologooro 1	Upper Gearle Siltstone	301.55	73	0.0565299	3.39179E-06	0.0067497	4.04982E-07	0.7074373	3.53708E-06	0.707416	0.707401572	-176.6428322	0.707415
B4	TW-03-12	Boologooro 1	Upper Gearle Siltstone	305.15	62	0.0565305	3.05265E-06	0.0067497	3.64484E-07	0.7074468	3.53713E-06	0.707425	0.707411071	-175.6928802	0.707424
B4	TW-03-12	Boologooro 1	Upper Gearle Siltstone	305.15	62	0.0565305	3.05265E-06	0.0067497	3.64484E-07	0.7074468	3.53713E-06	0.707425	0.707411071	-175.6928802	0.707424
B4	TW-03-12 RRL	Boologooro 1	Upper Gearle Siltstone	305.15	52	0.0565282	4.4092E-06	0.0067495	5.26461E-07		3.53704E-06	0.707407	0.707393456	-177.4543988	0.707406
B4	TW-03-12 RRLR	Boologooro 1	Upper Gearle Siltstone	305.15	44	0.0565257	2.93934E-06	0.0067492	3.50958E-07		3.53695E-06	0.707390	0.707376156	-179.1843647	0.707389
B5	TW-03-16	Boologooro 1	Upper Gearle Siltstone	308.80	62	0.0565309	3.39185E-06	0.0067498	4.04988E-07	0.7074435	4.24453E-06	0.707422	0.707407771	-176.0228635	0.707421
B6	TW-03-18	Boologooro 1	Upper Gearle Siltstone	311.60	56	0.0565276	3.39166E-06	0.0067494	4.04964E-07	0.7074677	4.24468E-06	0.707446	0.70743197	-173.6029858	0.707445
B6	TW-03-18RR	Boologooro 1	Upper Gearle Siltstone	311.60	71	0.0565434	3.73186E-06	0.0067513	4.45586E-07		4.24465E-06	0.707441	0.707427155	-174.0844652	0.707440
B7	TW-03-19	Boologooro 1	Upper Gearle Siltstone	326.60	66	0.0565371	3.16608E-06	0.0067505	3.78028E-07	0.7074801	4.24475E-06	0.707458	0.70744437	-172.3630484	0.707457
B7	TW-03-19R	Boologooro 1	Upper Gearle Siltstone	326.60	68	0.0565403	5.88019E-06	0.0067509	7.02094E-07	0.7074875	7.07466E-06	0.707466	0.707451769	-171.6230858	0.707465
B8	TW-03-20	Boologooro 1	Upper Gearle Siltstone	330.70	64	0.0565273	3.39164E-06	0.0067494	4.04964E-07	0.707512	4.24494E-06	0.707490	0.707476268	-169.1732095	0.707489
B8	TW-03-20R	Boologooro 1	Upper Gearle Siltstone	330.70	72	0.0565296	3.84401E-06	0.0067496	4.58973E-07	0.7075016	4.24488E-06	0.707480	0.707465868	-170.213157	0.707479
B9	TW-03-22	Boologooro 1	Upper Gearle Siltstone	339.14	78	0.0565367	3.05298E-06	0.0067505	3.64527E-07	0.7074635	3.53721E-06	0.707442	0.70742777	-174.0229645	0.707441
B9	TW-03-22RR	Boologooro 1	Upper Gearle Siltstone	339.14	50	0.0565402	3.16625E-06	0.0067509	3.7805E-07		4.24472E-06	0.707454	0.707439555	-172.8444897	0.707453
B9	TW-03-22RR	Boologooro 1	Upper Gearle Siltstone	339.14	54	0.056537	3.27915E-06	0.0067505	3.91529E-07		4.24482E-06	0.707469	0.707455255	-171.2745206	0.707468
B10	TW-03-26	Boologooro 1	Upper Gearle Siltstone	345.35	75	0.0565244	3.39146E-06	0.006749	4.0494E-07	0.7074612	4.24464E-06	0.707439	0.70742547	-174.2529529	0.707438
B10	TW-03-26R	Boologooro 1	Upper Gearle Siltstone	345.35	71	0.0565271	3.16552E-06	0.0067493	3.77961E-07	0.7074741	3.53726E-06	0.707452	0.70743837	-172.9630181	0.707451
B11	TW-03-29	Boologooro 1	Upper Gearle Siltstone	346.90	60	0.056525	3.1654E-06	0.0067491	3.7795E-07	0.7074868	3.53733E-06	0.707465	0.707451069	-171.6930822	0.707464
B11	TW-03-29R	Boologooro 1	Upper Gearle Siltstone	346.90	65	0.0565267	3.50466E-06	0.0067493	4.18457E-07	0.7074808	3.5373E-06	0.707459	0.707445069	-172.2930519	0.707458
B12	TW-03-30	Boologooro 1	Lower Gearle Siltstone	347.40	52	0.0565244	3.05232E-06	0.006749	3.64446E-07	0.7074554	3.53717E-06	0.707434	0.707419671	-174.8329236	0.707433
B12	TW-03-30R	Boologooro 1	Lower Gearle Siltstone	347.40	60	0.0565354	3.16598E-06	0.0067503	3.78017E-07	0.7074733	4.24471E-06	0.707452	0.70743757	-173.043014	0.707451
B13	TW-03-33	Boologooro 1	Lower Gearle Siltstone	350.65	78	0.0565235	3.39141E-06	0.0067489	4.04934E-07	0.7075046	3.53741E-06	0.707483	0.707468868	-169.9131721	0.707482
B13	TW-03-33RR	Boologooro 1	Lower Gearle Siltstone	350.65	99	0.0565173	3.05193E-06	0.0067482	3.64403E-07		3.53739E-06	0.707478	0.707463655	-170.4345372	0.707477
B14	TW-03-35	Boologooro 1	Lower Gearle Siltstone	351.42	69	0.0565224	3.39134E-06	0.0067488	4.04928E-07	0.7075345	3.53756E-06	0.707513	0.707498767	-166.9233231	0.707512
B14	TW-03-35	Boologooro 1	Lower Gearle Siltstone	351.42	69	0.0565224	3.39134E-06	0.0067488	4.04928E-07	0.7075345	3.53756E-06	0.707513	0.707498767	-166.9233231	0.707512
B14	TW-03-35 R	Boologooro 1	Lower Gearle Siltstone	351.42	59	0.0565389	3.27926E-06	0.0067507	3.91541E-07		4.24503E-06	0.707504	0.707490254	-167.7745896	0.707503
B15	TW-03-41	Boologooro 1	Lower Gearle Siltstone	352.95	99	0.0565299	3.50485E-06	0.0067497	4.18481E-07	0.7074798	4.24475E-06	0.707458	0.70744407	-172.3930469	0.707457
B16	TW-03-42	Boologooro 1	Lower Gearle Siltstone	357.00	44	0.0565315	3.0527E-06	0.0067494	3.64468E-07	0.707469	4.24468E-06	0.707447	0.70743327	-173.4729923	0.707446
B17	TW-03-45	Boologooro 1	Lower Gearle Siltstone	359.90	55	0.0565297	3.16566E-06	0.0067496	3.77978E-07	0.7074179	4.24438E-06	0.707396	0.707382173	-178.5827342	0.707395
B17	TW-03-45R	Boologooro 1	Lower Gearle Siltstone	359.90	51	0.0565303	3.1657E-06	0.0067497	3.77983E-07	0.7074437	3.53711E-06	0.707422	0.707407971	-176.0028645	0.707421
B17	TW-03-45RG	Boologooro 1	Lower Gearle Siltstone	359.90	51	0.0565335	2.93974E-06	0.0067501	3.51005E-07	0.7074319	3.53705E-06	0.707410	0.707396172	-177.182805	0.707409
B18	TW-03-48R	Boologooro 1	Lower Gearle Siltstone	361.05	67	0.0565266	3.27854E-06	0.0067493	3.91459E-07	0.7074893	3.53734E-06	0.707468	0.707453569	-171.4430948	0.707467
B18	TW-03-48RG	Boologooro 1	Lower Gearle Siltstone	361.05	51	0.0565303	3.39182E-06	0.0067497	4.04982E-07	0.7075072	3.53743E-06	0.707485	0.707471468	-169.6531852	0.707484
B19	TW-03-52R	Boologooro 1	Lower Gearle Siltstone	365.63	74	0.0565256	3.50459E-06	0.0067492	4.1845E-07	0.7074698	4.24469E-06	0.707448	0.70743407	-173.3929964	0.707447
B19	TW-03-52RG	Boologooro 1	Lower Gearle Siltstone	365.63	75	0.0565362	2.93988E-06	0.0067504	3.51021E-07	0.7074678	3.53723E-06	0.707446	0.70743207	-173.5929863	0.707445
B20	TW-03-54	Boologooro 1	Lower Gearle Siltstone	374.00	74	0.0565384	3.3923E-06	0.0067507	4.05042E-07	0.7074214	3.537E-06	0.707400	0.707385672	-178.2327519	0.707399

Sample No	Lab No	Well	Formation	Depth (m)	ZBias	$^{84}Sr/^{86}Sr$	Error %sem	$^{84}Sr/^{88}Sr$	Error %sem	$^{87}Sr/^{86}Srm$	Error %sem	$^{87}Sr/^{86}Srm$ N = 0.710249	$^{84}Sr/^{88}Sr$ 0.710235	ΔSW 0.709168	$^{87}Sr/^{86}Srm$ 0.710248
B20	TW-03-54R	Boologooro 1	Lower Gearle Siltstone	374.00	73	0.0565355	3.05292E-06	0.0067503	3.64516E-07	0.7074153	3.53697E-06	0.707394	0.707379573	-178.8427211	0.707393
B20	TW-03-54RG	Boologooro 1	Lower Gearle Siltstone	374.00	65	0.0565428	3.50565E-06	0.0067512	4.18574E-07	0.7074106	3.53694E-06	0.707389	0.707374873	-179.3126974	0.707388
B21	TW-03-57R	Boologooro 1	Lower Gearle Siltstone	377.65	36	0.0565399	3.16623E-06	0.0067509	3.7805E-07	0.7074009	3.5369E-06	0.707379	0.707365174	-180.2826484	0.707378
B21	TW-03-57RG	Boologooro 1	Lower Gearle Siltstone	377.65	34	0.0565354	3.16598E-06	0.0067503	3.78017E-07	0.7074025	3.5369E-06	0.707381	0.707366773	-180.1226565	0.707380
B22	TW-03-59R	Boologooro 1	Windalia Radiolarite	378.42	44	0.0565243	4.06975E-06	0.006749	4.85928E-07	0.7072016	4.24308E-06	0.707180	0.707165884	-200.2116418	0.707179
B22	TW-03-59RG	Boologooro 1	Windalia Radiolarite	378.42	60	0.0565264	3.8438E-06	0.0067493	4.58952E-07	0.7072096	3.53594E-06	0.707188	0.707173883	-199.4116823	0.707187
B23	TW-03-62	Boologooro 1	Windalia Radiolarite	382.70	?	0.0565196	3.05206E-06	0.0067484	3.64414E-07	0.707283	3.53631E-06	0.707261	0.707247279	-192.0720529	0.707260
B23	TW-03-62R	Boologooro 1	Windalia Radiolarite	382.70	99	0.0565271	3.50468E-06	0.0067493	4.18457E-07	0.707279	4.24354E-06	0.707257	0.70724328	-192.4720327	0.707256
B23	TW-03-62RG	Boologooro 1	Windalia Radiolarite	382.70	96	0.056538	3.16613E-06	0.0067506	3.78034E-07	0.7072772	3.53628E-06	0.707255	0.70724148	-192.6520237	0.707254
	TW-03-65	Edaggee 1	Lower Gearle Siltstone	256.80	?	0.0565392	2.94004E-06	0.0067508	3.51042E-07	0.7073934	3.53686E-06	0.707372	0.707357674	-181.0326105	0.707371
	TW-03-65R	Edaggee 1	Lower Gearle Siltstone	259.60	?	0.0565378	3.16612E-06	0.0067506	3.78034E-07	0.707395	3.53687E-06	0.707373	0.707359274	-180.8726186	0.707372
	TW-03-65RG	Edaggee 1	Lower Gearle Siltstone	260.30	51	0.056536	3.39216E-06	0.0067504	4.05024E-07	0.7073866	4.24419E-06	0.707365	0.707350874	-181.7125762	0.707364
BA1	TW-03-66R	Barrabiddy 1	Lower Gearle Siltstone	84.10	?	0.056532	3.27886E-06	0.0067499	3.91494E-07	0.7074732	4.24471E-06	0.707451	0.70743747	-173.0530135	0.707450
BA1	TW-03-66RG	Barrabiddy 1	Lower Gearle Siltstone	84.10	66	0.0565307	3.61796E-06	0.0067498	4.31987E-07	0.7074776	3.53728E-06	0.707456	0.70744187	-172.6130358	0.707455
Y1	TW-03-68	Yinni 1	Windalia Radiolarite	59.03	?	0.0565408	3.61861E-06	0.006751	4.32064E-07	0.7072437	3.53611E-06	0.707222	0.707207981	-196.0018545	0.707221
Y1	TW-03-68RG	Yinni 1	Windalia Radiolarite	59.03	61	0.0565345	3.50514E-06	0.0067502	4.18512E-07	0.7072023	4.24308E-06	0.707181	0.707166584	-200.1416454	0.707180
Y1	TW-03-68	Yinni 1	Windalia Radiolarite	59.03	?	0.0565408	3.61861E-06	0.006751	4.32064E-07	0.7072437	3.53611E-06	0.707222	0.707207981	-196.0018545	0.707221
Y1	TW-03-68 R	Yinni 1	Windalia Radiolarite	59.03	53	0.0565318	2.82659E-06	0.0067499	3.37495E-07		3.53606E-06	0.707212	0.70719836	-196.9640142	0.707211
BA2	TW-03-69	Barrabiddy 1	Munderong Sandstone	150.75	?	0.056536	3.05294E-06	0.0067504	3.64522E-07	0.7075177	4.24498E-06	0.707496	0.707481968	-168.6032383	0.707495
BA2	TW-03-69R	Barrabiddy 1	Munderong Sandstone	150.75	80	0.0565234	3.27836E-06	0.0067499	3.91494E-07	0.7074924	4.24482E-06	0.707471	0.707456669	-171.1331105	0.707470
BA2	TW-03-69 R	Barrabiddy 1	Munderong Sandstone	150.75	85	0.0565282	3.05252E-06	0.0067495	3.64473E-07		3.53762E-06	0.707524	0.707510494	-165.7506295	0.707523
	TW-03-70	Boologooro 1	Average		?	0.0565255	3.39153E-06	0.0067492	4.04952E-07	0.7074435	3.53711E-06	0.707422	0.707407771	-176.0228635	0.707421
	TW-03-70 R	Boologooro 1	Average		68	0.0565339	2.93976E-06	0.0067501	3.51005E-07		3.53711E-06	0.707423	0.707408956	-175.9044294	0.707422
	TW-03-71	Barrabiddy 1	Munderong Sandstone	150.75	?	0.0565285	5.99202E-06	0.0067495	7.15447E-07	0.7074972	5.6598E-06	0.707475	0.707461469	-170.6531347	0.707474
M4	TW-03-T1	Qld Eromanga	Toolebuc Limestone		68	0.0565446	3.1665E-06	0.0067514	3.78078E-07	0.7074053	4.2443E-06	0.707384	0.707369573	-179.8426706	0.707383
M3	TW-03-T2	Qld Eromanga	Toolebuc Limestone		51	0.056532	3.05273E-06	0.0067499	3.64495E-07	0.7074865	3.53732E-06	0.707465	0.707450769	-171.7230807	0.707464
C1	TW-03-EC1	Carpentaria	Blackdown Formation		83	0.0565341	3.73125E-06	0.0067502	4.45513E-07	0.7072597	4.24343E-06	0.707238	0.707223981	-194.4019353	0.707237
L3	TW-03-LA1	Qld Eromanga	Allaru Mudstone		99	0.056534	2.93977E-06	0.0067502	3.5101E-07	0.7074639	3.53721E-06	0.707442	0.70742817	-173.9829666	0.707441
L2	TW-03-LA2	Qld Eromanga	Allaru Mudstone		99	0.0565325	3.61808E-06	0.00675	0.000000432	0.7074151	4.24436E-06	0.707393	0.707379373	-178.8627201	0.707392
C3	TW-03-WR1	Carpentaria	Blackdown Formation		64	0.056544	3.05338E-06	0.0067514	3.64576E-07	0.7072234	3.53601E-06	0.707202	0.707187682	-198.0317519	0.707201
C3	TW-03-WR1 R	Carpentaria	Blackdown Formation		62	0.0565342	3.27898E-06	0.0067502	3.91512E-07		3.53606E-06	0.707212	0.70719766	-197.0340129	0.707211
C5	TW-03-WR2	Carpentaria	Blackdown Formation		71	0.0565414	2.82707E-06	0.006751	3.3755E-07	0.7072538	3.53616E-06	0.707232	0.707218081	-194.9919055	0.707231
C5	TW-03-WR2 R	Carpentaria	Blackdown Formation		71	0.056549	2.60125E-06	0.006752	3.10592E-07		3.53631E-06	0.707261	0.707247459	-192.054111	0.707260
C4	TW-03-WR3	Carpentaria	Blackdown Formation		99	0.0565352	3.27904E-06	0.0067503	3.91517E-07	0.7072669	4.24347E-06	0.707245	0.70723118	-193.6819716	0.707244
	TW-03-RM1	Qld Eromanga	Minmi Member		75	0.0565304	3.1657E-06	0.0067497	3.77983E-07	0.7073203	3.53649E-06	0.707299	0.707284578	-188.3422413	0.707298
FR6	TW-03-FR1	Qld Eromanga	Lower Doncaster Member		65	0.0565383	2.93999E-06	0.0067507	3.51036E-07	0.7072922	3.53635E-06	0.707270	0.707256479	-191.1520994	0.707269
M2	TW-03-FRA1	Qld Eromanga	Allaru Mudstone		99	0.0565471	3.05354E-06	0.0067517	3.64592E-07	0.7074145	3.53696E-06	0.707393	0.707378773	-178.9227171	0.707392
	TW-03-RW1 R	Qld Eromanga	Lower Wallumbilla Formation		72	0.0565307	3.16572E-06	0.0067498	3.77989E-07		3.53639E-06	0.707279	0.707264959	-190.3041455	0.707278
	TW-03-RW2	Qld Eromanga	Lower Wallumbilla Formation		50	0.0565484	3.73219E-06	0.0067519	4.45625E-07	0.7072608	4.24343E-06	0.707239	0.707225081	-194.2919408	0.707238
	TW-03-RW2	Qld Eromanga	Lower Wallumbilla Formation		50	0.0565484	3.73219E-06	0.0067519	4.45625E-07	0.7072608	4.24343E-06	0.707239	0.707225081	-194.2919408	0.707238
	TW-03-RW2 R	Qld Eromanga	Lower Wallumbilla Formation		64	0.0565411	2.71397E-06	0.006751	3.24048E-07		3.53613E-06	0.707226	0.70721236	-195.5640418	0.707225

Sample No	Lab No	Well	Formation	Depth (m)	ZBias	$^{84}Sr/^{86}Sr$	Error %sem	$^{84}Sr/^{88}Sr$	Error %sem	$^{87}Sr/^{86}Srm$	Error %sem	$^{87}Sr/^{86}Srm$ N = 0.710249	$^{84}Sr/^{88}Sr$ 0.710235	ΔSW 0.709168	$^{87}Sr/^{86}Srm$ 0.710248
L6	TW-03-LC1	Qld Eromanga	Coreena Member		80	0.0565234	3.27836E-06	0.0067499	3.91494E-07	0.7074924	4.24482E-06	0.707471	0.707456669	-171.1331105	0.707470
L6	TW-03-LC1	Qld Eromanga	Coreena Member		45	0.0565346	3.05287E-06	0.0067502	3.64511E-07		4.24457E-06	0.707428	0.707413656	-175.4344386	0.707427
La1	TW-03-5297-01	Laura	Wollena Claystone		55	0.0565254	3.16542E-06	0.0067491	3.7795E-07		4.24437E-06	0.707394	0.707380256	-178.7743728	0.707393
E2	TW-03-5297-11	SA Eromanga	Oodnadatta Formation		69	0.0565347	3.50515E-06	0.0067502	4.18512E-07		4.95211E-06	0.707444	0.707429955	-173.8044708	0.707443
E2	TW-03-5297-11 R	SA Eromanga	Oodnadatta Formation		73	0.0565293	2.82647E-06	0.0067496	3.3748E-07		3.5371E-06	0.707419	0.707405156	-176.2844219	0.707418
E2	TW-03-5297-11 RR	SA Eromanga	Oodnadatta Formation		60	0.0565234	2.82617E-06	0.0067489	3.37445E-07		2.82969E-06	0.707421	0.707407356	-176.0644262	0.707420
E1	TW-03-5297-12	SA Eromanga	Oodnadatta Formation		36	0.0565249	2.93929E-06	0.0067491	3.50953E-07		3.53708E-06	0.707416	0.707401956	-176.6044156	0.707415
E1	TW-03-5297-12 R	SA Eromanga	Oodnadatta Formation		20	0.0565312	2.60044E-06	0.0067498	3.10491E-07		3.53713E-06	0.707427	0.707412656	-175.5344367	0.707426
E3	TW-03-5297-14	SA Eromanga	Bulldog Shale		57	0.0565428	3.50565E-06	0.0067512	4.18574E-07		4.24386E-06	0.707310	0.707296158	-187.184207	0.707309
E3	TW-03-5297-14 R	SA Eromanga	Bulldog Shale		69	0.0565395	2.94005E-06	0.0067508	3.51042E-07		3.5364E-06	0.707280	0.707265559	-190.2441467	0.707279
L4	TW-03-5297-19	Qld Eromanga	Toolebuc Limestone		52	0.0565409	3.61862E-06	0.006751	4.32064E-07		3.53707E-06	0.707414	0.707400456	-176.7544126	0.707413
L4	TW-03-5297-19 RR	Qld Eromanga	Toolebuc Limestone		58	0.0565151	2.82576E-06	0.0067483	3.37415E-07		3.53707E-06	0.707415	0.707400656	-176.734413	0.707414
	TW-03-5297-20	Qld Eromanga	Lower Allaru Mudstone		64	0.0565344	3.05286E-06	0.0067502	3.64511E-07		4.24463E-06	0.707439	0.707424855	-174.3144607	0.707438
	TW-03-5297-20 R	Qld Eromanga	Lower Allaru Mudstone		72	0.0565327	2.71357E-06	0.00675	0.000000324		3.53708E-06	0.707416	0.707402456	-176.5544165	0.707415
L1	TW-03-5297-21	Qld Eromanga	Mackunda Formation		48	0.0565306	4.18326E-06	0.0067489	4.99419E-07		4.24449E-06	0.707416	0.707401856	-176.6144154	0.707415
L5	TW-03-5297-24	Qld Eromanga	Coreena Member		57	0.0565357	3.50521E-06	0.0067504	4.18525E-07		3.53686E-06	0.707372	0.707357757	-181.0243284	0.707371
L5	TW-03-5297-24 R	Qld Eromanga	Coreena Member		53	0.0565353	2.71369E-06	0.0067503	3.24014E-07		2.82945E-06	0.707361	0.707347457	-182.0543081	0.707360
C2	TW-03-5297-26	Carpentaria	Blackdown Formation		68	0.0565439	3.39263E-06	0.0067513	4.05078E-07		4.95037E-06	0.707196	0.70718176	-198.6239815	0.707195
FR5	TW-03-5297-32	Qld Eromanga	Upper Doncaster Member		64	0.0565298	3.16567E-06	0.0067497	3.77983E-07		3.53688E-06	0.707375	0.707361257	-180.6743353	0.707374
FR5	TW-03-5297-32R	Qld Eromanga	Upper Doncaster Member		46	0.0565381	2.93998E-06	0.0067507	3.51036E-07		3.53687E-06	0.707374	0.707359757	-180.8243324	0.707373
FR4	TW-03-5297-34	Qld Eromanga	Lower Jones Valley Member		57	0.0565357	3.50521E-06	0.0067504	4.18525E-07		4.24379E-06	0.707298	0.707283958	-188.404183	0.707297
FR4	TW-03-5297-34 R	Qld Eromanga	Lower Jones Valley Member		53	0.0565353	2.71369E-06	0.0067503	3.24014E-07		2.82911E-06	0.707278	0.707264259	-190.3741441	0.707277
FR2	TW-03-5297-38	Qld Eromanga	Lower Ranmoor Member		46	0.0565394	3.39236E-06	0.0067508	4.05048E-07		4.24312E-06	0.707187	0.70717326	-199.4739648	0.707186
FR2	TW-03-5297-38 R	Qld Eromanga	Lower Ranmoor Member		47	0.0565264	2.82632E-06	0.0067493	3.37465E-07		3.53592E-06	0.707184	0.70717016	-199.7839587	0.707183
FR1	TW-03-5297-39 R	Qld Eromanga	Upper Ranmmor Member		78	0.0565354	3.16598E-06	0.0067489	3.77938E-07		4.24411E-06	0.707352	0.707338157	-182.9842898	0.707351
FR1	TW-03-5297-39 RR	Qld Eromanga	Upper Ranmmor Member		65	0.0565227	3.50441E-06	0.0067488	4.18426E-07		4.24434E-06	0.707390	0.707375956	-179.2043643	0.707389
FR1	TW-03-5297-39 RRR	Qld Eromanga	Upper Ranmmor Member		46	0.0565381	2.93998E-06	0.0067507	3.51036E-07		3.53687E-06	0.707374	0.707359757	-180.8243324	0.707373
FR3	TW-03-5297-45	Qld Eromanga	Jones Valley Member		81	0.0565482	4.18457E-06	0.0067519	4.99641E-07		4.95038E-06	0.707197	0.70718306	-198.4939841	0.707196

Lab No	Date	ZBias	$^{84}Sr/^{86}Sr$	Error %sem	$^{84}Sr/^{88}Sr$	Error %sem	$^{87}Sr/^{86}Srm$	Error %sem	$^{87}Sr/^{86}Srm$ N = 0.710249	$^{84}Sr/^{88}Sr$ 0.710235	ΔSW 0.709168
NBS-987	Nov 18 03	68	0.0565085	0.000004	0.006747	0.0000005	0.710319	4.26135E-06	0.710226	0.710211613	
NBS-987	Nov 18 03	31	0.0565275	0.000004	0.006749	0.0000004	0.710337	4.9717E-06	0.710244	0.71022951	
NBS-987	Nov 19 03	49	0.056512	0.000003	0.006748	0.0000004	0.710257	4.26154E-06	0.710257	0.7102427	
NBS-987	Nov 19 03	53	0.0565122	0.000003	0.006748	0.0000004	0.710273	4.97191E-06	0.710273	0.7102588	
NBS-987	Nov 19 03	55	0.0565125	0.000003	0.006748	0.0000004	0.710273	4.26164E-06	0.710273	0.7102594	
NBS-987	Nov 19 03	24	0.0565111	0.000003	0.006747	0.0000004	0.710259	4.97181E-06	0.710259	0.7102447	
NBS-987	Nov 19 03	99	0.0565099	0.000004	0.006747	0.0000004	0.710276	4.26166E-06	0.710276	0.710262199	
NBS-987	Nov 20 03	45	0.0565274	0.000003	0.006749	0.0000004	0.710239	3.5512E-06	0.710239	0.7102252	
NBS-987	Nov 20 03	53	0.0565156	0.000004	0.006748	0.0000005	0.710238	4.26143E-06	0.710238	0.7102241	
NBS-987	Nov 20 03	34	0.0565187	0.000004	0.006748	0.0000005	0.710256	4.26154E-06	0.710256	0.710242	
NBS-987	Nov 20 03	19	0.0565229	0.000003	0.006749	0.0000004	0.710242	3.55121E-06	0.710242	0.7102277	
NBS-987	Nov 20 03	99	0.056518	0.000003	0.006748	0.0000004	0.710243	4.26146E-06	0.710243	0.710229	
NBS-987	Nov 21 03	63	0.0565158	0.000003	0.006748	0.0000003	0.710260	3.5513E-06	0.710260	0.710246	
NBS-987	Nov 21 04	60	0.0565309	0.000003	0.006750	0.0000004	0.710255	3.55127E-06	0.710255	0.7102405	
NBS-987	Nov 25 03	73	0.0565181	0.000003	0.006748	0.0000004	0.710225	4.97158E-06	0.710225	0.7102111	
NBS-987	Nov 25 03	51	0.0565222	0.000003	0.006749	0.0000004	0.710247	3.55123E-06	0.710247	0.7102326	106.4600047
NBS-987	Nov 25 03	45	0.0565109	0.000003	0.006747	0.0000004	0.710262	3.55131E-06	0.710262	0.7102479	107.9899746
NBS-987	Nov 28 03	56	0.0565136	0.000003	0.006748	0.0000003	0.710241	2.84096E-06	0.710241	0.7102265	105.85
NBS-987	Nov 28 03	80	0.0565234	0.000003	0.006749	0.0000004	0.710271	3.55125E-06	0.710250	0.710235529	106.75
NBS-987	Nov 29 03	48	0.0565294	0.000004	0.006750	0.0000004	0.710277	3.55128E-06	0.710255	0.710241428	107.34
NBS-987	Nov 30 03	74	0.0565335	0.000003	0.006750	0.0000004	0.710276	3.55127E-06	0.710254	0.710239728	107.17
NBS-987	Nov 30 03	52	0.0565328	0.000004	0.006750	0.0000004	0.710287	3.55133E-06	0.710265	0.710251028	108.30
NBS-987	Dec 2 03	47	0.0565179	0.000003	0.006748	0.0000004	0.710266	3.55122E-06	0.710244	0.710229829	106.18
NBS-987-60RG-1	Dec 2 03	68	0.056535	0.0000032	0.0067503	0.0000004	0.710278	0.000004	0.710256	0.710242	107.38
NBS-987-60RG	Dec 2 03	60	0.0565276	0.0000028	0.0067494	0.0000003	0.7102546	3.55116E-06	0.7102327	0.710218729	105.07
NBS-987-61RG	Dec 2 03	47	0.0565375	0.0000036	0.0067506	0.0000004	0.7091952	4.25504E-06	0.7091734	0.709159383	-0.86
NBS-987-62RG	Dec 3 03	50	0.0565272	0.0000032	0.0067493	0.0000004	0.7102598	4.26143E-06	0.7102379	0.710223929	105.59
NBS-987-63	Dec 3 03	33	0.0565325	0.0000032	0.0067500	0.0000004	0.7102427	3.5511E-06	0.7102208	0.71020683	103.8829994
EN-1	Nov 18 03	37	0.0565025	4.4072E-06	0.0067464	0.0000005	0.709261	2.83667E-06	0.709168	0.709154172	-1.382753516
EN-1	Nov 18 03	44	0.0565283	4.29615E-06	0.0067495	0.0000005	0.709279	3.54593E-06	0.709186	0.70917187	0.38697964
EN-1	Nov 19 03	34	0.0565281	3.27863E-06	0.0067494	0.0000004	0.709174	2.8367E-06	0.709174	0.709160321	-0.767881616
EN-1	Nov 19 03	37	0.056521	3.27822E-06	0.0067486	0.0000004	0.709189	3.54595E-06	0.709189	0.709175221	0.722089014
EN-1	Nov 20 03	53	0.0565187	2.82594E-06	0.0067483	0.0000003	0.709173	3.54587E-06	0.709173	0.709159121	-0.887879251
EN-1	Nov 20 03	32	0.0565316	3.16577E-06	0.0067499	0.0000004	0.709141	3.5457E-06	0.709141	0.709126922	-4.10781578
EN-1	Nov 20 03	39	0.0565328	3.16584E-06	0.00675	0.0000004	0.709151	4.2549E-06	0.709151	0.709136522	-3.147834703
EN-1	Nov 20 03	14	0.0565237	2.60009E-06	0.0067486	0.0000003	0.709144	3.54572E-06	0.709144	0.709129922	-3.807821694
EN-1	Nov 21 03	99	0.0565248	2.93929E-06	0.0067491	0.0000004	0.709175	3.54588E-06	0.709175	0.709161021	-0.697882996
EN-1	Nov 22 03	24	0.0565031	2.71215E-06	0.0067465	0.0000003	0.709163	3.54581E-06	0.709163	0.709148921	-1.907859145
EN-1	Nov 23 03	98	0.0565204	2.82602E-06	0.0067485	0.0000003	0.709175	3.54588E-06	0.709175	0.709161421	-0.657883784
EN-1 New Load	Nov 23 03	83	0.0565152	3.27788E-06	0.0067479	0.0000004	0.709169	3.54585E-06	0.709169	0.709155321	-1.26787176

Lab No	Date	ZBias	$^{84}Sr/^{86}Sr$	Error	$^{84}Sr/^{88}Sr$	Error	$^{87}Sr/^{86}Srm$	Error	$^{87}Sr/^{86}Srm$	$^{84}Sr/^{88}Sr$	ΔSW
				%sem		%sem		%sem	N = 0.710249	0.710235	0.709168
EN-1	Nov 25 03	53	0.0565176	3.05195E-06	0.0067483	0.0000004	0.7091627	3.54581E-06	0.709163	0.709148721	-1.927858751
EN-1	Nov 25 03	99	0.0565136	3.05173E-06	0.0067477	0.0000004	0.7091567	3.54578E-06	0.709157	0.709142722	-2.527846924
EN-1	Nov 25 03	42	0.0565297	2.71343E-06	0.0067496	0.0000003	0.7091581	3.54591E-06	0.709183	0.709168664	0.066411535
EN-1	Nov 28 03	34	0.0565297	3.6179E-06	0.0067496	0.0000004	0.7092098	4.96432E-06	0.709188	0.709173982	0.598215964
EN-1	Nov 28 03	65	0.0565325	3.16582E-06	0.00675	0.0000004	0.7092463	3.54612E-06	0.709224	0.70921048	4.248031625
EN-1	Nov 30 03	63	0.0565254	3.84373E-06	0.0067491	0.0000005	0.7092412	4.96454E-06	0.709219	0.709205381	3.738057382
EN-1	Nov 30 03	64	0.0565353	2.82677E-06	0.0067503	0.0000003	0.7091801	3.54579E-06	0.709158	0.709144284	-2.371634039
EN-1/03/29 R	Dec 2 03	46	0.0565254	2.82627E-06	0.0067491	3.37455E-07	0.7092571	0	0	0	-70916.8
EN-1/03-28RG	Dec 2 03	89	0.056529	0.000003	0.006750	3.91477E-07	0.7092269	3.54603E-06	0.709205	0.709191081	2.308129603
EN-1/03-29RG	Dec 3 03	45	0.056525	3.2785E-06	0.006749	3.91448E-07	0.7092675	3.54623E-06	0.709246	0.709231679	6.367924557
EN-1/03-31	Dec 3 03	57	0.0565374	0.000003	6.7506E-03	0.000000	0.7091938	4.25503E-06	0.709171962	0.709157983	-1.001703229

Western Australian Samples

Carnarvon Basin

Upper Gearle Siltstone Cenomanian Boloogooroo 283.3 - 347.1 m

Boologooro 293.1 m
Upper Gearle Siltstone
B1
5591-002

Element	Conc	S.D.	Unit	ppm
Ca	398	6	mg/g	
Fe	<= 0.1		mg/g	<=100
Mg	1.84	0.03	mg/g	1840
Mn	<= 0.1		mg/g	<=100
Sr	1.33	0.01	mg/g	1330

Boologooro 297.95 m
Upper Gearle Siltstone
B2
5591-004

Element	Conc	S.D.	Unit	ppm
Ca	401	2	mg/g	
Fe	<= 0.1		mg/g	<=100
Mg	2.24	0.02	mg/g	2240
Mn	<= 0.1		mg/g	<=100
Sr	1.24	0.01	mg/g	1240

Boologooro 301.55 m
Upper Gearle Siltstone
B3
5591-009

Element	Conc	S.D.	Unit	ppm
Ca	393	6	mg/g	
Fe	0.176	0.007	mg/g	176
Mg	1.90	0.05	mg/g	1900
Mn	<= 0.1		mg/g	<=100
Sr	0.608	0.016	mg/g	608

Boologooro 305.15 m
Upper Gearle Siltstone
B4
5591-012

Element	Conc	S.D.	Unit	ppm
Ca	401	2	mg/g	
Fe	<= 0.1		mg/g	<=100
Mg	2.56	0.01	mg/g	2560
Mn	<= 0.1		mg/g	<=100
Sr	1.24	0.02	mg/g	1240

Boologooro 308.80 m (p)
Upper Gearle Siltstone
B5
5591-016

Element	Conc	S.D.	Unit	ppm
Ca	417	7	mg/g	
Fe	<= 0.1		mg/g	<=100
Mg	1.22	0.01	mg/g	1220
Mn	<= 0.1		mg/g	<=100
Sr	0.941	0.013	mg/g	941

Boologooro 311.6 m (p)
Upper Gearle Siltstone
B6
5591-018

Element	Conc	S.D.	Unit	ppm
Ca	368	3	mg/g	
Fe	6.54	0.09	mg/g	6540
Mg	1.76	0.01	mg/g	1760
Mn	<= 0.1		mg/g	<=100
Sr	1.05	0.02	mg/g	1050

Boologooro 326.6 m (p)
Upper Gearle Siltstone
B7
5591-019

Element	Conc	S.D.	Unit	ppm
Ca	376	5	mg/g	
Fe	0.252	0.008	mg/g	252
Mg	3.10	0.02	mg/g	3100
Mn	<= 0.1		mg/g	<=100
Sr	1.12	0.01	mg/g	1120

Boologooro 330.7 m
Upper Gearle Siltstone
B8
5591-020

Element	Conc	S.D.	Unit	ppm
Ca	376	3	mg/g	
Fe	<= 0.1		mg/g	<=100
Mg	2.25	0.01	mg/g	2250
Mn	<= 0.1		mg/g	<=100
Sr	1.13	0.01	mg/g	1130

Boologooro 339.14 m
Upper Gearle Siltstone
B9
5591-022

Element	Conc	S.D.	Unit	ppm
Ca	393	2	mg/g	
Fe	<= 0.1		mg/g	<=100
Mg	2.75	0.03	mg/g	2750
Mn	<= 0.1		mg/g	<=100
Sr	1.18	0.01	mg/g	1180

Boologooro 345.35 m
Upper Gearle Siltstone
B10
5591-026

Element	Conc	S.D.	Unit	ppm
Ca	372	6	mg/g	
Fe	0.195	0.004	mg/g	195
Mg	2.57	0.01	mg/g	2570
Mn	<= 0.1		mg/g	<=100
Sr	1.24	0.01	mg/g	1240

Boologooro 346.9 m
Upper Gearle Siltstone
B11
5591-029

Element	Conc	S.D.	Unit	ppm
Ca	389	3	mg/g	
Fe	0.553	0.014	mg/g	553
Mg	2.33	0.03	mg/g	2330
Mn	<= 0.1		mg/g	<=100
Sr	1.13	0.03	mg/g	1130

Lower Gearle Siltstone Albian Boloogooroo 347.1 - 378.0 m

Boologooro 347.4 m
Lower Gearle Siltstone
B12
5591-030

Element	Conc	S.D.	Unit	ppm
Ca	384	2	mg/g	
Fe	<= 0.1		mg/g	<=100
Mg	2.34	0.01	mg/g	2340
Mn	<= 0.1		mg/g	<=100
Sr	1.23	0.02	mg/g	1230

Boologooro 350.65 m
Lower Gearle Siltstone
B13
5591-033

Element	Conc	S.D.	Unit	ppm
Ca	378	2	mg/g	
Fe	<= 0.1		mg/g	<=100
Mg	2.35	0.04	mg/g	2350
Mn	<= 0.1		mg/g	<=100
Sr	1.19	0.01	mg/g	1190

Boologooro 351.42 m
Lower Gearle Siltstone
B14
5591-035

Element	Conc	S.D.	Unit	ppm
Ca	379	3	mg/g	
Fe	0.145	0.007	mg/g	145
Mg	2.41	0.01	mg/g	2410
Mn	<= 0.1		mg/g	<=100
Sr	1.47	0.01	mg/g	1470

Boologooro 352.95 m (p)
Lower Gearle Siltstone
B15
5591-041

Element	Conc	S.D.	Unit	ppm
Ca	384	3	mg/g	
Fe	<= 0.1		mg/g	<=100
Mg	2.63	0.01	mg/g	2630
Mn	<= 0.1		mg/g	<=100
Sr	1.27	0.01	mg/g	1270

Boologooro 357.0 m
Lower Gearle Siltstone n
B16
5591-042

Element	Conc	S.D.	Unit	ppm
Ca	378	7	mg/g	
Fe	<= 0.1		mg/g	<=100
Mg	2.37	0.01	mg/g	2370
Mn	<= 0.1		mg/g	<=100
Sr	1.31	0.01	mg/g	1310

Boologooro 359.9 m
Lower Gearle Siltstone
B17
5591-045

Element	Conc	S.D.	Unit	ppm
Ca	382	5	mg/g	
Fe	<= 0.1		mg/g	<=100
Mg	2.16	0.03	mg/g	2160
Mn	<= 0.1		mg/g	<=100
Sr	1.15	0.01	mg/g	1150

Boologooro 361.05 m
Lower Gearle Siltstone
B18
5591-048

Element	Conc	S.D.	Unit	ppm
Ca	393	7	mg/g	
Fe	<= 0.1		mg/g	<=100
Mg	2.23	0.01	mg/g	2230
Mn	<= 0.1		mg/g	<=100
Sr	1.17	0.02	mg/g	1170

Boologooro 365.63 m
Lower Gearle Siltstone
B19
5591-052

Element	Conc	S.D.	Unit	ppm
Ca	396	1	mg/g	
Fe	<= 0.1		mg/g	<=100
Mg	1.13	0.01	mg/g	1130
Mn	<= 0.1		mg/g	<=100
Sr	1.19	0.01	mg/g	1190

Boologooro 374.0 m
Lower Gearle Siltstone
B20
5591-054

Element	Conc	S.D.	Unit	ppm
Ca	408	2	mg/g	
Fe	0.196	0.019	mg/g	196
Mg	1.54	0.02	mg/g	1540
Mn	<= 0.1		mg/g	<=100
Sr	1.64	0.01	mg/g	1640

Boologooro 377.65 m
Lower Gearle Siltstone
B21
5591-057

Element	Conc	S.D.	Unit	ppm
Ca	406	2	mg/g	
Fe	<= 0.1		mg/g	<=100
Mg	2.08	0.01	mg/g	2080
Mn	<= 0.1		mg/g	<=100
Sr	1.15	0.01	mg/g	1150

Edaggee 264.85 m
Lower Gearle Siltstone Albian
E1
5591-065

Element	Conc	S.D.	Unit	ppm
Ca	444	2	mg/g	
Fe	<= 0.1		mg/g	<=100
Mg	1.44	0.02	mg/g	1440
Mn	<= 0.1		mg/g	<=100
Sr	1.77	0.04	mg/g	1770

Barrabiddy 84.1 m
Lower Gearle Siltstone Albian
Ba1
5591-066

Element	Conc	S.D.	Unit	ppm
Ca	445	6	mg/g	
Fe	<= 0.1		mg/g	<=100
Mg	1.59	0.01	mg/g	1590
Mn	<= 0.1		mg/g	<=100
Sr	1.85	0.04	mg/g	1850

Windalia Radiolarite 378.0 - 400 m Boloogooroo

Boologooro 378.42 m
Windalia Radiolarite Upper Aptian
B22
5591-059

Element	Conc	S.D.	Unit	ppm
Ca	428	1	mg/g	
Fe	0.113	0.021	mg/g	113
Mg	1.13	0.01	mg/g	1130
Mn	<= 0.1		mg/g	<=100
Sr	1.42	0.03	mg/g	1420

Boologooro 382.7 m
Windalia Radiolarite Upper Aptian
B23
5591-062

Element	Conc	S.D.	Unit	ppm
Ca	376	4	mg/g	
Fe	0.221	0.004	mg/g	221
Mg	1.63	0.01	mg/g	1630
Mn	<= 0.1		mg/g	<=100
Sr	1.09	0.01	mg/g	1090

Yinni 59.03 m
Windalia Radiolarite Upper Aptian
Y1
5591-068

Element	Conc	S.D.	Unit	ppm
Ca	432	3	mg/g	
Fe	<= 0.1		mg/g	<=100
Mg	1.13	0.01	mg/g	1130
Mn	<= 0.1		mg/g	<=100
Sr	1.22	0.01	mg/g	1220

Boologooro
Average seasonal results
5591-070

Element	Conc	S.D.	Unit	ppm
Ca	452	4	mg/g	
Fe	<= 0.1		mg/g	<=100
Mg	1.97	0.01	mg/g	1970
Mn	<= 0.1		mg/g	<=100
Sr	1.92	0.02	mg/g	1920

Barrabiddy 150.75 m
Munderong Sandstone Lower Aptian
Ba2
5591-069

Element	Conc	S.D.	Unit	ppm
Ca	420	6	mg/g	
Fe	0.189	0.006	mg/g	189
Mg	3.39	0.02	mg/g	3390
Mn	<= 0.1		mg/g	<=100
Sr	1.89	0.01	mg/g	1890

Eastern Australian Platform Samples

Laura Basin

Wolena Claystone Late Albian

La1 **JCU F11623**

5297-001

Element	Conc	S.D.	Unit	ppm
Ca	364	2	mg/g	
Fe	<= 0.1		mg/g	<=100
Mg	1.94	0.01	mg/g	1940
Mn	<= 0.1		mg/g	<=100
Sr	1.55	0.02	mg/g	1550

South Australia Eromanga Basin

Oodnadatta Formation Early Albian

E2 **NMV P310431**

5297-011

Element	Conc	S.D.	Unit	ppm
Ca	336	4	mg/g	
Fe	<= 0.1		mg/g	<=100
Mg	1.49	0.03	mg/g	1490
Mn	<= 0.1		mg/g	<=100
Sr	1.28	0.02	mg/g	1280

Oodnadatta Formation Late Albian

E1 **NMV P310468**

Element	Conc	S.D.	Unit	ppm
Ca	310	3	mg/g	
Fe	<= 0.1		mg/g	<=100
Mg	1.11	0.02	mg/g	1110
Mn	<= 0.1		mg/g	<=100
Sr	1.39	0.03	mg/g	1390

Bulldog Shale Late Aptian-Ealry Albian

E3 **SAM P19229**

5297-014

Element	Conc	S.D.	Unit	ppm
Ca	270	1	mg/g	
Fe	<= 0.1		mg/g	<=100
Mg	2.29	0.02	mg/g	2290
Mn	<= 0.1		mg/g	<=100
Sr	1.28	0.01	mg/g	1280

Carpentaria Basin - Elizabeth Creek

Blackdown Formation

C1 **QGS 8430 W10**

5867-005

Element	Conc	S.D.	Unit	ppm
Ca	471	8	mg/g	
Fe	<= 0.1		mg/g	<=100
Mg	1.40	0.01	mg/g	1400
Mn	<= 0.1		mg/g	<=100
Sr	1.30	0.01	mg/g	1300

Blackdown Formation

C2 **QGS F8773**

5297-026

Element	Conc	S.D.	Unit	ppm
Ca	266	3	mg/g	
Fe	<= 0.1		mg/g	<=100
Mg	0.636	0.009	mg/g	636
Mn	<= 0.1		mg/g	<=100
Sr	0.470	0.006	mg/g	470

Walsh River Samples

Blackdown Formation

C3 **JCU F8123**

5867-006

Element	Conc	S.D.	Unit	ppm
Ca	453	4	mg/g	
Fe	<= 0.1		mg/g	<=100
Mg	1.33	0.03	mg/g	1330
Mn	<= 0.1		mg/g	<=100
Sr	1.24	0.01	mg/g	1240

Blackdown Formation

C5 **JCU F5171**

5867-007

Element	Conc	S.D.	Unit	ppm
Ca	424	1	mg/g	
Fe	<= 0.1		mg/g	<=100
Mg	1.35	0.02	mg/g	1350
Mn	<= 0.1		mg/g	<=100
Sr	0.559	0.008	mg/g	559

Blackdown Formation

C4 **QM F33252 L681**

5867-008

Element	Conc	S.D.	Unit	ppm
Ca	422	5	mg/g	
Fe	<= 0.1		mg/g	<=100
Mg	1.12	0.01	mg/g	1120
Mn	<= 0.1		mg/g	<=100
Sr	1.02	0.01	mg/g	1020

Flinders River Section

Upper Doncaster Member
FR2 **L908**
5297-038

Element	Conc	S.D.	Unit	ppm
Ca	292	4	mg/g	
Fe	<= 0.1		mg/g	<=100
Mg	0.813	0.013	mg/g	813
Mn	<= 0.1		mg/g	<=100
Sr	0.693	0.012	mg/g	693

Lower Doncaster Member
FR6 **L907**
5867-001

Element	Conc	S.D.	Unit	ppm
Ca	439	2	mg/g	
Fe	<= 0.1		mg/g	<=100
Mg	2.30	0.02	mg/g	2300
Mn	<= 0.1		mg/g	<=100
Sr	1.10	0.02	mg/g	1100

Upper Ranmoor Member
FR1 **L910**
5297-039

Element	Conc	S.D.	Unit	ppm
Ca	297	4	mg/g	
Fe	<= 0.1		mg/g	<=100
Mg	1.34	0.02	mg/g	1340
Mn	<= 0.1		mg/g	<=100
Sr	0.932	0.025	mg/g	932

Upper Ranmoor Member
FR5 **L914**
5297-032

Element	Conc	S.D.	Unit	ppm
Ca	256	2	mg/g	
Fe	<= 0.1		mg/g	<=100
Mg	0.921	0.005	mg/g	921
Mn	<= 0.1		mg/g	<=100
Sr	0.542	0.009	mg/g	542

Jones Valley Member
FR4 **L916**
5297-034

Element	Conc	S.D.	Unit	ppm
Ca	207	2	mg/g	
Fe	<= 0.1		mg/g	<=100
Mg	1.33	0.02	mg/g	1330
Mn	<= 0.1		mg/g	<=100
Sr	0.374	0.022	mg/g	374

Jones Valley Member
FR3 **L912**
5297-045

Element	Conc	S.D.	Unit	ppm
Ca	321	5	mg/g	
Fe	<= 0.1		mg/g	<=100
Mg	0.830	0.003	mg/g	830
Mn	<= 0.1		mg/g	<=100
Sr	0.538	0.015	mg/g	538

Northern Eromanga Basin

Toolebuc Limestone
M4 **JCU F11616**
5867-002

Element	Conc	S.D.	Unit	ppm
Ca	497	6	mg/g	
Fe	<= 0.1		mg/g	<=100
Mg	1.65	0.05	mg/g	1650
Mn	<= 0.1		mg/g	<=100
Sr	1.61	0.03	mg/g	1610

Toolebuc Limestone
M3 **JCU F11615**
5867-003

Element	Conc	S.D.	Unit	ppm
Ca	461	2	mg/g	
Fe	<= 0.1		mg/g	<=100
Mg	1.43	0.02	mg/g	1430
Mn	<= 0.1		mg/g	<=100
Sr	1.75	0.01	mg/g	1750

Toolebuc Limestone
L4 **GSQ F1369**
5297-019

Element	Conc	S.D.	Unit	ppm
Ca	279	2	mg/g	
Fe	<= 0.1		mg/g	<=100
Mg	0.969	0.010	mg/g	969
Mn	<= 0.1		mg/g	<=100
Sr	1.17	0.03	mg/g	1170

Mackunda Formation

L1 **QM F27918**

5297-021

Element	Conc	S.D.	Unit	ppm
Ca	244	2	mg/g	
Fe	<= 0.1		mg/g	<=100
Mg	1.35	0.02	mg/g	1350
Mn	<= 0.1		mg/g	<=100
Sr	1.21	0.02	mg/g	1210

Mackunda Formation

M2 **QM F2105**

5867-004

Element	Conc	S.D.	Unit	ppm
Ca	434	5	mg/g	
Fe	<= 0.1		mg/g	<=100
Mg	1.98	0.01	mg/g	1980
Mn	<= 0.1		mg/g	<=100
Sr	1.79	0.03	mg/g	1790

Lower Allaru Mudstone

M1 **QM F27742**

5297-020

Element	Conc	S.D.	Unit	ppm
Ca	257	2	mg/g	
Fe	<= 0.1		mg/g	<=100
Mg	1.45	0.01	mg/g	1450
Mn	<= 0.1		mg/g	<=100
Sr	1.39	0.01	mg/g	1390

Allaru Mudstone

L3 **UQ F16922**

LA1

Element	Conc	S.D.	Unit	ppm
Ca	431	3	mg/g	
Fe	<= 0.1		mg/g	<=100
Mg	2.11	0.02	mg/g	2110
Mn	<= 0.1		mg/g	<=100
Sr	1.40	0.01	mg/g	1400

Allaru Mudstone

L2 **JCU 1987**

LA2

Element	Conc	S.D.	Unit	ppm
Ca	345	3	mg/g	
Fe	<= 0.1		mg/g	<=100
Mg	0.509	0.007	mg/g	509
Mn	<= 0.1		mg/g	<=100
Sr	0.940	0.014	mg/g	940

Coreena Member

L5 **GSQ F 1759**

5297-024

Element	Conc	S.D.	Unit	ppm
Ca	279	2	mg/g	
Fe	<= 0.1		mg/g	<=100
Mg	1.11	0.01	mg/g	1110
Mn	<= 0.1		mg/g	<=100
Sr	1.08	0.01	mg/g	1080

Coreena Member

L6 **GSQ F1370**

LC1

Element	Conc	S.D.	Unit	ppm
Ca	455	3	mg/g	
Fe	<= 0.1		mg/g	<=100
Mg	1.38	0.02	mg/g	1380
Mn	<= 0.1		mg/g	<=100
Sr	1.58	0.03	mg/g	1580